

Computational Electromagnetics: The Finite-Difference Time-Domain

*Stephen Gedney
Department of Electrical Engineering
University of Kentucky*

EE699

Fall 2003

© Copyright, Stephen Gedney

Computational Electromagnetics via The Finite-Difference Time-Domain Method

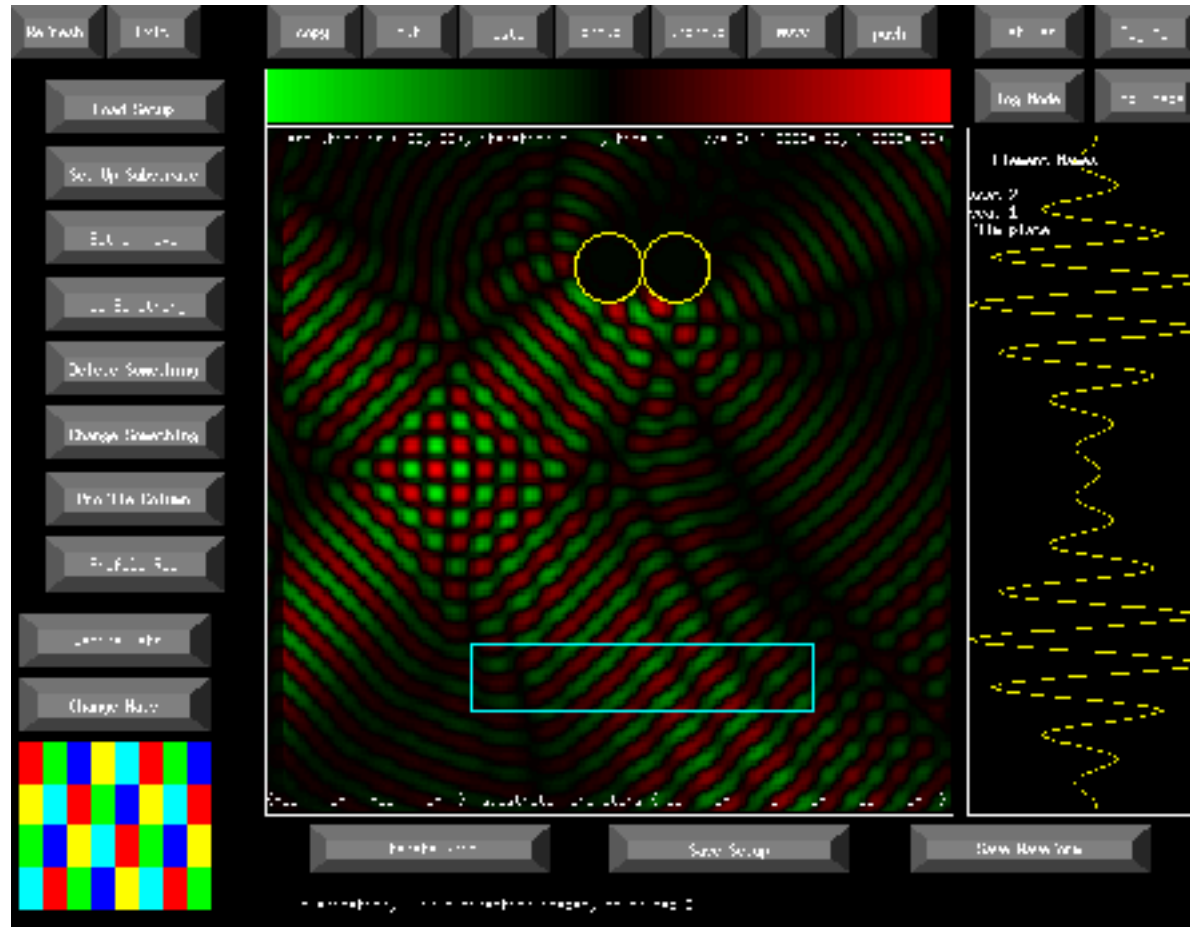
- FDTD is One of the Most Popular Computational Techniques of Current Date for Simulation of Electromagnetic Phenomona
- Based on 2nd Order Accurate Central Difference Approximations in Space and Time of Maxwell's Eqns.
- Provides a Direct Solution of Time-Dependent EM Fields in a Volumetric Region
- Advantages over Moment Method or Finite Element Method:
 - Inhomogeneous Media is Inherently Modeled
 - Lossy, Non-Linear and Anisotropic Media Supported
 - Boundary Conditions are Inherently Represented
 - Broad Band Response Obtained with Single Simulations
 - Robustness and Ease of Implementation
 - Much Broader Range of Direct Applicability

- Some Disadvantages:
 - Accuracy
 - The standard Yee-algorithm is second order accurate
 - Error is generally dispersive
 - Error accumulates as the wave propagates through the mesh
 - Large problems require finer meshing!
 - Computationally Intensive
 - requires 3D orthogonal gridding
 - staircase approximation of curved surfaces
 - Time stepping is a function of the grid dimension
 - smallest detail in the geometry can thus determine grid size (Yee-algorithm) and
the time step

- Application areas of FDTD:
 - EM Scattering
 - EMC
 - Microwave Circuits
 - Non-linear device modeling
 - Antenna modeling & Design
 - Geo-sensing
 - Photonic device modeling
 - Optical gratings, periodic structures
 -

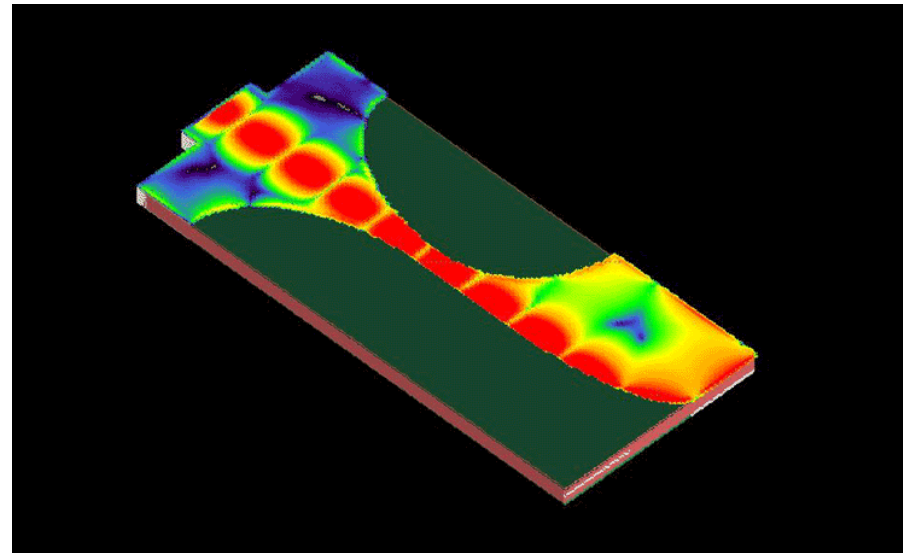
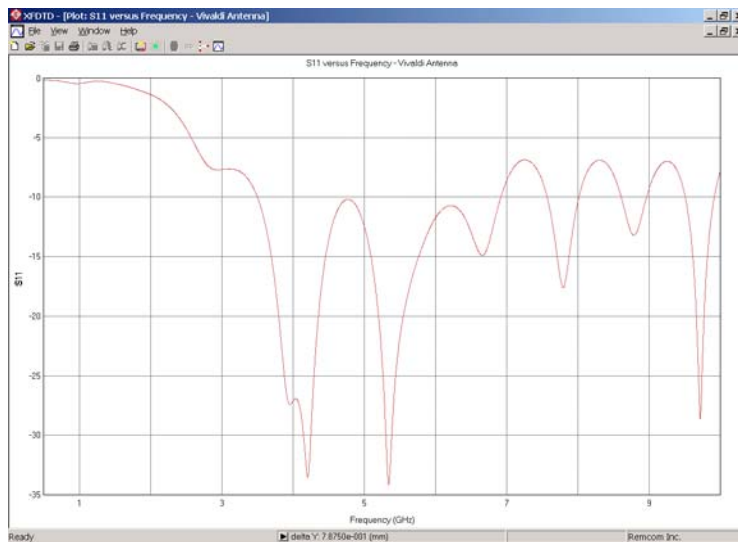
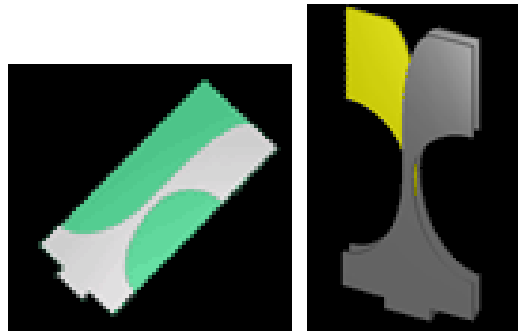
Applications

Optical Interference Due to Two PEC Spheres (Computed using LLNL Tsar-Lite)



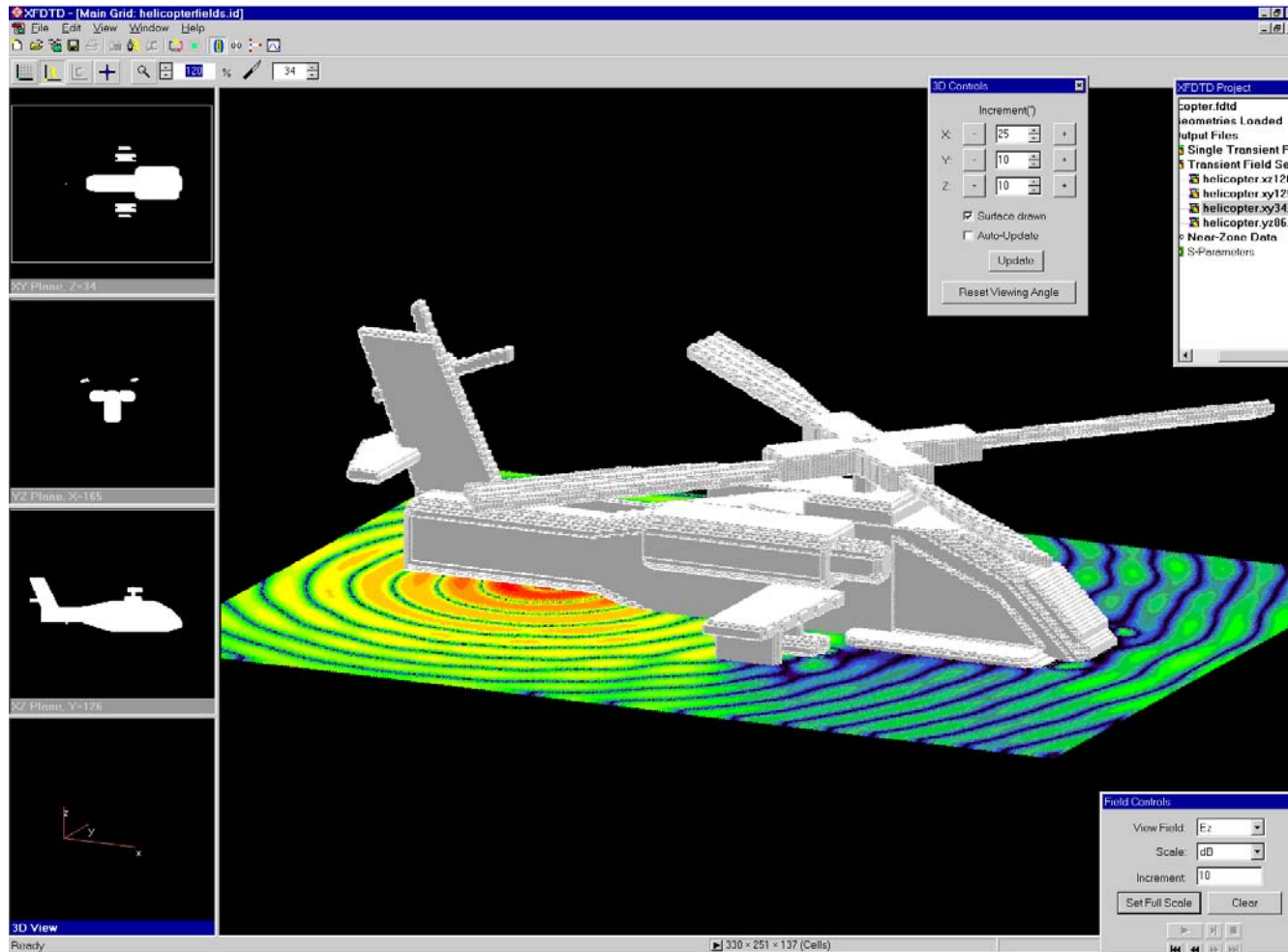
Balanced Antipodal Vivaldi Antenna (REMCOM X-FDTD)

Source: <http://www.remcom.com/html/cad-vivaldi.html>

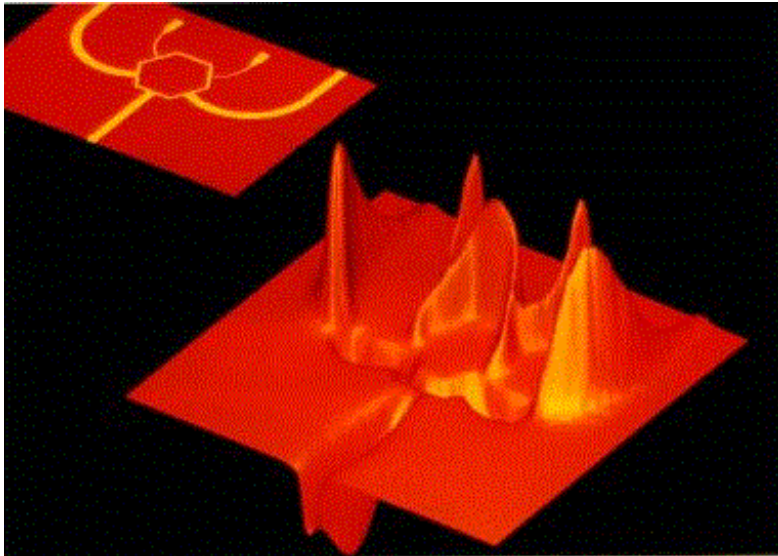


Electromagnetic Interaction with a Helicopter (REMCOM X-FDTD)

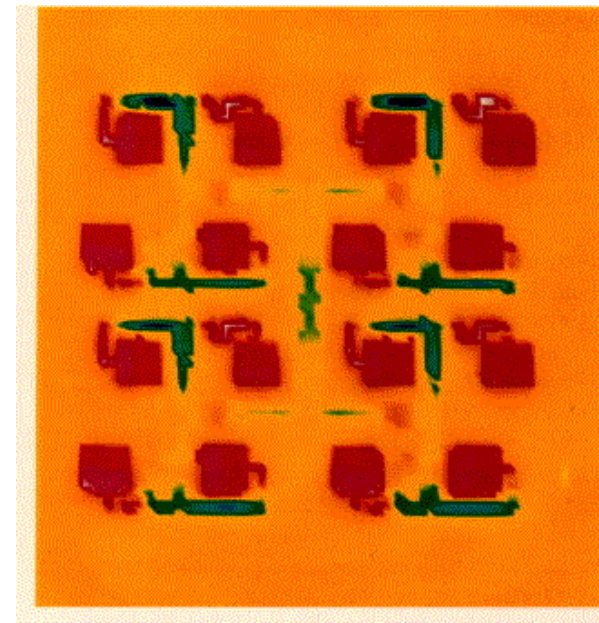
Source: <http://www.remcom.com/html/cad-helicopter.html>



Microwave Circuit Device Modeling
(Simulated Using UK/JPL PGY Simulator)



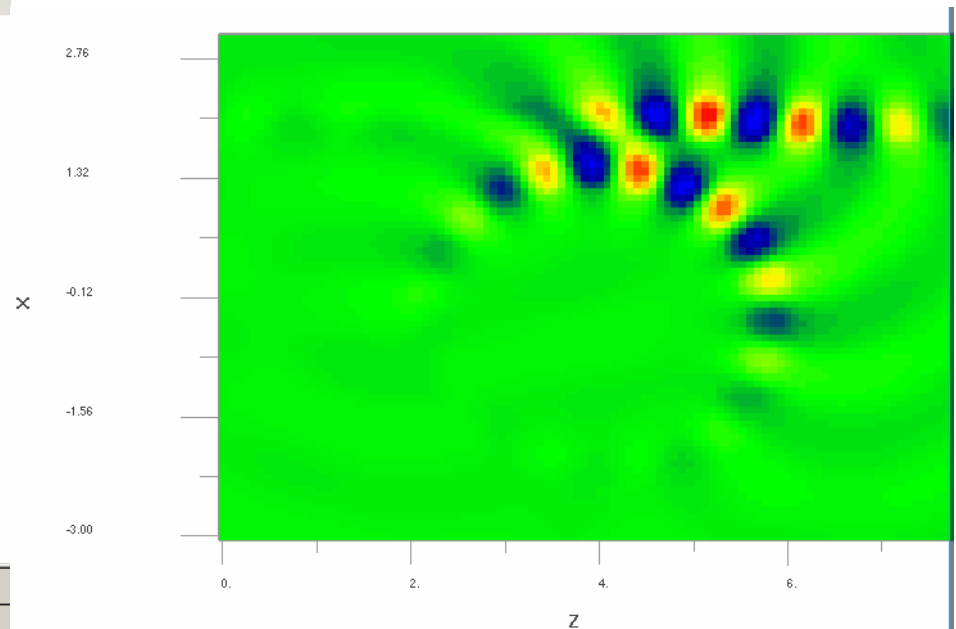
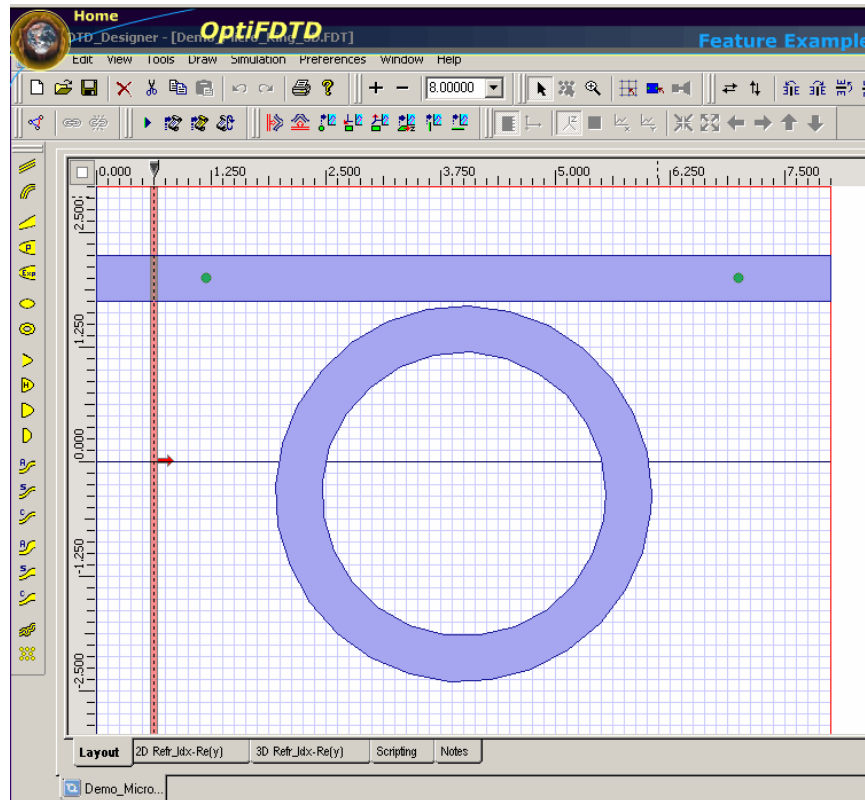
*Vertical Electric Field Beneath the Substrate of a
3 dB Gysel Power Divider*



*Vertical Electric Field Beneath the Substrate of a
16-Element Phased Array*

Micro-Ring Resonator (OptiFDTD)

Source: <http://www.optiwave.com>



1.1 One-Dimensional Scalar Wave Equation

$$\frac{\partial^2 f}{\partial t^2} = c^2 \frac{\partial^2 f}{\partial x^2}$$

- Assume an infinite homogeneous space
- The wave equation supports the general solutions

$$f(x, t) = F_1(x - ct) + F_2(x + ct)$$

- Represents superposition of forward and backward traveling waves

$$c = \frac{1}{\sqrt{\mu\epsilon}}$$

Taylor's series expansion of $f(x,t)$ about the point x to the point $x \pm \Delta x$ at a fixed time t

$$f(x + \Delta x, t) = f(x, t) + \frac{\partial f(x, t)}{\partial x} \Delta x + \frac{\partial^2 f(x, t)}{\partial x^2} \frac{\Delta x^2}{2} + \frac{\partial^3 f(x, t)}{\partial x^3} \frac{\Delta x^3}{6} + \frac{\partial^4 f(x, t)}{\partial x^4} \frac{\Delta x^4}{24} + \dots$$

$$f(x - \Delta x, t) = f(x, t) - \frac{\partial f(x, t)}{\partial x} \Delta x + \frac{\partial^2 f(x, t)}{\partial x^2} \frac{\Delta x^2}{2} - \frac{\partial^3 f(x, t)}{\partial x^3} \frac{\Delta x^3}{6} + \frac{\partial^4 f(x, t)}{\partial x^4} \frac{\Delta x^4}{24} + \dots$$

Adding these two expressions

$$f(x + \Delta x, t) + f(x - \Delta x, t) = 2f(x, t) + \frac{\partial^2 f(x, t)}{\partial x^2} \Delta x^2 + \frac{\partial^4 f(x, t)}{\partial x^4} \frac{\Delta x^4}{12} + \dots$$

$$\Rightarrow \frac{\partial^2 f(x,t)}{\partial x^2} = \left[\frac{f(x+\Delta x,t) - 2f(x,t) + f(x-\Delta x,t)}{(\Delta x)^2} \right] + O[(\Delta x)^2]$$

This expression is commonly referred to as the ***CENTRAL DIFFERENCE*** approximation of the second-order derivative. It is said to be second-order accurate since the error is of order $(\Delta x)^2$. Namely, the error decays as $(\Delta x)^2$ with decreasing values of Δx . It is noted that the error is also dependent on the *smoothness* of $f(x,t)$.

Similarly,

$$\frac{\partial^2 f(x,t)}{\partial t^2} = \left[\frac{f(x,t+\Delta t) - 2f(x,t) + f(x,t-\Delta t)}{(\Delta t)^2} \right] + O[(\Delta t)^2]$$

Combining to Form a Discrete Wave Equation

$$\left[\frac{f(x,t+\Delta t) - 2f(x,t) + f(x,t-\Delta t)}{(\Delta t)^2} \right] + O[(\Delta t)^2] = c^2 \left\{ \left[\frac{f(x+\Delta x,t) - 2f(x,t) + f(x-\Delta x,t)}{(\Delta x)^2} \right] + O[(\Delta x)^2] \right\}$$

DISCRETE SPACE

Let

$$\begin{aligned} x_i &= i\Delta x, \\ t_n &= n\Delta t, \quad \text{and} \\ f_i^n &= f(x_i, t_n) \end{aligned}$$

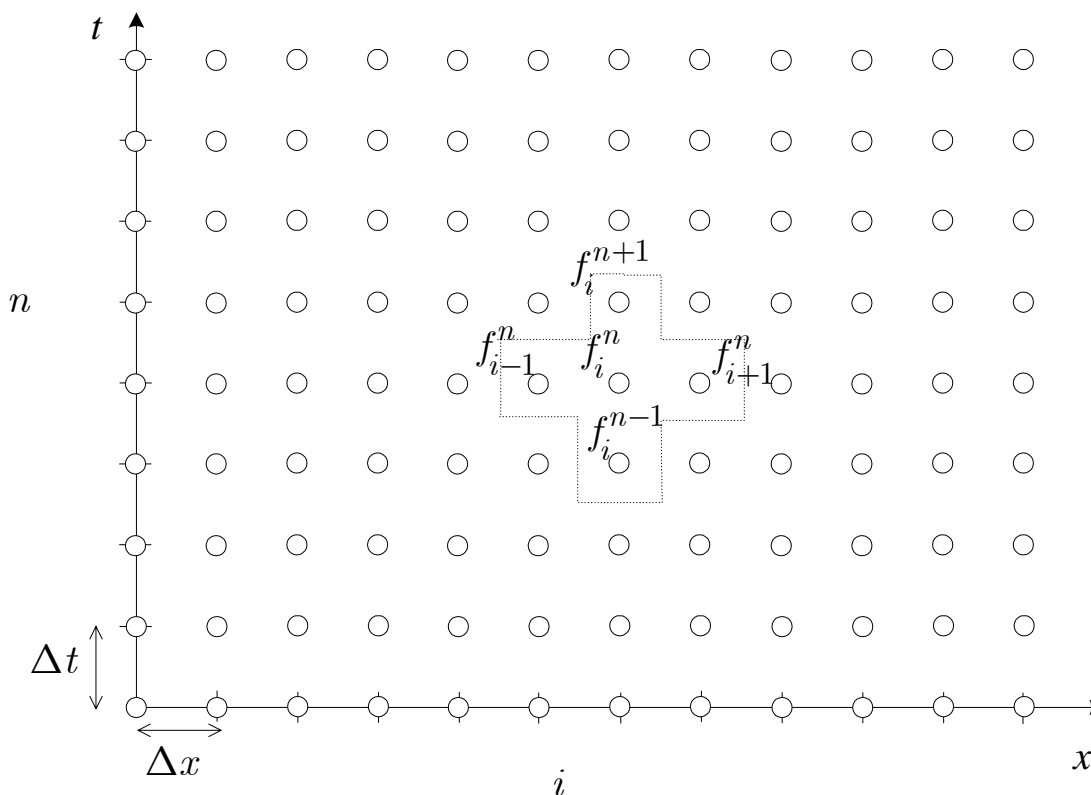
Discrete Wave Equation:

$$\left[\frac{f_i^{n+1} - 2f_i^n + f_i^{n-1}}{(\Delta t)^2} \right] + O[(\Delta t)^2] = c^2 \left\{ \left[\frac{f_{i+1}^n - 2f_i^n + f_{i-1}^n}{(\Delta x)^2} \right] + O[(\Delta x)^2] \right\}$$

Explicit Time-Marching Solution for f :

$$f_i^{n+1} = (c\Delta t)^2 \left[\frac{f_{i+1}^n - 2f_i^n + f_{i-1}^n}{(\Delta x)^2} \right] + 2f_i^n - f_i^{n-1} + O[(\Delta x)^2] + O[(\Delta t)^2]$$

1-D FDTD Stencil



- Given the Initial Conditions: f_i^{-1} , f_i^0
- Given the Boundary Conditions: f_0^n , $f_{N_x}^n$
- Solve for f_i^{n+1} , \forall_i

DISCRETIZATION

The **Stability and Accuracy** of the Explicit Solution will be Dependent on the values of Δx and Δt .

MAGIC TIME STEP:

$$\Delta x = c \Delta t.$$

Discrete Wave Equation Using the Magic Time Step:

$$\begin{aligned} f_i^{n+1} &= \left[f_{i+1}^n - 2f_i^n + f_{i-1}^n \right] + 2f_i^n - f_i^{n-1} \\ &= \left[f_{i+1}^n + f_{i-1}^n - f_i^{n-1} \right] \end{aligned}$$

Analysis:

Let

$$f_i^n = F_1(i\Delta x - cn\Delta t), \text{ and } g_i^n = G_2(i\Delta x + cn\Delta t)$$

and

$$\Delta t = \Delta x/c$$

$$f_i^{n+1} = F_1((i - n - 1)\Delta x) = f_{i-1}^n,$$

$$g_i^{n+1} = G_2((i + n + 1)\Delta x) = g_{i+1}^n!$$

This is the exact solution! In fact, for this choice of discretization parameters, the discrete solution is exact! This choice of Δt is referred to as the ***magic time step***. Unfortunately, we only have this luxury for one-dimensional problems with homogeneous material regions, however, in the following discussions, it will provide useful insight into understanding the discrete solution.

Dispersion for 1D Wave Equation

- **Dispersion:** Variation of the propagating velocity as a function of frequency.

Time-Harmonic Plane Wave Analysis

Let

$$f(x, t) = e^{j(\omega t - kx)}$$

From the wave equation ($\frac{\partial^2 f}{\partial t^2} = c^2 \frac{\partial^2 f}{\partial x^2}$)

$$-\omega^2 e^{j(\omega t - kx)} = -c^2 k^2 e^{j(\omega t - kx)}$$

or

$$k = \omega / c$$

$c = \text{phase velocity of the wave} = v_p$, where

$$v_p = \omega / k$$

Group velocity (velocity of energy transport):

$$v_g = \frac{\partial \omega}{\partial k} = 1 / \frac{\partial k}{\partial \omega} = c$$

Numerical Dispersion for 1D Wave Equation

- Discrete Space

$$f(x, t) = f_i^n = e^{j(\omega n \Delta t - \tilde{k} i \Delta x)}$$

Explicit Update Equation:

$$f_i^{n+1} = (c\Delta t)^2 \left[\frac{f_{i+1}^n - 2f_i^n + f_{i-1}^n}{\Delta x^2} \right] + 2f_i^n - f_i^{n-1}$$

Plugging the discrete form of $f(x, t)$ into the update expression:

$$e^{j(\omega(n+1)\Delta t - \tilde{k} i \Delta x)} = (c\Delta t)^2 \left[\frac{e^{j(\omega n \Delta t - \tilde{k}(i+1)\Delta x)} - 2e^{j(\omega n \Delta t - \tilde{k} i \Delta x)} + e^{j(\omega n \Delta t - \tilde{k}(i-1)\Delta x)}}{\Delta x^2} \right] + 2e^{j(\omega n \Delta t - \tilde{k} i \Delta x)} - e^{j(\omega(n-1)\Delta t - \tilde{k} i \Delta x)}$$

Factor out the term $e^{j(\omega n \Delta t - \tilde{k} i \Delta x)}$, and grouping terms, this reduces to:

$$\frac{e^{j\omega\Delta t} + e^{-j\omega\Delta t}}{2} = \frac{(c\Delta t)^2}{\Delta x^2} \left[\frac{e^{j\tilde{k}\Delta x} + e^{-j\tilde{k}\Delta x}}{2} - 1 \right] + 1$$

Dispersion Relationship of the Discrete Space:

$$\cos(\omega\Delta t) = \frac{(c\Delta t)^2}{\Delta x^2} [\cos(\tilde{k}\Delta x) - 1] + 1$$

Numerical Phase Velocity:

1. Assume: $\Delta t \rightarrow 0$, $\Delta x \rightarrow 0$. Dispersion Relationship becomes

$$1 - \frac{(\omega \Delta t)^2}{2} \cong \frac{(c \Delta t)^2}{\Delta x^2} \left[1 - \frac{(\tilde{k} \Delta x)^2}{2} - 1 \right] + 1$$

which reduces to:

$$\frac{(\omega \Delta t)^2}{2} \cong \frac{(c \Delta t)^2}{\Delta x^2} \frac{(\tilde{k} \Delta x)^2}{2} \Rightarrow \omega^2 = c^2 \tilde{k}^2 \Rightarrow \tilde{k} = \pm \frac{\omega}{c}$$

2. Magic Time Step: $c \Delta t = \Delta x$

$$\cos(\omega \Delta t) = 1 \cdot [\cos(\tilde{k} \Delta x) - 1] + 1 = \cos(\tilde{k} \Delta x)$$

$$\therefore \omega \Delta t = \pm \tilde{k} \Delta x \rightarrow \tilde{k} = \pm \omega / c$$

3. Numerical Dispersion:

$$\tilde{k} = \frac{1}{\Delta x} \cos^{-1} \left\{ \frac{\Delta x^2}{(c\Delta t)^2} [\cos(\omega\Delta t) - 1] + 1 \right\}$$

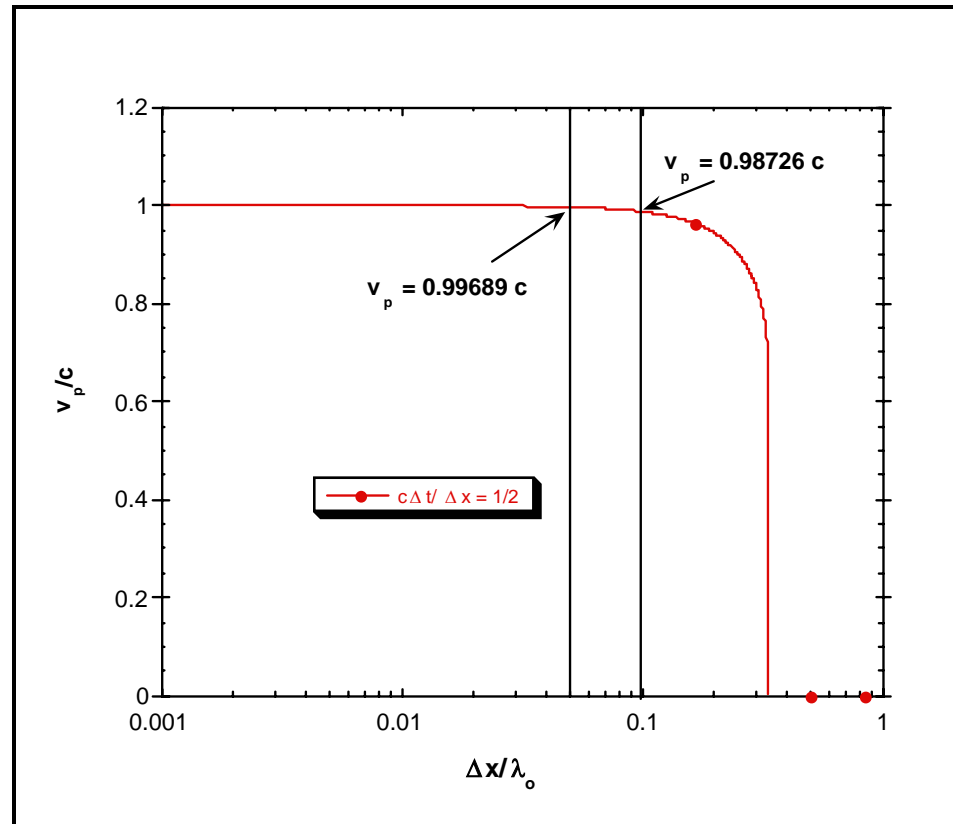
$$v_p = \omega / \tilde{k} = \frac{2\pi c}{\cos^{-1} \left\{ \frac{\Delta x^2}{(c\Delta t)^2} [\cos(\omega\Delta t) - 1] + 1 \right\}} \frac{\Delta x}{\lambda_o}$$

Example: $\Delta x = \lambda_o / 10$ and $c\Delta t = \Delta x / 2$. Then

$$\tilde{k} = \frac{1}{\Delta x} \cos^{-1} \left\{ 1 + 4 \left[\cos\left(\frac{2\pi\Delta x}{2\lambda_o}\right) - 1 \right] \right\} = \frac{0.63642}{\Delta x} = 6.3642 / \lambda_o$$

$$v_p = \omega / \tilde{k} = 0.9873c$$

Example: $c\Delta t = \Delta x / 2$



$$\frac{\text{Phase Error}}{\lambda} = \frac{(\tilde{k} - k)}{k} \cdot \frac{360^\circ}{\lambda} = \frac{\left(\frac{\omega}{v_p} - \frac{\omega}{c}\right)}{\frac{\omega}{c}} \cdot \frac{360^\circ}{\lambda} = \left(\frac{c}{v_p} - 1\right) \cdot \frac{360^\circ}{\lambda}$$

Calculate the Phase Error over 10 λ_o when $c\Delta t = \Delta x / 2$ and:

1. $\Delta x = 0.1 \lambda_o, v_p = 0.98726 c$

$$\text{Phase Error: } 10 [1/0.98726 - 1] 360^\circ = 46.45^\circ$$

2. $\Delta x = 0.05 \lambda_o, v_p = 0.99689 c$

$$\text{Phase Error: } 10[1/0.99689 - 1] 360^\circ = 11.23^\circ$$

Phase Error Reduces by a Factor of 4!

STABILITY

- Stability of the Formulation Implies that the Eigenvalues of the linear update expression are within the unit circle.

Starting with:

$$f_i^{n+1} = (c\Delta t)^2 \left[\frac{f_{i+1}^n - 2f_i^n + f_{i-1}^n}{\Delta x^2} \right] + 2f_i^n - f_i^{n-1}$$

Rewrite this as:

$$f^{n+1} = 2[A]f^n - f^{n-1}$$

where $[A]$ is a matrix. Stability requires that the energy is bounded. That is: $\frac{|f^{n+1}|^2}{|f^n|^2} \leq 1$.

To analyze the stability problem, we will analyze the eigenspectrum of the difference operator and determine the relationship of Δt and Δx that leads to bounded energy within the system.

STABILITY ANALYSIS

The difference operator is re-written in matrix format:

$$f_i^{n+1} = \frac{(c\Delta t)^2}{\Delta x^2} [f_{i+1}^n - 2f_i^n + f_{i-1}^n] + 2f_i^n - f_i^{n-1}$$

$$\Rightarrow f^{n+1} = 2[A]f^n - [I]f^{n-1} \quad (i)$$

where,

$$[A] = [I] - \frac{(c\Delta t)^2}{2\Delta x^2} [L],$$

$[I]$ is the Identity Matrix, and $[L]$ is a tridiagonal Matrix and is defined as:

$$[L]_{i-th \text{ row}} = [0, 0, \dots, 0, -1, 2, -1, 0, \dots, 0, 0]$$

$[L]$ is Positive Semi-Definite with eigenvalues $0 \leq \lambda \leq 4$.

Currently, our update operator is in the form of a 2^{nd} Order Difference Operator.

Reducing 1st Order Difference Eqn. to 2nd Order

To study stability, we will reduce the 2nd order difference equation into a 1st order expression. To this end, let

$$\mathbf{y}^{n+1} = \begin{bmatrix} f^{n+1} \\ f^n \end{bmatrix}, \quad \mathbf{y}^n = \begin{bmatrix} f^n \\ f^{n-1} \end{bmatrix}.$$

Then, (i) can be rewritten as a 1st order difference equation

$$\mathbf{y}^{n+1} = [\mathbf{M}] \mathbf{y}^n; \quad [\mathbf{M}] = \begin{bmatrix} 2[\mathbf{A}] & -[\mathbf{I}] \\ [\mathbf{I}] & 0 \end{bmatrix}$$

Each iteration of the difference operator is simply a matrix product. Therefore, given the initial condition \mathbf{y}^o , we can define:

$$\mathbf{y}^n = [\mathbf{M}]^n \mathbf{y}^o$$

Stability of the first-order equation thus requires

$$\lim_{n \rightarrow \infty} |[\mathbf{M}]^n| < K$$

where K is a constant that is finite. This will be satisfied if $\rho([\mathbf{M}]) \leq 1$, that is, if the eigenvalues of \mathbf{M} are within or on the unit circle in the complex plane.

Define (λ, \mathbf{x}_i) to be an eigensolution of $[A]$, or

$$[A]\mathbf{x} - \lambda\mathbf{x} = 0$$

and $([x, y]^T, \xi)$ to be an eigen solution of $[M]$:

$$[M] \begin{bmatrix} \mathbf{x} \\ \mathbf{y} \end{bmatrix} = \xi \begin{bmatrix} \mathbf{x} \\ \mathbf{y} \end{bmatrix}.$$

Assume the eigenvalues of $[A]$ are real and distinct, such that $[A]$ is diagonalizable. Then

$$[A] = [P][D][P]^{-1}$$

where $[P]$ is the matrix of eigenvectors of $[A]$ and $[D]$ is a diagonal matrix containing the eigenvalues of $[A]$. Subsequently,

$$\begin{bmatrix} [P] & 0 \\ 0 & [P] \end{bmatrix} \begin{bmatrix} 2[D] & -[I] \\ [I] & 0 \end{bmatrix} \begin{bmatrix} [P]^{-1} & 0 \\ 0 & [P]^{-1} \end{bmatrix} \begin{bmatrix} \mathbf{x} \\ \mathbf{y} \end{bmatrix} = \xi \begin{bmatrix} \mathbf{x} \\ \mathbf{y} \end{bmatrix}$$

Transforming

$$\begin{bmatrix} 2[D] & -[I] \\ [I] & 0 \end{bmatrix} \begin{bmatrix} \mathbf{x}' \\ \mathbf{y}' \end{bmatrix} = \xi \begin{bmatrix} \mathbf{x}' \\ \mathbf{y}' \end{bmatrix}, \text{ where } \begin{bmatrix} \mathbf{x}' \\ \mathbf{y}' \end{bmatrix} = \begin{bmatrix} [P]^{-1} & 0 \\ 0 & [P]^{-1} \end{bmatrix} \begin{bmatrix} \mathbf{x} \\ \mathbf{y} \end{bmatrix}$$

Stability Criterion of Explicit Method

This is then reduced to 2 x 2 matrices for each eigenvalue λ

$$\begin{bmatrix} 2\lambda & -1 \\ 1 & 0 \end{bmatrix} \begin{bmatrix} x' \\ y' \end{bmatrix} = \xi \begin{bmatrix} x' \\ y' \end{bmatrix}$$

The eigenvalues ξ can then be easily derived from the characteristic equation

$$\xi^2 - 2\lambda\xi + 1 = 0$$

which has solutions $\xi = \lambda \pm \sqrt{\lambda^2 - 1}$. Stability requires that $|\xi| \leq 1$, which is true if $|\lambda| < 1$, or, if $\rho([A]) \leq 1$.

The spectral radius of $[A]$ is determined from the generalized eigenvalue equation

$$[A]x - \lambda x = 0$$

or

$$\left\{ [I] - \frac{(c\Delta t)^2}{2\Delta x^2} [L] \right\} x - \lambda [I]x = 0$$

This can be rewritten as:

$$[L]x = (1 - \lambda) \frac{2\Delta x^2}{(c_o \Delta t)^2} [I]x$$

or

$$[L]x = \kappa [I]x$$

Therefore,

$$\kappa = (1 - \lambda) \frac{2\Delta x^2}{(c_o \Delta t)^2} \Rightarrow \lambda = 1 - \kappa \frac{(c_o \Delta t)^2}{2\Delta x^2}$$

Stability requires $|\lambda| \leq 1$. Also, κ is the eigenvalues of $[L]$, and by definition: $0 < \kappa \leq 4$

Therefore, stability requires:

$$\kappa \frac{(c_o \Delta t)^2}{2\Delta x^2} \leq 2$$

or,

$$\frac{\kappa}{4} \leq \frac{\Delta x^2}{(c_o \Delta t)^2}$$

This inequality must satisfy all eigenvalues κ . Consequently, choosing the largest value $\kappa = 4$, leads to:

$$1 \leq \frac{\Delta x^2}{(c_o \Delta t)^2} \Rightarrow c_o \Delta t \leq \Delta x$$

Thus, for stability, we must have that:

1. The eigenvalues of A are real and distinct (inherently true)
2. The space and time steps satisfy the *Courant Stability Limit*:

$$\Delta t \leq \frac{\Delta x}{c}$$

If this inequality is not satisfied, the energy in the system will grow unboundedly.

An Implicit 1-Dimensional Formulation with Unconditional Stability

$$\frac{\partial^2 f}{\partial t^2} = c^2 \frac{\partial^2 f}{\partial x^2}$$

Using the *Newmark-Beta* Time-Integration Scheme, we can approximate the wave equation in the discrete space as

$$\begin{aligned} \frac{\Delta x^2}{(c_o \Delta t)^2} (f_i^{n+1} - 2f_i^n + f_i^{n-1}) = & \beta (f_{i+1}^{n+1} - 2f_i^{n+1} + f_{i-1}^{n+1}) \\ & + (1 - 2\beta) (f_{i+1}^n - 2f_i^n + f_{i-1}^n) \\ & + \beta (f_{i+1}^{n-1} - 2f_i^{n-1} + f_{i-1}^{n-1}) \end{aligned}$$

$$\Rightarrow [A]f^{n+1} = 2[B]f^n - [C]f^{n-1}$$

or

$$f^{n+1} = 2[A]^{-1}[B]f^n - [A]^{-1}[C]f^{n-1}$$

where,

$$[A] = [C] = \beta[L] + \frac{\Delta x^2}{(c_o \Delta t)^2} [I], \quad [B] = \frac{2\beta-1}{2}[L] + \frac{\Delta x^2}{(c_o \Delta t)^2} [I]$$

$[I]$ is the Identity Matrix, and $[L]$ is a tridiagonal Matrix and is defined as:

$$[L]_{i-th\ row} = [0, 0, \dots, 0, -1, 2, -1, 0, \dots, 0, 0]$$

$[L]$ is Positive Semi-Definite with eigenvalues $0 \leq \lambda \leq 4$.

With $[A] = [C]$, the implicit update expression is

$$f^{n+1} = 2[A]^{-1}[B]f^n - f^{n-1} \quad (i)$$

This scheme is implicit since it requires the inversion of A . For the one-dimensional problem, A is tri-diagonal, and can be factorized in $O(N)$ operations.

Question: What is the range of stability for this implicit operator as a function of β , $c\Delta t$, and Δx ?

Reducing 1st Order Difference Eqn. to 2nd Order

Again, reduce the 2nd order difference equation into a 1st order expression by letting:

$$y^{n+1} = \begin{bmatrix} f^{n+1} \\ f^n \end{bmatrix}, \quad y^n = \begin{bmatrix} f^n \\ f^{n-1} \end{bmatrix}.$$

Then, (i) can be rewritten as a 1st order difference equation

$$y^{n+1} = [M]y^n; \quad [M] = \begin{bmatrix} 2[A]^{-1}[B] & -[I] \\ [I] & 0 \end{bmatrix}$$

Stability of the first-order equation requires

$$\lim_{n \rightarrow \infty} |[M]^n| < K$$

where K is a constant that is finite. This will be satisfied if $\rho([M]) \leq 1$.

Define (λ, \mathbf{x}_l) to be an eigensolution of $[A]^{-1}[B]$, or
 $[B]x - \lambda[A]x = 0$

The eigenspectrum of $[M]$ is found from

$$[M] \begin{bmatrix} \mathbf{x} \\ \mathbf{y} \end{bmatrix} = \xi \begin{bmatrix} \mathbf{x} \\ \mathbf{y} \end{bmatrix}.$$

Assume that the eigenvalues of $[A]^{-1}[B]$ are real and distinct. Then, it is diagonalizable:

$$[A]^{-1}[B] = [P][D][P]^{-1}$$

$[D]$ is a diagonal matrix containing the eigenvalues of $[A]^{-1}[B]$. Subsequently,

$$\begin{bmatrix} [P] & 0 \\ 0 & [P] \end{bmatrix} \begin{bmatrix} 2[D] & -[I] \\ [I] & 0 \end{bmatrix} \begin{bmatrix} [P]^{-1} & 0 \\ 0 & [P]^{-1} \end{bmatrix} \begin{bmatrix} \mathbf{x} \\ \mathbf{y} \end{bmatrix} = \xi \begin{bmatrix} \mathbf{x} \\ \mathbf{y} \end{bmatrix}$$

Let:

$$\begin{bmatrix} \mathbf{x}' \\ \mathbf{y}' \end{bmatrix} = \begin{bmatrix} [P]^{-1} & 0 \\ 0 & [P]^{-1} \end{bmatrix} \begin{bmatrix} \mathbf{x} \\ \mathbf{y} \end{bmatrix}$$

Leads to:

$$\begin{bmatrix} 2[D] & -[I] \\ [I] & 0 \end{bmatrix} \begin{bmatrix} \mathbf{x}' \\ \mathbf{y}' \end{bmatrix} = \xi \begin{bmatrix} \mathbf{x}' \\ \mathbf{y}' \end{bmatrix}$$

Stability Criterion of Explicit Method

This is then reduced to 2×2 matrices for each eigenvalue λ

$$\begin{bmatrix} 2\lambda & -1 \\ 1 & 0 \end{bmatrix} \begin{bmatrix} x' \\ y' \end{bmatrix} = \xi \begin{bmatrix} x' \\ y' \end{bmatrix}$$

The eigenvalues ξ can then be easily derived from the characteristic equation

$$\xi^2 - 2\lambda\xi + 1 = 0$$

which has solutions $\xi = \lambda \pm \sqrt{\lambda^2 - 1}$. Stability requires that $|\xi| \leq 1$, which is true if $|\lambda| < 1$, or, if $\rho([A]^{-1}[B]) \leq 1$.

The spectral radius of $[A]^{-1}[B]$ is determined from the generalized eigenvalue equation

$$[B]x - \lambda[A]x = 0$$

or

$$\left\{ \frac{2\beta-1}{2}[L] + \frac{\Delta x^2}{(c_o \Delta t)^2}[I] \right\} x - \lambda \left\{ \beta[L] + \frac{\Delta x^2}{(c_o \Delta t)^2}[I] \right\} = 0$$

$$[L]x = \frac{\lambda - 1}{\frac{2\beta-1}{2} - \lambda\beta} \frac{\Delta x^2}{(c_o \Delta t)^2} [I]x$$

or

$$[L]x = \kappa[I]x$$

However, by definition, $0 < \kappa \leq 4$. Finally, solving for λ ,

$$\lambda = \frac{\frac{\Delta x^2}{(c \Delta t)^2} - \kappa \left(\frac{1-2\beta}{2} \right)}{\frac{\Delta x^2}{(c \Delta t)^2} + \kappa \beta}$$

Regions of Stability

Stability requires $|\lambda| \leq 1$

1. $\beta = 0$ (Central Difference Approximation)

$$\lambda = \frac{\frac{\Delta x^2}{(c\Delta t)^2} - \left(\frac{\kappa}{2}\right)}{\frac{\Delta x^2}{(c\Delta t)^2}} = 1 - \left(\frac{\kappa}{2}\right) \frac{(c\Delta t)^2}{\Delta x^2}$$

$$\text{For } |\lambda| \leq 1; \quad \left(\frac{\kappa}{2}\right) \frac{(c\Delta t)^2}{\Delta x^2} \leq 2$$

$$\because \kappa_{\max} = 4, \rightarrow \frac{(c\Delta t)^2}{\Delta x^2} \leq 1, \quad \text{or} \quad \Delta t \leq \frac{\Delta x}{c}$$

2. $\beta > 0$.

$$\lambda = \frac{1 - \kappa \left(\frac{1-2\beta}{2} \right) \frac{(c\Delta t)^2}{\Delta x^2}}{1 + \kappa \beta \frac{(c\Delta t)^2}{\Delta x^2}}$$

If $|\lambda| \leq 1$, $0 \leq \kappa \leq 4$ and $\forall_{\Delta t > 0}$ then we can write this as:

$$\lambda = \frac{1 - \left(\frac{1-2\beta}{2} \right) \alpha}{1 + \beta \cdot \alpha}$$

where $\alpha = \kappa \frac{(c\Delta t)^2}{\Delta x^2}$ For this to have a magnitude greater than one for $0 \leq \alpha \leq \infty$

$$\left(\frac{1-2\beta}{2} \right) \leq \beta, \text{ or}$$

$$\boxed{\beta \geq \frac{1}{4}}$$

In this instance, the formulation is unconditionally stable! Namely, $|\lambda| \leq 1$ for all time steps.

Question: What are practical values for β and Δt ?

- $\beta = 1/4$ - the Newmark scheme is equivalent to 2nd order trapezoidal integration rule. This is the most accurate.

$$\begin{aligned} \frac{\Delta x^2}{(c_o \Delta t)^2} (f_i^{n+1} - 2f_i^n + f_i^{n-1}) &= \frac{1}{4} (f_{i+1}^{n+1} - 2f_i^{n+1} + f_{i-1}^{n+1}) \\ &\quad + \frac{1}{2} (f_{i+1}^n - 2f_i^n + f_{i-1}^n) \\ &\quad + \frac{1}{4} (f_{i+1}^{n-1} - 2f_i^{n-1} + f_{i-1}^{n-1}) \end{aligned}$$

- $\beta = 1/2$ - the Newmark scheme is equivalent to a 1st order Simpson integration rule:

$$\begin{aligned} \frac{\Delta x^2}{(c_o \Delta t)^2} (f_i^{n+1} - 2f_i^n + f_i^{n-1}) &= \frac{1}{2} (f_{i+1}^{n+1} - 2f_i^{n+1} + f_{i-1}^{n+1}) \\ &\quad + \frac{1}{2} (f_{i+1}^{n-1} - 2f_i^{n-1} + f_{i-1}^{n-1}) \end{aligned}$$

- Typically, you should choose $\beta = 1/4$ for 2nd order accuracy.
- Next, Δt must still be small enough to minimize dispersion error, and to maintain the proper sampling rate.
- A good choice is $\Delta t \leq \lambda_o/20/c$, where, λ_o is the wavelength, of the highest frequency within the Fourier spectrum of the propagating signal.

Transmission-Line Equations

$$\frac{\partial V(x,t)}{\partial x} = -RI(x,t) - L \frac{\partial I(x,t)}{\partial t},$$

$$\frac{\partial I(x,t)}{\partial x} = -GV(x,t) - C \frac{\partial V(x,t)}{\partial t}.$$

C – Capacitance per unit length

L – Inductance per unit length

R – Resistance per unit length

G – Conductance per unit length

Scalar Wave Equations – Transmission Line

$$\frac{\partial^2 V(x,t)}{\partial x^2} = LC \frac{\partial^2 V(x,t)}{\partial t^2} + (RC + GL) \frac{\partial V(x,t)}{\partial t} + RGV(x,t)$$

$$\frac{\partial^2 I(x,t)}{\partial x^2} = LC \frac{\partial^2 I(x,t)}{\partial t^2} + (RC + GL) \frac{\partial I(x,t)}{\partial t} + RGI(x,t)$$

Lossless Transmission Lines ($R = G = 0$)

Lossless Transmission Line Equations:

$$\frac{\partial V(x,t)}{\partial x} = -L \frac{\partial I(x,t)}{\partial t}, \quad \frac{\partial I(x,t)}{\partial x} = -C \frac{\partial V(x,t)}{\partial t}.$$

Taylor's series expansion function $f(x,t)$

$$\begin{aligned} f(x + \Delta x/2, t) = & f(x, t) + \frac{\partial f(x, t)}{\partial x} \frac{\Delta x}{2} \frac{1}{1!} + \frac{\partial^2 f(x, t)}{\partial x^2} \left(\frac{\Delta x}{2} \right)^2 \frac{1}{2!} \\ & + \frac{\partial^3 f(x, t)}{\partial x^3} \left(\frac{\Delta x}{2} \right)^3 \frac{1}{3!} + \frac{\partial^4 f(x, t)}{\partial x^4} \left(\frac{\Delta x}{2} \right)^4 \frac{1}{4!} + \dots \end{aligned}$$

Similarly,

$$\begin{aligned} f(x - \Delta x/2, t) = & f(x, t) - \frac{\partial f(x, t)}{\partial x} \frac{\Delta x}{2} + \frac{\partial^2 f(x, t)}{\partial x^2} \left(\frac{\Delta x}{2} \right)^2 \frac{1}{2!} \\ & - \frac{\partial^3 f(x, t)}{\partial x^3} \left(\frac{\Delta x}{2} \right)^3 \frac{1}{3!} + \frac{\partial^4 f(x, t)}{\partial x^4} \left(\frac{\Delta x}{2} \right)^4 \frac{1}{4!} + \dots \end{aligned}$$

Subtracting

$$f(x + \Delta x/2, t) - f(x - \Delta x/2, t) = \frac{\partial f(x, t)}{\partial x} \Delta x + \frac{1}{24} \frac{\partial^3 f(x, t)}{\partial x^3} (\Delta x)^3 + \dots$$

$$\frac{\partial f(x, t)}{\partial x} = \left[\frac{f(x + \Delta x/2, t) - f(x - \Delta x/2, t)}{\Delta x} \right] + O[(\Delta x)^2]$$

$$\frac{\partial f(x, t)}{\partial t} = \left[\frac{f(x, t + \Delta t/2) - f(x, t - \Delta t/2)}{\Delta t} \right] + O[(\Delta t)^2]$$

Note that second-order accuracy is obtained at (x,t) by differencing two discrete points centered by (x,t). Hence, this is called a central difference approximation.

Discrete Transmission Line Equations:

$$\frac{I_{i+1/2}^n - I_{i-1/2}^n}{\Delta x} = -C \frac{\partial V_i^n}{\partial t}$$

Second-order accurate iff V is evaluated at x_i and I is evaluated at $x_i \pm \Delta x / 2$.

$$\frac{I_{i+1/2}^n - I_{i-1/2}^n}{\Delta x} = -C \frac{V_i^{n+1/2} - V_i^{n-1/2}}{\Delta t}.$$

Second-order accurate iff I is evaluated at t_n and V is evaluated at $t_n \pm \Delta t / 2$.

Observing the equation, we can write a recursive relationship to compute $V_i^{n+1/2}$ given the previous values of V and I :

$$V_i^{n+1/2} = V_i^{n-1/2} - \frac{\Delta t}{C} \frac{I_{i+1/2}^n - I_{i-1/2}^n}{\Delta x}$$

FULLY EXPLICIT TIME-MARCHING SOLUTION OF THE DISCRETE LOSSLESS TRANSMISSION LINE EQUATIONS

$$V_i^{n+1/2} = V_i^{n-1/2} - \frac{\Delta t}{C} \frac{I_{i+1/2}^n - I_{i-1/2}^n}{\Delta x}$$

$$I_{i+1/2}^{n+1} = I_{i+1/2}^n - \frac{\Delta t}{L} \frac{V_{i+1}^{n+1/2} - V_i^{n+1/2}}{\Delta x}$$

- Explicit update expression based on 1D coupled eqns
- V and I are staggered in both space and time.
- Given the initial condition of V and I along the entire line length, V and I can be time advanced
- We still need to guarantee stability and understand the error properties

STABILITY OF 1D TX-LINE EQUATIONS

$$I_{i+1/2}^{n+1} = I_{i+1/2}^n - \frac{\Delta t}{L} \frac{V_{i+1}^{n+1/2} - V_i^{n+1/2}}{\Delta x}, \quad V_i^{n+1/2} = V_i^{n-1/2} - \frac{\Delta t}{C} \frac{I_{i+1/2}^n - I_{i-1/2}^n}{\Delta x}$$

Plug in the expressions for V into the first equation:

$$I_{i+1/2}^{n+1} = I_{i+1/2}^n - \frac{\Delta t}{L} \frac{V_{i+1}^{n-1/2} - \frac{\Delta t}{C} \frac{I_{i+3/2}^n - I_{i+1/2}^n}{\Delta x} - V_i^{n-1/2} + \frac{\Delta t}{C} \frac{I_{i+1/2}^n - I_{i-1/2}^n}{\Delta x}}{\Delta x}$$

Noting that:

$$V_{i+1}^{n-1/2} - V_i^{n-1/2} = -\frac{L\Delta x}{\Delta t} [I_{i+1/2}^n - I_{i-1/2}^n]$$

$$I_{i+1/2}^{n+1} = 2I_{i+1/2}^n - I_{i-1/2}^n - \frac{(c\Delta t)^2}{\Delta x^2} [I_{i+3/2}^n - 2I_{i+1/2}^n + I_{i-1/2}^n]$$

This can again be repeated for V :

$$V_i^{n+1/2} = 2V_i^{n-1/2} - V_i^{n-3/2} - \frac{(c\Delta t)^2}{\Delta x^2} [V_{i+1}^{n-1/2} - 2V_i^{n-1/2} + V_{i-1}^{n-1/2}]$$

These equations are identical to those derived via the 2nd-order wave equation using central difference approximations! (with the exception of a shifted time or space index.)

Stability and Dispersion:

- Same as One-Dim. Scalar Wave Equation
- Stability of the coupled 1D difference operators satisfies the Courant limit:

$$\Delta t \leq \frac{\Delta x}{c}, \text{ where } c = \frac{1}{\sqrt{LC}} \text{ is the wave speed.}$$

Example 1.

Assume a uniform transmission-line with $C = 100.0$ pf/m, and $L = 250.0$ nH/m ($Z = 50 \Omega$, and $c = 2 \times 10^8$ m/s). The transmission-line has a length of 1 m, and is terminated by a short circuit at each end. The spatial discretization Δx is 0.1 m.

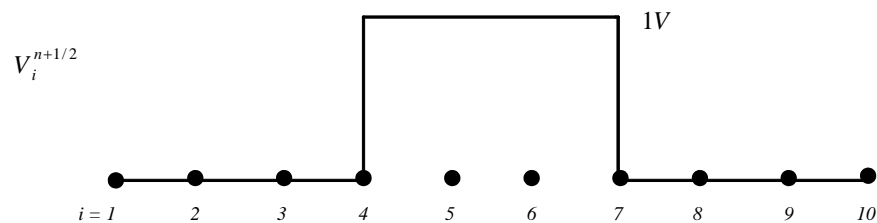
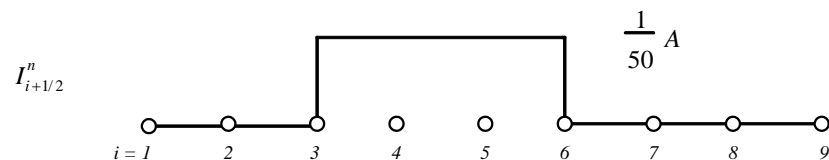
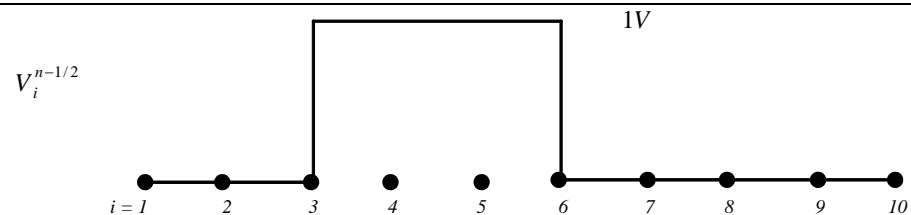
! Initial condition, a rectangular pulse with amplitude of 1 V –

Given $V_i^{n-1/2}$ and $I_{i+1/2}^n$. Find $V_i^{n+1/2}$ if $\Delta t = \frac{\Delta x}{c}$.

Solution:

$$\text{At } \Delta t = \frac{\Delta x}{c} = \sqrt{LC} \Delta x$$

$$V_i^{n+1/2} = V_i^{n-1/2} - \sqrt{\frac{L}{C}} [I_{i+1/2}^n - I_{i-1/2}^n], \quad I_{i+1/2}^{n+1} = I_{i+1/2}^n - \sqrt{\frac{C}{L}} (V_{i+1}^{n+1/2} - V_i^{n+1/2})$$



where, $V_i^{n+1/2} = V_i^{n-1/2} - 50(I_{i+1/2}^n - I_{i-1/2}^n)$

Substituting $I_{i+1/2}^{n+1}$ and $I_{i-1/2}^{n+1}$, leads to: $V_i^{n+1/2} = V_{i+1}^{n-1/2} + V_{i-1}^{n-1/2} - V_i^{n-3/2}$

Lossy Transmission Lines

Transmission Line Equations:

$$\frac{\partial I(x,t)}{\partial x} = -GV(x,t) - C \frac{\partial V(x,t)}{\partial t}$$

$$\frac{\partial V(x,t)}{\partial x} = -RI(x,t) - L \frac{\partial I(x,t)}{\partial t}$$

Discrete Transmission Line Equations:

$$\frac{I_{i+1/2}^n - I_{i-1/2}^n}{\Delta x} = -GV_i^n - C \frac{V_i^{n+1/2} - V_i^{n-1/2}}{\Delta t}$$

$$\frac{V_{i+1}^{n+1/2} - V_i^{n+1/2}}{\Delta x} = -RI_{i+1/2}^{n+1/2} - L \frac{I_{i+1/2}^{n+1} - I_{i+1/2}^n}{\Delta t}$$

Averaging Loss Terms in Time for 2nd Order Accuracy

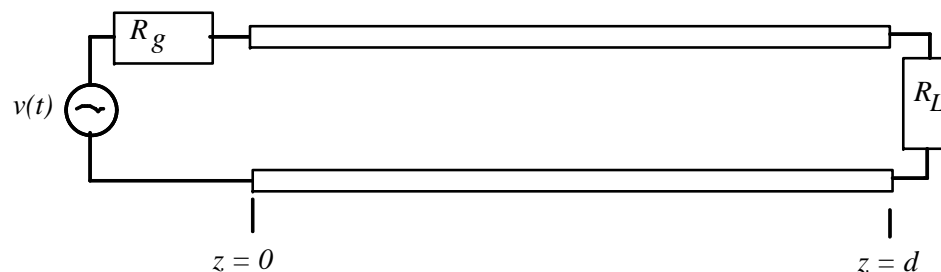
$$\frac{I_{i+1/2}^n - I_{i-1/2}^n}{\Delta x} = -G \frac{V_i^{n+1/2} + V_i^{n-1/2}}{2} - C \frac{V_i^{n+1/2} - V_i^{n-1/2}}{\Delta t}$$

$$\frac{V_{i+1}^{n+1/2} - V_i^{n+1/2}}{\Delta x} = -R \frac{I_{i+1/2}^{n+1} + I_{i+1/2}^n}{2} - L \frac{I_{i+1/2}^{n+1} - I_{i+1/2}^n}{\Delta t}$$

$$V_i^{n+1/2} = \left[\frac{\frac{C}{\Delta t} - \frac{G}{2}}{\frac{C}{\Delta t} + \frac{G}{2}} \right] V_i^{n-1/2} - \left[\frac{1}{\frac{C}{\Delta t} + \frac{G}{2}} \right] \frac{I_{i+1/2}^n - I_{i-1/2}^n}{\Delta x}$$

$$I_{i+1/2}^{n+1} = \left[\frac{\frac{L}{\Delta t} - \frac{R}{2}}{\frac{L}{\Delta t} + \frac{R}{2}} \right] I_{i+1/2}^n - \left[\frac{1}{\frac{L}{\Delta t} + \frac{R}{2}} \right] \frac{V_i^{n+1/2} - V_i^{n-1/2}}{\Delta x}$$

Boundary Conditions: Loads and Sources



Constraints must be introduced to properly terminate the mesh since V^n cannot be updated at the terminating load

$$V_i^{n+1/2} = V_i^{n-1/2} - \frac{\Delta t}{C} \frac{I_i^n - I_{i-1}^n}{\Delta x}$$

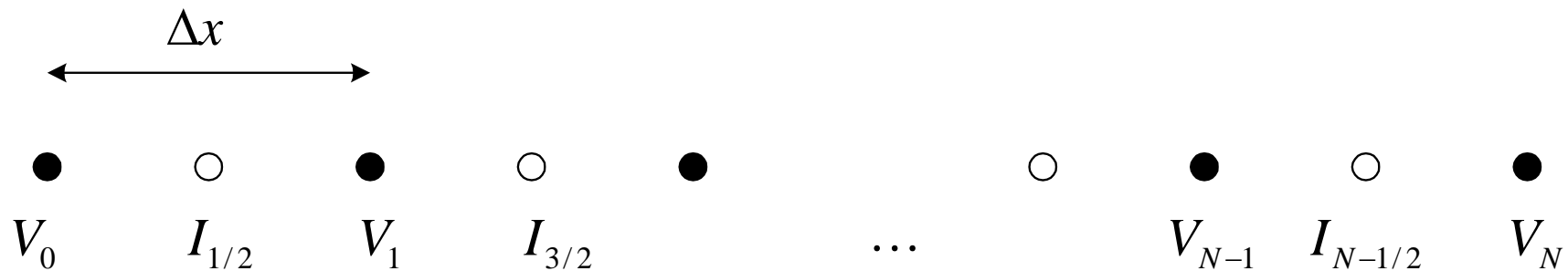
and

$$I_i^{n+1} = I_i^n - \frac{\Delta t}{L} \frac{V_{i+1}^{n+1/2} - V_i^{n+1/2}}{\Delta x}$$

.

To update V_1 or V_N we need to have $I_{-1/2}$ and $I_{N+1/2}$. Unfortunately, neither of these quantities are in our solution space. As a result, an additional constraint must be introduced in order to update the voltages at the endpoints of the grid.

Such constraints must preserve stability and accuracy in the solution.



Short and Open Circuit Loads

1. $R_L = 0$ and $R_g = 0$

$$V_1^{n+1/2} = v(n\Delta t), \quad V_N^{n+1/2} = 0; \quad \forall_n$$

2 $R_g = 0$, and $R_L = \infty$?

$$V_1^{n+1/2} = v(n\Delta t), \quad I_{N-1}^{n+1} = 0; \quad \forall_n$$

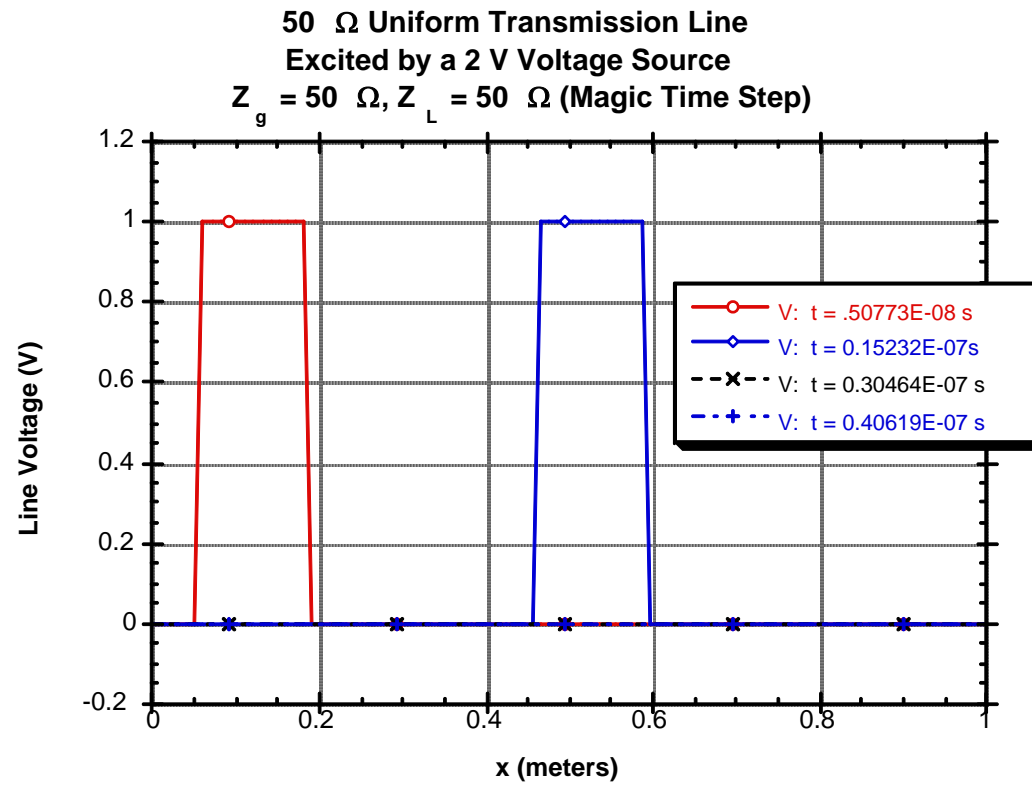
[Note: $\Delta x = L / (N - 1.5)$]

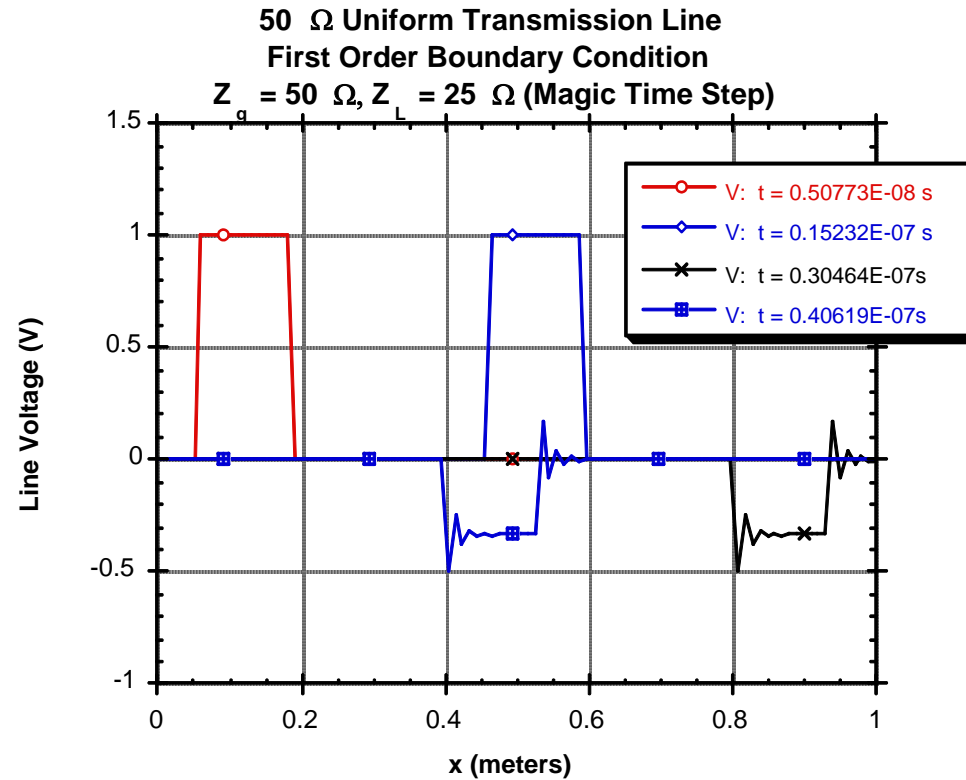
Arbitrary Loads

Poor First-Order Approximation:

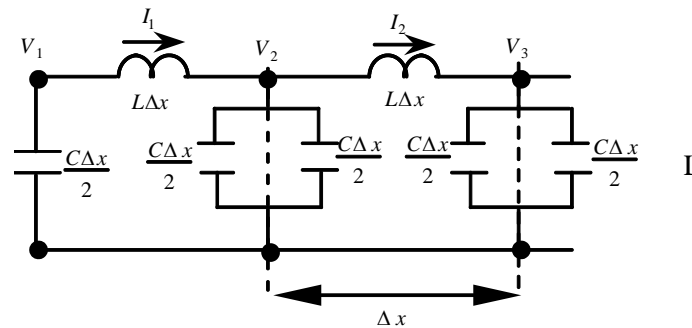
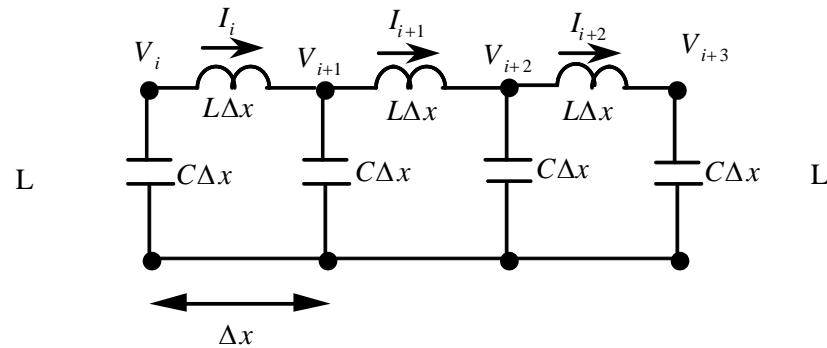
$$V_N^{n+1/2} = I_{N-1}^n R_L \quad (R_L \leq Z_o)$$

- $\Delta t/2$ displacement in time and $\Delta x/2$ displacement in space
- *Unconditionally Unstable* if $R_L > Z_o$ ($\because I_{N-1}^{n+1} = V_{N-1}^{n+1/2} / R_L$)





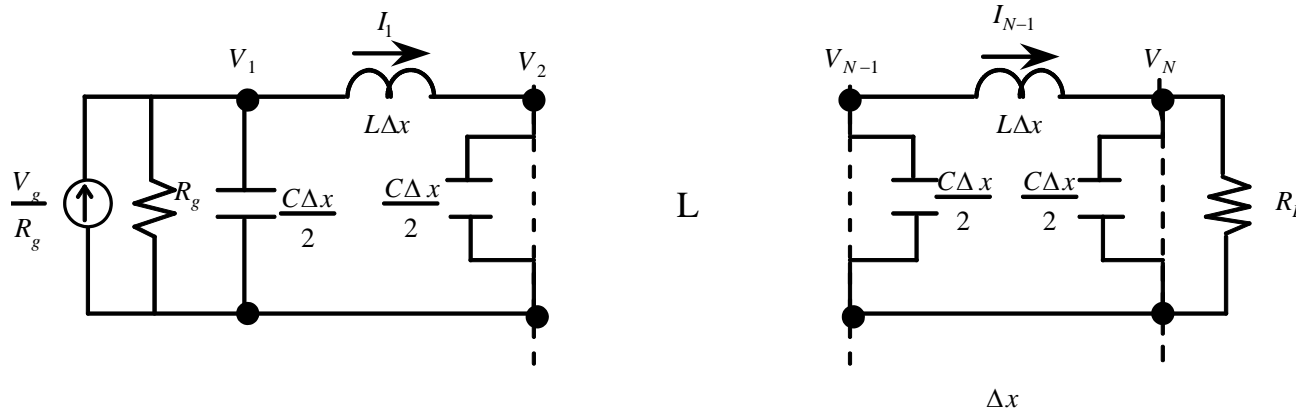
Equivalent Distributed Circuit Model of a Uniform Transmission Line



At the source end, we need to account for the affects of the discrete current source.

$$\frac{\partial I(x,t)}{\partial x} = -GV(x,t) - C \frac{\partial V(x,t)}{\partial t} - I_s(x,t)$$

Second-Order Accurate Source and Load Models for the Finite-Length Transmission Line



Applying KCL at Node 1:

$$\frac{V_g^n}{R_g} = I_1^n + C \frac{\Delta x}{2} \frac{\partial V_1^n}{\partial t} + \frac{V_1^n}{R_g}$$

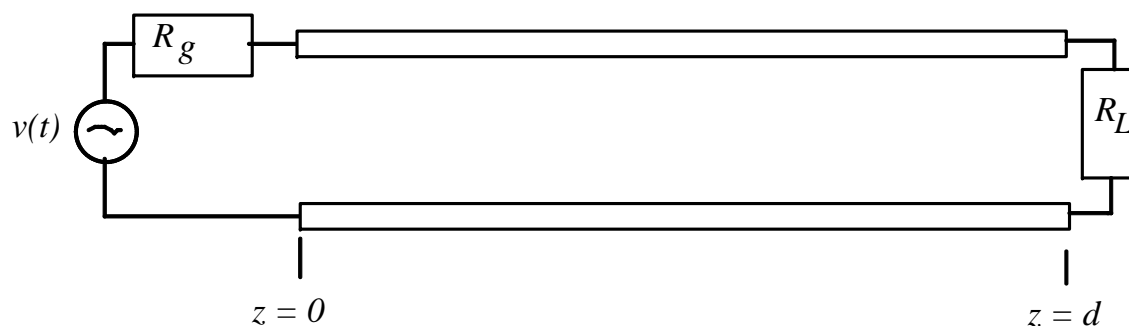
$$\frac{V_g^{n+1/2} + V_g^{n-1/2}}{2R_g\Delta x} = \frac{I_1^n}{\Delta x} + C \frac{V_i^{n+1/2} - V_i^{n-1/2}}{2\Delta t} + \frac{1}{R_g\Delta x} \frac{V_i^{n+1/2} + V_i^{n-1/2}}{2}$$

Finally,

$$V_1^{n+1/2} = \left[\frac{R_g \frac{C\Delta x}{2\Delta t} - \frac{1}{2}}{R_g \frac{C\Delta x}{2\Delta t} + \frac{1}{2}} \right] V_1^{n-1/2} - \left[\frac{1}{R_g \frac{C\Delta x}{2\Delta t} + \frac{1}{2}} \right] \left\{ R_g I_1^n - \frac{V_g^{n+1/2} + V_g^{n-1/2}}{2} \right\}$$

Similarly, at the load end:

$$V_N^{n+1/2} = \left[\frac{R_L \frac{C\Delta x}{2\Delta t} - \frac{1}{2}}{R_L \frac{C\Delta x}{2\Delta t} + \frac{1}{2}} \right] V_N^{n-1/2} + \left[\frac{1}{R_L \frac{C\Delta x}{2\Delta t} + \frac{1}{2}} \right] R_L I_{N-1}^n$$

EXAMPLE**Steady State Response of a Uniform Transmission Line Excited by A Unit Step Function**

$$C = 100.0 \text{ pf/m}, L = 250 \text{ nH/m}, d = 10 \text{ m}$$

$$Z_o = \sqrt{\frac{L}{C}} = 50 \Omega, \quad v_p = \frac{1}{\sqrt{LC}} = 2 \times 10^8 \text{ m/s}$$

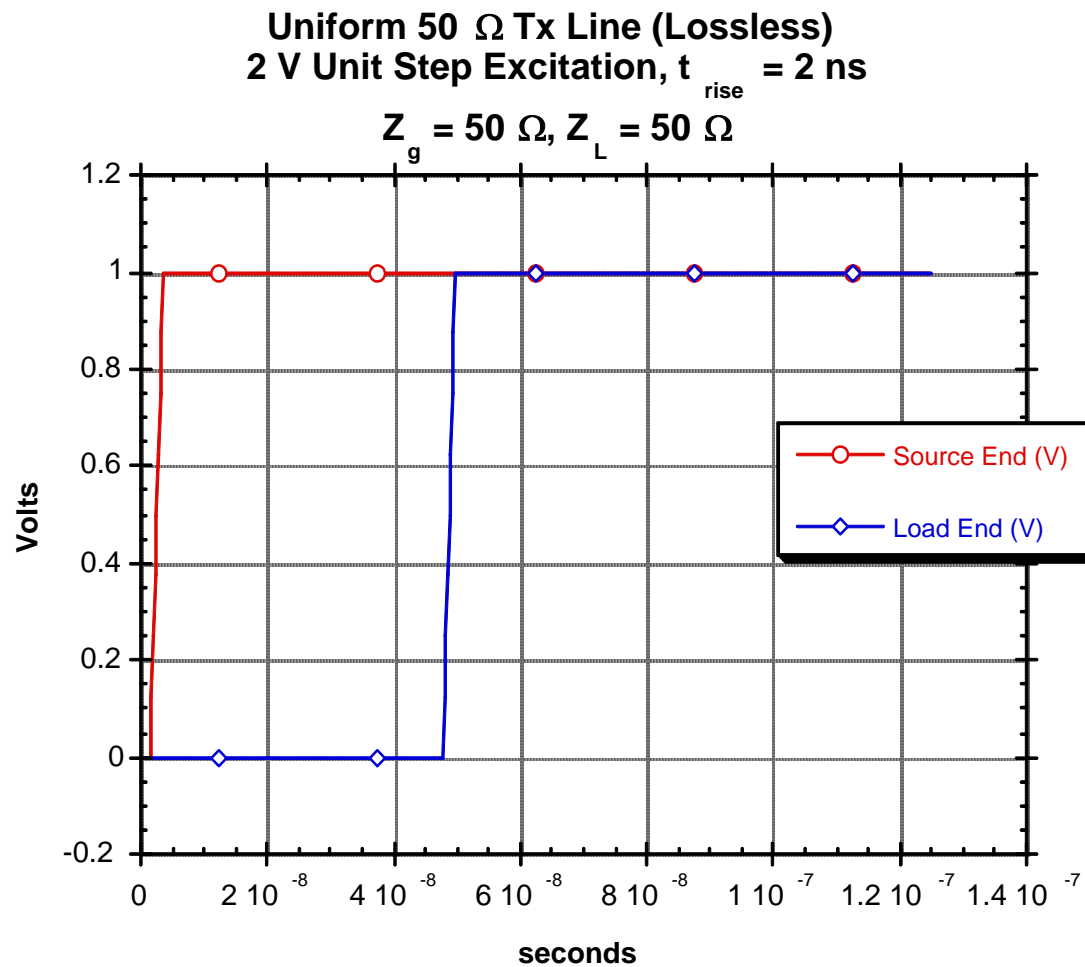
$$\text{transit time} = d / v_p = 50 \text{ ns}$$

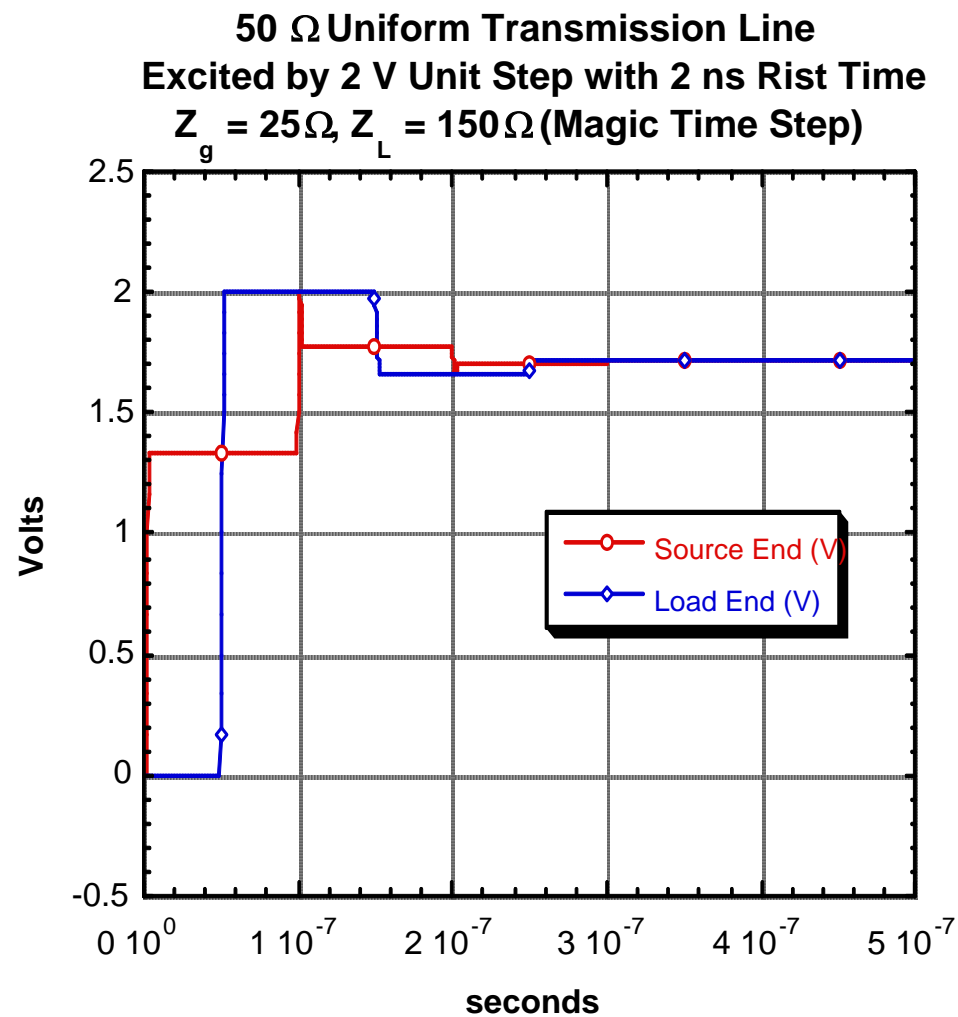
Assume a source voltage $v(t) = 2u(t)$.

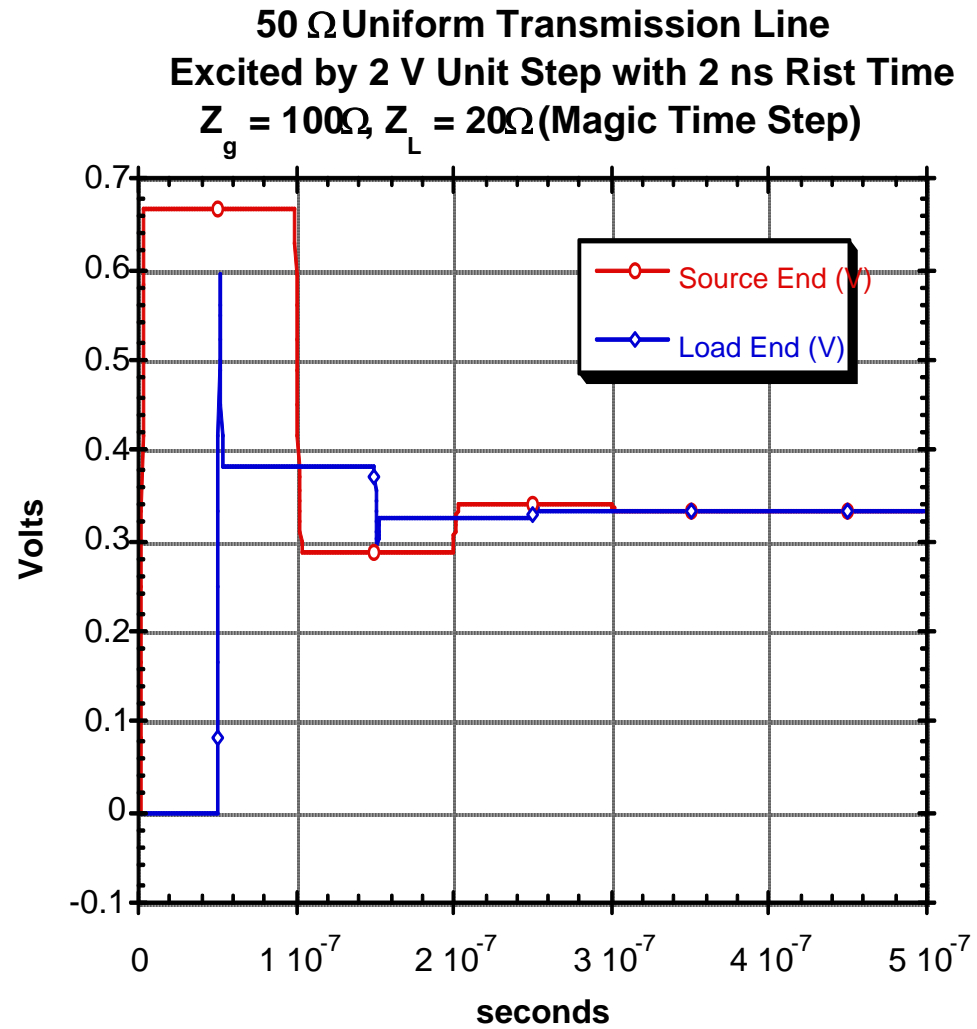
Example 1: $Z_g = 50 \Omega$, $Z_L = 50 \Omega$, Example 2: $Z_g = 25 \Omega$, $Z_L = 150 \Omega$

Example 2: $Z_g = 100 \Omega$, $Z_L = 20 \Omega$

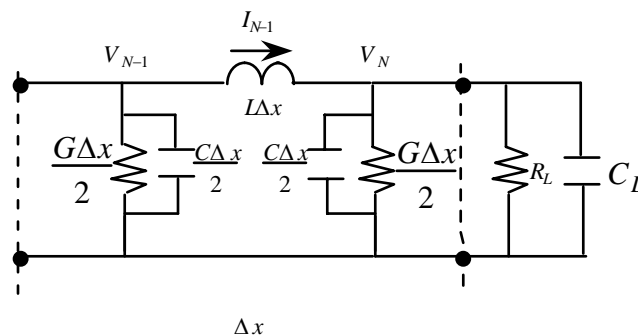
probe the near and far end voltages.







Reactive Load Models for the Finite-Length Transmission Line



Parallel Capacitance/Resistance

From KCL at node N :

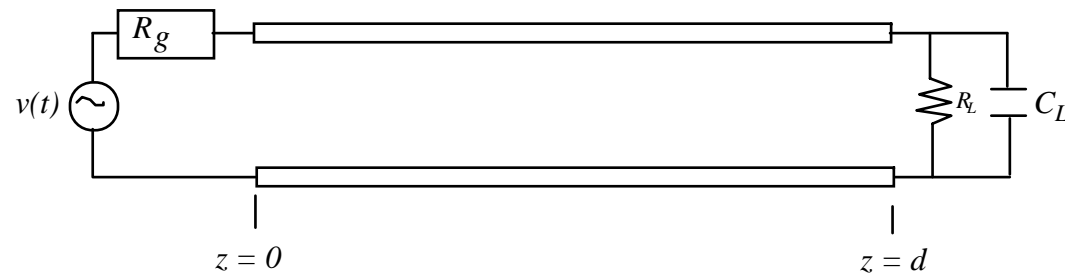
$$I_{N-1}^n = V_N^n \left(\frac{G\Delta x}{2} + \frac{1}{R_L} \right) + \frac{C\Delta x}{2} \frac{\partial V_N^n}{\partial t} + C_L \frac{\partial V_N^n}{\partial t}$$

Central difference the time derivatives, and using linear interpolation of V_N^n

$$\Rightarrow I_{N-1}^n = \frac{V_i^{n+1/2} + V_i^{n-1/2}}{2} \left(\frac{G\Delta x}{2} + \frac{1}{R_L} \right) + \left(\frac{C\Delta x}{2} + C_L \right) \frac{V_i^{n+1/2} - V_i^{n-1/2}}{\Delta t}$$

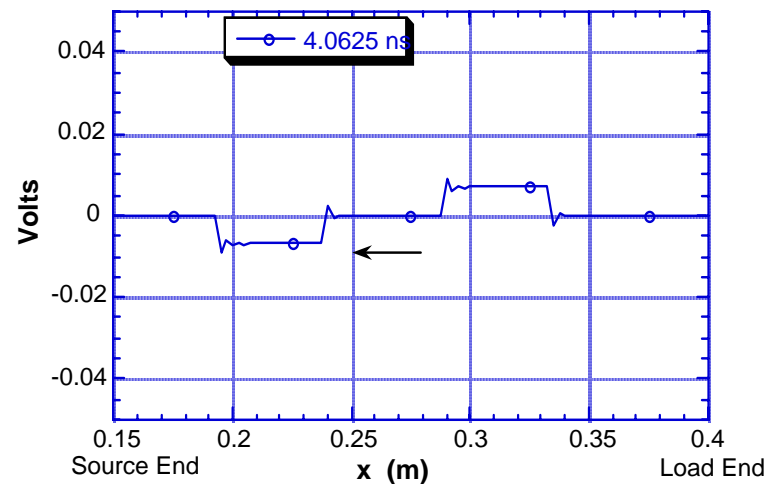
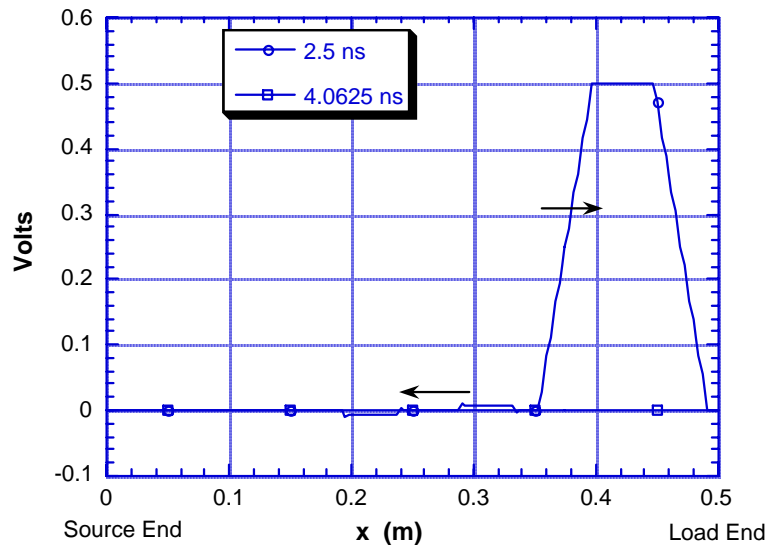
Finally,

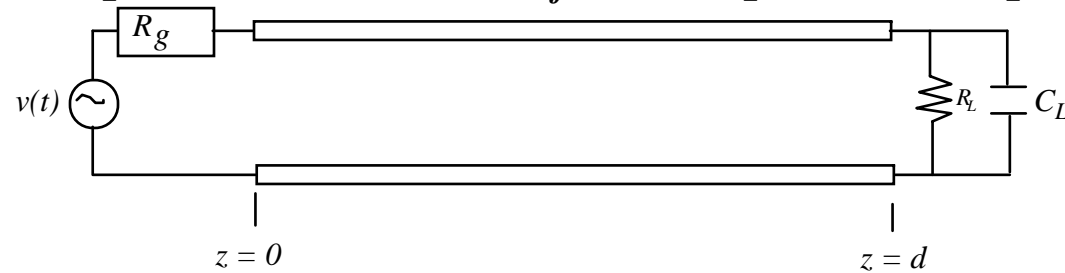
$$V_N^{n+1/2} = \left[\frac{\frac{C\Delta x + 2C_L}{2\Delta t} - \frac{1}{2} \left(\frac{G\Delta x}{2} + \frac{1}{R_L} \right)}{\frac{C\Delta x + 2C_L}{2\Delta t} + \frac{1}{2} \left(\frac{G\Delta x}{2} + \frac{1}{R_L} \right)} \right] V_N^{n-1/2} + \left[\frac{1}{\frac{C\Delta x + 2C_L}{2\Delta t} + \frac{1}{2} \left(\frac{G\Delta x}{2} + \frac{1}{R_L} \right)} \right] I_{N-1}^n$$

EXAMPLE**Steady State Response of a Uniform Transmission Line Excited by A Trapezoidal Pulse ($t_{rise} = t_{fall} = 250$ ps, $t_{dur} = 250$ ps)**

$$C = 100.0 \text{ pf/m}, L = .250 \text{ } \mu\text{H/m} (Z_o = 50 \text{ } \Omega) d = 0.5 \text{ m}$$

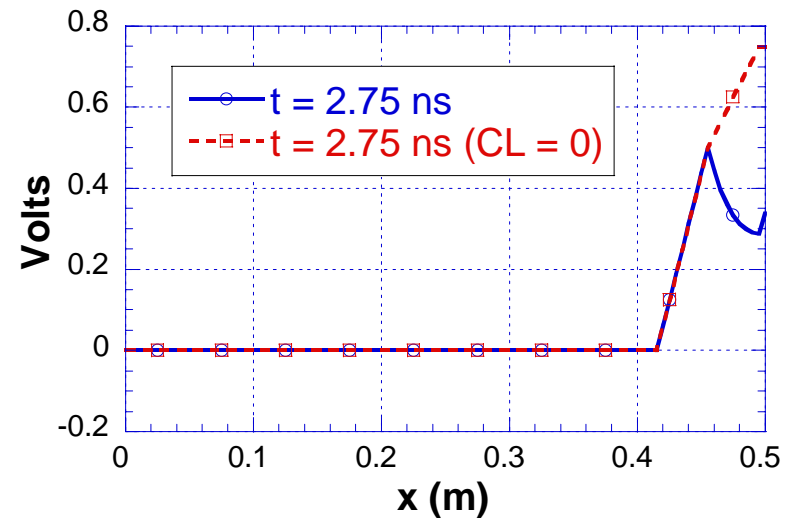
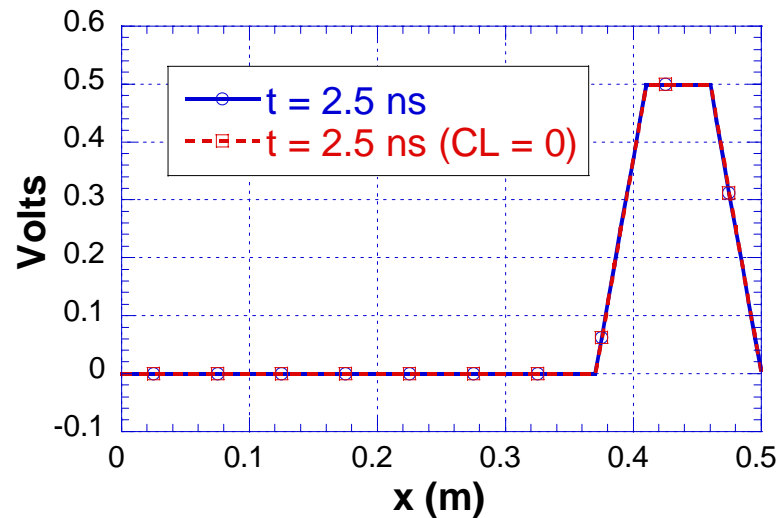
Case 1: $R_L = 50 \text{ } \Omega$, $C_L = 0.1 \text{ pf}$, $R_g = 50 \text{ } \Omega$

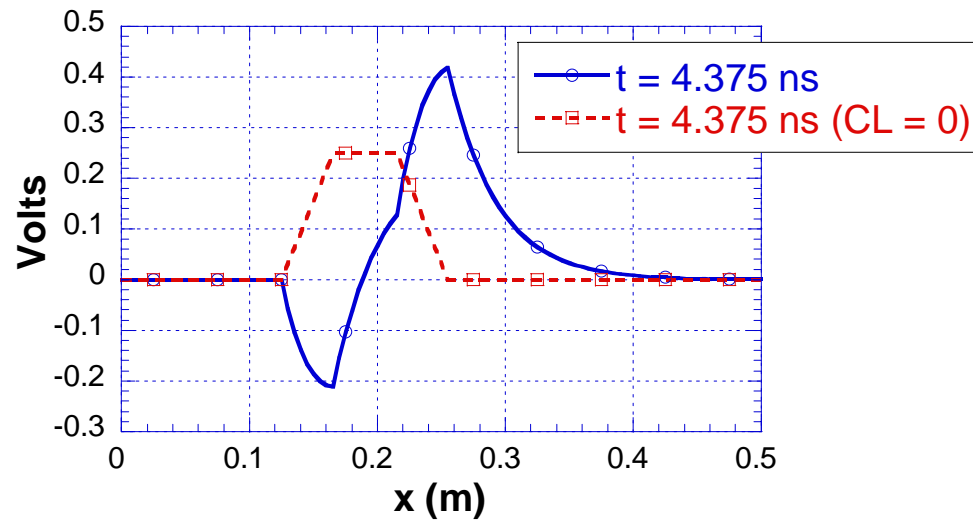
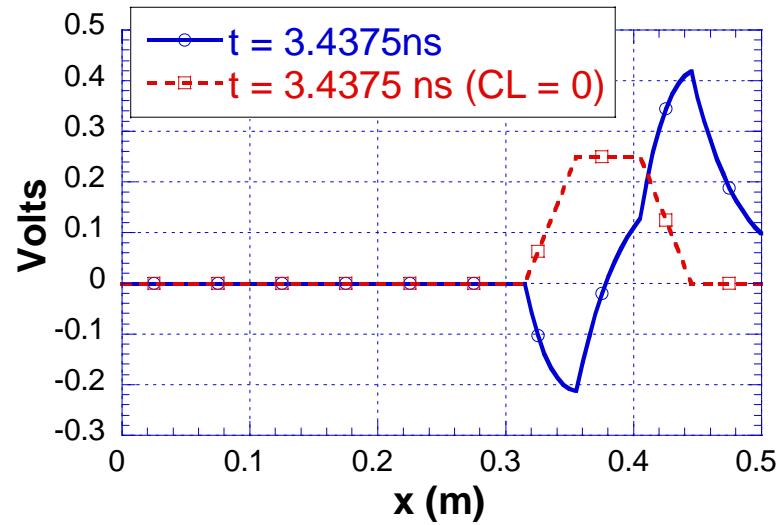
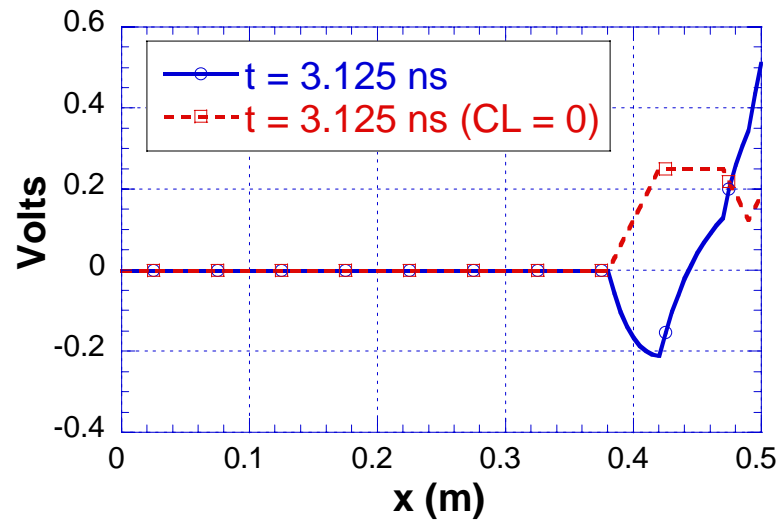


EXAMPLE 2**Trapezoidal Pulse ($t_{rise} = t_{fall} = 200$ ps, $t_{dur} = 250$ ps)**

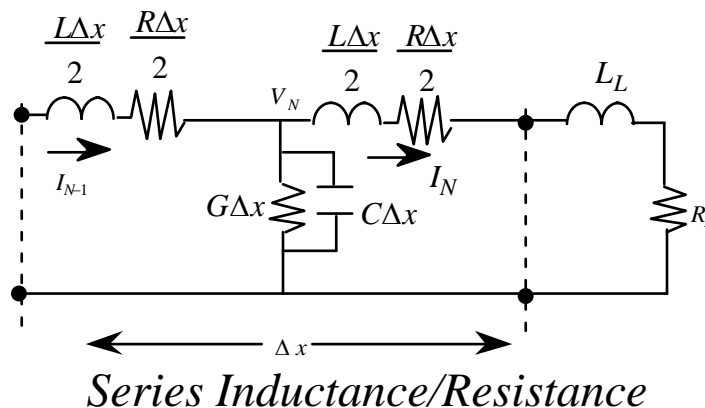
$$C = 100.0 \text{ pf/m}, L = .250 \text{ } \mu\text{H/m} (Z_o = 50 \text{ } \Omega) d = 0.5 \text{ m}$$

Case 2: $R_L = 150 \text{ } \Omega$, $C_L = 5 \text{ pf}$, $R_g = 50 \text{ } \Omega$





Inductive Load Models



Typical Model for Wire Bond to load, or via.

From KVL at *current* node N :

$$V_N^{n+1/2} = I_N^{n+1/2} \left(R_L + \frac{R\Delta x}{2} \right) + \frac{L\Delta x}{2} \frac{\partial I_N^{n+1/2}}{\partial t} + L_L \frac{\partial I_N^{n+1/2}}{\partial t}$$

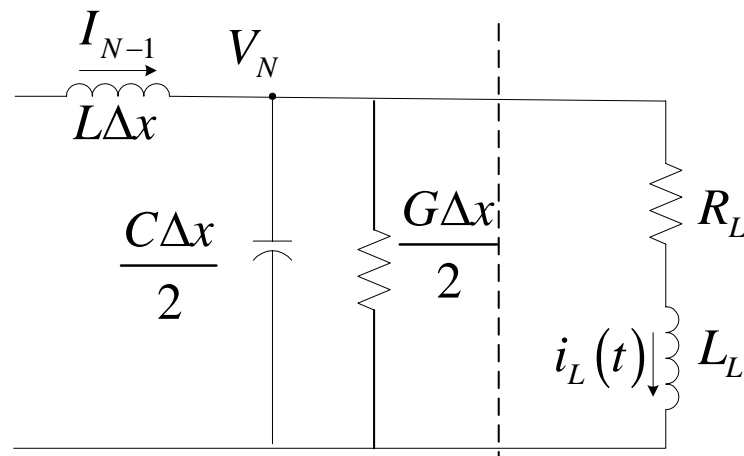
Central difference the time derivatives, and using linear interpolation of $I_N^{n+1/2}$

$$\Rightarrow V_N^{n+1/2} = \frac{I_N^{n+1} + I_N^n}{2} \left(R_L + \frac{R\Delta x}{2} \right) + \left(\frac{L\Delta x}{2} + L_L \right) \frac{I_N^{n+1} - I_N^n}{\Delta t}$$

Finally,

$$I_N^{n+1} = \left[\frac{\frac{L\Delta x + 2L_L}{2\Delta t} - \frac{R\Delta x + 2R_L}{4}}{\frac{L\Delta x + 2L_L}{2\Delta t} + \frac{R\Delta x + 2R_L}{4}} \right] I_N^n + \left[\frac{1}{\frac{L\Delta x + 2L_L}{2\Delta t} + \frac{R\Delta x + 2R_L}{4}} \right] V_N^{n+1/2}$$

Inductive Load at a Voltage Node



$$\text{KCL: } I_{N-1}(t) = \frac{C\Delta x}{2} \frac{\partial V_N(t)}{\partial t} + \frac{G\Delta x}{2} V_N(t) + i_L(t) \quad \text{KVL: } V_N(t) = i_L(t) R_L + L_L \frac{\partial i_L(t)}{\partial t}$$

Discretize in time:

$$(1) \quad I_{N-1}^n = \frac{C\Delta x}{2} \frac{V_N^{n+1/2} - V_N^{n-1/2}}{\Delta t} + \frac{G\Delta x}{2} \frac{V_N^{n+1/2} + V_N^{n-1/2}}{2} + \frac{I_L^{n+1/2} + I_L^{n-1/2}}{2}$$

$$(2) \quad \frac{V_N^{n+1/2} + V_N^{n-1/2}}{2} = \frac{I_L^{n+1/2} + I_L^{n-1/2}}{2} R_L + L_L \frac{I_L^{n+1/2} - I_L^{n-1/2}}{\Delta t}$$

Where, the load current is expressed at the same time as the load voltage. This is due to the fact that they are co-located in space, and there is no time-delay between them.

(1) and (2) lead to a coupled set of equations. This can be expressed in matrix form as:

$$\begin{pmatrix} \left(\frac{C\Delta x}{2\Delta t} + \frac{G\Delta x}{4} \right) & +\frac{1}{2} \\ +\frac{1}{2} & -\left(\frac{L}{\Delta t} + \frac{R_L}{2} \right) \end{pmatrix} \begin{pmatrix} V_N^{n+\frac{1}{2}} \\ I_L^{n+\frac{1}{2}} \end{pmatrix} = \begin{pmatrix} \left(\frac{C\Delta x}{2\Delta t} - \frac{G\Delta x}{4} \right) & +\frac{1}{2} \\ +\frac{1}{2} & -\left(\frac{L}{\Delta t} - \frac{R_L}{2} \right) \end{pmatrix} \begin{pmatrix} V_N^{n-\frac{1}{2}} \\ I_L^{n-\frac{1}{2}} \end{pmatrix} - \begin{pmatrix} I_{N-1}^n \\ 0 \end{pmatrix}$$

which can be written in reduced notation as:

$$\mathbf{P}\mathbf{x}^{n+\frac{1}{2}} = \mathbf{Q}\mathbf{x}^{n-\frac{1}{2}} + \mathbf{y}^n$$

Where, \mathbf{P} and \mathbf{Q} are 2×2 matrices. Therefore, at each time step, we can solve:

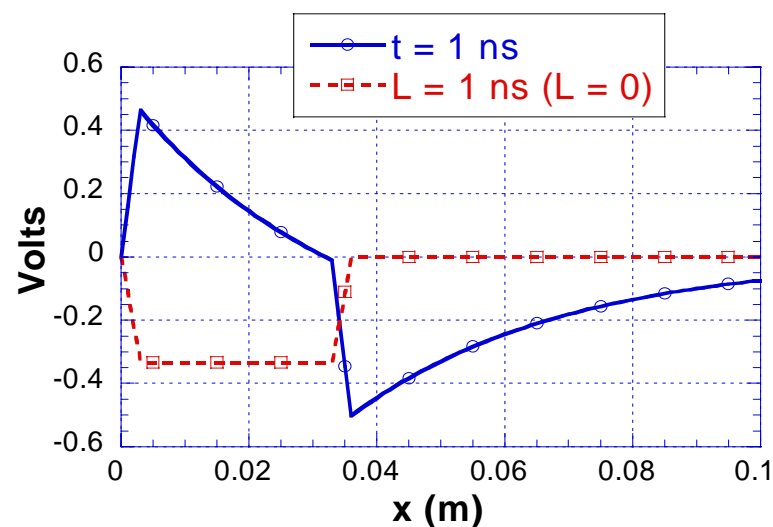
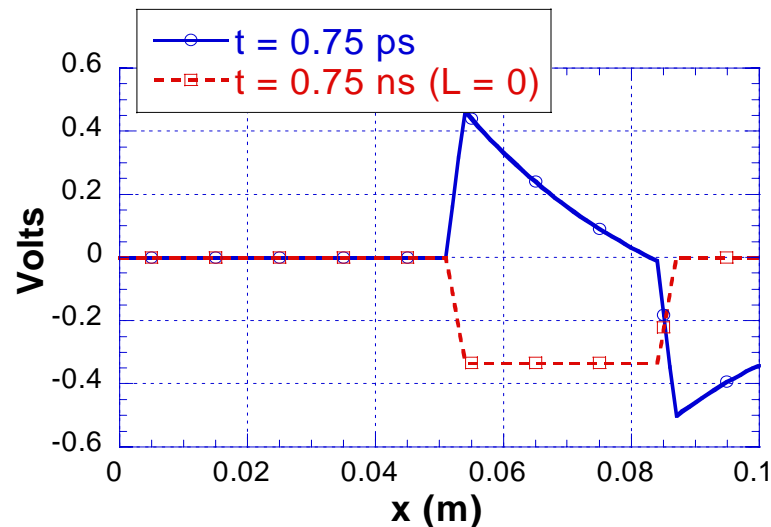
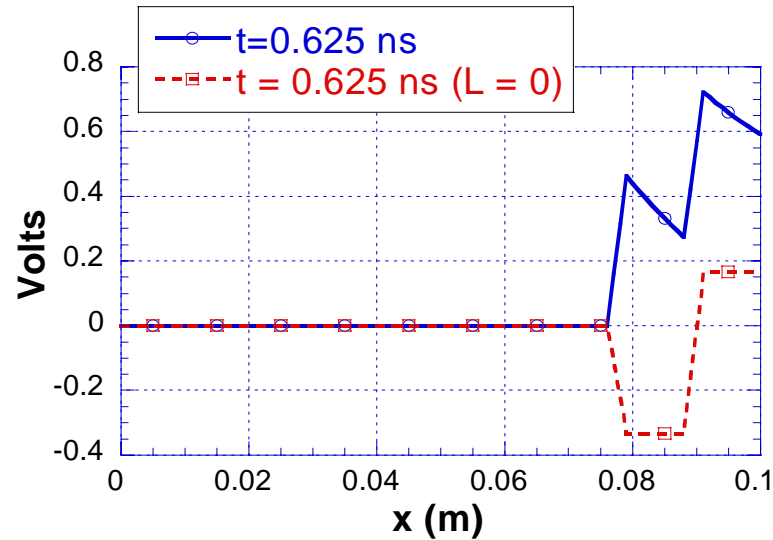
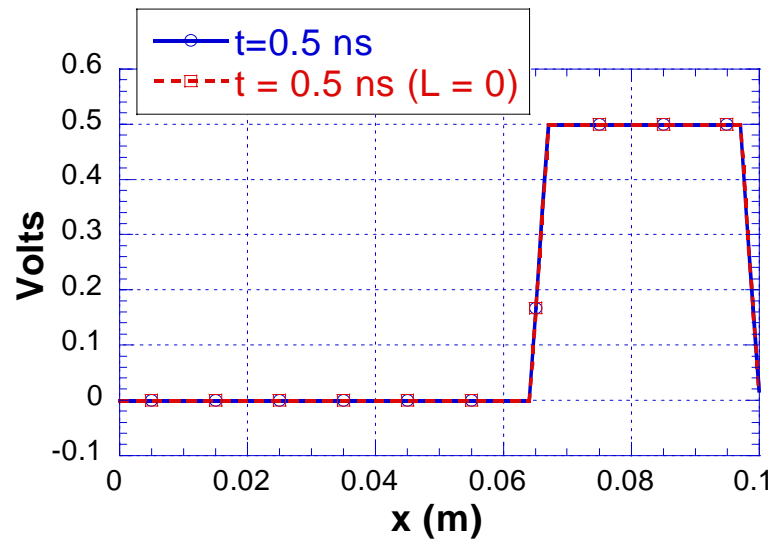
$$\begin{pmatrix} V_N^{n+\frac{1}{2}} \\ I_L^{n+\frac{1}{2}} \end{pmatrix} = \mathbf{x}^{n+\frac{1}{2}} = \mathbf{P}^{-1} \left(\mathbf{Q}\mathbf{x}^{n-\frac{1}{2}} + \mathbf{y}^n \right)$$

EXAMPLE 3

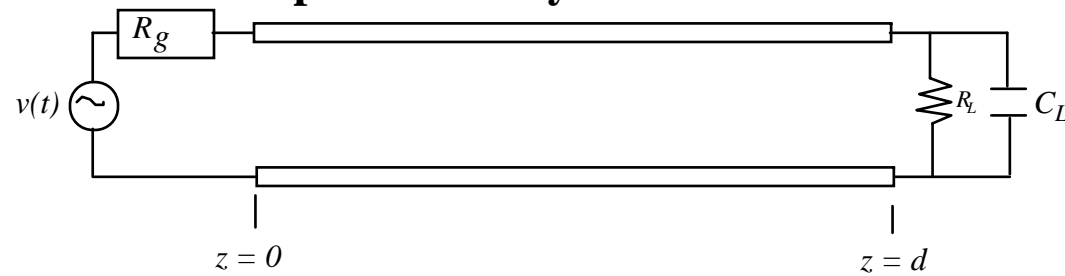
Trapezoidal Pulse ($t_{rise} = t_{fall} = 15 \text{ ps}$, $t_{dur} = 150 \text{ ps}$)

$C = 100.0 \text{ pF/m}$, $L = .250 \text{ } \mu\text{H/m}$ ($Z_o = 50 \text{ } \Omega$), $d = 0.1 \text{ m}$

$R_L = 10 \text{ } \Omega$, $L_L = 10 \text{ nF}$, $R_g = 50 \text{ } \Omega$, $\Delta x = .001 \text{ m}$, $\Delta t = \Delta x / v = 5 \text{ ps}$



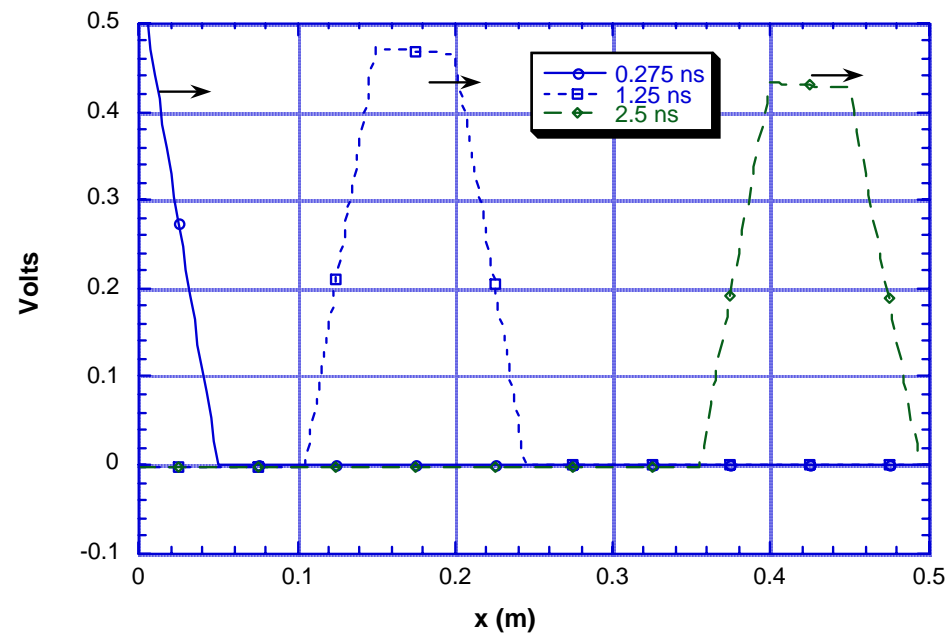
Example of a Lossy Transmission Line



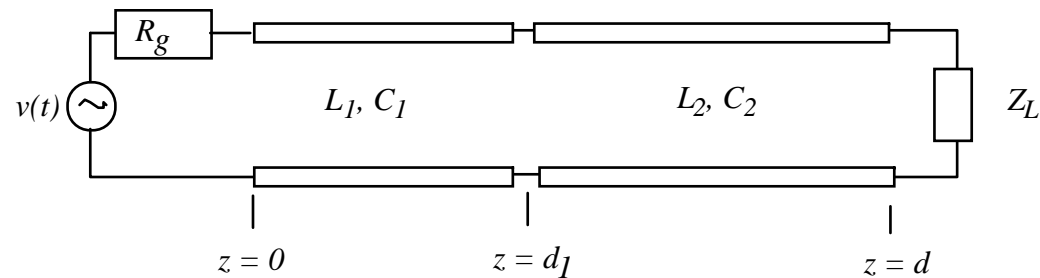
$$C = 100.0 \text{ pf/m}, L = .250 \text{ } \mu\text{H/m}, d = 0.5 \text{ m}$$

$$G = 0.01 \text{ s/m}, R = 10 \text{ } \Omega/\text{m}$$

(Z_o , v_p are dispersive)



NON-UNIFORM TRANSMISSION LINES

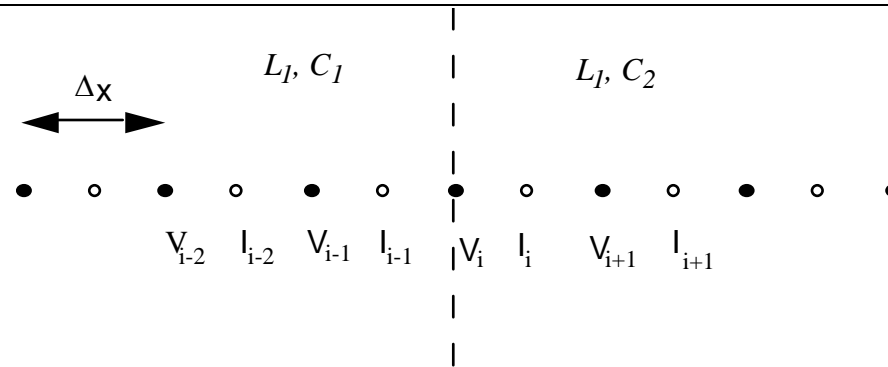


Line 1: $Z_1 = \sqrt{L_1/C_1}$, $v_1 = 1/\sqrt{L_1 C_1}$

Line 2: $Z_2 = \sqrt{L_2/C_2}$, $v_2 = 1/\sqrt{L_2 C_2}$

- Impact:
- a. Lines have different impedances
 - b. Lines have different phase velocities (affects Δt)
 - c. Differential Operators invalid at interface

Assume $L_1 = L_2$:



At node V_i :

$$\frac{\partial I(x,t)}{\partial x} = -C \frac{\partial V(x,t)}{\partial t}$$

V is continuous, however, C is not! Therefore, $\frac{\partial I(x,t)}{\partial x}$ not defined at interface

Split into two regions and approximate:

$$\frac{I_i^- - I_{i-1}}{\Delta x / 2} = -C_1 \frac{V_i^{n+1/2} - V_i^{n-1/2}}{\Delta t}; \quad \frac{I_i - I_i^+}{\Delta x / 2} = -C_2 \frac{V_i^{n+1/2} - V_i^{n-1/2}}{\Delta t}$$

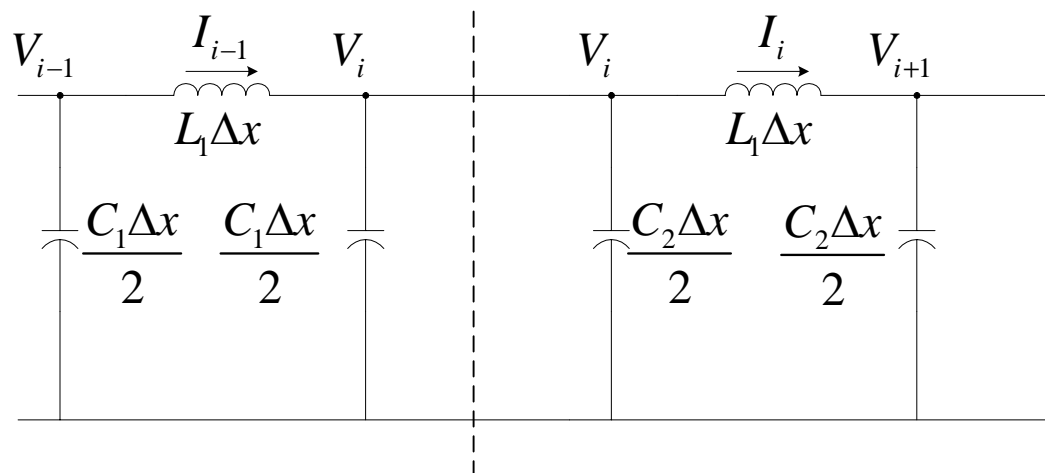
Adding the two and enforcing current continuity:

$$\frac{I_i^n - I_{i-1}^n}{\Delta x} = -\left(\frac{C_1 + C_2}{2}\right) \frac{V_i^{n+1/2} - V_i^{n-1/2}}{\Delta t}$$

Average Value of the Capacitance per unit length. Similarly, for discontinuity in the line inductance:

$$\frac{V_i^{n+1/2} - V_{i-1}^{n+1/2}}{\Delta x} = -\left(\frac{L_1 + L_2}{2}\right) \frac{I_i^{n+1} - I_i^n}{\Delta t}$$

An alternate derivation is presented via a distributed circuit model:



The interface is represented by the interface of the cascaded pi-networks.

Applying KCL at the interface:

$$I_{i-1}^n = \left(\frac{C_1 \Delta x}{2} + \frac{C_2 \Delta x}{2} \right) \frac{\partial V_i^n}{\partial t} + I_i^n$$

Applying a central difference approximation for the time derivative:

$$\frac{I_i^n - I_{i-1}^n}{\Delta x} = - \left(\frac{C_1 + C_2}{2} \right) \frac{V_i^{n+1/2} - V_i^{n-1/2}}{\Delta t}$$

Which is identical to that derived previously. Note that this is easily extendable to lossy lines.

Conclusion: FDTD approximation of a step discontinuity is approximated by a linear approximation. Also, discontinuity in C and L are separated by $\frac{1}{2}$ of a space cell.

FDTD Solution of Maxwell's Equations

Faraday's Law:

$$\frac{\partial \vec{B}}{\partial t} = -\nabla \times \vec{E} - \vec{M}_{imp}$$

$$\frac{\partial}{\partial t} \iint_S \vec{B} \cdot d\vec{S} = -\oint_C \vec{E} \cdot d\vec{\ell} - \iint_S \vec{M}_{imp} \cdot d\vec{S}$$

$$-\sigma \vec{E} - \vec{J}_{imp}$$

Ampere's Law:

$$\frac{\partial \vec{D}}{\partial t} = \nabla \times \vec{H} - \sigma \vec{E} - \vec{J}_{imp}$$

$$\frac{\partial}{\partial t} \iint_S \vec{D} \cdot d\vec{S} = \oint_C \vec{H} \cdot d\vec{\ell} - \iint_S \sigma \vec{E} \cdot d\vec{S} - \iint_S \vec{J}_{imp} \cdot d\vec{S}$$

Gauss' Laws:

$$\nabla \cdot \vec{D} = \rho \qquad \nabla \cdot \vec{B} = 0$$

$$\oiint_S \vec{D} \cdot d\vec{S} = \iiint_V \rho dV \qquad \oiint_S \vec{B} \cdot d\vec{S} = 0$$

$$\text{Constitutive Relations: } \vec{D} = \epsilon \vec{E}, \qquad \vec{B} = \mu \vec{H}, \qquad \vec{J} = \sigma \vec{E}$$

Maxwell's Curl Equations

From Faraday's and Ampere's Laws:

$$\begin{aligned}
 -\frac{\partial B_x}{\partial t} &= \frac{\partial E_z}{\partial y} - \frac{\partial E_y}{\partial z} & \frac{\partial D_x}{\partial t} &= \frac{\partial H_z}{\partial y} - \frac{\partial H_y}{\partial z} - J_x \\
 -\frac{\partial B_y}{\partial t} &= \frac{\partial E_x}{\partial z} - \frac{\partial E_z}{\partial x} & \frac{\partial D_y}{\partial t} &= \frac{\partial H_x}{\partial z} - \frac{\partial H_z}{\partial x} - J_y \\
 -\frac{\partial B_z}{\partial t} &= \frac{\partial E_y}{\partial x} - \frac{\partial E_x}{\partial y} & \frac{\partial D_z}{\partial t} &= \frac{\partial H_y}{\partial x} - \frac{\partial H_x}{\partial y} - J_z
 \end{aligned}$$

2-Dimensional Form of Maxwell's Equations:

1. TM_z ($H_z = 0$, $E_z = E_z(x,y)$).

$$-\frac{\partial B_x}{\partial t} = \frac{\partial E_z}{\partial y} \qquad \frac{\partial D_z}{\partial t} = \frac{\partial H_y}{\partial x} - \frac{\partial H_x}{\partial y} - J_z$$

$$\frac{\partial B_y}{\partial t} = \frac{\partial E_z}{\partial x}$$

2. TE_z ($E_z = 0$, $H_z = H_z(x,y)$).

$$\frac{\partial D_x}{\partial t} = \frac{\partial H_z}{\partial y} - J_x \qquad -\frac{\partial B_z}{\partial t} = \frac{\partial E_y}{\partial x} - \frac{\partial E_x}{\partial y}$$

$$\frac{\partial D_y}{\partial t} = -\frac{\partial H_z}{\partial x} - J_y$$

1-Dimensional Form of Maxwell's Equations:

1. TM_z ($H_z = 0$, $E_z = E_z(y)$).

$$-\frac{\partial B_x}{\partial t} = \frac{\partial E_z}{\partial y} \quad \frac{\partial D_z}{\partial t} = \frac{\partial H_x}{\partial y} - J_z$$

or,

$$\frac{\partial H_x}{\partial t} = -\frac{1}{\mu} \frac{\partial E_z}{\partial y} \quad \frac{\partial E_z}{\partial t} = -\frac{1}{\epsilon} \frac{\partial H_x}{\partial y} - \frac{1}{\epsilon} J_z$$

2. TE_z ($E_z = 0$, $H_z = H_z(y)$).

$$\frac{\partial D_x}{\partial t} = \frac{\partial H_z}{\partial y} - J_x \quad -\frac{\partial B_z}{\partial t} = -\frac{\partial E_x}{\partial y}$$

or,

$$\frac{\partial E_x}{\partial t} = \frac{1}{\epsilon} \frac{\partial H_z}{\partial y} - \frac{1}{\epsilon} J_x \quad \frac{\partial H_z}{\partial t} = \frac{1}{\mu} \frac{\partial E_x}{\partial y}$$

Can Model 1-Dimensional Maxwell's Equations in a manner identical to the 1-Dimensional Transmission Line Equations.

The Yee Algorithm in 2D, TM_z Case

Maxwell's Equations TM_z ($H_z = 0$, $E_z = E_z(x,y)$).

$$-\frac{\partial B_x}{\partial t} = \frac{\partial E_z}{\partial y} \qquad \frac{\partial D_z}{\partial t} = \frac{\partial H_y}{\partial x} - \frac{\partial H_x}{\partial y} - J_z$$

$$-\frac{\partial B_y}{\partial t} = -\frac{\partial E_z}{\partial x}$$

Discrete Space

Let

$$x_i = i\Delta x, \quad y_j = j\Delta y,$$

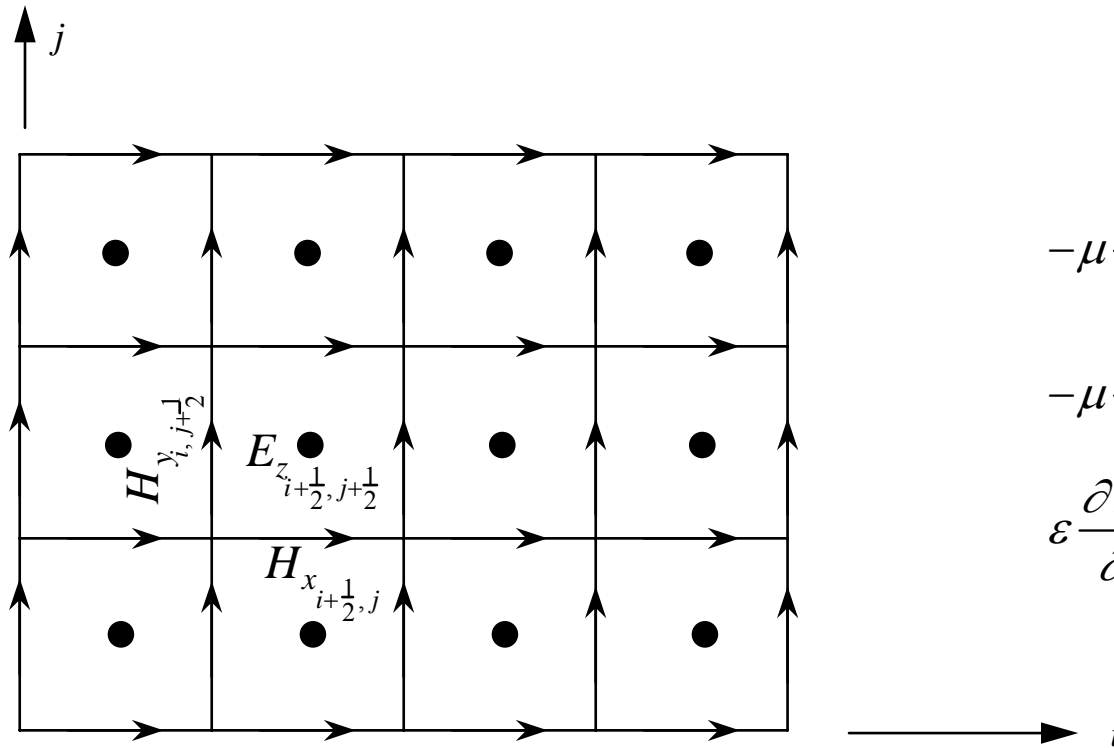
$$t_n = n\Delta t, \quad \text{and}$$

$$f_{i,j}^n = f(x_i, y_j, t_n)$$

Use Central Differences

$$\frac{\partial f(x, y, t)}{\partial x} = \frac{f_{i+\frac{1}{2},j}^n - f_{i-\frac{1}{2},j}^n}{\Delta x} + O(\Delta x^2), \quad \frac{\partial f(x, y, t)}{\partial y} = \frac{f_{i,j+\frac{1}{2}}^n - f_{i,j-\frac{1}{2}}^n}{\Delta y} + O(\Delta y^2)$$

Staggered Grid:



$$-\mu \frac{\partial H_x}{\partial t} = \frac{\partial E_z}{\partial y}$$

$$-\mu \frac{\partial H_y}{\partial t} = -\frac{\partial E_z}{\partial x}$$

$$\epsilon \frac{\partial E_z}{\partial t} = \frac{\partial H_y}{\partial x} - \frac{\partial H_x}{\partial y} - J_z$$

E_z is located at center of grid cells

H_x is located at the center of horizontal edges

H_y is located at the center of vertical edges

Discrete coupled 1st-order equations for linear, homogeneous, isotropic medium:

$$-\mu \frac{H_{x_{i+1/2,j}}^{n+1/2} - H_{x_{i+1/2,j}}^{n-1/2}}{\Delta t} = \frac{E_{z_{i+1/2,j+1/2}}^n - E_{z_{i+1/2,j-1/2}}^n}{\Delta y}$$

$$-\mu \frac{H_{y_{i,j+1/2}}^{n+1/2} - H_{y_{i,j+1/2}}^{n-1/2}}{\Delta t} = -\frac{E_{z_{i+1/2,j+1/2}}^n - E_{z_{i-1/2,j+1/2}}^n}{\Delta x}$$

$$\varepsilon \frac{E_{z_{i+1/2,j+1/2}}^{n+1} - E_{z_{i+1/2,j+1/2}}^n}{\Delta t} = \frac{H_{y_{i+1,j+1/2}}^{n+1/2} - H_{y_{i,j+1/2}}^{n+1/2}}{\Delta x}$$

$$-\frac{H_{x_{i+1/2,j+1}}^{n+1/2} - H_{x_{i+1/2,j}}^{n+1/2}}{\Delta y} - \sigma \frac{\left(E_{z_{i+1/2,j+1/2}}^n + E_{z_{i+1/2,j+1/2}}^{n+1} \right)}{2}$$

Constitutive relations:

$$D_{z_{i+1/2,j+1/2}}^{n+1} = \varepsilon E_{z_{i+1/2,j+1/2}}^{n+1}, \quad B_{x_{i+1/2,j}}^{n+1/2} = \mu H_{x_{i+1/2,j}}^{n+1/2}, \quad B_{y_{i,j+1/2}}^{n+1/2} = \mu H_{y_{i,j+1/2}}^{n+1/2}$$

Fully Explicit Time-Marching Solution of the Discretized Maxwell's Equations in 2-D (TM_z)

$$H_{x_{i+1/2,j}}^{n+1/2} = H_{x_{i+1/2,j}}^{n-1/2} - \frac{\Delta t}{\mu} \frac{E_{z_{i+1/2,j+1/2}}^n - E_{z_{i+1/2,j-1/2}}^n}{\Delta y}$$

$$H_{y_{i,j+1/2}}^{n+1/2} = H_{y_{i,j+1/2}}^{n-1/2} + \frac{\Delta t}{\mu} \frac{E_{z_{i+1/2,j+1/2}}^n - E_{z_{i-1/2,j+1/2}}^n}{\Delta x}$$

$$E_{z_{i+1/2,j+1/2}}^{n+1} = \frac{1-\xi}{1+\xi} E_{z_{i+1/2,j+1/2}}^n + \frac{1}{1+\xi} \frac{\Delta t}{\varepsilon} \frac{H_{y_{i+1,j+1/2}}^{n+1/2} - H_{y_{i,j+1/2}}^{n+1/2}}{\Delta x} - \frac{1}{1+\xi} \frac{\Delta t}{\varepsilon} \frac{H_{x_{i+1/2,j+1}}^{n+1/2} - H_{x_{i+1/2,j}}^{n+1/2}}{\Delta y}$$

where

$$\xi = \frac{\sigma \Delta t}{2\varepsilon}$$

Stability for the 2-D TM_z Finite Difference Equations

- Stability ensures that the energy is bounded within our system. That is, for all n :

$$\frac{|f^{n+1}|^2}{|f^n|^2} \leq 1.$$

where here f represents the electric and magnetic fields.

Solving the Stability Problem:

Again, we will derive the relationships between $(\Delta x, \Delta y)$ and Δt that is sufficient to ensure that the energy is bounded.

This will be done in combination of a Von-Neumann analysis and an eigenvalues problem.

Von Neumann Stability Analysis

- Due to the regularity of the grid, a *Von Neumann* stability analysis can be used. To this end, the grid is assumed infinite in extent, and regularly spaced.
- As done for the dispersion analysis, assume a TM_Z Plane Wave Solution in the discrete space:

$$H_{x_{i,j}}^n = H_{x_0}^n e^{j(\tilde{k}_x i \Delta x + \tilde{k}_y j \Delta y)}$$

$$H_{y_{i,j}}^n = H_{y_0}^n e^{j(\tilde{k}_x i \Delta x + \tilde{k}_y j \Delta y)}$$

$$E_{z_{i,j}}^n = E_{z_0}^n e^{j(\tilde{k}_x i \Delta x + \tilde{k}_y j \Delta y)}$$

- The plane wave expansion is then inserted into the update equations on page 4-7. Note, that we will coincide the electric and magnetic fields in time.

- Looking first at the H_x update:

$$H_{x_0}^{n+\frac{1}{2}} e^{j(\tilde{k}_x(i+\frac{1}{2})\Delta x + \tilde{k}_y j \Delta y)} = H_{x_0}^{n-\frac{1}{2}} e^{j(\tilde{k}_x(i+\frac{1}{2})\Delta x + \tilde{k}_y j \Delta y)} - \frac{\Delta t}{\mu \Delta y} E_{z_0}^n \left(e^{j(\tilde{k}_x(i+\frac{1}{2})\Delta x + \tilde{k}_y(j+\frac{1}{2})\Delta y)} - e^{j(\tilde{k}_x(i+\frac{1}{2})\Delta x + \tilde{k}_y(j-\frac{1}{2})\Delta y)} \right)$$

- Canceling exponentials, and applying Euler's law:

$$H_{x_0}^{n+\frac{1}{2}} = H_{x_0}^{n-\frac{1}{2}} - 2j \frac{\Delta t}{\mu \Delta y} E_{z_0}^n \sin\left(\frac{\tilde{k}_y \Delta y}{2}\right)$$

- This is repeated for the other updates, leading to:

$$H_{x_0}^{n+\frac{1}{2}} = H_{x_0}^{n-\frac{1}{2}} - 2j \frac{\Delta t}{\mu} Y E_{z_0}^n, \quad H_{y_0}^{n+\frac{1}{2}} = H_{y_0}^{n-\frac{1}{2}} + 2j \frac{\Delta t}{\mu} X E_{z_0}^n$$

$$E_{z_0}^{n+\frac{1}{2}} = E_{z_0}^{n-\frac{1}{2}} + 2j \frac{\Delta t}{\epsilon} (X H_{y_0}^n - Y H_{x_0}^n)$$

where

$$Y = \frac{\sin\left(\frac{\tilde{k}_y \Delta y}{2}\right)}{\Delta y}, \quad X = \frac{\sin\left(\frac{\tilde{k}_x \Delta x}{2}\right)}{\Delta x}$$

- These equations can be combined in a linear form as:

$$x^{n+\frac{1}{2}} = -2j[A]x^n + I x^{n-\frac{1}{2}} \quad (ii)$$

- where

$$x^{n+\frac{1}{2}} = \begin{bmatrix} H_{x_0}^{n+\frac{1}{2}} \\ H_{y_0}^{n+\frac{1}{2}} \\ E_{z_0}^{n+\frac{1}{2}} \end{bmatrix}, \quad [A] = c\Delta t \begin{bmatrix} 0 & 0 & \frac{Y}{\eta} \\ 0 & 0 & -\frac{X}{\eta} \\ Y\eta & -X\eta & 0 \end{bmatrix}$$

and

$$\eta = \sqrt{\frac{\mu}{\varepsilon}}$$

- Equation (ii) can be reduced to a first order equation by introducing the vectors

$$\mathbf{y}^{n+\frac{1}{2}} = \begin{bmatrix} x^{n+\frac{1}{2}} \\ x^n \end{bmatrix}, \quad \mathbf{y}^n = \begin{bmatrix} x^n \\ x^{n-\frac{1}{2}} \end{bmatrix}$$

and then expressing it as

$$\mathbf{y}^{n+\frac{1}{2}} = [M] \mathbf{y}^n; \quad [M] = \begin{bmatrix} -2j[A] & [I] \\ [I] & 0 \end{bmatrix}.$$

- Stability of the first-order equation requires $\rho([M]) < 1$, where $\rho([M])$ is the spectral radius of M . Following the arguments from Set 2 of the notes, it can be shown that if $\rho([A]) < 1$, then it will follow that $\rho([M]) < 1$.

$$[A] = c\Delta t \begin{bmatrix} 0 & 0 & \frac{Y}{\eta} \\ 0 & 0 & -\frac{X}{\eta} \\ Y\eta & -X\eta & 0 \end{bmatrix}$$

- The eigenvalues of $[A]$ can be determined analytically as:

$$\lambda_A = 0, c\Delta t\sqrt{X^2 + Y^2}, -c\Delta t\sqrt{X^2 + Y^2}$$

- We are interested in the extremum of λ_A . Thus, the maximum value of λ_A for all possible values of \tilde{k}_x and \tilde{k}_y is

$$|\lambda_A|_{\max} = c\Delta t \sqrt{\frac{1}{\Delta x^2} + \frac{1}{\Delta y^2}}$$

Stability of the Explicit 2-Dimensional Formulation

- If $\rho([A]) < 1$, then $|\lambda_A|_{\max} < 1$. Hence, this leads to the stability limit for the two-dimensional explicit update equations:

$$\Delta t < \frac{1}{c \sqrt{\frac{1}{\Delta x^2} + \frac{1}{\Delta y^2}}}$$

- Note, that under the conditions $\Delta x = \Delta y = \Delta$, this is expressed as

$$\Delta t < \frac{\Delta}{c\sqrt{2}}$$

- It is noted that the stability limit excludes the limiting value $\Delta t = \Delta / c\sqrt{2}$. This is because this limit is the *weak* stability limit. In fact, due to numerical rounding error, at the weak stability limit, the simulation may go unstable.
- It will be interesting to observe in the following studies that the dispersive error of the discrete approximation is actually minimized by choosing the time step as close as possible to this limit. Thus, typically one would choose the time step to be at least 99 % of the stability limit.

Study of TM_z Wave Propagation in an Unbounded Medium

Time-Harmonic Plane Wave Analysis – Continuous Space

Let

$$f(x, y, t) = e^{j(\omega t - k_x x - k_y y)}$$

From the wave equation $\left(\frac{\partial^2 f}{\partial t^2} = c^2 \left(\frac{\partial^2 f}{\partial x^2} + \frac{\partial^2 f}{\partial y^2} \right) \right)$

$$-\omega^2 e^{j(\omega t - k_x x - k_y y)} = -c^2 (k_x^2 + k_y^2) e^{j(\omega t - k_x x - k_y y)}$$

This leads to the *dispersion relationship*:

$$k_x^2 + k_y^2 = \frac{\omega^2}{c^2} = k^2$$

c = phase velocity of the wave = v_p , where

$$v_p = \omega / k$$

Group velocity (velocity of energy transport):

$$v_g = \frac{\partial \omega}{\partial k} = 1 / \frac{\partial k}{\partial \omega} = c$$

Numerical Dispersion for Maxwell's Equations in 2D

- Assume a TM_Z Plane Wave Solution for the discrete difference equations:

$$E_{z_{i,j}}^n = E_{z_0} e^{j(\tilde{k}_x i \Delta x + \tilde{k}_y j \Delta y - \omega n \Delta t)}$$

$$H_{x_{i,j}}^n = H_{x_0} e^{j(\tilde{k}_x i \Delta x + \tilde{k}_y j \Delta y - \omega n \Delta t)}$$

$$H_{y_{i,j}}^n = H_{y_0} e^{j(\tilde{k}_x i \Delta x + \tilde{k}_y j \Delta y - \omega n \Delta t)}$$

where, ω is a constant, and we have defined \tilde{k}_x and \tilde{k}_y as the *numerical wave-numbers* that will be solved for.

Plugging the discrete form of the *plane wave solution* into the update expression for H_X:

$$\frac{\mu_o}{\Delta t} H_{x_0} \sin\left(\frac{\omega \Delta t}{2}\right) = \frac{E_{z_0}}{\Delta y} \sin\left(\frac{\tilde{k}_y \Delta y}{2}\right)$$

Repeat for H_y and E_z gives:

$$\begin{bmatrix} \frac{\mu_o}{\Delta t} \sin\left(\frac{\omega\Delta t}{2}\right) & 0 & -\frac{1}{\Delta y} \sin\left(\frac{\tilde{k}_y \Delta y}{2}\right) \\ 0 & \frac{\mu_o}{\Delta t} \sin\left(\frac{\omega\Delta t}{2}\right) & \frac{1}{\Delta x} \sin\left(\frac{\tilde{k}_x \Delta x}{2}\right) \\ -\frac{1}{\Delta y} \sin\left(\frac{\tilde{k}_y \Delta y}{2}\right) & \frac{1}{\Delta x} \sin\left(\frac{\tilde{k}_x \Delta x}{2}\right) & \frac{\varepsilon_o}{\Delta t} \sin\left(\frac{\omega\Delta t}{2}\right) \end{bmatrix} \begin{bmatrix} H_{x_0} \\ H_{y_0} \\ E_{z_0} \end{bmatrix} = 0$$

Dispersion Relationship of the Discrete Space:

$$\frac{1}{c^2 \Delta t^2} \sin^2 \left(\frac{\omega \Delta t}{2} \right) - \frac{1}{\Delta x^2} \sin^2 \left(\frac{\tilde{k}_x \Delta x}{2} \right) - \frac{1}{\Delta y^2} \sin^2 \left(\frac{\tilde{k}_y \Delta y}{2} \right) = 0$$

Numerical Phase Velocity:

1. Assume: $\Delta t \rightarrow 0, \Delta x \rightarrow 0$. Dispersion Relationship becomes

$$\frac{\omega^2}{c^2} - \tilde{k}_x^2 - \tilde{k}_y^2 = 0$$

2. Magic Time Step?

Try $c\Delta t = \Delta x = \Delta y$ for plane wave propagation at an angle α with respect to the x axis:

$$\begin{aligned} & \frac{1}{c^2 \Delta t^2} \sin^2 \left(\frac{\omega \Delta t}{2} \right) - \frac{1}{c^2 \Delta t^2} \sin^2 \left(\frac{\omega \Delta t \cos \alpha}{2} \right) \\ & - \frac{1}{c^2 \Delta t^2} \sin^2 \left(\frac{\omega \Delta t \sin \alpha}{2} \right) \neq 0 \end{aligned}$$

3. Numerical Dispersion: In general, one should choose $(\Delta x, \Delta y) \leq \frac{\lambda}{20}$.

CHARACTERISTICS OF NUMERICAL DISPERSION OF 2-DIM. GRID

DISPERSION RELATIONSHIP IN DISCRETE SPACE:

$$\frac{1}{c^2 \Delta t^2} \sin^2 \left(\frac{\omega \Delta t}{2} \right) - \frac{1}{\Delta x^2} \sin^2 \left(\frac{\tilde{k}_x \Delta x}{2} \right) - \frac{1}{\Delta y^2} \sin^2 \left(\frac{\tilde{k}_y \Delta y}{2} \right) = 0$$

Let,

$$\tilde{k}_x = \tilde{k} \cos(\theta), \quad \tilde{k}_y = \tilde{k} \sin(\theta)$$

Then,

$$\frac{1}{c^2 \Delta t^2} \sin^2 \left(\frac{\omega \Delta t}{2} \right) = \frac{1}{\Delta x^2} \sin^2 \left(\frac{\tilde{k} \cos(\theta) \Delta x}{2} \right) + \frac{1}{\Delta y^2} \sin^2 \left(\frac{\tilde{k} \sin(\theta) \Delta y}{2} \right)$$

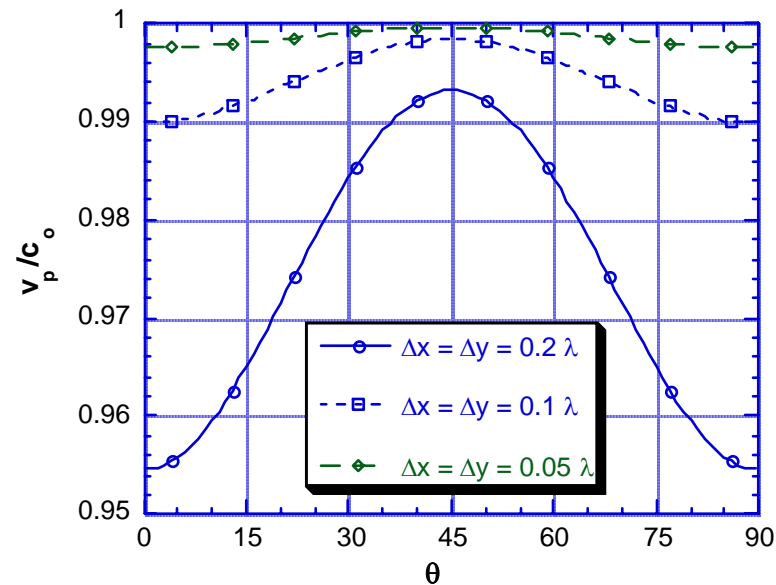
\tilde{k} is solved with a non-linear solver. Apply Newton's method $\tilde{k}_{i+1} = \tilde{k}_i - f(\tilde{k}_i) / f'(\tilde{k}_i)$

$$\tilde{k}_{i+1} = \tilde{k}_i - \frac{\frac{1}{\Delta x^2} \sin^2 \left(\frac{\tilde{k}_i \cos(\theta) \Delta x}{2} \right) + \frac{1}{\Delta y^2} \sin^2 \left(\frac{\tilde{k}_i \sin(\theta) \Delta y}{2} \right) - \frac{1}{c^2 \Delta t^2} \sin^2 \left(\frac{\omega \Delta t}{2} \right)}{\frac{\cos(\theta)}{2\Delta x} \sin(\tilde{k}_i \cos(\theta) \Delta x) + \frac{\sin(\theta)}{2\Delta y} \sin(\tilde{k}_i \sin(\theta) \Delta y)}$$

Numerical Dispersion - Examples

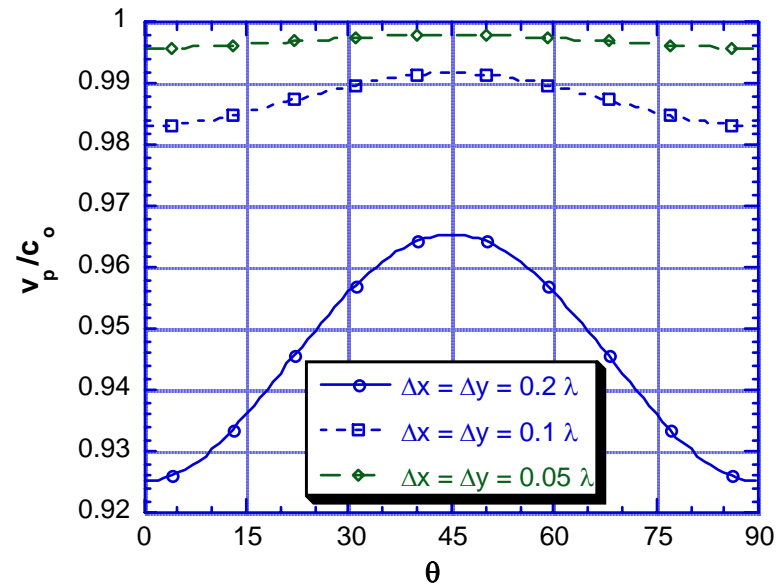
- Numerical Dispersion:

Numerical Phase Velocity: $\Delta t = 0.9$ C.L.



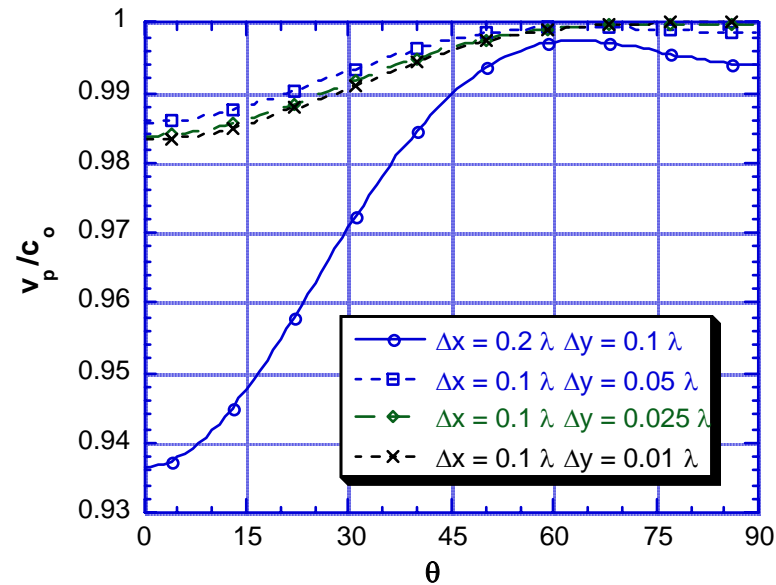
- $v_p < c_o$
- Anisotropic Behavior

Numerical Phase Velocity: $\Delta t = 0.1$ C.L.



Note that the error increases as the time step decreases! We find that the dispersion error is minimized at the stability limit.

Numerical Phase Velocity: $\Delta t = 0.9 \text{ C.L.}$, $dx \neq dy$



- $v_p < c_o$
- Anisotropic Behavior
- Accuracy of wave propagating along y-direction increases.
- Accuracy of wave propagating along the x-direction actually decreases!

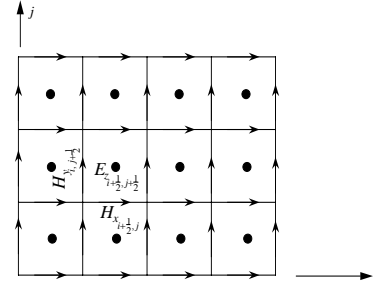
Numerical Implementation (TM_z - Polarization)

In Discrete Homogeneous Space:

$$H_{x_{i+1/2,j}}^{n+1/2} = H_{x_{i+1/2,j}}^{n-1/2} - \frac{\Delta t}{\mu_o} \frac{E_{z_{i+1/2,j+1/2}}^n - E_{z_{i+1/2,j-1/2}}^n}{\Delta y}$$

$$H_{y_{i,j+1/2}}^{n+1/2} = H_{y_{i,j+1/2}}^{n-1/2} + \frac{\Delta t}{\mu_o} \frac{E_{z_{i+1/2,j+1/2}}^n - E_{z_{i-1/2,j+1/2}}^n}{\Delta x}$$

$$E_{z_{i+1/2,j+1/2}}^{n+1} = E_{z_{i+1/2,j+1/2}}^n + \frac{\Delta t}{\epsilon_o} \frac{H_{y_{i+1,j+1/2}}^{n+1/2} - H_{y_{i,j+1/2}}^{n+1/2}}{\Delta x} - \frac{\Delta t}{\epsilon_o} \frac{H_{x_{i+1/2,j+1}}^{n+1/2} - H_{x_{i+1/2,j}}^{n+1/2}}{\Delta y}$$



High-Level Language Implementation (FORTRAN)

```

real hx(maxi,maxj), hy(maxi,maxj)
real ez(maxi,maxj)
co = 2.998e8
dtoco = 0.95/(sqrt(1./dx**2+1./dy**2))
eta = 120*Pi
c1 = dtoco/eta/dy  c2 = dtoco/eta/dx
c3 = dtoco*eta/dx  c4 = dtoco*eta/dy
do it = 1,maxits
  do 10 j = 1,ny
    do 10 i = 1,nx-1
      hx(i,j) = hx(i,j)-c1*(ez(i,j)-ez(i,j-1))
10    continue
    do 20 j = 1,ny-1
      do 20 i = 1,nx
        hy(i,j) = hy(i,j)+c2*(ez(i,j)-ez(i-1,j))
20    continue
    do 30 j = 1,ny-1
      do 30 i = 1,nx-1
        ez(i,j) = ez(i,j)+c3*(hy(i+1,j)-hy(i,j))-c4*(hx(i,j+1)-hx(i,j))
30    continue
  enddo

```

Dirichlet and Neumann Boundary Conditions

- Are the Explicit Update Operators Well-Posed as Stated on the Exterior Boundaries? (i.e., $i = 1; i = nx; j = 1; j = ny$).
- PMC Boundary:
$$H_t = 0, \text{ and } \frac{1}{\mu} \frac{\partial}{\partial n} E_t = 0$$

Dirichlet boundary condition:

$$hx(i,1) = 0, hx(i,ny) = 0$$

$$hy(1,j) = 0, hy(nx,j) = 0$$

- PEC Boundary

$$E_z = 0, \text{ and } \frac{1}{\varepsilon} \frac{\partial}{\partial n} H_t = 0, \hat{n} \cdot \vec{H} = 0$$

Cannot Strictly Enforce as Neumann Boundary Condition on H_t

Use Image Theory:

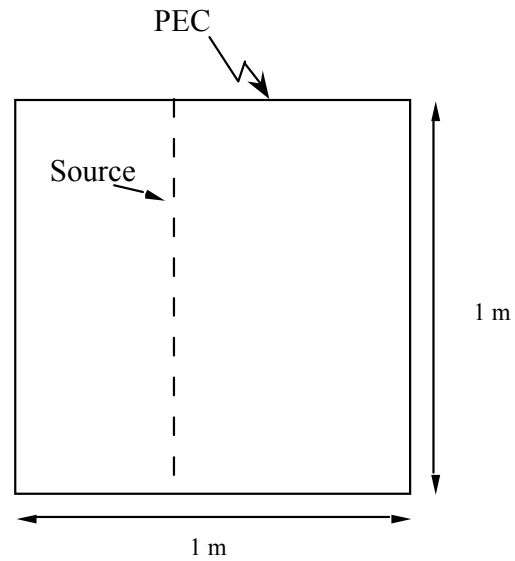
Let $i = 1$ be a PEC wall, then

$$ez(0,j) = -ez(1,j).$$

Therefore, update becomes:

```
do 25 j = 1,ny-1
    hy(1,j) = hy(1,j)+2*c2*ez(1,j)
25 continue
```

- Exterior Radiation Conditions:
-Will Discuss in Set 7 of notes



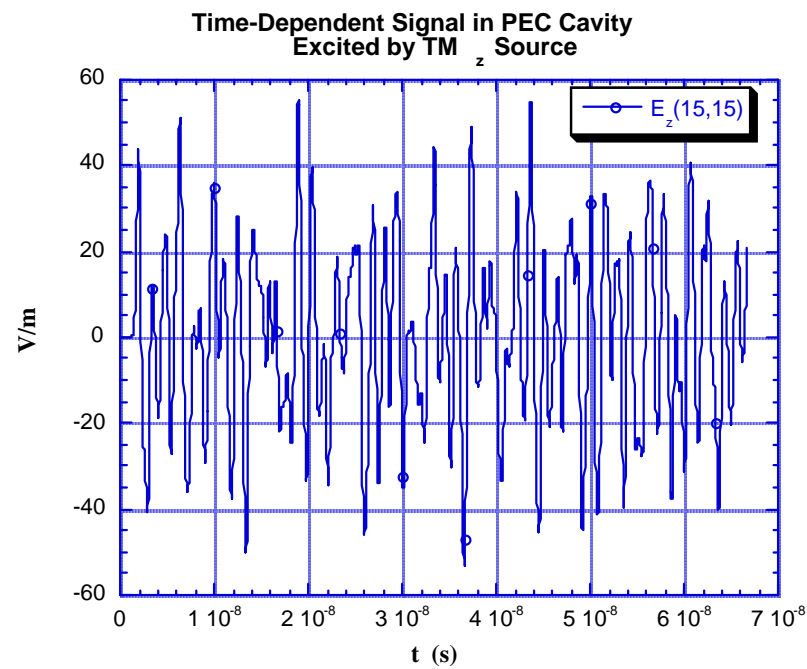
Statistics:

$\Delta x = 0.01$ m, $\Delta y = 0.01$ m, $nx = 101$, $ny = 101$, $\Delta t = 2.1213203\text{E-}11$
10,000 time iterations

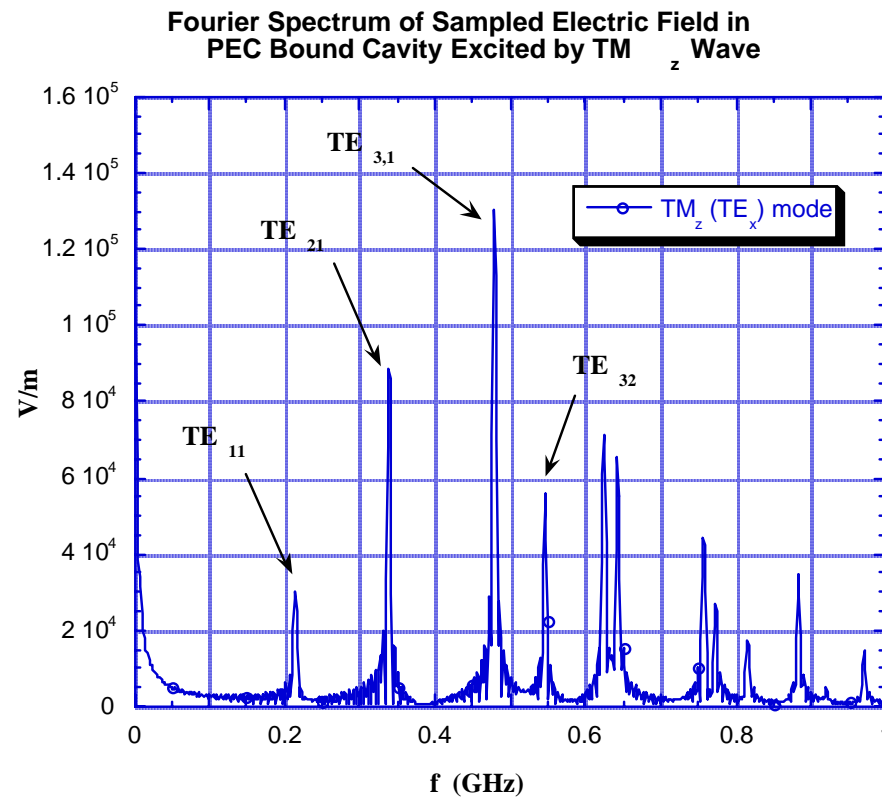
Source (Soft Source):

- Gaussian Profile

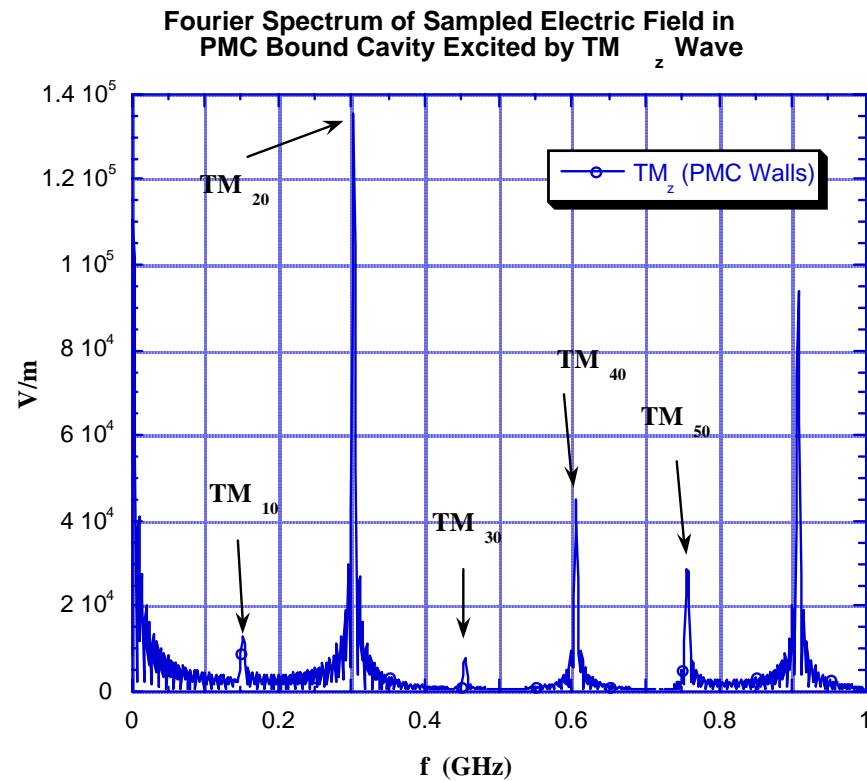
$$E_{z_{i+1/2},j+1/2}^n = E_{z_{i+1/2},j+1/2}^n + \exp\left(-\frac{(n\Delta t - t_0)^2}{t_w^2}\right) / \Delta y$$



Fourier transform the time-dependent data using a FFT:



Cavity Mode	Approx. (FDTD)	Exact
TM_{11}	212.2 MHz	212.1 MHz
TM_{21}	334.7 MHz	335.4 MHz
$TM_{3,1}$	474.2 MHz	474.3 MHz
$TM_{3,2}$	541.2 MHz	540.8 MHz

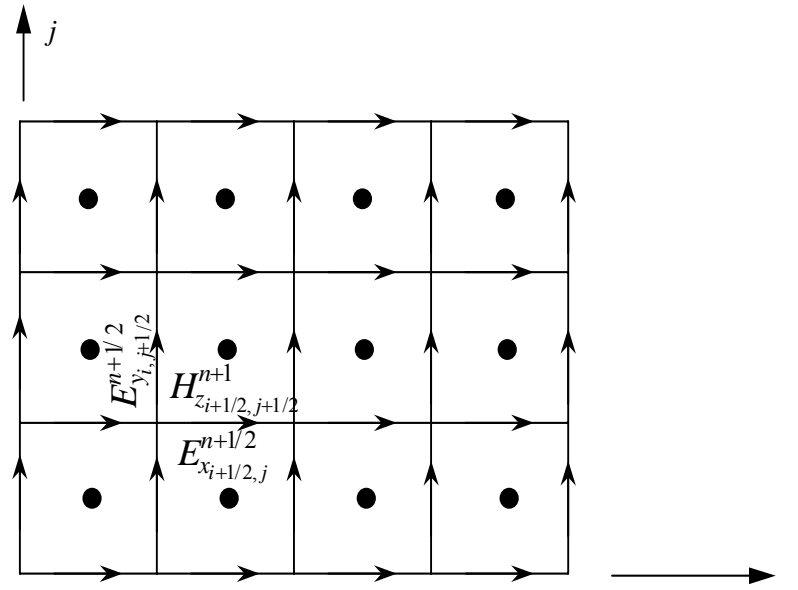


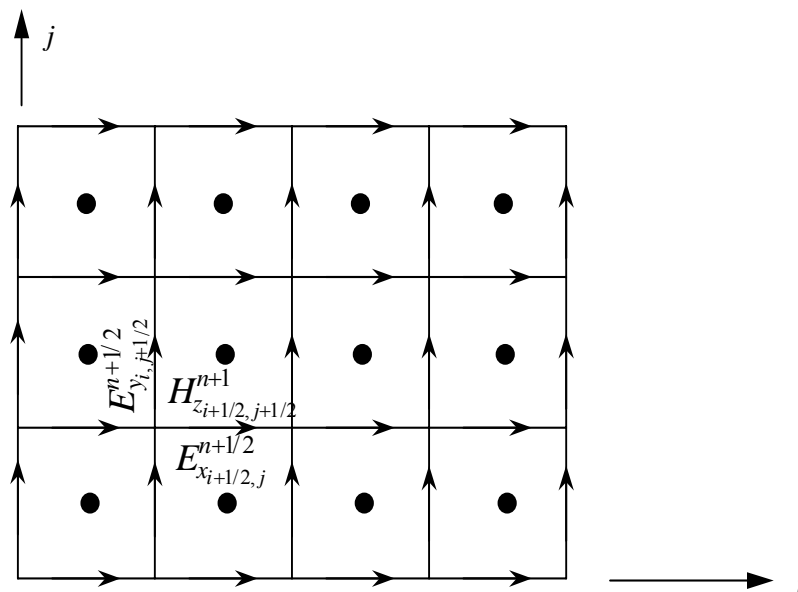
Cavity Mode	Approx. (FDTD)	Exact
TM_{10}	150.8 MHz	150.0 MHz
TM_{20}	300.5 MHz	300.0 MHz
TM_{30}	450.2 MHz	450.0 MHz
TM_{40}	599.5 MHz	600.0 MHz
TM_{50}	749.1 MHz	750.0 MHz

TE_z POLARIZATION - DISCRETE SOLUTION

$$\frac{\partial D_x}{\partial t} = \frac{\partial H_z}{\partial y} \qquad -\frac{\partial B_z}{\partial t} = \frac{\partial E_y}{\partial x} - \frac{\partial E_x}{\partial y}$$

$$\frac{\partial D_y}{\partial t} = -\frac{\partial H_z}{\partial x}$$





In Discrete Homogeneous Space:

$$E_{x_{i+1/2,j}}^{n+1/2} = E_{x_{i+1/2,j}}^{n-1/2} + \frac{\Delta t}{\epsilon_o} \frac{H_{z_{i+1/2,j+1/2}}^n - H_{z_{i+1/2,j-1/2}}^n}{\Delta y}$$

$$E_{y_{i,j+1/2}}^{n+1/2} = E_{y_{i,j+1/2}}^{n-1/2} - \frac{\Delta t}{\epsilon_o} \frac{H_{z_{i+1/2,j+1/2}}^n - H_{z_{i-1/2,j+1/2}}^n}{\Delta x}$$

$$H_{z_{i+1/2,j+1/2}}^{n+1} = H_{z_{i+1/2,j+1/2}}^n - \frac{\Delta t}{\mu_o} \frac{E_{y_{i+1,j+1/2}}^{n+1/2} - E_{y_{i,j+1/2}}^{n+1/2}}{\Delta x} + \frac{\Delta t}{\mu_o} \frac{E_{x_{i+1/2,j+1}}^{n+1/2} - E_{x_{i+1/2,j}}^{n+1/2}}{\Delta y}$$

High-Level Language Implementation (FORTRAN)

```

real ex(maxi,maxj), ey(maxi,maxj)
real hz(maxi,maxj)
co = 2.998e8
dtoco = 0.98/(sqrt(1./dx**2+1./dy**2))
eta = 120*Pi
c1 = dtoco*eta/dy  c2 = dtoco*eta/dx
c3 = dtoco/eta/dx  c4 = dtoco/eta/dy
do it = 1,maxits
  do 10 j = 1,ny
    do 10 i = 1,nx-1
      ex(i,j) = ex(i,j)+c1*(hz(i,j)-hz(i,j-1))
10    continue
    do 20 j = 1,ny-1
      do 20 i = 1,nx
        ey(i,j) = ey(i,j)-c2*(hz(i,j)-hz(i-1,j))
20    continue
    do 30 j = 1,ny-1
      do 30 i = 1,nx-1
        hz(i,j) = hz(i,j)-c3*(ey(i+1,j)-ey(i,j))+c4*(ex(i,j+1)-ex(i,j))
30    continue
  enddo

```

Dirichlet and Neumann Boundary Conditions for TE_z Polarization

- The Explicit Update Operators are Ill-Posed as Stated on the Exterior Boundaries (i.e., $i = 1$; $i = nx$; $j = 1$; $j = ny$).

- PEC Boundary:

$$E_t = 0, \text{ and } \frac{1}{\varepsilon} \frac{\partial}{\partial n} H_t = 0$$

Dirichlet boundary condition:

$$ex(i,1) = 0, ex(i,ny) = 0$$

$$ey(1,j) = 0, ey(nx,j) = 0$$

- PMC Boundary

$$H_z = 0, \text{ and } \frac{1}{\mu} \frac{\partial}{\partial n} E_t = 0$$

Cannot Strictly Enforce as Neumann Boundary Condition

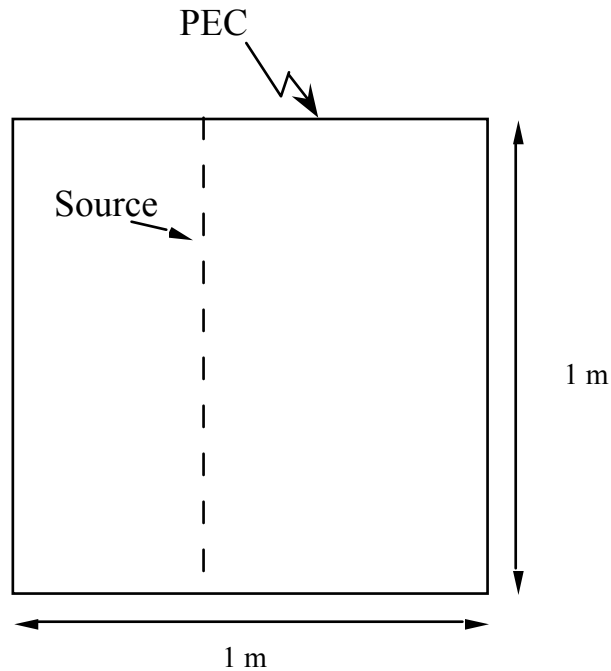
Use Image Theory:

Let $i = 1$ be a PMC wall, then

$$h_z(-1, j) = -h_z(1, j).$$

Therefore, update for PMC boundary becomes:

```
do 25 j = 1, ny-1
    ey(1, j) = ey(1, j) - 2*c2*hz(1, j)
25 continue
```



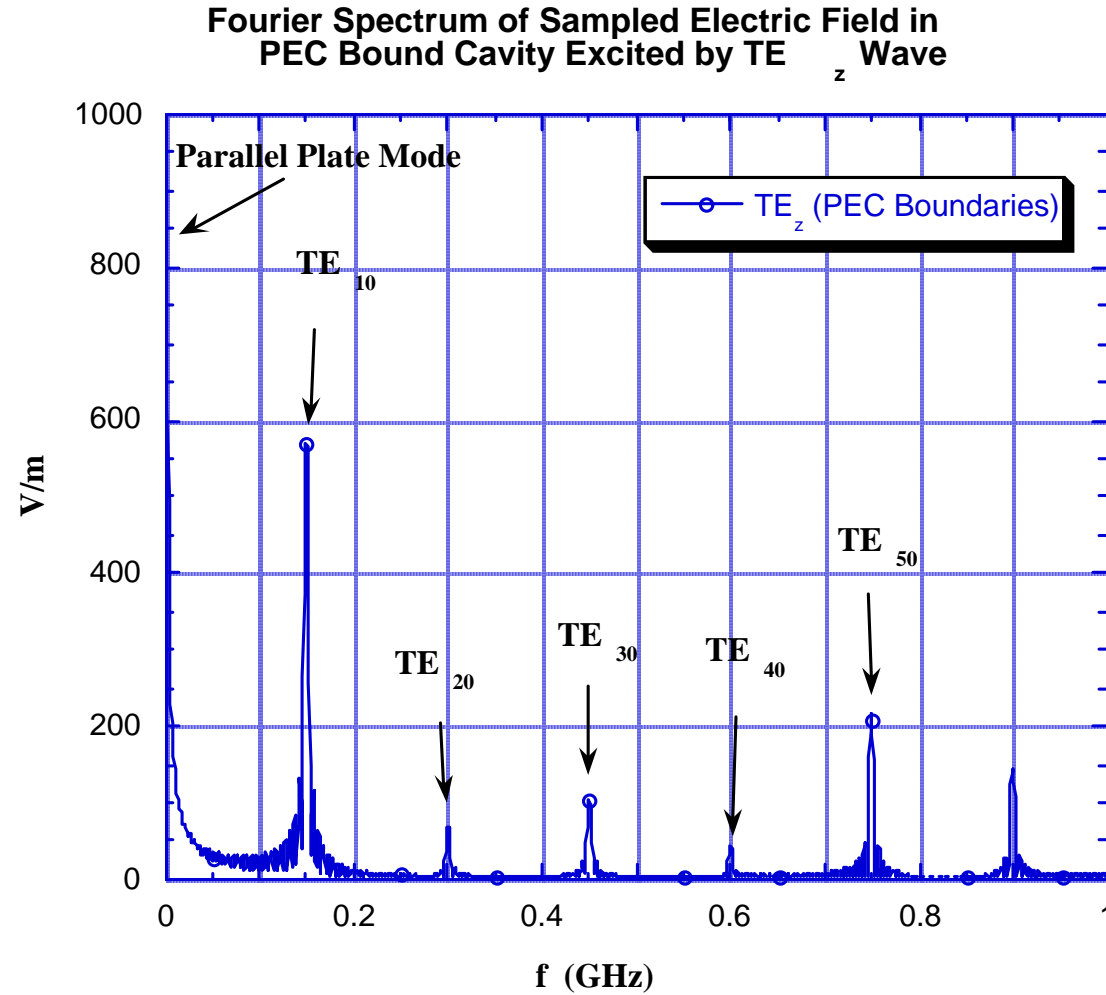
Statistics:

$\Delta x = 0.01$ m, $\Delta y = 0.01$ m, $nx = 101$, $ny = 101$, $\Delta t = 2.1213203\text{E-}11$
10,000 time iterations

Source (Soft Source):

- Gaussian Profile

$$E_{y_{i,j+1/2}}^n = E_{y_{i,j+1/2}}^n + \exp\left(-\frac{(n\Delta t - t_0)^2}{t_w^2}\right) / \Delta y; \quad j = 1, ny - 1$$



Cavity Mode	Approx. (FDTD)	Exact
TE ₁₀	150.0 MHz	150.0 MHz
TE ₂₀	299.92 MHz	300.0 MHz
TE ₃₀	449.97 MHz	450.0 MHz
TE ₄₀	599.94 MHz	600.0 MHz
TE ₅₀	749.53 MHz	750.0 MHz
TE ₆₀	899.17 MHz	900 MHz

THREE-DIMENSIONAL FDTD SOLUTION OF MAXWELL'S EQUATIONS - THE YEE ALGORITHM

- **Maxwell's Curl Equations in Cartesian Coordinates:**

$$\begin{aligned}
 -\frac{\partial B_x}{\partial t} &= \frac{\partial E_z}{\partial y} - \frac{\partial E_y}{\partial z} & \frac{\partial D_x}{\partial t} &= \frac{\partial H_z}{\partial y} - \frac{\partial H_y}{\partial z} - J_x \\
 -\frac{\partial B_y}{\partial t} &= \frac{\partial E_x}{\partial z} - \frac{\partial E_z}{\partial x} & \frac{\partial D_y}{\partial t} &= \frac{\partial H_x}{\partial z} - \frac{\partial H_z}{\partial x} - J_y \\
 -\frac{\partial B_z}{\partial t} &= \frac{\partial E_y}{\partial x} - \frac{\partial E_x}{\partial y} & \frac{\partial D_z}{\partial t} &= \frac{\partial H_y}{\partial x} - \frac{\partial H_x}{\partial y} - J_z
 \end{aligned}$$

- **Mapping the Curl Equations into the Discrete Space**

Define a regular orthogonal grid. A function $f(x,y,z,t)$ evaluated at the vertices of the grid is defined in the discrete coordinate space as

$$f(x,y,z,t) = f(i\Delta x, j\Delta y, k\Delta z, n\Delta t) = f_{i,j,k}^n$$

\Rightarrow Central Difference Approximation of Derivatives:

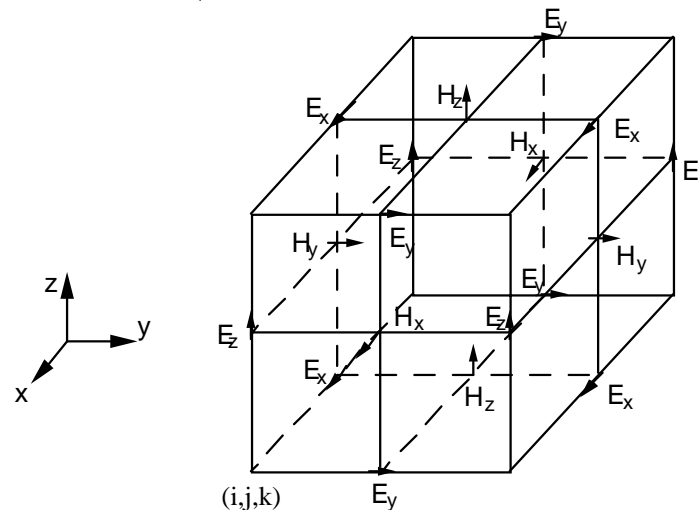
$$-\frac{\partial B_x}{\partial t} = \frac{\partial E_z}{\partial y} - \frac{\partial E_y}{\partial z} \Rightarrow$$

$$\begin{aligned} \frac{1}{\Delta t} \left[B_{x, j+\frac{1}{2}, k+\frac{1}{2}}^{n+\frac{1}{2}} - B_{x, j+\frac{1}{2}, k+\frac{1}{2}}^{n-\frac{1}{2}} \right] &= \frac{1}{\Delta z} \left[E_{y, j+\frac{1}{2}, k+1}^n - E_{y, j+\frac{1}{2}, k}^n \right] - \\ &\quad \frac{1}{\Delta y} \left[E_{z, j+1, k+\frac{1}{2}}^n - E_{z, j, k+\frac{1}{2}}^n \right] \end{aligned}$$

$$\frac{\partial D_x}{\partial t} = \frac{\partial H_z}{\partial y} - \frac{\partial H_y}{\partial z} - J_x \Rightarrow$$

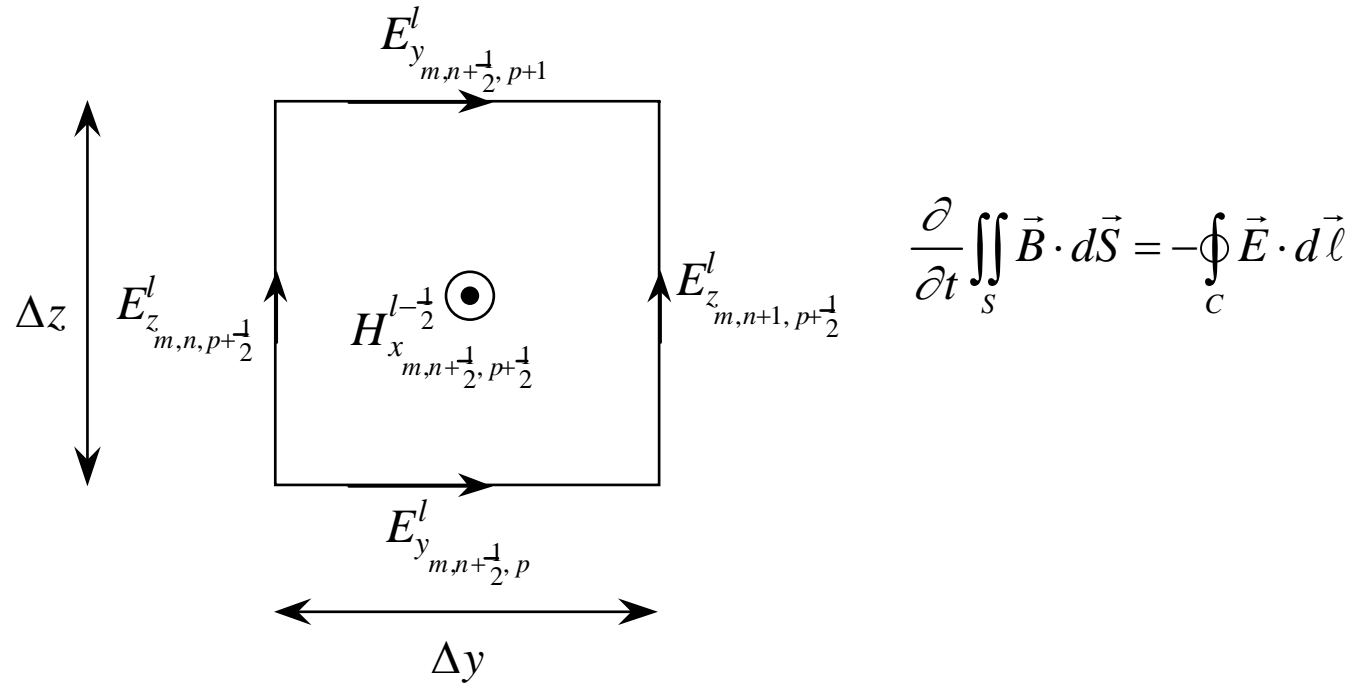
$$\begin{aligned} \frac{1}{\Delta t} \left[D_{x, i+\frac{1}{2}, j, k}^n - D_{x, i+\frac{1}{2}, j, k}^{n-1} \right] &= \frac{1}{\Delta y} \left[H_{z, i+\frac{1}{2}, j+\frac{1}{2}, k}^{n-\frac{1}{2}} - H_{z, i+\frac{1}{2}, j-\frac{1}{2}, k}^{n-\frac{1}{2}} \right] - \\ &\quad \frac{1}{\Delta z} \left[H_{y, i+\frac{1}{2}, j, k+\frac{1}{2}}^{n-\frac{1}{2}} - H_{y, i+\frac{1}{2}, j, k-\frac{1}{2}}^{n-\frac{1}{2}} \right] - J_{x, i+\frac{1}{2}, j, k}^{n-\frac{1}{2}} \end{aligned}$$

YEE-CELL (PRIMARY LATTICE CELL)



- Assumptions:
 - Discrete Vector Electric Fields are parallel to and are constant along the edges of the *Primary* Lattice.
 - Discrete Vector Magnetic Fields are normal to and constant throughout each face of the Primary Lattice.
 - Discrete Vector Magnetic Fields are parallel to and are constant along the edges of the *Secondary* Lattice.
 - Discrete Vector Electric Fields are normal to and constant throughout each face of the Secondary Lattice.
- Secondary Lattice edges connect the cell centers of the Primary Lattice.

DERIVATION OF YEE-ALGORITHM FROM MAXWELL'S EQUATIONS IN INTEGRAL FORM



Let $d\vec{S} = \hat{x}dydz$. Then, within the discrete space:

$$\frac{\Delta z \Delta y}{\Delta t} \left[B_{x, j+\frac{1}{2}, k+\frac{1}{2}}^{n+\frac{1}{2}} - B_{x, j+\frac{1}{2}, k+\frac{1}{2}}^{n-\frac{1}{2}} \right] = - \left[E_{y, j+\frac{1}{2}, k}^n \Delta y + E_{z, j+1, k+\frac{1}{2}}^n \Delta z - E_{y, j+\frac{1}{2}, k+1}^n \Delta y - E_{z, j, k+\frac{1}{2}}^n \Delta z \right]$$

$$\frac{\Delta z \Delta y}{\Delta t} \left[B_{x, j+\frac{1}{2}, k+\frac{1}{2}}^{n+\frac{1}{2}} - B_{x, j+\frac{1}{2}, k+\frac{1}{2}}^{n-\frac{1}{2}} \right] = - \left[E_{y, j+\frac{1}{2}, k}^n \Delta y + E_{z, j+\frac{1}{2}, k+\frac{1}{2}}^n \Delta z \right. \\ \left. - E_{y, j+\frac{1}{2}, k+1}^n \Delta y - E_{z, j, k+\frac{1}{2}}^n \Delta z \right]$$

Multiply this expression by $1/\Delta z \Delta y$ leads to

$$B_{x, j+\frac{1}{2}, k+\frac{1}{2}}^{n+\frac{1}{2}} = B_{x, j+\frac{1}{2}, k+\frac{1}{2}}^{n-\frac{1}{2}} + \frac{\Delta t}{\Delta z} \left[E_{y, j+\frac{1}{2}, k+1}^n - E_{y, j+\frac{1}{2}, k}^n \right] - \\ \frac{\Delta t}{\Delta y} \left[E_{z, j+1, k+\frac{1}{2}}^n - E_{z, j, k+\frac{1}{2}}^n \right]$$

Similarly, from a Secondary Lattice Face:

$$D_{x, i+\frac{1}{2}, j, k}^n = D_{x, i+\frac{1}{2}, j, k}^{n-1} + \frac{\Delta t}{\Delta y} \left[H_{z, i+\frac{1}{2}, j+\frac{1}{2}, k}^{n-\frac{1}{2}} - H_{z, i+\frac{1}{2}, j-\frac{1}{2}, k}^{n-\frac{1}{2}} \right] - \\ \frac{\Delta t}{\Delta z} \left[H_{y, i+\frac{1}{2}, j, k+\frac{1}{2}}^{n-\frac{1}{2}} - H_{y, i+\frac{1}{2}, j, k-\frac{1}{2}}^{n-\frac{1}{2}} \right] - J_{x, i+\frac{1}{2}, j, k}^{n-\frac{1}{2}}$$

Similar approximations for the remaining components of **B** and **D** are also derived.

STABILITY

- The study of the one-dimensional problem demonstrated that the explicit update scheme was conditionally stable. The stability of the three-dimensional scheme is also conditionally stable. Stability is again analyzed here using a Von Neumann scheme. Specifically, all the fields will be expanded into a Fourier Plane Wave Spectrum, which can be thought of as a plane wave expansion, e.g. $\vec{E} = \vec{E}_o e^{-jk_x x - jk_y y - jk_z z}$.
- Following the analogy of the 1D problem, The 6 update equations are written as a coupled 2nd order difference operator:

$$x^{n+1} = 2j[A]x^{n+\frac{1}{2}} + x^n$$

$$x^n = \begin{bmatrix} E_x^n \\ E_y^n \\ E_z^n \\ H_x^n \\ H_y^n \\ H_z^n \end{bmatrix} [A] = \begin{bmatrix} 0 & 0 & 0 & 0 & \eta S_z & -\eta S_y \\ 0 & 0 & 0 & -\eta S_z & 0 & \eta S_x \\ 0 & 0 & 0 & \eta S_y & -\eta S_x & 0 \\ 0 & -S_z/\eta & S_y/\eta & 0 & 0 & 0 \\ S_z/\eta & 0 & -S_x/\eta & 0 & 0 & 0 \\ -S_y/\eta & S_x/\eta & 0 & 0 & 0 & 0 \end{bmatrix}$$

where:

$$S_x = \frac{c\Delta t \sin\left(\frac{k_x\Delta x}{2}\right)}{\Delta x}, S_y = \frac{c\Delta t \sin\left(\frac{k_y\Delta y}{2}\right)}{\Delta y}, S_z = \frac{c\Delta t \sin\left(\frac{k_z\Delta z}{2}\right)}{\Delta z}$$

- From the previous analysis, it is sufficient to show that a stable solution requires $|\lambda_A| < 1$ (strict stability).
- Computing the eigenvalues using Maple™, shows there are two sets of degenerate eigenvalues:

$$\lambda_A = 0, \pm \sqrt{S_x^2 + S_y^2 + S_z^2}$$

STABILITY CONTINUED

- Note that stability requires $|\lambda_A| < 1$ for all Fourier Harmonics. Therefore, one needs to choose the maximum eigenvalues for all k_x , k_y , and k_z . To this end,

$$\max(S_x) = \frac{c\Delta t}{\Delta x}, \quad \max(S_y) = \frac{c\Delta t}{\Delta y}, \quad \max(S_z) = \frac{c\Delta t}{\Delta z}$$

- Enforcing $|\lambda_A| < 1$, this leads to the strict stability limit:

$$\Delta t < \frac{1}{c} \frac{1}{\sqrt{\frac{1}{\Delta x^2} + \frac{1}{\Delta y^2} + \frac{1}{\Delta z^2}}}$$

- The CFL (Courant-Friedrichs-Lewy) number is expressed as:

$$CFL = \Delta t c \sqrt{\frac{1}{\Delta x^2} + \frac{1}{\Delta y^2} + \frac{1}{\Delta z^2}} < 1$$

- Thus, the CFL number must always be less than unity for strict stability. For the sake of numerical dispersion, one typically wants to run the simulation with as large a CFL number as possible. This will be demonstrated when studying dispersion error.

GAUSS' LAWS

- For the Yee-algorithm to be well-posed, the approximate fields must also satisfy Gauss' Laws. If the fields do not satisfy Gauss' Laws, then spurious charge will result, leading to an erroneous solution.
- It will be shown that Gauss' Laws are satisfied in a global sense, by treating each unit cell individually.
- Electric Flux:

- Gauss' Law

$$\oiint_S \vec{D} \cdot d\vec{s} = \iiint_V \rho dV = 0 \Big|_{\text{charge free media}}$$

- Differentiate with respect to time:

$$\frac{\partial}{\partial t} \oiint_S \vec{D} \cdot d\vec{s} = 0$$

- Integrate over a single Yee-cell, and superimpose faces

$$\frac{\partial}{\partial t} \oiint_S \vec{D} \cdot d\vec{s} = \sum_{i=1}^6 \frac{\partial}{\partial t} \iint_{S_i} \vec{D} \cdot d\vec{s}_i = \sum_{i=1}^6 \oint_{C_i} \vec{H} \cdot d\vec{\ell} \stackrel{?}{=} 0$$

- The line integrals of the magnetic fields around the contours bounding the cell faces will cancel out along each edge. Therefore, the right-hand-side is zero.
- Since this is true for all time-dependent fields in a source free media, then we can conclude for the discrete fields that Gauss' law is satisfied over each Yee-cell.

$$\oiint_{S_{\text{Yee-cell}}} \vec{D} \cdot d\vec{s} = 0$$

NUMERICAL DISPERSION

- Due to the 2nd-Order Nature of the Algorithm, the Discrete Solution is Inherently Dispersive. A Harmonic Analysis based on the Discrete Operators can Again be Performed, as Discussed in Section 4. This Leads to the Dispersion Relationship:

$$\frac{1}{c^2 \Delta t^2} \sin^2 \left(\frac{\omega \Delta t}{2} \right) = \frac{1}{\Delta x^2} \sin^2 \left(\frac{\tilde{k}_x \Delta x}{2} \right) + \frac{1}{\Delta y^2} \sin^2 \left(\frac{\tilde{k}_y \Delta y}{2} \right) + \frac{1}{\Delta z^2} \sin^2 \left(\frac{\tilde{k}_z \Delta z}{2} \right)$$

- Limit $\Delta t, \Delta x, \Delta y, \Delta z \rightarrow 0$:

$$\frac{(\omega \Delta t)^2}{c^2 \Delta t^2} = \frac{(\tilde{k}_x \Delta x)^2}{\Delta x^2} + \frac{(\tilde{k}_y \Delta y)^2}{\Delta y^2} + \frac{(\tilde{k}_z \Delta z)^2}{\Delta z^2}$$

or

$$k^2 = \tilde{k}_x^2 + \tilde{k}_y^2 + \tilde{k}_z^2$$

DISPERSION RELATIONSHIP FOR THE DISCRETE SPACE:

Plane Wave Expansion of the field components, e.g.,

$$E_z = E_o e^{-j(\tilde{k} \cos \phi \sin \theta x + \tilde{k} \sin \phi \sin \theta y + \tilde{k} \cos \theta z)}$$

Leads to the Dispersion Relationship:

$$\frac{1}{\Delta x^2} \sin^2 \left(\frac{\tilde{k}_x \Delta x}{2} \right) + \frac{1}{\Delta y^2} \sin^2 \left(\frac{\tilde{k}_y \Delta y}{2} \right) + \frac{1}{\Delta z^2} \sin^2 \left(\frac{\tilde{k}_z \Delta z}{2} \right) - \frac{1}{c \Delta t^2} \sin^2 \left(\frac{\omega \Delta t}{2} \right) = 0$$

Let,

$$\tilde{k}_x = \tilde{k} \cos \phi \sin \theta, \quad \tilde{k}_y = \tilde{k} \sin \phi \sin \theta, \quad \tilde{k}_z = \tilde{k} \cos \theta$$

Then solve for \tilde{k} using a non-linear solver. Again, use Newton's method [Numerical Recipes]:

$$\tilde{k}_{i+1} = \tilde{k}_i - \frac{f(\tilde{k}_i)}{f'(\tilde{k}_i)}$$

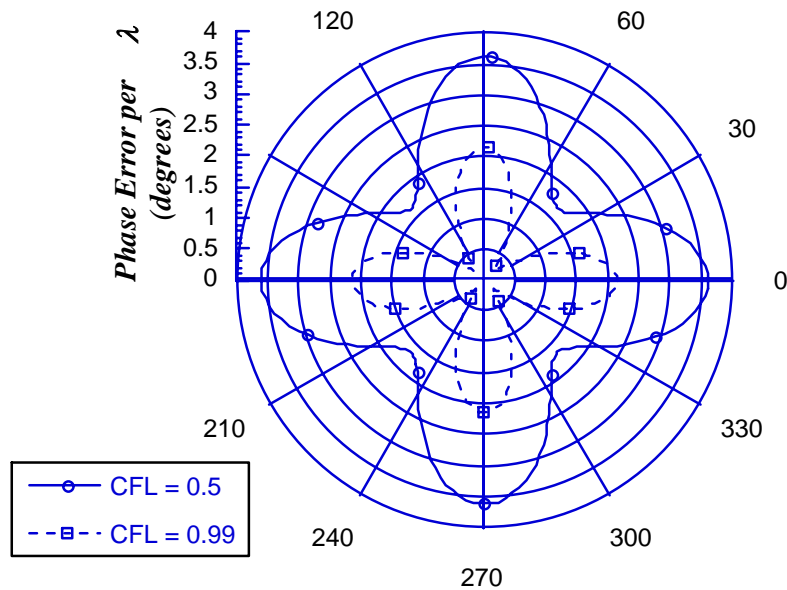
where the initial condition is assumed to be: $\tilde{k}_0 = 2\pi / \lambda$. This method converges in a few iterations.

- From \tilde{k} the numerical phase velocity is estimated ($\tilde{v}_p = \omega / \tilde{k}$) and the phase error is estimated as a function of ϕ and θ .

NUMERICAL DISPERSION 3-DIMENSIONS

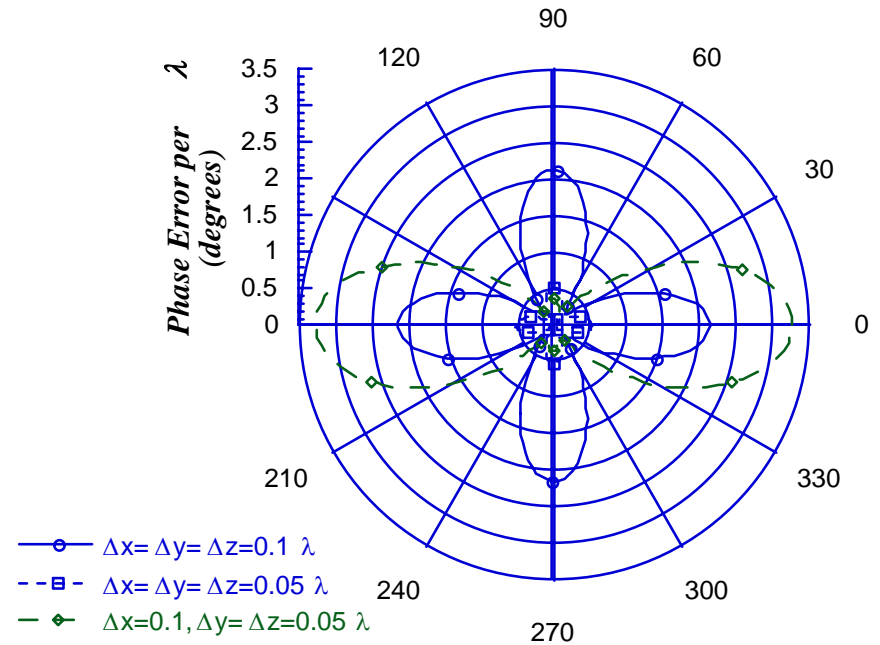
Dispersion vs. CFL Number

($\theta = 90^\circ$, $\Delta x = \Delta y = \Delta z = 0.1 \lambda$)

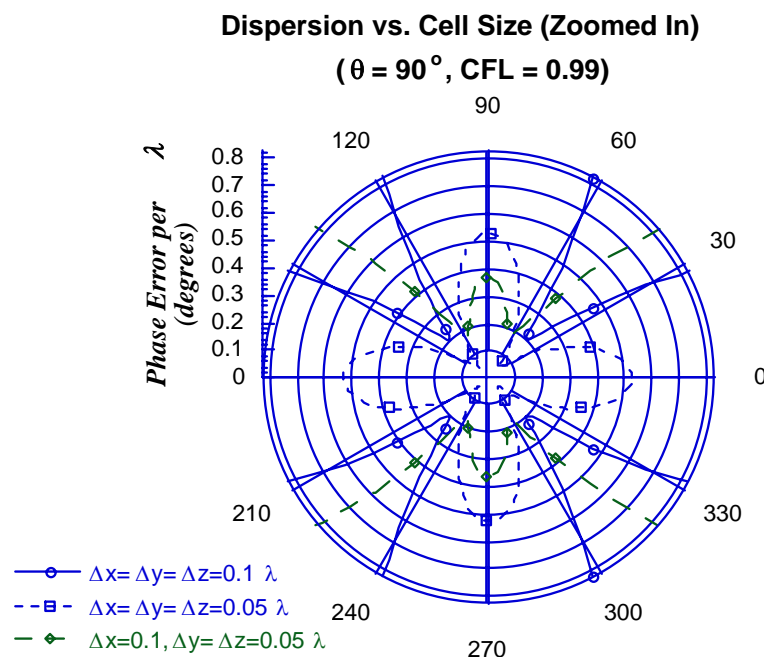


Dispersion vs. Cell Size

($\theta = 90^\circ$, CFL = 0.99)

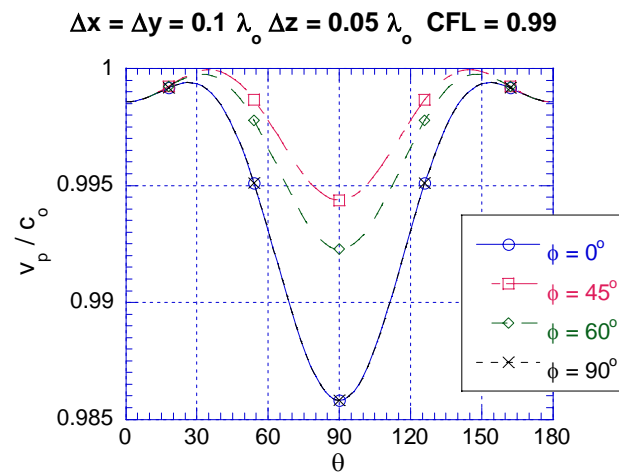
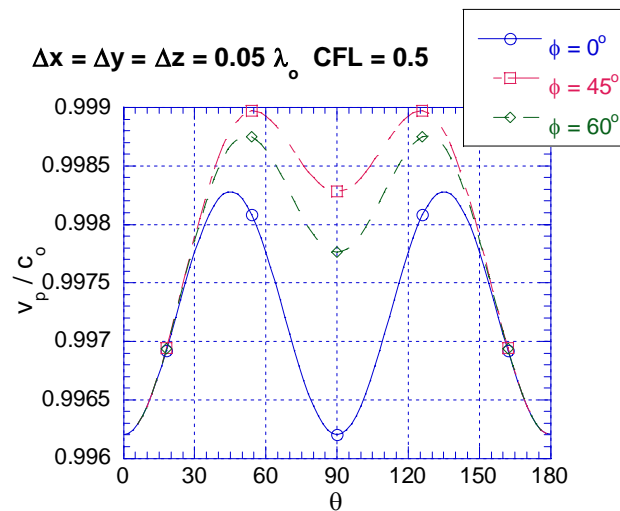
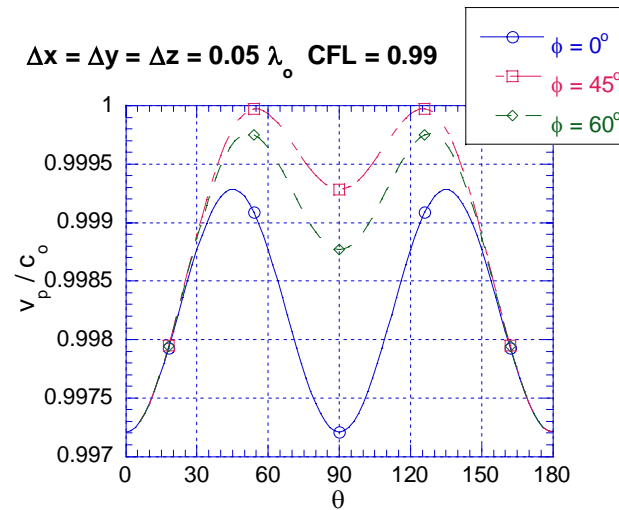
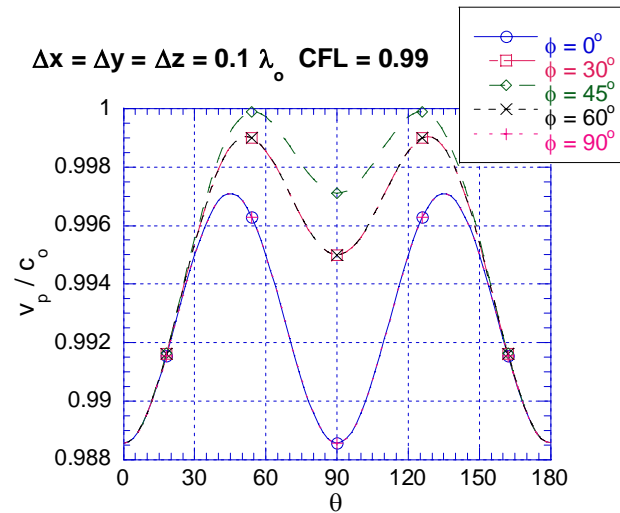


NUMERICAL DISPERSION 3-DIMENSIONS

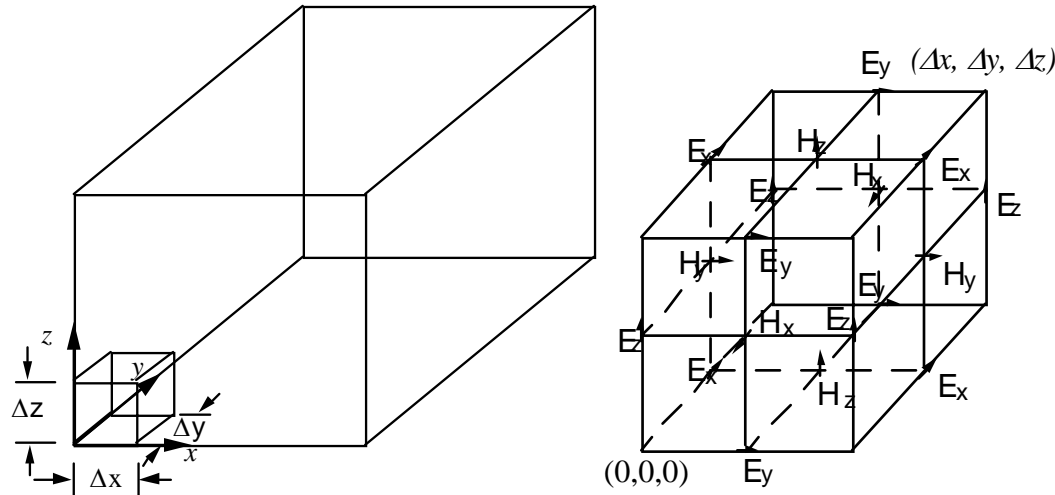


- The Numerical Grid is a Dispersive and Anisotropic Medium.
- Cell sizes should be on the order of $\lambda/15$ ($\sim 1^\circ$ error/ λ) to $\lambda/20$ ($\sim 0.5^\circ$ error/ λ).
- The CFL # should be as large as possible (0.999).
- Square meshes minimize anisotropy and phase error.
- This study assumes smooth boundaries. When geometric singularities are present in a model (e.g., the edge of a microstrip line) the fields typically become singular in their near vicinity. As a result, the spatial frequency spectrum of the fields in these regions are much higher, and much finer discretization will be needed (recall the error is $\propto f^{(3)}$.)

NUMERICAL DISPERSION 3-DIMENSIONS



Numerical Implementation



- Data Array Storage:

$$\tilde{E}_x(i, j, k) = E_x((i - \frac{1}{2})\Delta x, (j - 1)\Delta y, (k - 1)\Delta z)$$

$$\tilde{E}_y(i, j, k) = E_y((i - 1)\Delta x, (j - \frac{1}{2})\Delta y, (k - 1)\Delta z)$$

$$\tilde{E}_z(i, j, k) = E_z((i - 1)\Delta x, (j - 1)\Delta y, (k - \frac{1}{2})\Delta z)$$

$$\tilde{H}_x(i, j, k) = H_x((i - 1)\Delta x, (j - \frac{1}{2})\Delta y, (k - \frac{1}{2})\Delta z)$$

$$\tilde{H}_y(i, j, k) = H_y((i - \frac{1}{2})\Delta x, (j - 1)\Delta y, (k - \frac{1}{2})\Delta z)$$

$$\tilde{H}_z(i, j, k) = H_z((i - \frac{1}{2})\Delta x, (j - \frac{1}{2})\Delta y, (k - 1)\Delta z)$$

YEE-SCHEME

∴ Can Express Faraday's Law in Discrete Form as:

$$\begin{aligned}\tilde{H}_{x_{i,j,k}}^{n+\frac{1}{2}} &= \tilde{H}_{x_{i,j,k}}^{n-\frac{1}{2}} + \frac{\Delta t}{\mu\Delta z} \left[\tilde{E}_{y_{i,j,k+1}}^n - \tilde{E}_{y_{i,j,k}}^n \right] - \frac{\Delta t}{\mu\Delta y} \left[\tilde{E}_{z_{i,j+1,k}}^n - \tilde{E}_{z_{i,j,k}}^n \right] \\ \tilde{H}_{y_{i,j,k}}^{n+\frac{1}{2}} &= \tilde{H}_{y_{i,j,k}}^{n-\frac{1}{2}} + \frac{\Delta t}{\mu\Delta x} \left[\tilde{E}_{z_{i+1,j,k}}^n - \tilde{E}_{z_{i,j,k}}^n \right] - \frac{\Delta t}{\mu\Delta z} \left[\tilde{E}_{x_{i,j,k+1}}^n - \tilde{E}_{x_{i,j,k}}^n \right] \\ \tilde{H}_{z_{i,j,k}}^{n+\frac{1}{2}} &= \tilde{H}_{z_{i,j,k}}^{n-\frac{1}{2}} + \frac{\Delta t}{\mu\Delta y} \left[\tilde{E}_{x_{i,j+1,k}}^n - \tilde{E}_{x_{i,j,k}}^n \right] - \frac{\Delta t}{\mu\Delta x} \left[\tilde{E}_{y_{i+1,j,k}}^n - \tilde{E}_{y_{i,j,k}}^n \right]\end{aligned}$$

And can Express Ampere's Law in Discrete Form as:

$$\begin{aligned}\tilde{E}_{x_{i,j,k}}^{n+1} &= \tilde{E}_{x_{i,j,k}}^n - \frac{\Delta t}{\varepsilon\Delta z} \left[\tilde{H}_{y_{i,j,k}}^{n+\frac{1}{2}} - \tilde{H}_{y_{i,j,k-1}}^{n+\frac{1}{2}} \right] + \frac{\Delta t}{\varepsilon\Delta y} \left[\tilde{H}_{z_{i,j,k}}^{n+\frac{1}{2}} - \tilde{H}_{z_{i,j-1,k}}^{n+\frac{1}{2}} \right] \\ \tilde{E}_{y_{i,j,k}}^{n+1} &= \tilde{E}_{y_{i,j,k}}^n - \frac{\Delta t}{\varepsilon\Delta x} \left[\tilde{H}_{z_{i,j,k}}^{n+\frac{1}{2}} - \tilde{H}_{z_{i-1,j,k}}^{n+\frac{1}{2}} \right] + \frac{\Delta t}{\varepsilon\Delta z} \left[\tilde{H}_{x_{i,j,k}}^{n+\frac{1}{2}} - \tilde{H}_{x_{i,j,k-1}}^{n+\frac{1}{2}} \right] \\ \tilde{E}_{z_{i,j,k}}^{n+1} &= \tilde{E}_{z_{i,j,k}}^n - \frac{\Delta t}{\varepsilon\Delta y} \left[\tilde{H}_{x_{i,j,k}}^{n+\frac{1}{2}} - \tilde{H}_{x_{i,j-1,k}}^{n+\frac{1}{2}} \right] + \frac{\Delta t}{\varepsilon\Delta x} \left[\tilde{H}_{y_{i,j,k}}^{n+\frac{1}{2}} - \tilde{H}_{y_{i-1,j,k}}^{n+\frac{1}{2}} \right]\end{aligned}$$

Updates can be implemented using triple-vector loops for each field component. The bounds of the loops will be determined by the boundary conditions at the extremities of the lattice.

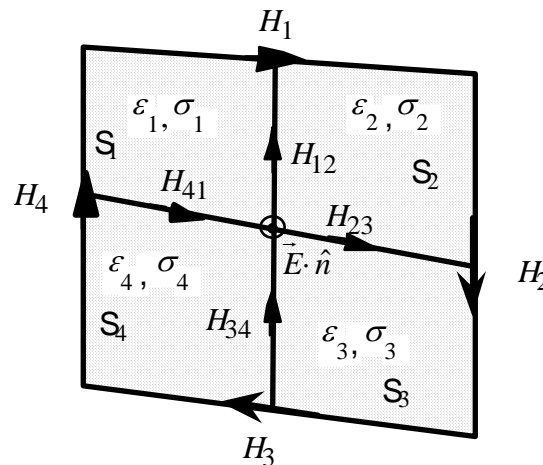
Treating Inhomogeneous Media

$$\frac{\partial D_x}{\partial t} + \sigma E_x = \frac{\partial H_z}{\partial y} - \frac{\partial H_y}{\partial z}$$

$$\frac{\partial D_y}{\partial t} + \sigma E_y = \frac{\partial H_x}{\partial z} - \frac{\partial H_z}{\partial x}$$

$$\frac{\partial D_z}{\partial t} + \sigma E_z = \frac{\partial H_y}{\partial x} - \frac{\partial H_x}{\partial y}$$

- Consider a Piece wise Homogeneous Medium. Let the Interface of this medium coincide with an edge of the Primary Lattice.
- The four regions surrounding the lattice are defined by the profile ε_i , σ_i , μ_o ($i = 1,2,3,4$)



Secondary cell face within an inhomogeneous medium.

$$\sum_{i=1}^4 \left(\frac{\partial}{\partial t} \iint_{S_i} \epsilon_i \vec{E} \cdot d\vec{s} + \iint_{S_i} \sigma_i \vec{E} \cdot d\vec{s} \right) = \sum_{i=1}^4 \left(\oint_{C_i} \vec{H} \cdot d\vec{\ell} \right)$$

- S_i is the surface of each sub-area that is bound by the contour C_i
- Perform the integrals over each S_i and the bounding C_i . For example, in region 1 leads to

$$\epsilon_1 \left(\frac{\vec{E}_1^{n+1} - \vec{E}_1^n}{\Delta t} \right) \cdot \hat{n} dA + \sigma_1 \left(\frac{\vec{E}_1^{n+1} + \vec{E}_1^n}{2} \right) \cdot \hat{n} dA =$$

$$\left[\vec{\ell}_1 \cdot \vec{H}_1^{n+\frac{1}{2}} - \vec{\ell}_{12} \cdot \vec{H}_{12}^{n+\frac{1}{2}} - \vec{\ell}_{41} \cdot \vec{H}_{41}^{n+\frac{1}{2}} + \vec{\ell}_4 \cdot \vec{H}_4^{n+\frac{1}{2}} \right]$$

- \vec{E}_1^n is the electric field in region 1, \hat{n} is the unit normal to the planar surface
- Repeat for Remaining Three Regions. Then Enforce the Continuity of the Tangential Electric Field:

$$\vec{E}_1^n \cdot \hat{n} = \vec{E}_2^n \cdot \hat{n} = \vec{E}_3^n \cdot \hat{n} = \vec{E}_4^n \cdot \hat{n}$$

- Adding the Results from the Four Regions:

$$\begin{aligned} & \left(\frac{\vec{E}_1^{n+1} - \vec{E}_1^n}{\Delta t} \right) \cdot \hat{n}(\varepsilon_1 + \varepsilon_2 + \varepsilon_3 + \varepsilon_4) dA + \\ & \left(\frac{\vec{E}_1^{n+1} + \vec{E}_1^n}{2} \right) \cdot \hat{n}(\sigma_1 + \sigma_2 + \sigma_3 + \sigma_4) dA = \\ & \left[\vec{\ell}_1 \cdot \vec{H}_1^{n+\frac{1}{2}} + \vec{\ell}_2 \cdot \vec{H}_2^{n+\frac{1}{2}} + \vec{\ell}_3 \cdot \vec{H}_3^{n+\frac{1}{2}} + \vec{\ell}_4 \cdot \vec{H}_4^{n+\frac{1}{2}} \right] \end{aligned}$$

- Since $dA = A/4$, this can be interpreted as an effective permittivity that is the average of the 4 surrounding regions:

$$\begin{aligned} \varepsilon_{ave} &= \frac{(\varepsilon_1 + \varepsilon_2 + \varepsilon_3 + \varepsilon_4)}{4} \\ \sigma_{ave} &= \frac{(\sigma_1 + \sigma_2 + \sigma_3 + \sigma_4)}{4} \end{aligned}$$

- Linear Interpolation of the Media. In the Discrete Space, the Media is not Truly Piece Wise Constant. Rather, it is Linearly Varying across a Discontinuity
- Second-Order Accurate Representation of an Inhomogeneous Interface.

Yee's Scheme in General Inhomogeneous Media

$$\begin{aligned}\tilde{H}_{x_{i,j,k}}^{n+\frac{1}{2}} = & \tilde{H}_{x_{i,j,k}}^{n-\frac{1}{2}} + \frac{\Delta t}{\mu_{i,j,k}\Delta z} \left[\tilde{E}_{y_{i,j,k+1}}^n - \tilde{E}_{y_{i,j,k}}^n \right] \\ & - \frac{\Delta t}{\mu_{i,j,k}\Delta y} \left[\tilde{E}_{z_{i,j+1,k}}^n - \tilde{E}_{z_{i,j,k}}^n \right]\end{aligned}$$

$$\begin{aligned}\tilde{E}_{x_{i,j,k}}^{n+1} = & \tilde{E}_{x_{i,j,k}}^n - \frac{\Delta t}{\varepsilon_{i,j,k}\Delta z} \left[\tilde{H}_{y_{i,j,k}}^{n+\frac{1}{2}} - \tilde{H}_{y_{i,j,k-1}}^{n+\frac{1}{2}} \right] \\ & + \frac{\Delta t}{\varepsilon_{i,j,k}\Delta y} \left[\tilde{H}_{z_{i,j,k}}^{n+\frac{1}{2}} - \tilde{H}_{z_{i,j-1,k}}^{n+\frac{1}{2}} \right]\end{aligned}$$

- Compute average ε for each edge of the primary lattice. Then store $\varepsilon_{i,j,k}$
- Compute average for μ for each edge of the secondary lattice and store $\mu_{i,j,k}$

Include File (fdtd.inc):

```
parameter(maxi=400,maxj=400,maxk=400, maxs=100)

real ex(maxi,maxj,maxk),ey(maxi,maxj,maxk),ez(maxi,maxj,maxk)
real hx(maxi,maxj,maxk),hy(maxi,maxj,maxk),hz(maxi,maxj,maxk)

integer is1(maxs),js1(maxs),ks1(maxs)
integer is2(maxs),js2(maxs),ks2(maxs)

common /efields/ ex,ey,ez
common /hfields/ hx,hy,hz
common /pec/ nsurf,is1,js1,ks2,is2,js2,ks2
```


H-Field Update

```

subroutine hupdate()
include 'fdtd. inc'
C
cx = co*dt/dx
cy = co*dt/dy
cz = co*dt/dz

do 10 k = 1,nk-1
  do 10 j = 1,ny-1
    do 10 i = 1,nx
      hx(i,j,k) = hx(i,j,k)+cz*(ey(i,j,k+1)-ey(i,j,k))
1      -cy*(ez(i,j+1,k)-ez(i,j,k))
10  continue

  do 20 k = 1,nk-1
    do 20 j = 1,ny
      do 20 i = 1,nx-1
        hy(i,j,k) = hy(i,j,k)+cx*(ez(i+1,j,k)-ez(i,j,k))
1        -cz*(ex(i,j,k+1)-ex(i,j,k))
1  continue
20  continue

  do 30 k = 1,nk
    do 30 j = 1,ny-1
      do 30 i = 1,nx-1
        hz(i,j,k) = hz(i,j,k)+cy*(ex(i,j+1,k)-ex(i,j,k))
1        -cx*(ey(i+1,j,k)-ey(i,j,k))
1  continue
30  continue

  return
end

```

E-Field Update (Lossless, Inhomogeneous)

```

subroutine eupdate()
include 'fdtd. inc'
C
cx = co*dt/dx
cy = co*dt/dy
cz = co*dt/dz

do 10 k = 2,nk-1                                ⇨ exclude exterior bdries at k=1 & k=nk
  do 10 j = 2,ny-1                                ⇨ exclude exterior bdries at j=1 & j=nj
    do 10 i = 1,nx-1
      ex(i,j,k) = ex(i,j,k) - cz*(hy(i,j,k) - hy(i,j,k-1))
1      +cy*(hz(i,j,k) - hz(i,j-1,k))/eps(iepx(i,j,k))
10  continue
C
  do 20 k = 2,nk-1
    do 20 j = 1,ny-1
      do 20 i = 2,nx-1
        ey(i,j,k) = ey(i,j,k) - cx*(hz(i,j,k) - hz(i-1,j,k))
1      +cz*(hx(i,j,k) - hx(i,j,k-1))/eps(iepy(i,j,k))
20  continue
C
  do 30 k = 1,nk-1
    do 30 j = 2,ny-1
      do 30 i = 2,nx-1
        ez(i,j,k) = ez(i,j,k) - cy*(hx(i,j,k) - hx(i,j-1,k))
1      +cx*(hy(i,j,k) - hy(i-1,j,k))/eps(iepz(i,j,k))
30  continue

  return
end

```

More Efficient Implementation of the Explicit Update Loops

- The number of floating-point operations can be further reduced by weighting the fields by their edge length, and normalize the magnetic field by η_o namely:

$$e_x = \Delta x E_x, \quad e_y = \Delta y E_y, \quad e_z = \Delta z E_z$$

$$h_x = \Delta x H_x / \eta_o, \quad h_y = \Delta y H_y / \eta_o, \quad h_z = \Delta z H_z / \eta_o$$

- Secondly, define $\text{eps}(i) = c_o \Delta t \Delta x / (\Delta y \Delta z \epsilon_r)$ The update loop can be rewriting as:

```

do 10 k = 2,nk-1
  do 10 j = 2,ny-1
    do 10 i = 1,nx-1
      ex(i,j,k) = ex(i,j,k) - (hy(i,j,k) - hy(i,j,k-1)
1      -hz(i,j,k) + hz(i,j-1,k)) * eps(iepx(i,j,k))
10 continue

```

- This has reduced the number of Floating point operations from $39 N$ to $33 N$ (~20 % speedup). Furthermore, we have eliminated a floating point division.
- Further speedup can be made on vector-based and RISC processor based computers via more advanced steps such as combining the three field update loops into a single loop, etc.[†].

[†] S. D. Gedney, "Finite-difference time-domain analysis of microwave circuit devices on high performance vector/parallel computers," *IEEE Trans. on MTT*, vol. 43, pp. 2510-2514, Oct. 1995.

SOURCE EXCITATIONS

- We have discussed 1D, 2D, and 3D FDTD Algorithms
 - Central Difference Approximations
 - Discrete Explicit Update Operations
 - Natural Boundary Conditions (PEC, PMC)
 - Inhomogeneous Media
- Need to Introduce Physical Source Models to Excite the Fields for Accurate Full Wave Analysis
- Choice of Source is Problem Dependent
 - Current Source (J_x , J_y , J_z , M_x , M_y , or M_z)
 - Voltage Source
 - Discrete Source Models (Thévenin or Norton)
 - Hard Source (eigen mode, fictitious voltage source)
 - Soft Source (analogous to current source)
 - Controlled Sources (non-linear device modeling)
 - Plane Wave Source

CURRENT SOURCES

- ELECTRIC CURRENT SOURCE

- Example: 2D, TM_z Polarization

$$-\frac{\partial B_x}{\partial t} = \frac{\partial E_z}{\partial y} \qquad \frac{\partial D_z}{\partial t} = \frac{\partial H_y}{\partial x} - \frac{\partial H_x}{\partial y} - J_z$$

$$\frac{\partial B_y}{\partial t} = \frac{\partial E_z}{\partial x}$$

- Discrete Form:

$$-\frac{B_{x_{i+1/2,j}}^{n+1/2} - B_{x_{i+1/2,j}}^{n-1/2}}{\Delta t} = \frac{E_{z_{i+1/2,j+1/2}}^n - E_{z_{i+1/2,j-1/2}}^n}{\Delta y}$$

$$-\frac{B_{y_{i,j+1/2}}^{n+1/2} - B_{y_{i,j+1/2}}^{n-1/2}}{\Delta t} = -\frac{E_{z_{i+1/2,j+1/2}}^n - E_{z_{i-1/2,j+1/2}}^n}{\Delta x}$$

$$\frac{D_{z_{i+1/2,j+1/2}}^{n+1} - D_{z_{i+1/2,j+1/2}}^n}{\Delta t} = \frac{H_{y_{i+1,j+1/2}}^{n+1/2} - H_{y_{i,j+1/2}}^{n+1/2}}{\Delta x} - \frac{H_{x_{i+1/2,j+1}}^{n+1/2} - H_{x_{i+1/2,j}}^{n+1/2}}{\Delta y} - \frac{(J_{z_{i+1/2,j+1/2}}^n + J_{z_{i+1/2,j+1/2}}^{n+1})}{2}$$

- Faraday's Law Remains Unchanged from Previous Analysis
- Ampere's Law leads to the explicit Update Expression:

$$E_{z_{i+1/2,j+1/2}}^{n+1} = E_{z_{i+1/2,j+1/2}}^n + \frac{\Delta t}{\varepsilon} \left[\frac{H_{y_{i+1,j+1/2}}^{n+1/2} - H_{y_{i,j+1/2}}^{n-1/2}}{\Delta x} - \frac{H_{x_{i+1/2,j+1}}^{n+1/2} - H_{x_{i+1/2,j}}^{n-1/2}}{\Delta y} - \frac{J_{z_{i+1/2,j+1/2}}^{n+1} + J_{z_{i+1/2,j+1/2}}^n}{2} \right]$$

- Applications: Current Sheet Excitation, Known Current Source

CURRENT SOURCES

- MAGNETIC CURRENT SOURCE
 - TE_z Polarization (M_z) - Dual of TM_z Electric Current Source (J_z)
 - TM_z Polarization (M_x, M_y)

- MAGNETIC CURRENT SOURCE
 - Example: 2D, TM_z Polarization

$$-\frac{\partial B_x}{\partial t} = \frac{\partial E_z}{\partial y} + M_x, \quad \frac{\partial B_y}{\partial t} = \frac{\partial E_z}{\partial x} + M_y$$

- Discrete Form:

$$H_{x_{i+1/2,j}}^{n+1/2} = H_{x_{i+1/2,j}}^{n-1/2} - \frac{\Delta t}{\mu} \left[\frac{E_{z_{i+1/2,j+1/2}}^n - E_{z_{i+1/2,j-1/2}}^n}{\Delta y} + \frac{M_{x_{i+1/2,j}}^{n+1/2} + M_{x_{i+1/2,j}}^{n-1/2}}{2} \right]$$

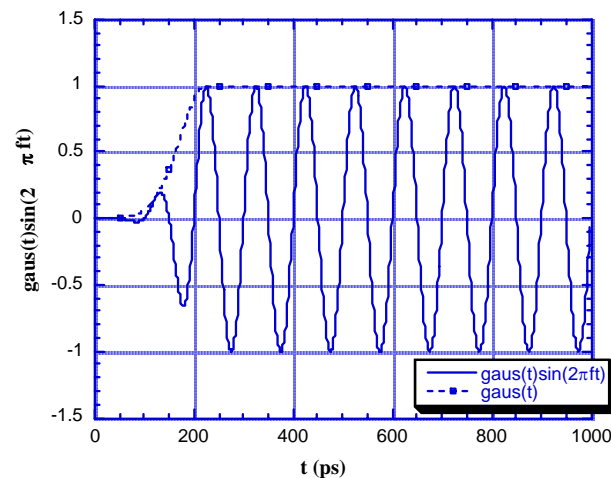
$$H_{y_{i,j+1/2}}^{n+1/2} = H_{y_{i,j+1/2}}^{n-1/2} + \frac{\Delta t}{\mu} \left[\frac{E_{z_{i+1/2,j+1/2}}^n - E_{z_{i-1/2,j+1/2}}^n}{\Delta x} + \frac{M_{y_{i,j+1/2}}^{n+1/2} + M_{y_{i,j+1/2}}^{n-1/2}}{2} \right]$$

- Observation
 - Magnetic Current Sources are Applied Along Secondary Grid Edges
 - Electric Current Sources are Applied Along Primary Grid Edges

TIME SIGNATURE OF SOURCES

- Initial Condition of Fields
 - E and H must be Specified Throughout Lattice
 - Must satisfy Maxwell's Equations throughout the entire space
 - Typically, Fields are Initialized to Zero
- At zero, source should be zero (if fields init. to zero), and smooth (\sim zero derivative).
- Typical Sources

1. CW response (ramped):
$$f(t) = \begin{cases} \sin(2\pi ft) \exp(-(t-t_o)^2 / t_w^2), & t \leq t_o \\ \sin(2\pi ft), & t > t_o \end{cases}$$



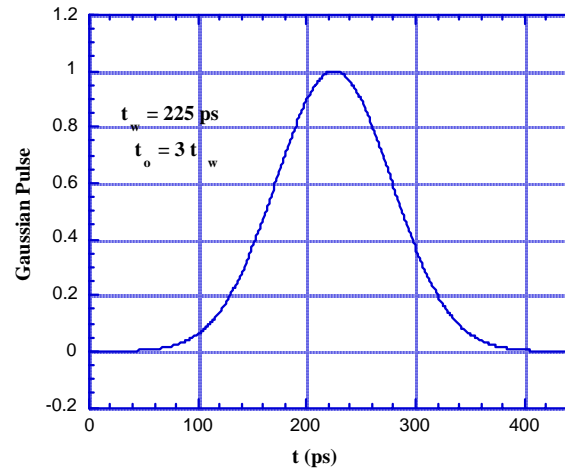
Broad Band Pulses with DC Component

2. Gaussian:

$$f(t) = \exp(-(t - t_o)^2 / t_w^2))$$

• Spectral Response:

$$F(f) = t_w \sqrt{\pi} \exp(-(\pi f)^2 t_w^2) \cdot \exp(-j2\pi f t_o)$$



Also a Gaussian Pulse centered
-3 dB Band Width $f_{-3\text{db}} = 1/\pi t_w$

at the Origin!

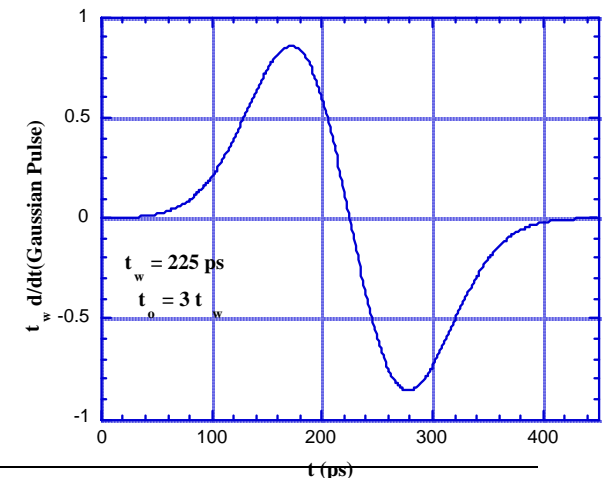
Broad Band Pulses with no DC Component

3. Gaussian Derivative:

$$f(t) = t_w \frac{\partial}{\partial t} \exp(-(t - t_o)^2 / t_w^2) = \frac{-2}{t_w} (t - t_o) \exp(-(t - t_o)^2 / t_w^2)$$

• Spectral Response:

$$F(f) = t_w^2 \sqrt{\pi} \exp(-(\pi f)^2 t_w^2) \cdot \exp(-j2\pi f t_o) \cdot j2\pi f$$



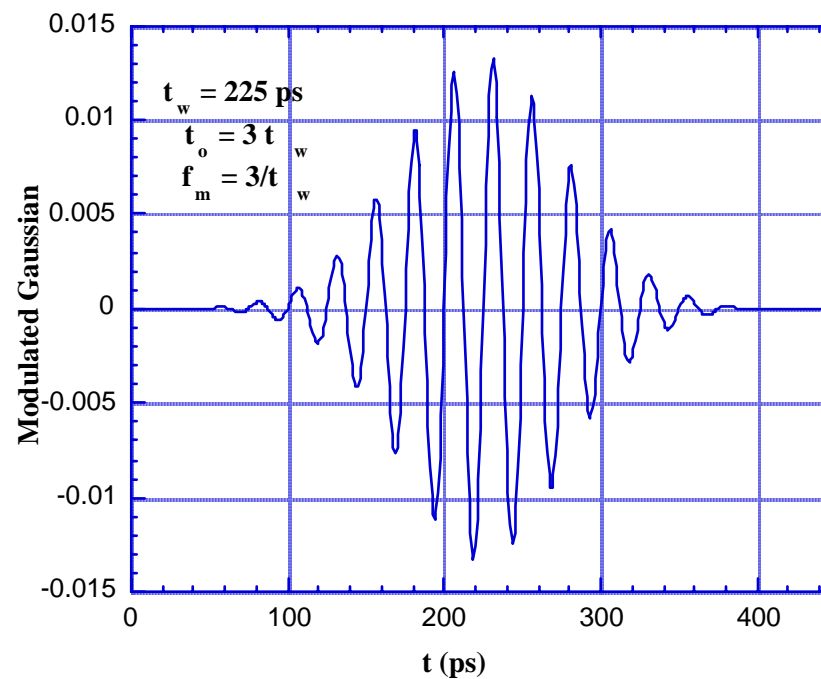
Broad Band Pulses with No DC (Continued)

- Modulated Gaussian:

$$f(t) = \exp(-(t - t_o)^2 / t_w^2) \cdot \sin(2\pi f_m t)$$

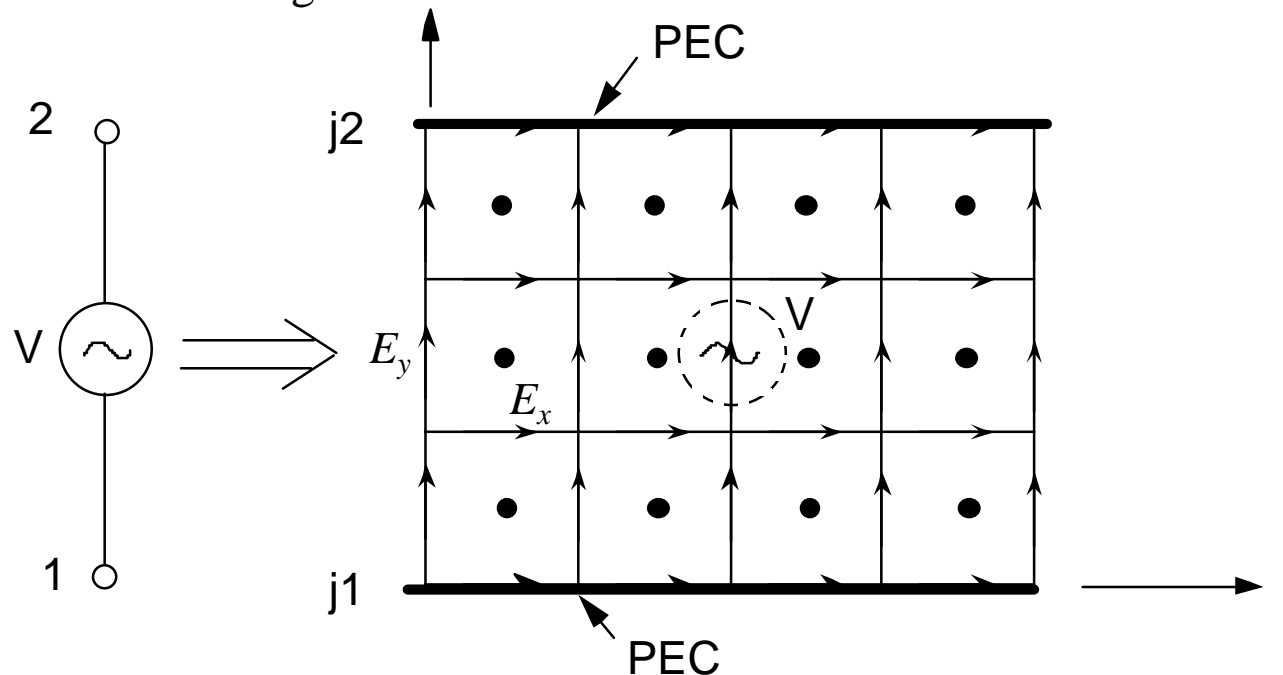
- Spectral Response:

$$F(f) = j \frac{\sqrt{\pi}}{t_w} \exp(-(\pi(f - f_m))^2 / t_w^2) \cdot \exp(-j2(f - f_m)ft_o)$$



VOLTAGE SOURCES

Discrete Voltage Source:



- Line Voltage:

$$V_{21} = -\int_1^2 \vec{E} \cdot d\vec{\ell} = -\sum_{j=j1}^{j2-1} E_{y_{i,j}} \Delta y$$

$$\therefore E_{y_{i,j}} = -\frac{V_{21}}{\Delta y(j2 - j1)}$$

- Hard Source:

$$E_{y_{i,j}}^n = -\frac{V_{21}^n}{\Delta y(j2 - j1)}; \quad j1 \leq j < j2$$

- Soft Source:

$$E_{y_{i,j}}^n = E_{y_{i,j}}^n - \frac{V_{21}^n}{\Delta y(j2 - j1)}; \quad j1 \leq j < j2$$

DISCRETE SOURCE MODELS WITH LUMPED LOADS

- Ampere's Law

$$\oint \vec{H} \cdot d\vec{\ell} = \int \frac{\partial \vec{D}}{\partial t} \cdot d\vec{s} + \int \sigma \vec{E} \cdot d\vec{s} + \int \vec{J} \cdot d\vec{s}$$

- Total Current

$$I = \int \frac{\partial \vec{D}}{\partial t} \cdot d\vec{s} + \int \sigma \vec{E} \cdot d\vec{s} + \int \vec{J} \cdot d\vec{s}$$

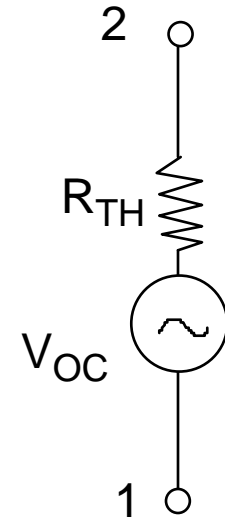
or,

$$I = I_d + I_c + I_l$$

I_d = displacement current,

I_c = conduction current,

I_l = impressed current, or the lumped current.



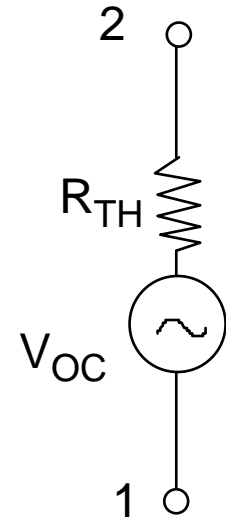
Expressing:

$$V_{21} = -\int_1^2 \vec{E} \cdot d\vec{\ell}$$

- Express Lumped Current Using a Voltage/Current Relationship

$$I_l = f(V_{21}) = f\left(\int_1^2 \vec{E} \cdot d\vec{\ell}\right)$$

- For Understanding, Let $V_{oc} = 0$ (Resistive Load Only). Thus, $I_l = V_{21}/R_{lTH}$.



LUMPED RESISTANCE

- Relationship for Lumped Resistance $I_l = V_{2l}/R_l$.
- Evaluate Ampere's Law over a Secondary Lattice Face:

$$\oint \vec{H} \cdot d\vec{\ell} = \int \frac{\partial \vec{D}}{\partial t} \cdot d\vec{s} + \int \sigma \vec{E} \cdot d\vec{s} + \int \vec{J} \cdot d\vec{s}$$

$$\left[\left(H_{z_{i+\frac{1}{2},j+\frac{1}{2},k}}^{n-\frac{1}{2}} - H_{z_{m+\frac{1}{2},n-\frac{1}{2},p}}^{n-\frac{1}{2}} \right) \Delta z - \left(H_{y_{i+\frac{1}{2},j,k+\frac{1}{2}}}^{n-\frac{1}{2}} - H_{y_{i+\frac{1}{2},j,k-\frac{1}{2}}}^{n-\frac{1}{2}} \right) \Delta y \right] = \frac{D_{x_{i+\frac{1}{2},j,k}}^n - D_{x_{i+\frac{1}{2},j,k}}^{n-1}}{\Delta t} \Delta y \Delta z + I_l^{n-\frac{1}{2}}$$

- From Voltage Current Relationship:

$$I_{l_{i+\frac{1}{2},j,k}}^{n-\frac{1}{2}} = \frac{V_{l_{i+\frac{1}{2},j,k}}^{n-\frac{1}{2}}}{R} = \frac{E_{x_{i+\frac{1}{2},j,k}}^{n-\frac{1}{2}} \Delta x}{R} = \frac{\Delta x}{R} \frac{E_{x_{i+\frac{1}{2},j,k}}^n + E_{x_{i+\frac{1}{2},j,k}}^{n-1}}{2}$$

- Inserting this Back into Ampere's Law (Discrete) Leads to:

$$\left[\left(H_{z_{i+\frac{1}{2},j+\frac{1}{2},k}}^{n-\frac{1}{2}} - H_{z_{m+\frac{1}{2},n-\frac{1}{2},p}}^{n-\frac{1}{2}} \right) \Delta z - \left(H_{y_{i+\frac{1}{2},j,k+\frac{1}{2}}}^{n-\frac{1}{2}} - H_{y_{i+\frac{1}{2},j,k-\frac{1}{2}}}^{n-\frac{1}{2}} \right) \Delta y \right] =$$

$$\varepsilon \frac{E_{x_{i+\frac{1}{2},j,k}}^n - E_{x_{i+\frac{1}{2},j,k}}^{n-1}}{\Delta t} \Delta y \Delta z + \frac{\Delta x}{R} \frac{E_{x_{i+\frac{1}{2},j,k}}^n + E_{x_{i+\frac{1}{2},j,k}}^{n-1}}{2}$$

- Explicit Update Expression:

$$E_{x_{i+\frac{1}{2},j,k}}^n = \frac{\frac{\varepsilon}{\Delta t} - \frac{\Delta x}{\Delta y \Delta z 2R}}{\frac{\varepsilon}{\Delta t} + \frac{\Delta x}{\Delta y \Delta z 2R}} E_{x_{i+\frac{1}{2},j,k}}^{n-1} + \frac{1}{\frac{\varepsilon}{\Delta t} + \frac{\Delta x}{\Delta y \Delta z 2R}} \cdot \left[\left(H_{z_{i+\frac{1}{2},j+\frac{1}{2},k}}^{n-\frac{1}{2}} - H_{z_{m+\frac{1}{2},n-\frac{1}{2},p}}^{n-\frac{1}{2}} \right) / \Delta y - \left(H_{y_{i+\frac{1}{2},j,k+\frac{1}{2}}}^{n-\frac{1}{2}} - H_{y_{i+\frac{1}{2},j,k-\frac{1}{2}}}^{n-\frac{1}{2}} \right) / \Delta z \right]$$

- Comparing with Previous Update Expressions For Lossy Media
 - Locally Lossy Media with $\sigma_{eff} = \frac{\Delta x}{\Delta y \Delta z R}$ (s/m)
 - Expression is Stable (local C. L. is less restrictive than lossless case)
 - Lumped Resistance Has an Effective Width of Secondary Grid Face, and Effective Length of Grid Edge

DISCRETE VOLTAGE SOURCE

- KVL:

$$V_{12} = I_l R_{TH} - V_{oc} \rightarrow I_l = (V_{12} + V_{oc})/R_{TH}$$

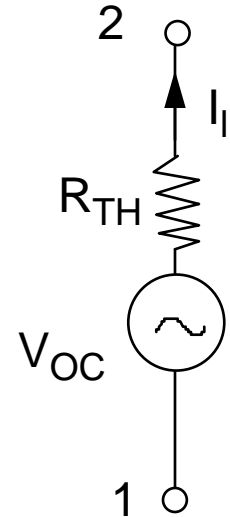
- In the Discrete Space:

$$I_{l_{i+\frac{1}{2},j,k}}^{n-\frac{1}{2}} = \frac{\left(E_{x_{i+\frac{1}{2},j,k}}^n + E_{x_{i+\frac{1}{2},j,k}}^{n-1} \right) \Delta x + 2V_{oc_{i+\frac{1}{2},j,k}}^{n-\frac{1}{2}}}{2R_{TH}}$$

- Applying this Discrete Form to Ampere's Law Leads to:

$$E_{x_{i+\frac{1}{2},j,k}}^n = \frac{\frac{\varepsilon}{\Delta t} - \frac{\Delta x}{\Delta y \Delta z 2R_{TH}}}{\frac{\varepsilon}{\Delta t} + \frac{\Delta x}{\Delta y \Delta z 2R_{TH}}} E_{x_{i+\frac{1}{2},j,k}}^{n-1} + \frac{1}{\frac{\varepsilon}{\Delta t} + \frac{\Delta x}{\Delta y \Delta z 2R_{TH}}} \cdot \left[\left(H_{z_{i+\frac{1}{2},j+\frac{1}{2},k}}^{n-\frac{1}{2}} - H_{z_{m+\frac{1}{2},n-\frac{1}{2},p}}^{n-\frac{1}{2}} \right) / \Delta y - \left(H_{y_{i+\frac{1}{2},j,k+\frac{1}{2}}}^{n-\frac{1}{2}} - H_{y_{i+\frac{1}{2},j,k-\frac{1}{2}}}^{n-\frac{1}{2}} \right) / \Delta z - \frac{V_{oc_{i+\frac{1}{2},j,k}}^{n-\frac{1}{2}}}{\Delta y \Delta z R_{TH}} \right]$$

- Implement as a Soft Source (to maintain Vectorization).
- Represents a Physical Source with Internal Resistance.



TOTAL FIELD SCATTERED FIELD FORMULATIONS **(PLANE WAVE)**

- Plane Wave Excitation Poses Challenge Since It Cannot Be Easily Generated By Finite Sources, as Posed Previously, in a Finite Volume
- Number of Techniques Have Been Presented To Excite Plane Wave. Most are Based on a Decomposition of the Total Field into Scattered and Incident Fields, i.e.,

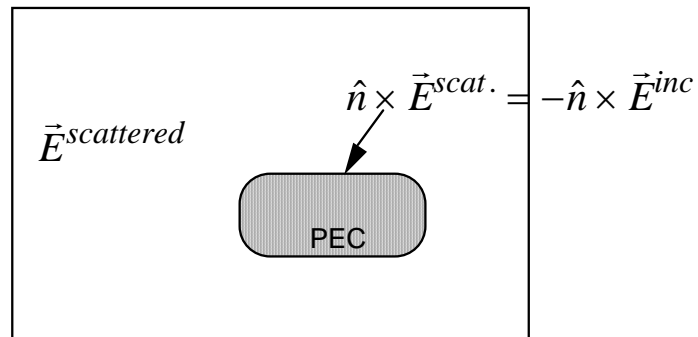
$$\vec{E}^{total} = \vec{E}^{inc} + \vec{E}^{scattered}, \quad \vec{H}^{total} = \vec{H}^{inc} + \vec{H}^{scattered}$$

where, the incident fields satisfy Maxwell's equations for a homogeneous free space:

$$\nabla \times \vec{E}^{inc} = -\mu_o \frac{\partial \vec{H}^{inc}}{\partial t}, \quad \nabla \times \vec{H}^{inc} = \varepsilon_o \frac{\partial \vec{E}^{inc}}{\partial t}$$

- Popular Techniques:
 1. Superimpose Scattered Field and Incident Fields Throughout the Space, where incident field is known.
 - problem: Have to include non-linear numerical dispersion in incident field

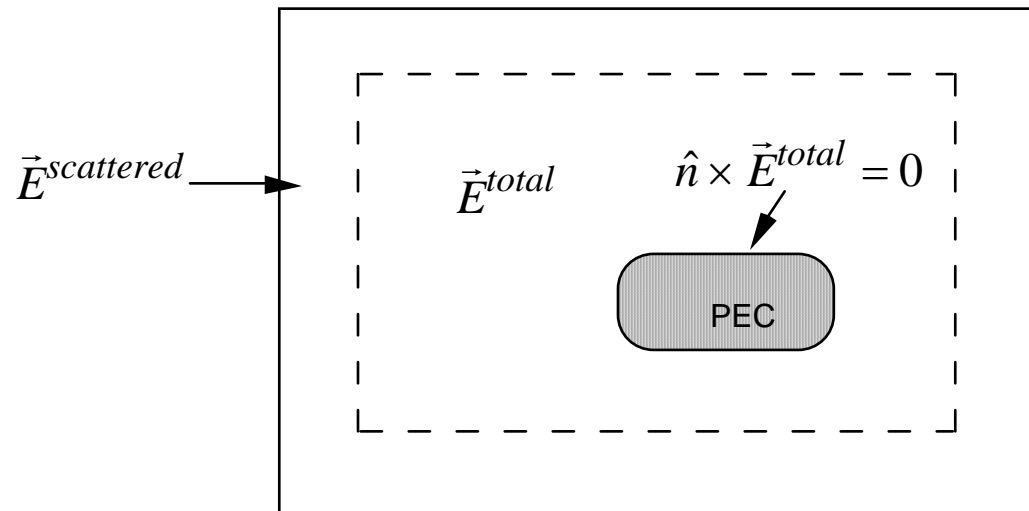
2. Solve for the Scattered Field Only.
 - Incident Field Arises from Boundary Conditions!
 - surface sources for perfectly conductor boundaries
 - volume sources for dielectric/magnetic medium



3. Solve for Total Field in the Interior Region of the Mesh, including all inhomogeneities, and Compute Scattered Field at the Extremities of the Mesh. Source is Excited at the Interface Between the Two Regions

TOTAL FIELD - SCATTERED FIELD FORMULATION

- Plane Wave Excited at the Interface Between the Total Field Region and the Scattered Field Region:



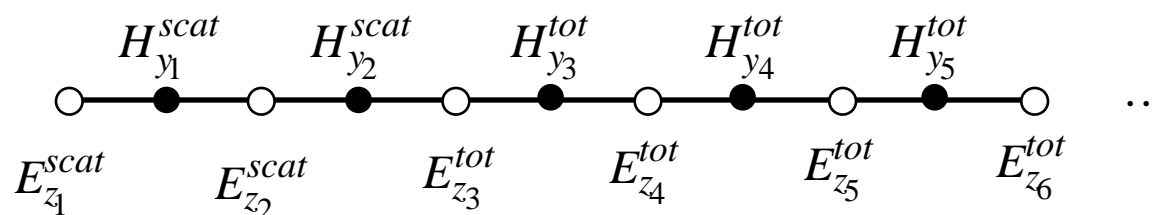
- At the Interface, make use of the fact that

$$\vec{E}^{total} = \vec{E}^{inc} + \vec{E}^{scattered}, \quad \vec{H}^{total} = \vec{H}^{inc} + \vec{H}^{scattered}$$

to transition between the scattered and total field regions

- Subsequently, the incident field is excited about the surface defining the interface between the two regions

One-Dimensional Example



- Updates in Total Field Region:

$$E_{z_i}^{tot^{n+1}} = E_{z_i}^{tot^n} + \frac{\Delta t}{\epsilon \Delta x} \left(H_{y_i}^{tot^{n+\frac{1}{2}}} - H_{y_{i-1}}^{tot^{n+\frac{1}{2}}} \right)$$

- Updates in Scattered Field Region:

$$E_{z_i}^{scat^{n+1}} = E_{z_i}^{scat^n} + \frac{\Delta t}{\epsilon \Delta x} \left(H_{y_i}^{scat^{n+\frac{1}{2}}} - H_{y_{i-1}}^{scat^{n+\frac{1}{2}}} \right)$$

- Update at the Interface

$$E_{z_3}^{tot^{n+1}} = E_{z_3}^{tot^n} + \frac{\Delta t}{\epsilon \Delta x} \left(H_{y_3}^{tot^{n+\frac{1}{2}}} - H_{y_2}^{scat^{n+\frac{1}{2}}} \right) - \frac{\Delta t}{\epsilon \Delta x} \left(H_{y_2}^{inc^{n+\frac{1}{2}}} \right)$$

- Similarly:

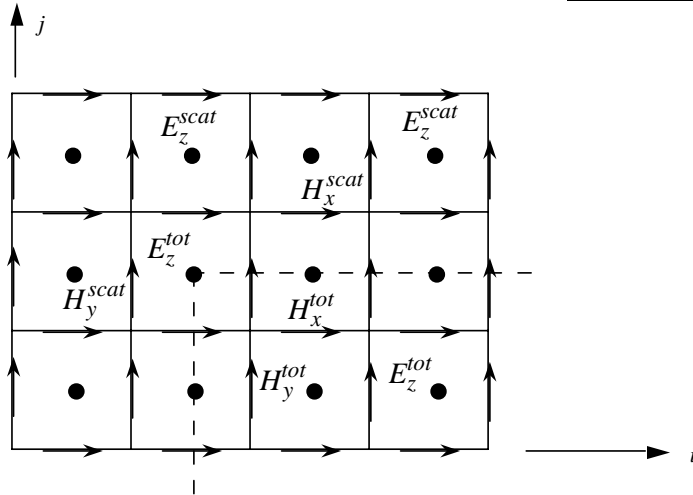
$$H_{y_2}^{scat^{n+\frac{1}{2}}} = H_{y_2}^{scat^{n-\frac{1}{2}}} + \frac{\Delta t}{\mu \Delta x} \left(E_{z_3}^{tot^n} - E_{z_2}^{scat^n} \right) - \frac{\Delta t}{\mu \Delta x} \left(E_{z_3}^{inc^n} \right)$$

- Incident fields satisfy independently Maxwell's equations for a homogeneous free space. For example, solution for a monochromatic plane wave propagating in the x-direction:

$$H_{y_2}^{inc^{n+\frac{1}{2}}} = -E_{z_0} \cos \left(\omega \left(n + \frac{1}{2} \right) \Delta t - \beta \left(\frac{5}{2} \Delta x \right) \right) / \eta$$

$$E_{z_3}^{inc^n} = E_{z_0} \cos \left(\omega n \Delta t - \beta (3 \Delta x) \right)$$

Two-Dimensions (TM_z)



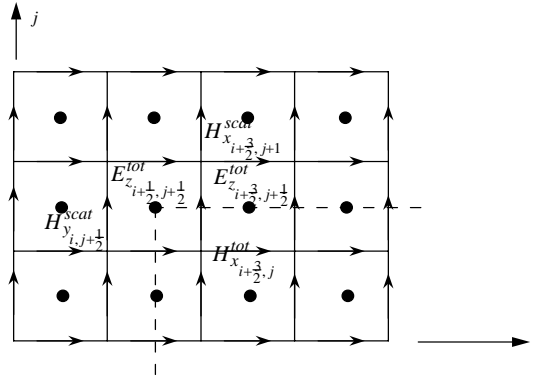
Total Field Region:

$$H_{x_{i+1/2,j}}^{tot^{n+1/2}} = H_{x_{i+1/2,j}}^{tot^{n-1/2}} - \frac{\Delta t}{\mu_{i+1/2,j}} \frac{E_{z_{i+1/2,j+1/2}}^{tot^n} - E_{z_{i+1/2,j-1/2}}^{tot^n}}{\Delta y}$$

$$H_{y_{i,j+1/2}}^{tot^{n+1/2}} = H_{y_{i,j+1/2}}^{tot^{n-1/2}} + \frac{\Delta t}{\mu_{i,j+1/2}} \frac{E_{z_{i+1/2,j+1/2}}^{tot^n} - E_{z_{i-1/2,j+1/2}}^{tot^n}}{\Delta x}$$

$$E_{z_{i+1/2,j+1/2}}^{tot^{n+1}} = \frac{1-\xi}{1+\xi} E_{z_{i+1/2,j+1/2}}^{tot^n} + \frac{1}{1+\xi} \frac{\Delta t}{\epsilon_{i+1/2,j+1/2}} \frac{H_{y_{i+1,j+1/2}}^{tot^{n+1/2}} - H_{y_{i,j+1/2}}^{tot^{n+1/2}}}{\Delta x} - \frac{1}{1+\xi} \frac{\Delta t}{\epsilon_{i+1/2,j+1/2}} \frac{H_{x_{i+1/2,j+1}}^{tot^{n+1/2}} - H_{x_{i+1/2,j}}^{tot^{n+1/2}}}{\Delta y}$$

$$\text{where, } \xi = \frac{\sigma_{i+1/2,j+1/2} \Delta t}{2 \epsilon_{i+1/2,j+1/2}}$$



Total Field/Scattered Field Interface:

$$E_{z_{i+3/2,j+1/2}}^{tot^{n+1}} = \frac{1-\xi}{1+\xi} E_{z_{i+3/2,j+1/2}}^{tot^n} + \frac{1}{1+\xi} \frac{\Delta t}{\epsilon_{i+3/2,j+1/2}} \frac{H_{y_{i+2,j+1/2}}^{tot^{n+1/2}} - H_{y_{i+1,j+1/2}}^{tot^{n+1/2}}}{\Delta x} - \frac{1}{1+\xi} \frac{\Delta t}{\epsilon_{i+3/2,j+1/2}} \left[\frac{H_{x_{i+3/2,j+1}}^{scat^{n+1/2}} - H_{x_{i+3/2,j}}^{tot^{n+1/2}}}{\Delta y} + \frac{H_{x_{i+3/2,j+1}}^{inc^{n+1/2}}}{\Delta y} \right]$$

Corner:

$$E_{z_{i+1/2,j+1/2}}^{tot^{n+1}} = \frac{1-\xi}{1+\xi} E_{z_{i+1/2,j+1/2}}^{tot^n} + \frac{1}{1+\xi} \frac{\Delta t}{\epsilon_{i+1/2,j+1/2}} \frac{H_{y_{i+1,j+1/2}}^{tot^{n+1/2}} - H_{y_{i,j+1/2}}^{scat^{n+1/2}}}{\Delta x} - \frac{1}{1+\xi} \frac{\Delta t}{\epsilon_{i+1/2,j+1/2}} \left[\frac{H_{x_{i+1/2,j+1}}^{scat^{n+1/2}} - H_{x_{i+1/2,j}}^{tot^{n+1/2}}}{\Delta y} + \frac{H_{x_{i+1/2,j+1}}^{inc^{n+1/2}}}{\Delta y} + \frac{H_{y_{i,j+1/2}}^{scat^{n+1/2}}}{\Delta x} \right]$$

H-Field Update:

$$H_{x_{i+3/2,j+1}}^{scat^{n+1/2}} = H_{x_{i+3/2,j+1}}^{scat^{n-1/2}} - \frac{\Delta t}{\mu_{i+3/2,j}} \frac{E_{z_{i+3/2,j+3/2}}^{scat^n} - E_{z_{i+3/2,j+1/2}}^{tot^n} + E_{z_{i+3/2,j+1/2}}^{inc^n}}{\Delta y}$$

FORTRAN IMPLEMENTATION 2D (TM_z)

E-Field Update:

```

      do 10 jj=2,ny-1
        do 10 ii=2,nx-1
          ez(ii,jj)=ca(ii,jj)*ez(ii,jj)
1          + cb(ii,jj)*(hy(ii+1,jj)-hy(ii,jj)+hx(ii,jj)-hx(ii,jj+1))
10    continue

```

- **Field is updated everywhere using the same update loop**
- **Preserves Vectorization**
- **Incident Field is Added in as a Soft Source**

```

      do 16 ii=i0,i1
c total-front face
      ez(ii,j0)=ez(ii,j0)+ cb(ii,j0)*hxinc(ii,j0,float(nt)-.5)

c total-back face
      ez(ii,j1)=ez(ii,j1)- cb(ii,j1)*hxinc(ii,(j1+1),float(nt)-.5)
16    continue

```



```
do 17 jj=j0,j1
* total-left face
    ez(i0,jj)=ez(i0,jj)- cb(i0,jj)*hyinc(i0,jj,float(nt)-.5)
c total-right face
    ez(i1,jj)=ez(i1,jj)+ cb(i1,jj)*hyinc((i1+1),jj,float(nt)-.5)

17    continue
```

- **hxinc, hyinc are functions**

H-Field Update:

** update hx-fields*

do 20 jj=1,ny

do 20 ii=1,nx-1

*hx(ii,jj)=dax(ii,jj)*hx(ii,jj) + dbx(ii,jj)*(ez(ii,jj-1)-ez(ii,jj))*

20 continue

** update hy-fields*

do 30 jj = 1,ny-1

do 30 ii=1,nx

*hy(ii,jj)=day(ii,jj)*hy(ii,jj) + dby(ii,jj)*(ez(ii,jj)-ez(ii-1,jj))*

350 continue

- **Again, Field is updated using a unified update loop**
- **Incident Field is added in as a Soft Source**

```
    do 40 ii=i0,i1
* scatt-front face
    hx(ii,j0)=hx(ii,j0)+ dbx(ii,j0)*ezinc(ii,j0,float(nt))
* scatt-back face
    hx(ii,(j1+1))=hx(ii,(j1+1))-dbx(ii,(j1+1))*ezinc(ii,j1,float(nt))
40  continue
    do 50 jj=j0,j1
* scatt-left face
    hy(i0,jj)=hy(i0,jj)- dby(i0,jj)*ezinc(i0,jj,float(nt))
* scatt-right face
    hy((i1+1),jj)=hy((i1+1),jj)+dby((i1+1),jj)*ezinc(i1,jj,float(nt))
50  continue
```

ABSORBING BOUNDARY CONDITIONS

- We have discussed 2D, and 3D FDTD Algorithms For the Analysis of Cavity Problems
- Desirable to Analyze Electromagnetic Interaction in Unbounded Media
- Have to Truncate the Mesh in a Manner that the Exterior Boundary Effective Looks Like an Unbounded Medium
- Essentially Need to Match the Exterior Region to the Interior Region
- Number of Techniques Can be Used to Achieve This:
 - Exact Radiation Boundary Condition Based on Green's Functions and a Surface or Volume Convolutional Integral in Time and Space
 - Local Radiation Boundary Condition, or Absorbing Boundary Condition Based on a Differential Operator, or Pseudo-Differential Operator
 - Absorbing Media that is Matched to the Interior Region and Rapidly Attenuates Electromagnetic Energy
- Desirables:
 - Reflectionless Boundary over Broad Spectrum, and for All Angles of Incidence and Polarizations
 - Minimal in Computational Cost and Memory Requirements

ENGQUIST-MAJDA ONE-WAY WAVE EQUATION

- Engquist-Majda one-way wave equation is based on enforcing the wave equation on the fields near the exterior boundary
- In 2D, each field component must satisfy the scalar wave equation. Let U represent an individual field component:

$$\frac{\partial^2 U}{\partial x^2} + \frac{\partial^2 U}{\partial y^2} - \frac{1}{c^2} \frac{\partial^2 U}{\partial t^2} = 0$$

where c is the wave phase velocity.

- Introducing the Operator L

$$L = \frac{\partial^2}{\partial x^2} + \frac{\partial^2}{\partial y^2} - \frac{1}{c^2} \frac{\partial^2}{\partial t^2} = D_x^2 + D_y^2 - \frac{1}{c^2} D_t^2$$

- The Wave Equation is then written in operator form as $L U = 0$, and L is factored as:
 $LU = L^+ L^- U = 0$, where:

$$L^- \equiv D_x - \frac{D_t}{c} \sqrt{1 - S^2}; \quad L^+ \equiv D_x + \frac{D_t}{c} \sqrt{1 - S^2}; \quad S = \frac{D_y}{D_t/c}$$

- Engquist and Majda showed that the application of the wave function L^- to the wave function U absorbs a plane wave impinging on a boundary at any angle θ ! Thus,

$$L^- U = 0$$

[B. Engquist and A. Majda, "Absorbing boundary conditions for the numerical simulation of waves", *Mathematics of Computation*, vol. 31, 1977, pp. 629-651]

- The difficulty with the Engquist-Majda boundary operator is that it is non-linear due to the square root.

$$\left[D_x - \frac{D_t}{c} \sqrt{1 - S^2} \right] U = 0$$

- Have to derive an approximate form, or a *pseudo-differential operator* that can be Implemented numerically.
- First-order Approximation based on a Taylor-series expansion:

$$\sqrt{1 - S^2} \approx 1$$

- Engquist-Majda Becomes:

$$\frac{\partial U}{\partial x} - \frac{1}{c} \frac{\partial U}{\partial t} = 0$$

- If we knew the phase-velocity exactly relative to the x-direction, this is exact! e.g., at the $x = 0$ Boundary:

$$U(x, y) = U_o e^{j(\beta_x x + \beta_y y)} e^{j\omega t}$$

$$\frac{\partial U}{\partial x} - \frac{1}{v_{p_x}} \frac{\partial U}{\partial t} = (j\beta_x - \frac{j\omega}{v_{p_x}})U = j\omega(\frac{\beta_x}{\omega} - \frac{1}{v_{p_x}})U = 0$$

- Difficulty: This requires a non-dispersive wave with a single angle of incidence. This is not practical for typical problems, such as scattering problems, which can have arbitrary angles of incidence on the exterior boundary.

- Second-Order Taylor-Series Expansion:

$$\sqrt{1-S^2} \approx 1 - \frac{1}{2}S^2$$

- This leads to:

$$L^- \cong D_x - \frac{D_t}{c} \left(1 - \frac{1}{2}S^2 \right) \cong D_x - \frac{D_t}{c} + \frac{cD_y^2}{2D_t}$$

- Introducing the ABC Operator:

$$L^-U \cong \left(D_x - \frac{D_t}{c} + \frac{cD_y^2}{2D_t} \right) U = 0 \quad \Rightarrow \quad \left(D_t D_x - \frac{D_t^2}{c} + \frac{cD_y^2}{2} \right) U = 0$$

which becomes:

$$\frac{\partial^2 U}{\partial x \partial t} - \frac{1}{c} \frac{\partial^2 U}{\partial t^2} + \frac{c}{2} \frac{\partial^2 U}{\partial y^2} = 0 \quad (x=0)$$

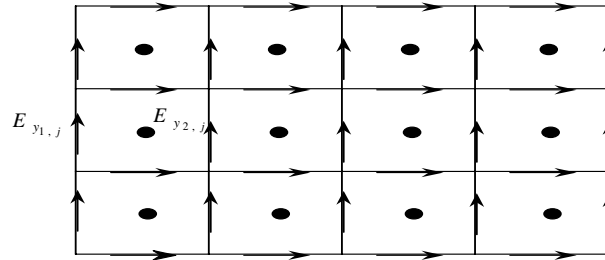
- Similarly for the Other Boundaries:

$$\frac{\partial^2 U}{\partial x \partial t} + \frac{1}{c} \frac{\partial^2 U}{\partial t^2} - \frac{c}{2} \frac{\partial^2 U}{\partial y^2} = 0 \quad (x=h), \quad \frac{\partial^2 U}{\partial y \partial t} - \frac{1}{c} \frac{\partial^2 U}{\partial t^2} + \frac{c}{2} \frac{\partial^2 U}{\partial x^2} = 0 \quad (y=0)$$

$$\frac{\partial^2 U}{\partial y \partial t} + \frac{1}{c} \frac{\partial^2 U}{\partial t^2} - \frac{c}{2} \frac{\partial^2 U}{\partial x^2} = 0 \quad (y=h)$$

MUR ABSORBING BOUNDARY OPERATOR

- Based on the Enquist-Majda Formulation
- Second-order accurate
- Standard ABC of the 80's and early 90's
- E-M ABC is based on mixed derivatives in space and time. Mur implemented these in a second-order accurate manner.



x = 0 Boundary:

$$\left. \frac{\partial^2 E_y}{\partial x \partial t} \right|_{\frac{3}{2},j}^n = \frac{1}{2\Delta t} \left(\frac{\partial E_{y_{\frac{3}{2},j}}^{n+1}}{\partial x} - \frac{\partial E_{y_{\frac{3}{2},j}}^{n-1}}{\partial x} \right) = \frac{1}{2\Delta t} \left(\frac{E_{y_{2,j}}^{n+1} - E_{y_{1,j}}^{n+1}}{\Delta x} - \frac{E_{y_{2,j}}^{n-1} - E_{y_{1,j}}^{n-1}}{\Delta x} \right)$$

$$\left. \frac{\partial^2 E_y}{\partial y^2} \right|_{\frac{3}{2},j}^n = \frac{1}{2} \left(\frac{E_{y_{2,j+1}}^n - 2E_{y_{2,j}}^n + E_{y_{2,j-1}}^n}{\Delta y^2} - \frac{E_{y_{1,j+1}}^n - 2E_{y_{1,j}}^n + E_{y_{1,j-1}}^n}{\Delta y^2} \right)$$

$$\left. \frac{\partial^2 E_y}{\partial t^2} \right|_{\frac{3}{2},j}^n = \frac{1}{2} \left(\frac{E_{y_{2,j}}^{n+1} - 2E_{y_{2,j}}^n + E_{y_{2,j}}^{n-1}}{\Delta t^2} - \frac{E_{y_{1,j}}^{n+1} - 2E_{y_{1,j}}^n + E_{y_{1,j}}^{n-1}}{\Delta t^2} \right)$$

- Assembling the terms, this leads to an update expression for the boundary field:

$$E_{y_{1,j}}^{n+1} = -E_{y_{1,j}}^{n-1} + \frac{c\Delta t - \Delta x}{c\Delta t + \Delta x} (E_{y_{2,j}}^{n+1} + E_{y_{1,j}}^{n-1}) + \frac{2\Delta x}{c\Delta t + \Delta x} (E_{y_{1,j}}^n + E_{y_{2,j}}^n) \\ + \frac{(c\Delta t)^2 \Delta x}{2(\Delta y)^2 (c\Delta t + \Delta x)} (E_{y_{1,j+1}}^n - 2E_{y_{1,j}}^n + E_{y_{1,j-1}}^n + E_{y_{2,j+1}}^n - 2E_{y_{2,j}}^n + E_{y_{2,j-1}}^n)$$

- This is known as the **2nd-Order Mur ABC**
- The first-order Mur is similarly derived from the Taylor Series Expansion $\sqrt{1 - S^2} \approx 1$, and evaluating at the center point between $i = 1$ and $i = 2$, leading to:

$$E_{y_{1,j}}^{n+1} = -E_{y_{1,j}}^{n-1} + \frac{c\Delta t - \Delta x}{c\Delta t + \Delta x} (E_{y_{2,j}}^{n+1} + E_{y_{1,j}}^{n-1}) + \frac{2\Delta x}{c\Delta t + \Delta x} (E_{y_{1,j}}^n + E_{y_{2,j}}^n)$$

- Second-Order Mur leads to a Second-Order Approximation of the *Difference Equation*. However, the Difference Equation only provides a 2-term T.S. approximation based on a normally incident plane wave (i.e., with phase velocity c).
- First-Order Mur is a second-order accurate approximation of a 1-term T.S., approximation of the wave annihilator

- Approximating the Reflection Coefficient Based on the First and Second-Order Mur ABCs

- Let:

$$E_y^{inc} = e^{j(\omega t + kx \cos \phi - ky \sin \phi)},$$

$$\rightarrow E_y^{total} = e^{j(\omega t + kx \cos \phi - ky \sin \phi)} + \text{Re} e^{j(\omega t - kx \cos \phi - ky \sin \phi)}$$

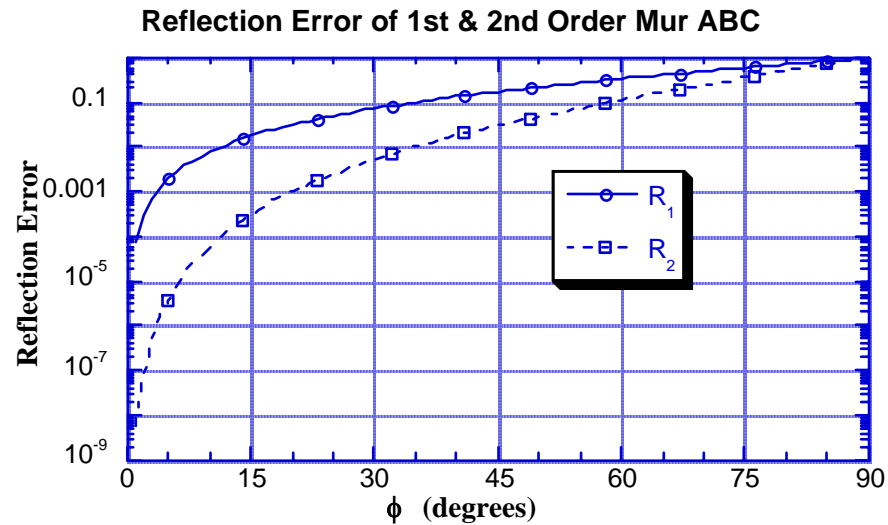
- First-Order Mur: E-field satisfies:

$$\frac{\partial E_y}{\partial x} - \frac{1}{c} \frac{\partial E_y}{\partial t} = 0 \Rightarrow R_1 = \frac{\cos \phi - 1}{\cos \phi + 1}$$

- Second-Order Mur: E-field satisfies:

$$\frac{\partial^2 E_y}{\partial x \partial t} - \frac{1}{c} \frac{\partial^2 E_y}{\partial t^2} + \frac{c}{2} \frac{\partial^2 E_y}{\partial y^2} = 0 \quad (x=0)$$

$$\Rightarrow R_2 = \frac{\cos \phi - 1 + \frac{1}{2} \sin^2 \phi}{\cos \phi + 1 - \frac{1}{2} \sin^2 \phi}$$



- Note that the Error is Based on Exact Differential Operators. The discrete Operators Approximate this (2nd-Order Accurate).

OTHER ABC OPERATORS

- The Mur ABC annihilates a normally incident wave highly accurately. However, for obliquely incident waves, large reflections can occur.
- Other boundary operators have been introduced to annihilate waves at multiple angles. This produces a higher levels of absorption over multiple angles.
- At least 2 schemes have been proposed with this intention
 - Trefethen-Halpern Generalized ABC
 - Higdon Boundary Operator.

Trefethen-Halpern Approximation

- Returning to the Approximation of $\sqrt{1-S^2}$. Let,

$$\sqrt{1-S^2} \cong p_o + p_2 S^2 \Rightarrow \frac{\partial^2 U}{\partial x \partial t} - \frac{p_o}{c} \frac{\partial^2 U}{\partial t^2} - p_2 c \frac{\partial^2 U}{\partial y^2} = 0$$

be a polynomial approximation. Then the coefficients can be determined by an interpolation technique such as a Padé, least-square, or Chebyshev approximation with the goal of interpolating $\sqrt{1-S^2}$ over the interval $[-1,1]$.

(see Tables 7.1, 7.2, pg. 162 of Text).

- Higher Order polynomial approximations:

$$\sqrt{1-S^2} \cong \frac{p_o + p_2 S^2}{q_o + q_2 S^2} \Rightarrow q_o \frac{\partial^3 U}{\partial x \partial t^2} + q_2 c^2 \frac{\partial^3 U}{\partial x \partial y^2} - \frac{p_o}{c} \frac{\partial^3 U}{\partial t^3} - p_2 c \frac{\partial^3 U}{\partial t \partial y^2} = 0$$

HIGDON BOUNDARY OPERATOR

- Consider the Wave Impinging on the Exterior Boundary to be a Linear Superposition of Plane Waves

$$U(x, y, t) = \sum_i f_i(ct + x \cos \phi_i \pm y \sin \phi_i)$$

- Higdon Proposed the Annihilator function [*Math. Comp.*, vol. 49, pp. 65-90, 1987]:

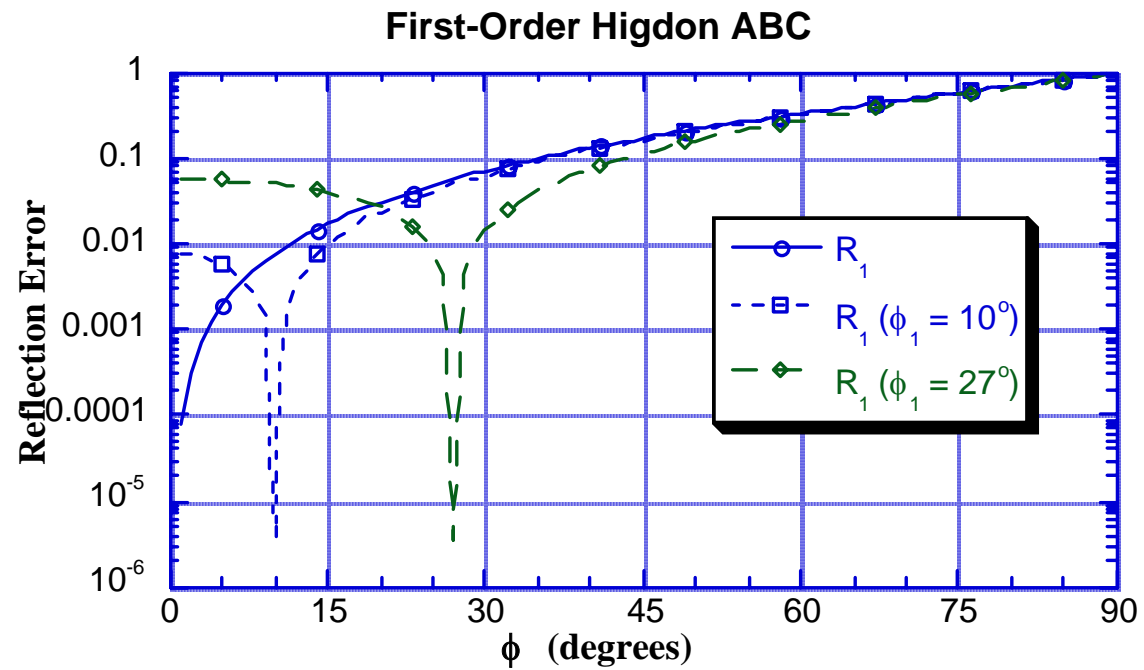
$$\left[\prod_{i=1}^n \left(\cos \phi_i \frac{\partial}{\partial t} - c \frac{\partial}{\partial x} \right) \right] U(x, y, t) = 0$$

- This operator is *exact* at each of the n angles ϕ_i .
- First-Order Higdon ($n = 1$):

$$\left(\cos \phi_1 \frac{\partial}{\partial t} - c \frac{\partial}{\partial x} \right) U(x, y, t) = 0$$

- Actually Equivalent to the First-Order Mur, with

$$v_p = c / \cos \phi_1$$



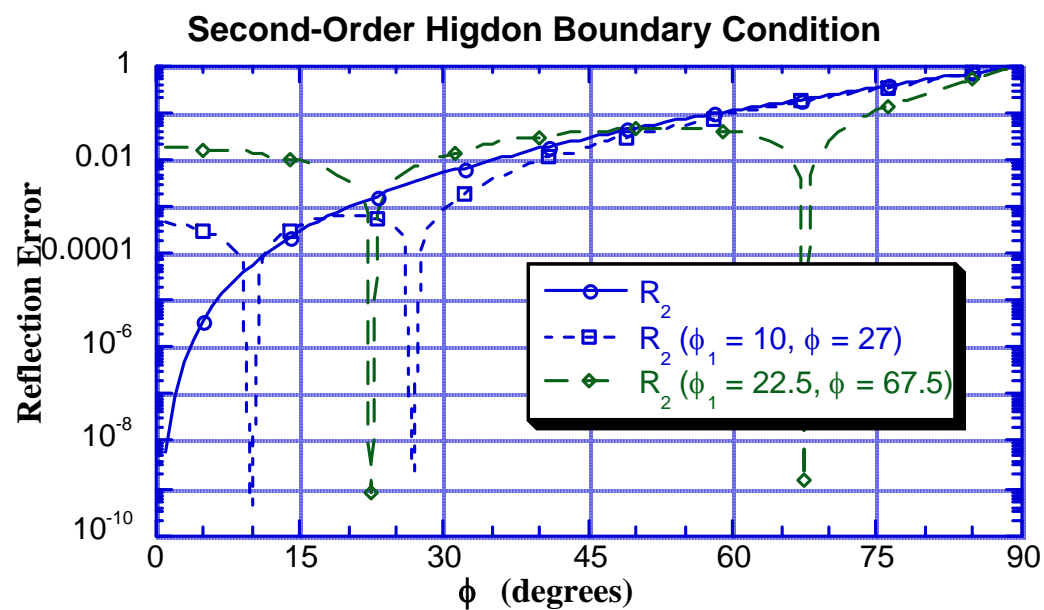
- Second-Order Higdon ($n = 1$):

$$\left(\cos \phi_1 \frac{\partial}{\partial t} - c \frac{\partial}{\partial x} \right) \left(\cos \phi_2 \frac{\partial}{\partial t} - c \frac{\partial}{\partial x} \right) U(x, y, t) = 0$$

- Equivalent to Trefethen-Halpern ABC, with p_o , and p_2 chosen to annihilate at angles ϕ_1 and ϕ_2 .

- Multiplying through leads to

$$\frac{\partial^2 U}{\partial x \partial t} - \frac{1}{c} \frac{1 + \cos \phi_1 \cos \phi_2}{(\cos \phi_1 + \cos \phi_2)} \frac{\partial^2 U}{\partial t^2} - \frac{c}{(\cos \phi_1 + \cos \phi_2)} \frac{\partial^2 U}{\partial y^2} = 0$$



- Implementing as a Difference Operator

$$\left(\frac{\partial}{\partial t} + \frac{c}{\cos \phi_1} \frac{\partial}{\partial x} \right) \left(\frac{\partial}{\partial t} + \frac{c}{\cos \phi_2} \frac{\partial}{\partial x} \right) U(x, y, t) = 0 \quad (x=h)$$

- Discretizing the Time and Space Derivatives at a half cell, as done previously with the Mur Boundary Operator, leads to:

$$\begin{aligned} U_M^n = & -(\gamma_1 + \gamma_2)U_{M-1}^n - \gamma_1\gamma_2 U_{M-2}^n + (\gamma_1 + \gamma_2)U_M^{n-1} \\ & + (2 + 2\gamma_1\gamma_2)U_{M-1}^{n-1} + (\gamma_2 + \gamma_1)U_{M-2}^{n-1} \\ & - \gamma_1\gamma_2 U_M^{n-2} - (\gamma_2 + \gamma_1)U_{M-1}^{n-2} - U_{M-2}^{n-2} \end{aligned}$$

where,

$$\gamma_i = \frac{1 - \rho_i}{1 + \rho_i}, \quad \rho_i = \frac{c\Delta t}{\cos \phi_i \Delta x}$$

- Advantages of Higdon Boundary Operator
 - Normal Derivative Only.
 - This is absolutely important for corners of the lattice, and for material inhomogeneities
 - Same Degree of Accuracy as 2nd Order Mur with added flexibility of broadening the absorption band
- Disadvantage
 - Can be Unstable in Late Time. Principally due to rounding error and the fact that the operator is weakly causal. Can be eradicated by adding a damping term:

- Modified Higdon Boundary Operator[†]

$$\left(\frac{\partial}{\partial t} + \frac{c}{\cos \phi_1} \frac{\partial}{\partial x} + \alpha_1 \right) \left(\frac{\partial}{\partial t} + \frac{c}{\cos \phi_2} \frac{\partial}{\partial x} \right) U(x, y, t) = 0 \quad (x=h)$$

- This leads to the Difference Operator:

$$\begin{aligned} U_M^n = & -(\gamma_1 + \gamma_2)U_{M-1}^n - \gamma_1\gamma_2 U_{M-2}^n + (\gamma_1 + \gamma_2)U_M^{n-1} \\ & + ((\beta + 1) + 2\gamma_1\gamma_2)U_{M-1}^{n-1} + (\beta\gamma_2 + \gamma_1)U_{M-2}^{n-1} \\ & - \gamma_1\gamma_2 U_M^{n-2} - (\beta\gamma_2 + \gamma_1)U_{M-1}^{n-2} - \beta U_{M-2}^{n-2} \end{aligned}$$

where,

$$\gamma_i = \frac{1 - \rho_i}{1 + \rho_i(1 + \alpha_1 \Delta x)}, \quad \rho_i = \frac{c \Delta t}{\cos \phi_i \Delta x}, \quad \beta = \frac{1 + \rho_i}{1 + \rho_i(1 + \alpha_1 \Delta x)}$$

- Typically, $\alpha_1 \Delta x = 0.1$ is chosen. This provides a stable formulation while maintaining the absorptive properties.

[†] V. Betz and R. Mittra, "Comparison and evaluation of boundary conditions for the absorption of guided waves in an FDTD simulation," *IEEE Microwave and Guided Wave Letters*, vol. 2, pp. 499-501, December 1992.

IMPLEMENTATION

- Example of update of Ex on the y = 0 plane

$$alp = 0.1$$

$$r1 = vi(1)*dt/dy$$

$$r2 = vi(2)*dt/dy$$

$$g1 = (1.-r1)/(1.+r1*(1.+alp))$$

$$g2 = (1.-r2)/(1.+r2)$$

$$bet = (1.+r1)/(1.+r1*(1.+alp))$$

$$c1 = g1+g2$$

$$c2 = g1*g2$$

$$c3 = bet*g2+g1$$

$$c4 = bet+1.+2.*c2$$

```

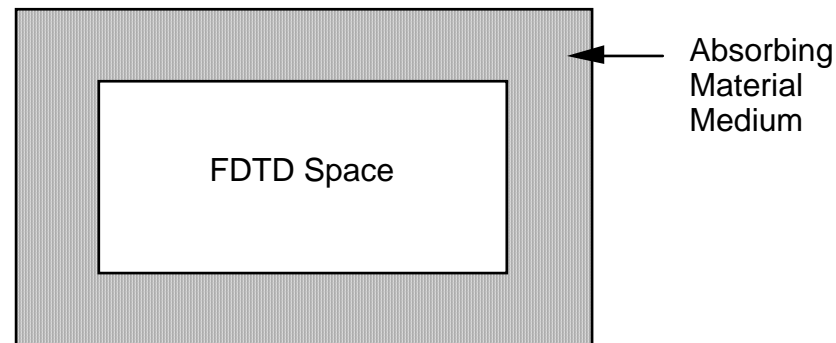
c j = 1 plane
c
c If r1 = 0, then assume j = 1 plane is a PEC wall. Else Update
c
  if(r1 .ne. 0.) then
c
  j = 1
  do 10 k = 2,nk-1
    do 10 i = 1,npx-1
      sv1 = ex(i,j,k)
      ex(i,j,k) = c4*exy2(i,k,1,1)-bet*exy3(i,k,2,1)+c1*ex(i,j,k)
1      -c1*ex(i,j+1,k)-c3*(exy2(i,k,2,1)-exy3(i,k,1,1))
2      -c2*(exy1(i,k,1)+ex(i,j+2,k))
      exy1(i,k,1) = sv1
10 continue

```

```
c
c Back store Field Information
c
  do 108 k = 2,nk-1
    do 108 i = 1,npx-1
      exy2(i,k,2,1) = exy2(i,k,1,1)
      exy3(i,k,2,1) = exy3(i,k,1,1)
108    continue
c
  do 110 k = 2,nk-1
    do 110 i = 1,npx-1
      exy2(i,k,1,1) = ex(i,2,k)
      exy3(i,k,1,1) = ex(i,3,k)
110    continue
c
```

PERFECTLY MATCHED LAYER ABC

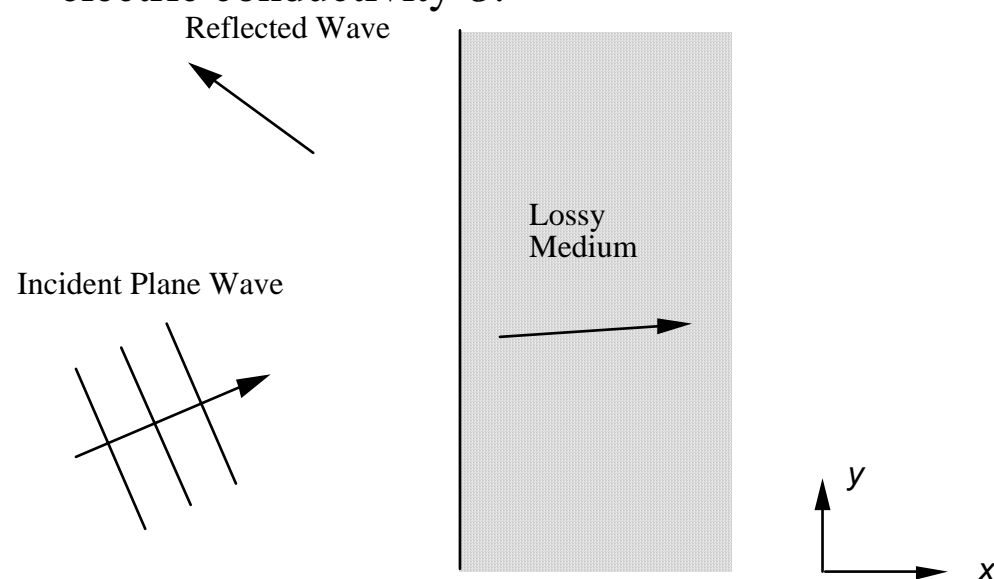
- Absorbing Material Boundary Condition'
- To Be Effective, Must:
 - Be thin (only a few lattice cells in thickness)
 - Be Effective in the Near Field of Source or Scatterer
 - Reflectionless to All Impinging Waves (Polarization, Angle)
 - Reflectionless over a Broad-Band



- Perfectly Matched Layer (PML) Material Medium First Introduced by J. P. Berenger Has Been Found to Meet all of these Criterion [J.-P. Berenger, "A perfectly matched layer for the absorption of electromagnetic waves," *Journal of Computational Physics*, October 1994]

Dispersionless Medium

- Consider a plane wave incident from a free space ($x < 0$) onto a material half space ($x > 0$)
- The material half space is assumed to have both a magnetic conductivity σ^* and an electric conductivity σ .



- TE_z polarized uniform plane wave incident upon this interface $\vec{H}^{inc} = \hat{z}H_o e^{-j\beta_x^i x - j\beta_y^i y}$, propagating with angle θ relative to the normal x -axis.
- The fields in the two regions are then posed as:

$$\left. \begin{aligned}
 \vec{H}_1 &= \hat{z} H_o (1 + \Gamma e^{2j\beta_x^i x}) e^{-j\beta_x^i x - j\beta_y^i y} \\
 \vec{E}_1 &= \left(-\hat{x} \frac{\beta_y^i}{\omega \epsilon_1} (1 + \Gamma e^{2j\beta_x^i x}) + \hat{y} \frac{\beta_x^i}{\omega \epsilon_1} (1 - \Gamma e^{2j\beta_x^i x}) \right) H_o e^{-j\beta_x^i x - j\beta_y^i y}
 \end{aligned} \right\} (x < 0)$$

$$\left. \begin{aligned}
 \vec{H}_2 &= \hat{z} H_o \tau e^{-j\beta_x^t x - j\beta_y^t y} \\
 \vec{E}_2 &= \left(-\hat{x} \frac{\beta_y^t}{\omega \epsilon_2 \left(1 + \frac{\sigma}{j\omega \epsilon_2}\right)} + \hat{y} \frac{\beta_x^t}{\omega \epsilon_2 \left(1 + \frac{\sigma}{j\omega \epsilon_2}\right)} \right) H_o \tau e^{-j\beta_x^t x - j\beta_y^t y}
 \end{aligned} \right\} (x > 0)$$

- From the dispersion relationships:

$$\left. \begin{aligned}
 \beta_x^i &= k_1 \cos \theta^i \\
 \beta_y^i &= k_1 \sin \theta^i
 \end{aligned} \right\} (x < 0)$$

$$\beta_x^t = \sqrt{k_2^2 \left(1 + \frac{\sigma}{j\omega \epsilon_2}\right) \left(1 + \frac{\sigma^*}{j\omega \mu_2}\right) - \beta_y^{t2}} \quad (x > 0)$$

- where $k_i = \omega \sqrt{\epsilon_i \mu_i}$ ($i = 1, 2$).
- Enforcing the continuity of the tangential fields across the boundary interface ($x = 0$), $\beta_y^t = \beta_y^i = k_1 \sin \theta^i$, and:

$$\Gamma = \frac{\frac{\beta_x^i}{\omega \varepsilon_1} - \frac{\beta_x^t}{\omega \varepsilon_2 \left(1 + \frac{\sigma}{j\omega \varepsilon_2}\right)}}{\frac{\beta_x^i}{\omega \varepsilon_1} + \frac{\beta_x^t}{\omega \varepsilon_2 \left(1 + \frac{\sigma}{j\omega \varepsilon_2}\right)}}; \quad \tau = 1 + \Gamma$$

- If the wave is normally incident ($\theta = 0$):

$$\Gamma = \frac{\eta_1 - \eta_2}{\eta_1 + \eta_2}$$

where

$$\eta_1 = \sqrt{\frac{\mu_1}{\varepsilon_1}}, \quad \eta_2 = \sqrt{\frac{\mu_2 \left(1 + \frac{\sigma^*}{j\omega \mu_2}\right)}{\varepsilon_2 \left(1 + \frac{\sigma}{j\omega \varepsilon_2}\right)}}$$

Subsequently, if $\mu_2 = \mu_1$, $\varepsilon_2 = \varepsilon_1$, and

$$\frac{\sigma^*}{\mu_1} = \frac{\sigma}{\varepsilon_1}$$

then, $\Gamma = 0$!

- Also,

$$\beta_x^t = \left(1 + \frac{\sigma}{j\omega \varepsilon_1}\right) k_1 = k_1 - j\sigma \eta_1.$$

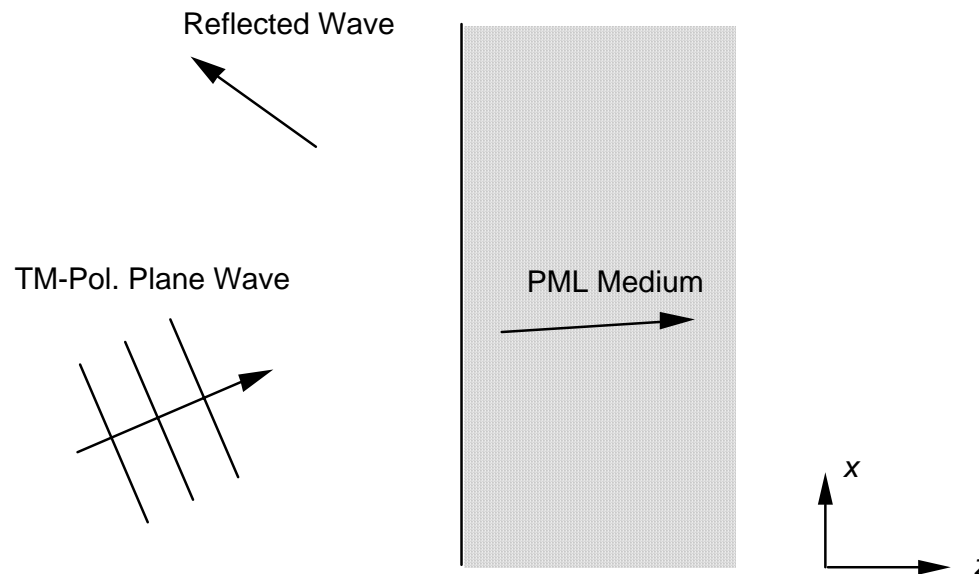
- The real part of β_x^t is the propagating component of the wave
- The imaginary part is the attenuative component.
- Thus, the wave speed in medium 2 is identical to that in medium 1. Furthermore, despite being a lossy medium, the wave is dispersionless – i.e., the wave speed is frequency independent for an axially propagating wave. Hence, this type of medium has been quantified as a dispersionless medium.
- From (7.1.b), the resultant fields in the dispersionless medium excited by a normally incident wave are expressed as:

$$\vec{H}_2 = \hat{z}H_o e^{-jk_1x} e^{-\sigma\eta_1x}$$

$$\vec{E}_2 = \hat{y}\eta_1H_o e^{-jk_1x} e^{-\sigma\eta_1x}$$

- In summary, it is seen that given a medium with magnetic and electric conductivity defined by $\frac{\sigma^*}{\mu_1} = \frac{\sigma}{\epsilon_1}$ the medium will be matched across a planar boundary for all *normally* incident waves. Furthermore, the wave propagating in the dispersionless medium has the same propagation characteristics as the incident wave, but will attenuate along the normal direction.

Berenger's PML



- The Dispersionless medium is matched only for normal incidence. J. P. Berenger was the first to introduce a technique that is matched for *all* angles of incidence and polarizations. This method is based on a mathematical step known as "Field splitting". This technique is now described.
- Consider again, a TE_z Polarized Incident Wave
- Within the lossy medium, Maxwell's curl equations are expressed in their time-harmonic form as:

$$j\omega\epsilon_2\left(1 + \frac{\sigma}{j\omega\epsilon_o}\right)E_x = \frac{\partial H_z}{\partial y}, \quad j\omega\epsilon_2\left(1 + \frac{\sigma}{j\omega\epsilon_o}\right)E_y = -\frac{\partial H_z}{\partial x},$$

$$j\omega\mu_2\left(1 + \frac{\sigma^*}{j\omega\mu_o}\right)H_z = \frac{\partial E_x}{\partial y} - \frac{\partial E_y}{\partial x}.$$

- It is noted that the electric and magnetic conductivities in (7.9.a) and (7.9.b) are intentionally normalized by the relative permittivity and permeability, respectively.
- These equations are then modified by splitting the transverse magnetic field into two orthogonal terms:

$$H_z = H_{zx} + H_{zy}$$

such that Faraday's Law is rewritten as:

$$j\omega\mu_2\left(1 + \frac{\sigma_x^*}{j\omega\mu_o}\right)H_{zx} = -\frac{\partial E_y}{\partial x},$$

$$j\omega\mu_2\left(1 + \frac{\sigma_y^*}{j\omega\mu_o}\right)H_{zy} = \frac{\partial E_x}{\partial y}.$$

- Introduce the variables:

$$\left\{ s_k = \left(1 + \frac{\sigma_k}{j\omega\epsilon_o} \right), s_k^* = \left(1 + \frac{\sigma_k^*}{j\omega\mu_o} \right); (k = x, y) \right\}$$

- The split field equations above are then rewritten as:

$$j\omega\mu_2 s_x^* H_{zx} = -\frac{\partial E_y}{\partial x},$$

$$j\omega\mu_2 s_y^* H_{zy} = \frac{\partial E_x}{\partial y}.$$

- Then, from Ampere's law:

$$j\omega\epsilon_2 s_y E_x = \frac{\partial (H_{zx} + H_{zy})}{\partial y}, j\omega\epsilon_2 s_x E_y = -\frac{\partial (H_{zx} + H_{zy})}{\partial x}$$

- From these equations, the wave equation can be derived:

$$-\omega^2 \mu_2 \epsilon_2 H_{zx} = -\frac{1}{s_x^*} \frac{\partial}{\partial x} \frac{1}{s_x} \frac{\partial}{\partial x} (H_{zx} + H_{zy})$$

$$-\omega^2 \mu_2 \epsilon_2 H_{zy} = -\frac{1}{s_y^*} \frac{\partial}{\partial y} \frac{1}{s_y} \frac{\partial}{\partial y} (H_{zx} + H_{zy})$$

- Adding these together and leads the representative wave equation:

$$\frac{1}{s_x^*} \frac{\partial}{\partial x} \frac{1}{s_x} \frac{\partial}{\partial x} H_z + \frac{1}{s_y^*} \frac{\partial}{\partial y} \frac{1}{s_y} \frac{\partial}{\partial y} H_z + \omega^2 \mu_2 \epsilon_2 H_z = 0$$

- This wave equation supports the solutions:

$$H_z = H_o \tau e^{-j\sqrt{s_x s_x^*} \beta_x x - j\sqrt{s_y s_y^*} \beta_y y}$$

with the dispersion relationship:

$$\beta_x^2 + \beta_y^2 = k_2^2 = \omega^2 \mu_2 \epsilon_2$$

- Then, from Ampere's law:

$$E_x = -H_o \tau \frac{\beta_y}{\omega \epsilon_2} \sqrt{\frac{s_y^*}{s_y}} e^{-j\sqrt{s_x s_x^*} \beta_x x - j\sqrt{s_y s_y^*} \beta_y y}$$

$$E_y = H_o \tau \frac{\beta_x}{\omega \epsilon_2} \sqrt{\frac{s_x^*}{s_x}} e^{-j\sqrt{s_x s_x^*} \beta_x x - j\sqrt{s_y s_y^*} \beta_y y}$$

- The object of this exercise is to determine the characteristics of s_x , s_x^* , s_y , and s_y^* such that the boundary interface is reflectionless.

- Despite the field splitting, the tangential fields must still be continuous across the $x = 0$ interface.
- Assuming a plane wave is assumed to be incident on this hypothetical material medium, the reflection and transmission coefficient are derived by enforcing the continuity of the tangential fields at $x = 0$, leading to:

$$\Gamma = \frac{\frac{\beta_x^i}{\omega\epsilon_1} - \frac{\beta_x}{\omega\epsilon_2} \sqrt{\frac{s_x^*}{s_x}}}{\frac{\beta_x^i}{\omega\epsilon_1} + \frac{\beta_x}{\omega\epsilon_2} \sqrt{\frac{s_x^*}{s_x}}}; \quad \tau = 1 + \Gamma$$

and $\beta_y = \beta_y^i = k_1 \sin \theta^i$.

- From the phase match condition, we see that $s_y = s_y^* = 1$.
- It is observed from the dispersion relationship that if $\epsilon_2 = \epsilon_l$, then $\beta_x = \beta_x^i$.
- Further, it is seen that if $s_x = s_x^*$ (or $\frac{\sigma_x}{\epsilon_o} = \frac{\sigma_x^*}{\mu_o}$), then $\Gamma = 0$ for all incident angles θ !

- The resultant TE_z field transmitted into the absorbing medium is then:

$$H_z = H_o e^{-js_x \beta_x^i x - j\beta_y^i y} = H_o e^{-j\beta_x^i x - j\beta_y^i y} e^{-\sigma \eta_1 \varepsilon_{r1} \cos \theta^i x}$$

$$E_x = -H_o \eta_1 \sin \theta^i e^{-j\beta_x^i x - j\beta_y^i y} e^{-\sigma \eta_1 \varepsilon_{r1} \cos \theta^i x},$$

$$E_y = H_o \eta_1 \cos \theta^i e^{-j\beta_x^i x - j\beta_y^i y} e^{-\sigma \eta_1 \varepsilon_{r1} \cos \theta^i x}.$$

- Thus, it is observed that the purely transmitted field propagates with the same wave speed as the impinging field, while attenuating along the normal direction with an attenuation constant of $\sigma \eta_1 \varepsilon_{r1} \cos \theta^i$.
- Unlike the dispersionless material in the previous section, this property applies to all angles incidence.
- This exercise can be repeated for the dual polarization splitting $E_z = E_{zx} + E_{zy}$. It is found that if $\mu_2 = \mu_1$, and $s_x = s_x^*$, then $\beta_x = \beta_x^i$ and $\Gamma = 0$ for all θ^i .
- In summary, if a wave impinges on a half space of this perfectly matched absorbing material, it will be perfectly transmitted for *all* polarizations, *all* frequencies, and *all* angles of incidence. Furthermore, the transmitted wave will propagate with the same wave speed as the incident wave, have the same characteristic impedance as the incident wave, but will attenuate along the normal direction. Finally, this hypothetical absorbing material can be used within the framework of a discrete numerical method such as FDTD to terminate all outward traveling waves.

FDTD Implementation of PML

- PML Equations (TE_y - 2 Dimemsional)

$$j\omega\epsilon_o\epsilon_r\left(1+\frac{\sigma_y}{j\omega\epsilon_o}\right)E_x = \frac{\partial}{\partial y}(H_{zx} + H_{zy}), \quad j\omega\epsilon_o\epsilon_r\left(1+\frac{\sigma_x}{j\omega\epsilon_o}\right)E_y = -\frac{\partial}{\partial x}(H_{zx} + H_{zy})$$

$$-j\omega\mu_o\mu_r\left(1+\frac{\sigma_x}{j\omega\epsilon_o}\right)H_{zx} = \frac{\partial}{\partial x}E_y, \quad -j\omega\mu_o\mu_r\left(1+\frac{\sigma_y}{j\omega\epsilon_o}\right)H_{zy} = -\frac{\partial}{\partial y}E_x$$

- Time-Dependent PML Equations (TE_y - 2 Dimemsional)

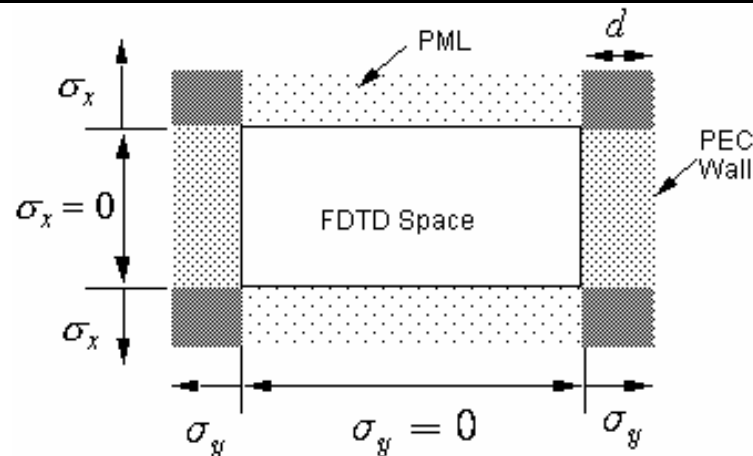
$$\epsilon_o\epsilon_r\frac{\partial E_x}{\partial t} + \sigma_y\epsilon_r E_x = \frac{\partial}{\partial y}(H_{zx} + H_{zy}), \quad \epsilon_o\epsilon_r\frac{\partial E_y}{\partial t} + \sigma_x\epsilon_r E_y = -\frac{\partial}{\partial x}(H_{zx} + H_{zy})$$

$$\mu_o\mu_r\frac{\partial H_{zx}}{\partial t} + \sigma_x\eta_o^2\mu_r H_{zx} = -\frac{\partial}{\partial x}E_y, \quad \mu_o\mu_r\frac{\partial H_{zy}}{\partial t} + \sigma_y\eta_o^2\mu_r H_{zy} = \frac{\partial}{\partial y}E_x$$

- Discrete Form Derived Using Central Difference Approximations. For example:

$$E_{x_{i+\frac{1}{2},j,k}}^{n+1} = \frac{\frac{\epsilon_o}{\Delta t} - \frac{\sigma_y}{2}}{\frac{\epsilon_o}{\Delta t} + \frac{\sigma_y}{2}} E_{x_{i+\frac{1}{2},j,k}}^n - \frac{1}{\frac{\epsilon_r\Delta y}{\frac{\epsilon_o}{\Delta t} + \frac{\sigma_z}{2}}} \left(H_{zx_{i+\frac{1}{2},j+\frac{1}{2},k}}^{n+\frac{1}{2}} - H_{zx_{i+\frac{1}{2},j-\frac{1}{2},k}}^{n+\frac{1}{2}} + H_{zy_{i+\frac{1}{2},j+\frac{1}{2},k}}^{n+\frac{1}{2}} - H_{zy_{i+\frac{1}{2},j-\frac{1}{2},k}}^{n+\frac{1}{2}} \right)$$

Theoretical Performance of the PML



- PML Backed by PEC Wall: $\sigma_y = 0$

$$R(\theta) = e^{-2\sigma_x \eta_o d \cos \theta}$$

- In practice, the abrupt transition between the discrete PML space and the discrete FDTD space can lead to a large reflection. One way to circumvent this is to scale the conductivity spatially along the normal axis:

$$\sigma_x = \sigma_{x_{\max}} \frac{|x - x_o|^m}{d_m}$$

This results in a reflection Coefficient:

$$R_m(\theta) = e^{-2\sigma_x \eta_o d \cos \theta / (m+1)}$$

THREE-DIMENSIONAL PML

- PML is easily represented in three-dimensions following the previous analogies:

$$\begin{aligned}
 \left(\epsilon_o \epsilon_r \frac{\partial}{\partial t} + \sigma_y \epsilon_r \right) E_{xy} &= \frac{\partial}{\partial y} (H_{zx} + H_{zy}) \\
 \left(\epsilon_o \epsilon_r \frac{\partial}{\partial t} + \sigma_z \epsilon_r \right) E_{xz} &= -\frac{\partial}{\partial z} (H_{yx} + H_{yz}) \\
 \left(\epsilon_o \epsilon_r \frac{\partial}{\partial t} + \sigma_z \epsilon_r \right) E_{yz} &= \frac{\partial}{\partial z} (H_{xy} + H_{xz}) \\
 \left(\epsilon_o \epsilon_r \frac{\partial}{\partial t} + \sigma_x \epsilon_r \right) E_{yx} &= -\frac{\partial}{\partial x} (H_{zx} + H_{zy}) \\
 \left(\epsilon_o \epsilon_r \frac{\partial}{\partial t} + \sigma_x \epsilon_r \right) E_{zx} &= \frac{\partial}{\partial x} (H_{yx} + H_{yz}) \\
 \left(\epsilon_o \epsilon_r \frac{\partial}{\partial t} + \sigma_y \epsilon_r \right) E_{zy} &= -\frac{\partial}{\partial y} (H_{xy} + H_{xz})
 \end{aligned}$$

$$\begin{aligned}
 -\left(\mu_o \mu_r \frac{\partial}{\partial t} + \sigma_y \eta_o^2 \mu_r \right) H_{xy} &= \frac{\partial}{\partial y} (E_{zx} + E_{zy}) \\
 -\left(\mu_o \mu_r \frac{\partial}{\partial t} + \sigma_z \eta_o^2 \mu_r \right) H_{xz} &= -\frac{\partial}{\partial z} (E_{yx} + E_{yz}) \\
 -\left(\mu_o \mu_r \frac{\partial}{\partial t} + \sigma_z \eta_o^2 \mu_r \right) H_{yz} &= \frac{\partial}{\partial z} (E_{xy} + E_{xz}) \\
 -\left(\mu_o \mu_r \frac{\partial}{\partial t} + \sigma_x \eta_o^2 \mu_r \right) H_{yx} &= -\frac{\partial}{\partial x} (E_{zx} + E_{zy}) \\
 -\left(\mu_o \mu_r \frac{\partial}{\partial t} + \sigma_x \eta_o^2 \mu_r \right) H_{zx} &= \frac{\partial}{\partial x} (E_{yx} + E_{yz}) \\
 -\left(\mu_o \mu_r \frac{\partial}{\partial t} + \sigma_y \eta_o^2 \mu_r \right) H_{zy} &= -\frac{\partial}{\partial y} (E_{xy} + E_{xz})
 \end{aligned}$$

UNIAXIAL PERFECTLY MATCHED LAYER ABSORBING MEDIUM

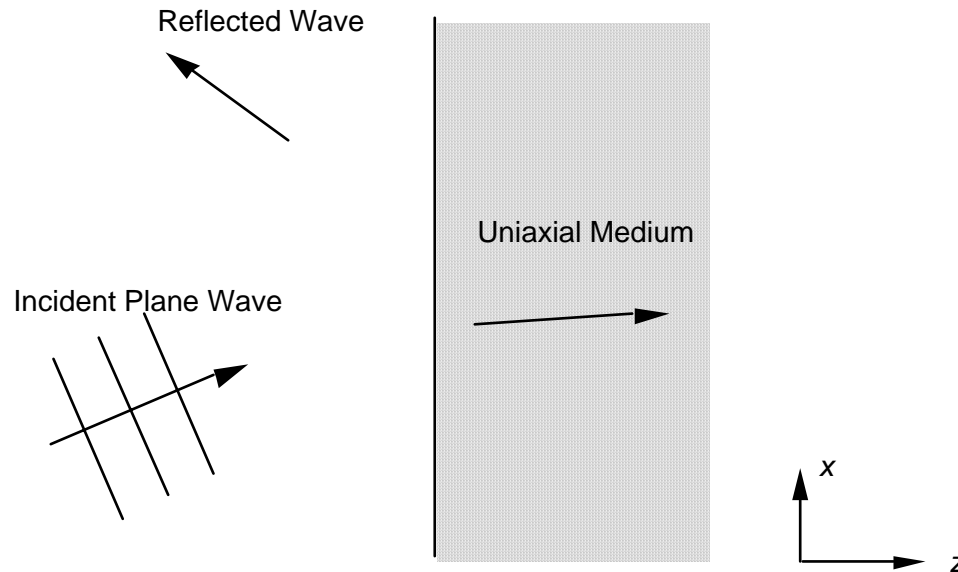
- Berenger's PML Provides an Efficient and Highly Accurate Means for Truncating the FDTD Lattice.
- Limitations of Berenger's Method:
 - + Based on a Non-Maxwellian Formulation.
 - + No Physical Insight for Application to General Problems.
 - + Results in a Field Splitting - Additional Memory and CPU Time.
- There are Alternate PML Based on a Uniaxial Anisotropic Media that also provides Perfect Absorption - but based directly on Maxwell's Equations.^{†,††}

[†] Z. S. Sacks, D. M. Kingsland, R. Lee, and J. F. Lee, "A perfectly matched anisotropic absorber for use as an absorbing boundary condition," *IEEE Transactions on Antennas and Propagation*, vol. 43, pp. 1460-1463, December 1995.

^{††} S. D. Gedney, "An Anisotropic PML Absorbing Media for FDTD Simulation of Fields in Lossy Dispersive Media," *Electromagnetics*, vol. 16, no. 3, July/August, 1996.

S. D. Gedney, "A Uniaxial PML Absorbing Media for FDTD Simulations," *IEEE Transactions on Antennas and Propagation*, vol. 44, pp. , December 1996.

UNIAXIAL PML - THEORY



- Assume a time-harmonic arbitrarily polarized plane wave, incident on a material half space described as a uniaxial anisotropic medium:

$$\vec{H}^{inc} = \vec{H}_o e^{-j\beta_x^i x - j\beta_z^i z}$$

- The interface between the two media is the $z = 0$ plane.
- The fields excited within the uniaxial medium are plane wave in nature and satisfy Maxwell's equations. In the plane wave space the curl equations are expressed as:

$$\vec{\beta}^a \times \vec{E} = \omega \mu_o \mu_r \bar{\bar{\mu}} \vec{H}, \quad \vec{\beta}^a \times \vec{H} = -\omega \varepsilon_o \varepsilon_r \bar{\bar{\varepsilon}} \vec{E}$$

where:

$$\vec{\beta}^a = \hat{x} \beta_x^i + \hat{z} \beta_z^a,$$

and:

$$\bar{\bar{\varepsilon}} = \begin{bmatrix} a & 0 & 0 \\ 0 & a & 0 \\ 0 & 0 & b \end{bmatrix}, \quad \bar{\bar{\mu}} = \begin{bmatrix} c & 0 & 0 \\ 0 & c & 0 \\ 0 & 0 & d \end{bmatrix}$$

UNIAXIAL PML - THEORY (cont'd)

- Derive the wave equation in the Uniaxial Medium equation:

$$\vec{\beta}^a \times \bar{\bar{\epsilon}}^{-1} \vec{\beta}^a \times \vec{H} + k^2 \bar{\bar{\mu}} \vec{H} = 0$$

where: $k^2 = \omega^2 \mu_o \mu_r \epsilon_o \epsilon_r$.

- Expressing the cross products as matrix operators, the wave equation can be expressed more suitably in matrix form as:

$$\begin{bmatrix} k^2 c - a^{-1} \beta_z^{a^2} & 0 & \beta_x^i \beta_z^a a^{-1} \\ 0 & k^2 c - \beta_z^{a^2} a^{-1} - \beta_x^{i^2} b^{-1} & 0 \\ \beta_x^i \beta_z^a a^{-1} & 0 & k^2 d - a^{-1} \beta_x^{i^2} \end{bmatrix} \begin{bmatrix} H_x \\ H_y \\ H_z \end{bmatrix} = 0$$

- The dispersion relationship for the uniaxial medium is derived from the determinant of the matrix operator:

$$\left(k^2 c - a^{-1} \beta_z^{a^2} - b^{-1} \beta_x^{i^2} \right) \left(k^2 a - c^{-1} \beta_z^{a^2} - d^{-1} \beta_x^{i^2} \right) = 0$$

- Conveniently, these solutions can be decoupled into forward and backward TE_y and TM_y modes, which satisfy the dispersion relationships:

$$k^2 c - a^{-1} \beta_z^{a^2} - b^{-1} \beta_x^{i^2} = 0 \quad \text{for (TE}_y\text{)}, \quad \& \quad k^2 a - c^{-1} \beta_z^{a^2} - d^{-1} \beta_x^{i^2} = 0 \quad \text{for (TM}_y\text{)}$$

UNIAXIAL PML - THEORY (cont'd)

- Initially, assume a TE_y incident wave impinging on the interface:

$$\vec{H}_1 = \hat{y} H_o (1 + \Gamma e^{2j\beta_z^i z}) e^{-j\beta_x^i x - j\beta_z^i z}$$

$$\vec{E}_1 = \left(\hat{x} \frac{\beta_z^i}{\omega \epsilon} (1 - \Gamma e^{2j\beta_z^i z}) - \hat{z} \frac{\beta_x^i}{\omega \epsilon} (1 + \Gamma e^{2j\beta_z^i z}) \right) H_o e^{-j\beta_x^i x - j\beta_z^i z}$$

$$\vec{H}_2 = \hat{y} H_o \tau e^{-j\beta_x^i x - j\beta_z^a z}$$

$$\vec{E}_2 = \left(\hat{x} \frac{\beta_z^a a^{-1}}{\omega \epsilon} - \hat{z} \frac{\beta_x^i b^{-1}}{\omega \epsilon} \right) H_o \tau e^{-j\beta_x^i x - j\beta_z^a z}$$

- Enforcing field continuity at the $z = 0$ interface:

$$\Gamma = \frac{\beta_z^i - \beta_z^a a^{-1}}{\beta_z^i + \beta_z^a a^{-1}}, \quad \tau = 1 + \Gamma = \frac{2\beta_z^i}{\beta_z^i + \beta_z^a a^{-1}}$$

- The underlying objective is to determine if there exists a choice of constitutive parameters for which $\Gamma = 0$ for all angles of incidence.
- A sufficient condition is if $\beta_z^i = \beta_z^a a^{-1}$.
- Given the TE_y dispersion relationship: $\beta_z^{a^2} = k^2 c a - a b^{-1} \beta_x^{i^2}$ or $\beta_z^{i^2} = k^2 c a^{-1} - \beta_x^{i^2} b^{-1} a^{-1}$
- Finally, if $c = a$ and $b = a^{-1}$, then:

$$\beta_z^{i^2} = k^2 - \beta_x^{i^2} !$$

- Repeating for the TM_y polarization, reflectionless conditions holds if $c = a$ and $d = c^{-1}$.

UNIAXIAL ABSORBING MEDIA

- In conclusion, if:

$$\bar{\bar{\epsilon}} = \begin{bmatrix} a & 0 & 0 \\ 0 & a & 0 \\ 0 & 0 & a^{-1} \end{bmatrix}, \bar{\bar{\mu}} = \begin{bmatrix} a & 0 & 0 \\ 0 & a & 0 \\ 0 & 0 & a^{-1} \end{bmatrix}$$

a plane wave of arbitrary polarization and angle of incidence will be purely transmitted into the uniaxial medium.

- For FDTD applications, the perfectly matched uniaxial medium is extremely useful if it is highly lossy such that any wave entrant upon the medium will quickly attenuate while no physical reflections will be encountered due to the interface.
- Terminating the uniaxial slab with a hard boundary such as a perfect electrical conductor (PEC), small reflections will be encountered due to the finite depth. However, if the medium is highly lossy, these reflections can be made to be extremely small.
- For a lossy uniaxial medium, one obvious choice for the constitutive parameters is $a = 1 + \frac{\sigma_z}{j\omega\epsilon_0}$. This leads to the relative permittivity and permeability tensors:

$$\bar{\bar{\epsilon}} = \begin{bmatrix} 1 + \frac{\sigma_z}{j\omega\epsilon_0} & 0 & 0 \\ 0 & 1 + \frac{\sigma_z}{j\omega\epsilon_0} & 0 \\ 0 & 0 & 1/(1 + \frac{\sigma_z}{j\omega\epsilon_0}) \end{bmatrix} = \bar{\bar{\mu}}$$

UNIAXIAL ABSORBING MEDIA (cont'd)

- The dispersion relationship is then expressed as:

$$k^2 = \beta_z^{a^2} / (1 + \frac{\sigma_z}{j\omega\epsilon_o})^2 + \beta_x^{i^2}$$

$$\text{which leads to: } \beta_z^a = \pm(1 - j\frac{\sigma_z}{\omega\epsilon_o})\beta_z^i$$

- This is identical to that derived for Berenger's PML.
- Given a TE_y incident wave, the field intensities in the uniaxial medium are given by:

$$\vec{H}_2 = \hat{y}H_o e^{-j\beta_x^i x - j\beta_z^i z} e^{-\alpha_z z}$$

$$\vec{E}_2 = \left(\hat{x} \frac{\beta_z^i}{\omega\epsilon_o\epsilon_r} - \hat{z} \frac{\beta_x^i (1 + \frac{\sigma_z}{j\omega\epsilon_o})}{\omega\epsilon_o\epsilon_r} \right) H_o e^{-j\beta_x^i x - j\beta_z^i z} e^{-\alpha_z z}$$

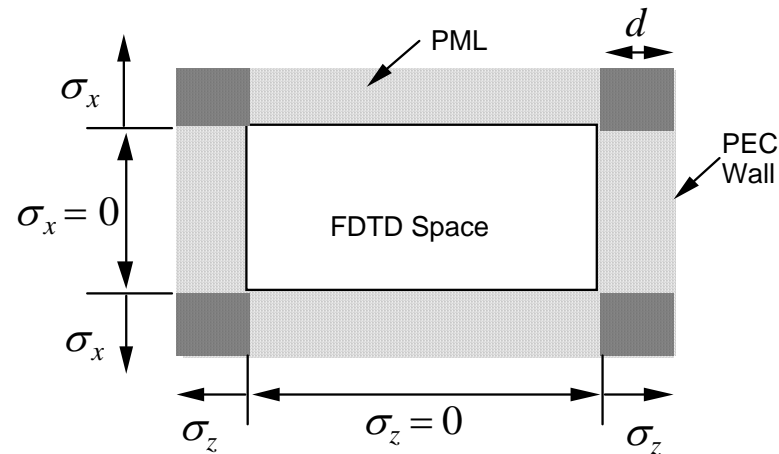
where:

$$\alpha_z = \frac{\sigma_z}{\omega\epsilon_o} \beta_z^i = \sigma_z \eta_o \sqrt{\epsilon_r} \cos \theta^i$$

- Which, again, is identical to that derived using Berenger's split field PML. In fact, the uniaxial PML can be derived from the split field formulation through a normalization of the normal field components[†].
- The principal advantage of the Uniaxial PML is that it is posed in a Maxwellian form. This lends to further physical insight to its properties, and has lead to the generalization of the PML to more generalized media, such as lossy, dispersive, and anisotropic media[†].

[†] S. D. Gedney, "An Anisotropic PML Absorbing Media for FDTD Simulation of Fields in Lossy Dispersive Media," *Electromagnetics*, vol. 16, no. 3, July/August, 1996.

Corner Regions



- In General, the FDTD lattice must be terminated by PML on all 6 sides. In the corner regions there are multiple interface boundaries.
- The constitutive relations in the corner regions are simply derived by matching two uniaxial media. This leads to the general expressions for Maxwell's curl equations:

$$\nabla \times \vec{H} = j\omega\epsilon_o\epsilon_r\vec{E}, \quad \nabla \times \vec{E} = -j\omega\mu_o\vec{H}$$

where:

$$\bar{\bar{\epsilon}} = \bar{\bar{\mu}} = \begin{bmatrix} \frac{s_y s_z}{s_x} & 0 & 0 \\ 0 & \frac{s_x s_z}{s_y} & 0 \\ 0 & 0 & \frac{s_x s_y}{s_z} \end{bmatrix}, s_x = (1 + \frac{\sigma_x}{j\omega\epsilon_0}), s_y = (1 + \frac{\sigma_y}{j\omega\epsilon_0}), s_z = (1 + \frac{\sigma_z}{j\omega\epsilon_0})$$

- s_x , s_y , and s_z are associated with the x , y , and z -normal planes, respectively. Outside of these regions, the respective $\sigma_i = 0$.

IMPLEMENTATION IN DISCRETE SPACE

- In the uniaxial medium, Ampère's law is expressed as:

$$\begin{bmatrix} \frac{\partial}{\partial y} H_z - \frac{\partial}{\partial z} H_y \\ \frac{\partial}{\partial z} H_x - \frac{\partial}{\partial x} H_z \\ \frac{\partial}{\partial x} H_y - \frac{\partial}{\partial y} H_x \end{bmatrix} = j\omega\epsilon_o\epsilon_r \begin{bmatrix} \frac{s_y s_z}{s_x} & 0 & 0 \\ 0 & \frac{s_x s_z}{s_y} & 0 \\ 0 & 0 & \frac{s_x s_y}{s_z} \end{bmatrix} \begin{bmatrix} E_x \\ E_y \\ E_z \end{bmatrix}$$

- Let's examine the update expression for E_z .
- Initially, define the constitutive relationship:

$$D_z = \epsilon_o\epsilon_r \frac{s_x}{s_z} E_z$$

where from Ampere's law, D_z satisfies:

$$\frac{\partial}{\partial x} H_y - \frac{\partial}{\partial y} H_x = j\omega s_y D_z = j\omega D_z + \frac{\sigma_y}{\epsilon_o} D_z$$

- D_z is then updated using the standard explicit FDTD formulation:

$$D_{z_{i,j,k+1/2}}^{n+1/2} = \frac{2\varepsilon_o - \Delta t \sigma_y}{2\varepsilon_o + \Delta t \sigma_y} D_{z_{i,j,k+1/2}}^{n-1/2} + \frac{2\varepsilon_o \Delta t}{2\varepsilon_o + \Delta t \sigma_y} \cdot \left\{ \left(H_{y_{i+\frac{1}{2},j,k+\frac{1}{2}}}^n - H_{y_{i-\frac{1}{2},j,k+\frac{1}{2}}}^n \right) / \Delta x - \left(H_{x_{i,j+\frac{1}{2},k+\frac{1}{2}}}^n - H_{x_{i,j-\frac{1}{2},k+\frac{1}{2}}}^n \right) / \Delta y \right\}$$

- Next, E_z must be determined from D_z . Recall,

$$s_z D_z = \varepsilon_o \varepsilon_r s_x E_z, \text{ or}$$

$$(1 + \frac{\sigma_z}{j\omega \varepsilon_o}) D_z = \varepsilon_o \varepsilon_r (1 + \frac{\sigma_x}{j\omega \varepsilon_o}) E_z, \text{ or}$$

$$j\omega D_z + \frac{\sigma_z}{\varepsilon_o} D_z = j\omega \varepsilon_o \varepsilon_r E_z + \varepsilon_o \varepsilon_r \frac{\sigma_x}{\varepsilon_o} E_z.$$

- Transforming into the time-domain: $j\omega \rightarrow \partial/\partial t$.

$$\frac{\partial}{\partial t} D_z + \frac{\sigma_z}{\varepsilon_o} D_z = \frac{\partial}{\partial t} \varepsilon_o \varepsilon_r E_z + \varepsilon_o \varepsilon_r \frac{\sigma_x}{\varepsilon_o} E_z$$

- Approximating the time derivatives using a central difference approximation and averaging $\frac{\sigma_z}{\varepsilon_o} D_z$ and $\frac{\sigma_y}{\varepsilon_o} E_z$ in time:

$$E_z^{n+\frac{1}{2}} = \frac{2\varepsilon_o - \Delta t \sigma_x}{2\varepsilon_o + \Delta t \sigma_x} E_z^{n-\frac{1}{2}} + \frac{2}{2\varepsilon_o + \Delta t \sigma_x} \frac{1}{\varepsilon_r} \left(D_z^{n+\frac{1}{2}} \left(1 + \frac{\sigma_z \Delta t}{2\varepsilon_o} \right) - D_z^{n-\frac{1}{2}} \left(1 - \frac{\sigma_z \Delta t}{2\varepsilon_o} \right) \right)$$

- Two-Step Update Process:
 - Maintains Second-Order Accuracy.
 - Requires Storage of D_z and E_z .
 - Stable within the Courant Limit.
- Similarly H_z is updated using a two-step process.

SAMPLE CODE FOR UPML-FDTD UPDATES:

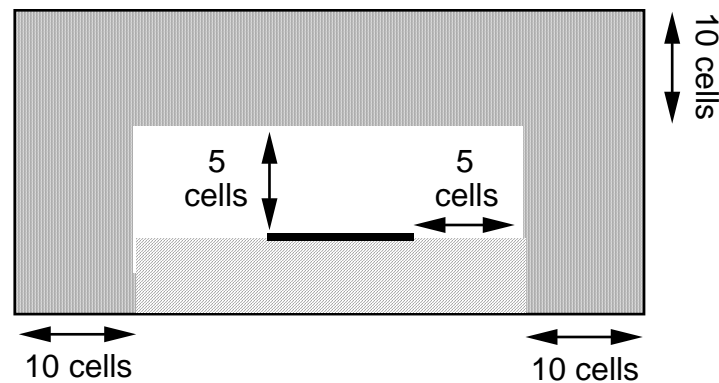
```

do 10 k = 2,nz-1      + Exclude k = 1 and k = nz since PEC bndaries are assumed
  do 10 j = 2,ny-1    + Exclude j = 1 and j = ny since PEC bndries are assumed
    do 10 i = 1,nx-1
      dxs = dex(i,j,k)
      dex(i,j,k)=aexz(k)*dex(i,j,k)+bexz(k)*(hz(i+1,j+1,k)-1
hz(i+1,j,k)-hy(i+1,j,k)+hy(i+1,j,k-1))*
2      epsc(iepx(i,j,k))
      ex(i,j,k)=aezy(j)*ex(i,j,k)+dexy(j)*(eexx(i)*dex(i,j,k)
1      +fexx(i)*dxs)
10  continue
do 20 k = 2,nz-1
  do 20 j = 1,ny-1
    do 20 i = 2,nx-1
      dys = dey(i,j,k)
      dey(i,j,k)=aeyx(i)*dey(i,j,k)+beyx(i)*(hx(i,j+1,k)-
1      hx(i,j+1,k-1)-hz(i+1,j+1,k)+hz(i,j+1,k))*
2      epsc(iepy(i,j,k))
      ey(i,j,k)=aexz(k)*ey(i,j,k)+deyz(k)*(eeyy(j)*dey(i,j,k)
1      +feyy(j)*dys)
20  continue
do 30 k = 1,nz-1
  do 30 j = 2,ny-1
    do 30 i = 2,nx-1
      dzs = dez(i,j,k)
      dez(i,j,k)=aezy(j)*dez(i,j,k)+bezy(j)*(hy(i+1,j,k)-
1      hy(i,j,k)-hx(i,j+1,k)+hx(i,j,k))*
2      epsc(iepz(i,j,k))
      ez(i,j,k)=aeyx(i)*ez(i,j,k)+dezx(i)*(eezz(k)*
1      dez(i,j,k)+fezz(k)*dzs)
30  continue

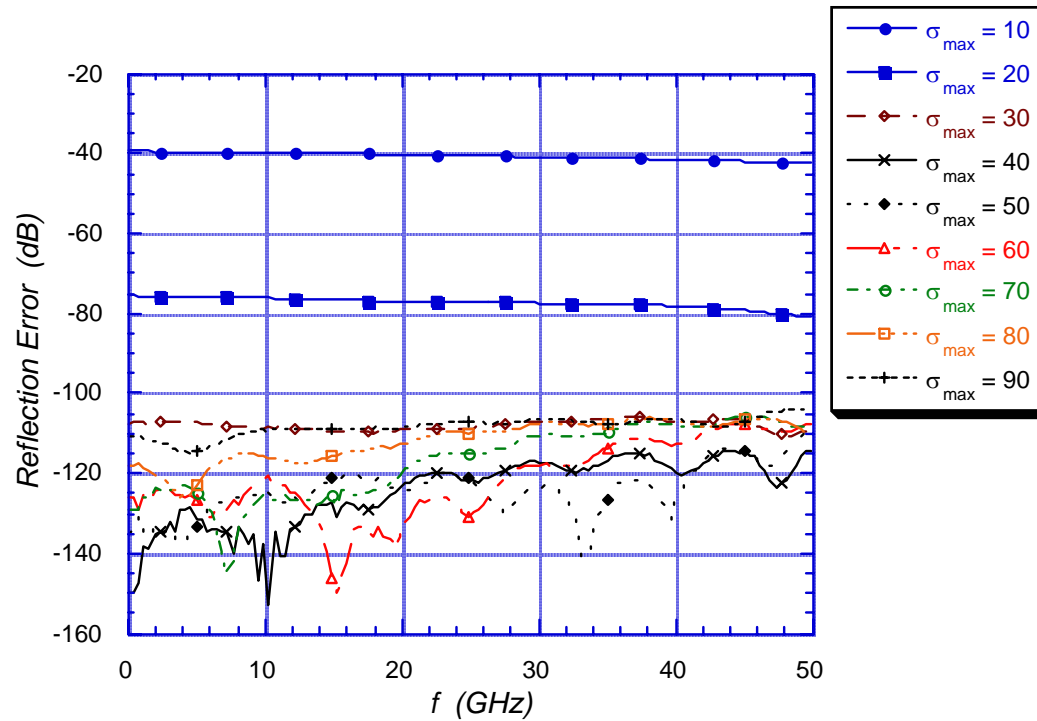
```

Actual Performance of PML

- Example: 50 Ω Microstrip Line printed on a 10 mil Alumina Substrate ($\epsilon_r = 9.8$) Terminating into a PML Interface. Side Walls and Ceiling also Terminating by PML walls.

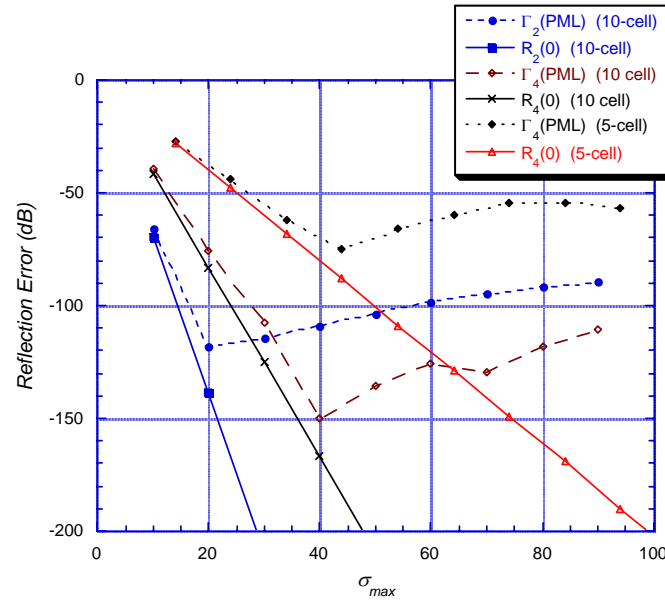


- End Wall Reflection Error:

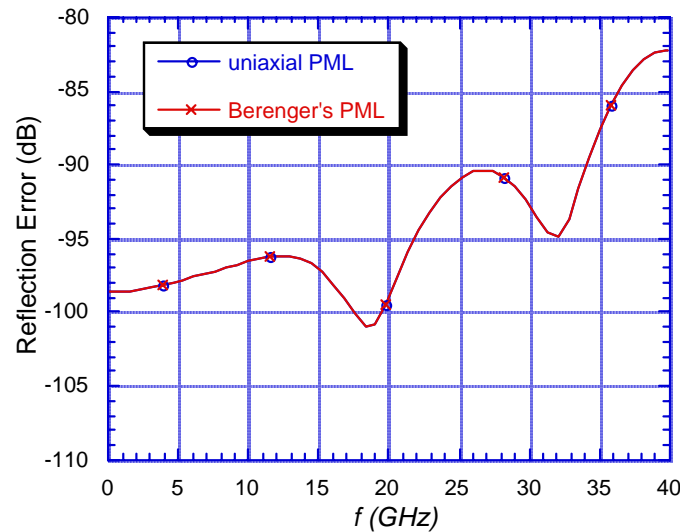


Reflection error due to a 10 cell thick uniaxial PML termination of the $50\ \Omega$ microstrip line ($m = 4$) for various values of σ_{\max} . (10 mil strip width).

- Comparison of the reflection error at $f = 0$ computed using the split field PML method compared with the theoretical reflection error due to a 10 cell thick PML termination of the microstrip line for $m = 4$ and $m = 2$, and due to a 5 and 10 cell thick PML termination of the microstrip line ($\Delta z = 0.12$ mm, and $\epsilon_{\text{reff}} = 6.62$).



- Comparison of the reflection error due to a 10 cell thick PML termination of a strip line with $\sigma_{\text{max}} = 90$, $m = 4$ encountered using the uniaxial PML method and Berenger's PML method.



Choosing the PML Material Parameters

- Due to the discontinuity in material profile at the PML interface, a large reflection can occur due to discretization error. It was proposed by Berenger, to spatially scale the conductivity profile to minimize this error, i.e., $\sigma(x)$.
- the reflection due to a purely propagating wave impinging at angle θ is then expressed as:

$$R(\theta) = e^{-2\eta\epsilon_r \cos\theta \int_0^d \sigma(x) dx}$$

- Polynomial Scaling:

$$\sigma(x) = \left(\frac{x}{d}\right)^m \sigma_{\max}, \quad R(\theta) = e^{-2\eta\epsilon_r\sigma_{\max}d\cos\theta/(m+1)}$$

- Where d is the thickness of the PML slab.

- Geometric Scaling:

$$\sigma(x) = \left(g^{\frac{1}{\Delta x}}\right)^x \sigma_o, \quad R(\theta) = e^{-2\eta\sigma_o\Delta x(g^N - 1)\cos\theta/\ln g}$$

- Specifically, the conductivity scales from σ_o at the PML interface to $g^N\sigma_o$ at the PEC boundary, where $d = N\Delta x$ is the thickness of the PML slab.

- The parameters can be determined for a given error estimate. For example, given m and d for polynomial scaling, it is desired to achieve a reflection error of $R(0)$, then σ_{\max} is:

$$\sigma_{\max} = -\frac{\ln(R(0))(m+1)}{2\eta\epsilon_r d}$$

- For geometric scaling, one would predetermine g , d , and $R(0)$. Then,

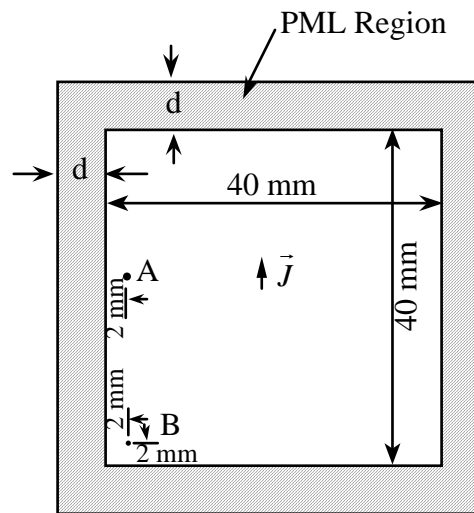
$$\sigma_o = -\frac{\ln(R(0))\ln(g)}{2\eta\epsilon_r\Delta x(g^N - 1)}$$

- The design of the optimal PML results in a delicate balance of the theoretical reflection error $R(\theta)$ and discretization error. If σ_{\max} is small, the predominant reflection of the finite PML will be due to PEC backed wall.
- In practice one would rather choose σ_{\max} to be as large as possible to minimize $R(\theta)$. Unfortunately, if σ_{\max} is too large, then discretization error due to the FDTD approximation will dominate. Subsequently, there is an optimal choice for $R(\theta)$ which balances reflection from the PEC wall and discretization error.
- Through extensive experimental study, it has been found that for a broad range of applications an optimal choice for a 10 cell thick polynomially scaled PML is $R(0) \approx e^{-16}$. For a 5 cell thick PML, $R(0) \approx e^{-8}$ is optimal. This leads to an optimal choice for σ_{\max} :

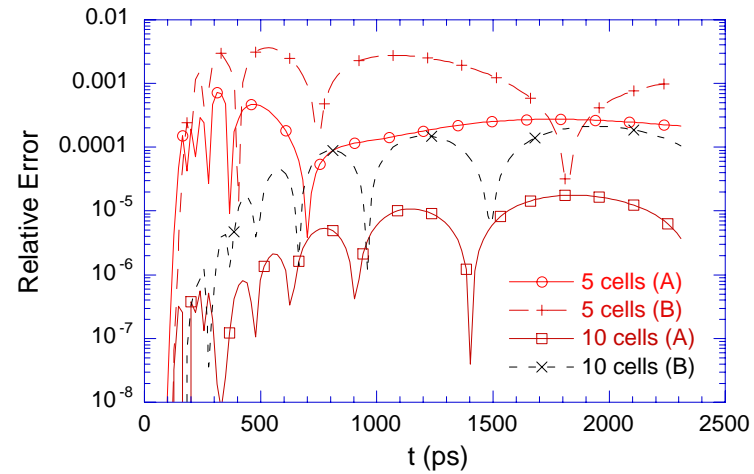
$$\sigma_{\text{opt}} = \frac{(m+1)}{150\pi\sqrt{\epsilon_r}\Delta x}$$

More Examples of PML

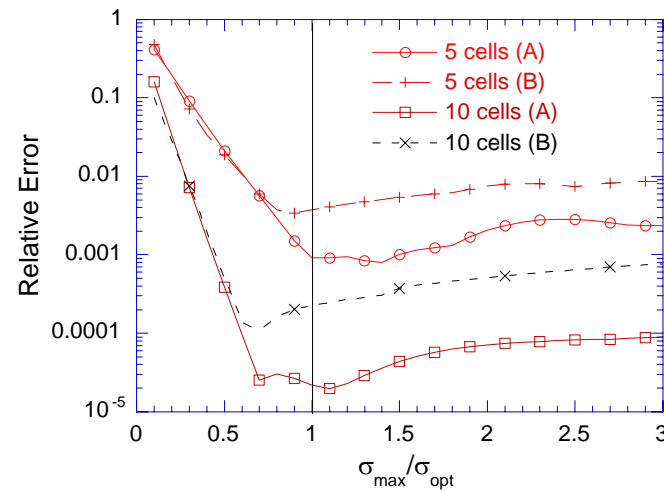
- TE-polarized wave excited by a vertically directed electric current source in a 2D region. The working volume is 40 mm x 40mm, and is surrounded by PML layers of thickness d . The source is located at the center of the region. The fields are probed at two observation points A and B .



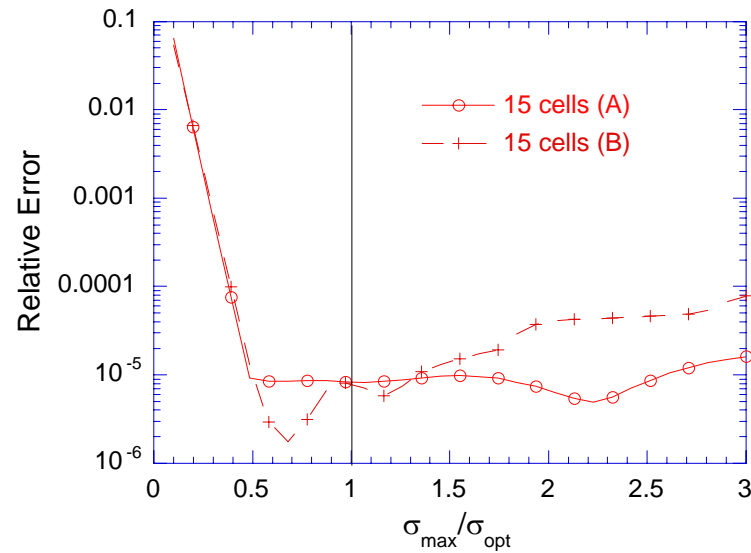
- Relative error at points A and B over 1,000 time iterations for 5 and 10 cell thick PMLs terminating a 40 x 40 cell lattice excited by a small dipole with $\sigma_{\max} = \sigma_{\text{opt}}$ and $\kappa = 1$.



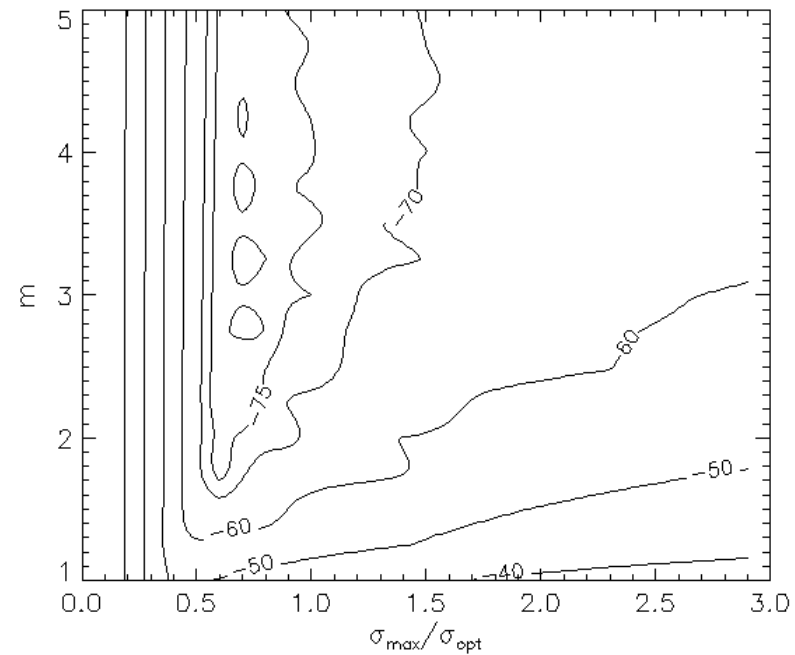
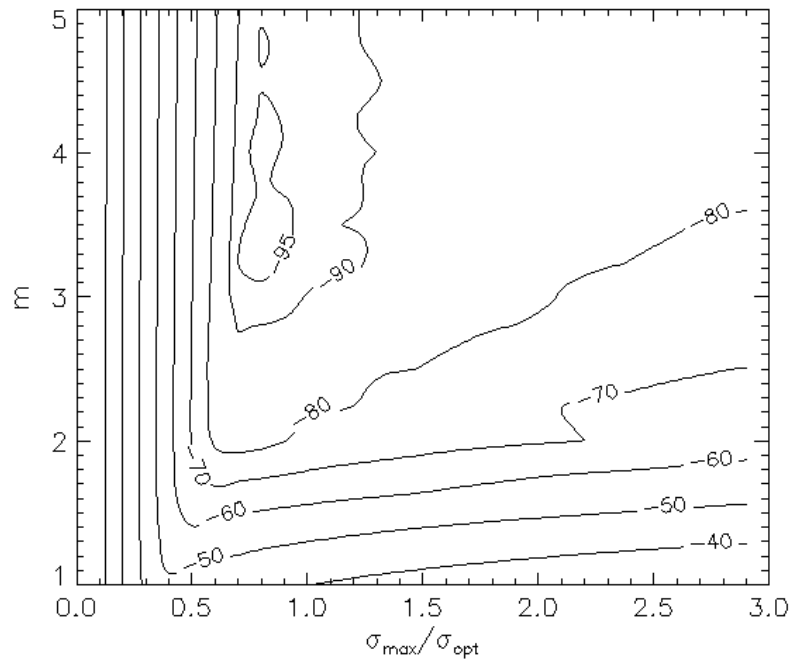
- Maximum relative error due to a 5 and 10 cell thick PML termination of a 40×40 cell lattice excited by a small dipole over 1,000 time iterations versus $\sigma_{\max}/\sigma_{\text{opt}}$. Polynomial spatial scaling with $m = 4$.



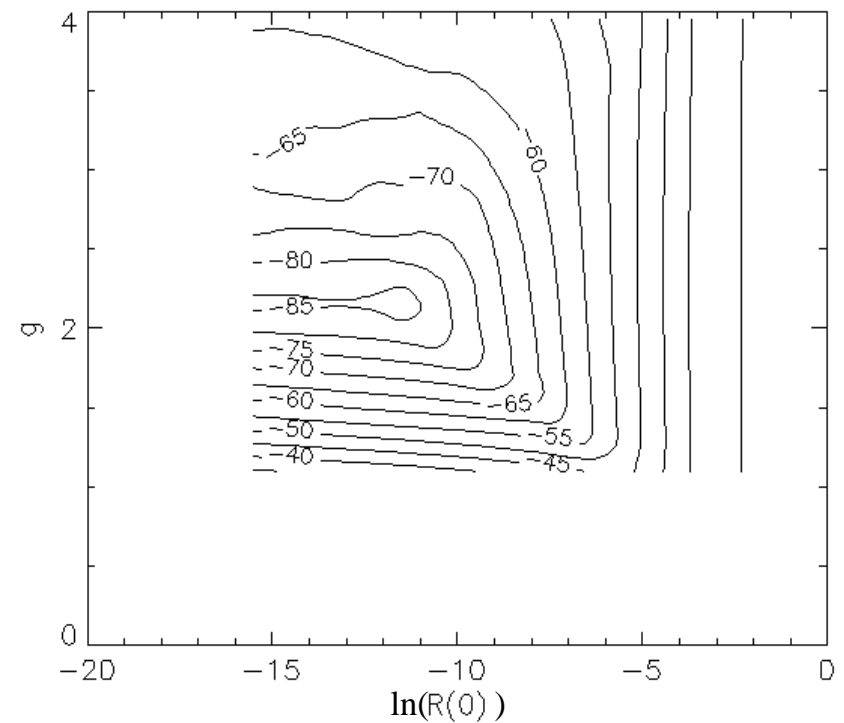
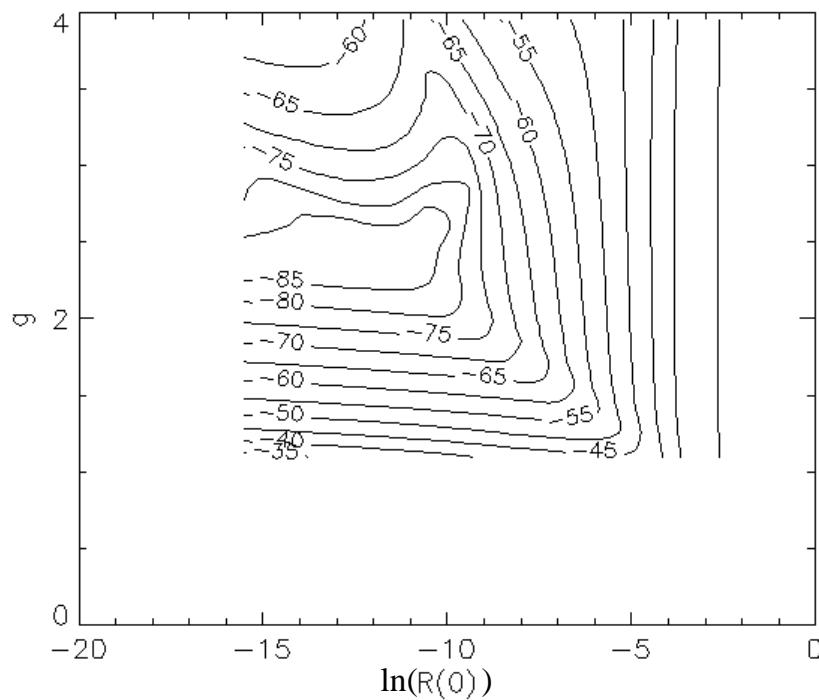
- Maximum relative error due to a 15 thick PML termination of a 40 x 40 cell lattice excited by a small dipole over 1,000 time iterations versus $\sigma_{\max}/\sigma_{\text{opt}}$. Polynomial spatial scaling with $m = 4$.



- Contour plot of the maximum relative error at points *A* and *B*, respectively, due to a polynomial scaled 10 cell thick PML termination of a 40 x 40 cell lattice excited by a small dipole over 1,000 time iterations versus $\sigma_{\max}/\sigma_{\text{opt}}$ and *m*.



- Maximum relative error at points *A* and *B*, respectively, due to a geometrically scaled 10 cell thick PML termination of a 40 x 40 cell lattice excited by a small dipole over 1,000 time iterations versus g and $\ln(R(0))$.



Alternate Forms of the PML Metric Tensor

- Berenger Originally proposed:

$$s_x = 1 + \frac{\sigma_x}{j\omega\epsilon_o}$$

- We found that for a plane wave incident on the boundary with normal dependence $e^{-j\beta_x^i x}$, the propagation constant in the PML will be

$$e^{-j\beta_x^i s_x x} = e^{-j\beta_x^i \left(1 + \frac{\sigma_x}{j\omega\epsilon_o}\right) x} = e^{-j\beta_x^i x} e^{-\sigma_x \eta \sqrt{\epsilon_r} \cos \theta^i x}$$

- Now consider a wave impinging on the boundary that has a complex wave number (e.g., lossy medium, guided mode below cutoff, or the evanescent part of a wave expansion):

$$e^{-\gamma_x^i x} = e^{-(\alpha_x^i + j\beta_x^i) x}$$

- If the wave is incident on the PML boundary, it can be shown that the wave transmitted in the PML is still perfectly matched with propagate along the normal direction as:

$$e^{-\gamma_x^i s_x x} = e^{-(\alpha_x^i + j\beta_x^i) s_x x} = e^{-(\alpha_x^i + j\beta_x^i) \left(1 + \frac{\sigma_x}{j\omega\epsilon_o}\right) x} = e^{-\alpha_x^i x} e^{j\alpha_x^i \frac{\sigma_x}{\omega\epsilon_o} x} e^{-j\beta_x^i x} e^{-\sigma_x \eta \sqrt{\epsilon_r} \cos \theta^i x}$$

- What if the wave was purely evanescent ($\beta_x^i = 0$)? The transmitted wave is:

$$e^{-\alpha_x^i x} e^{j\alpha_x^i \frac{\sigma_x}{\omega\epsilon_o} x}$$

which has no additional attenuation!

- Propose instead:

$$s_x = \kappa_x + \frac{\sigma_x}{j\omega\epsilon_o}$$

where $\kappa_x \geq 1$.

- Then, the transmitted wave behaves as:

$$e^{-\gamma_x^i s_x x} = e^{-(\alpha_x^i + j\beta_x^i) s_x x} = e^{-(\alpha_x^i + j\beta_x^i) \left(\kappa_x + \frac{\sigma_x}{j\omega\epsilon_o} \right) x} = e^{-\alpha_x^i \kappa_x x} e^{j\alpha_x^i \frac{\sigma_x}{\omega\epsilon_o} x} e^{-j\kappa_x \beta_x^i x} e^{-\sigma_x \eta \sqrt{\epsilon_r} \cos \theta^i x}$$

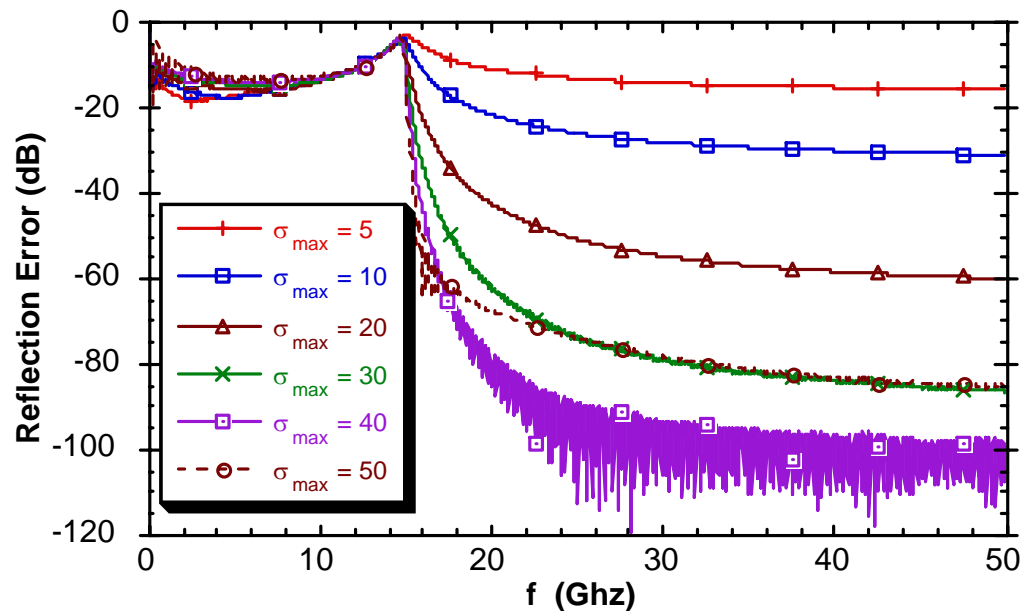
Now, the attenuation is amplified by κ_x . Also note that the wave speed is effectively reduced. Once again, κ_x cannot be increased indiscriminately. In fact, if κ_x becomes too large, it can actually degrade the reflection coefficient of a propagating wave impinging on the boundary, since it increases the time interaction with the PML medium.

- In practice, κ_x must be scaled to reduce discretization error. A recommended scaling is between 1 (at the front boundary) and κ_x^{\max} at the PEC wall. For a PML of depth d with boundary interface $x = 0$, set:

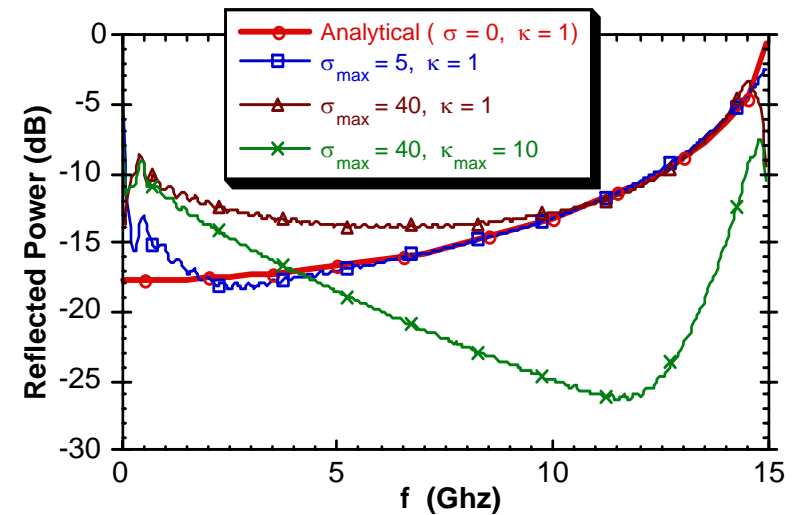
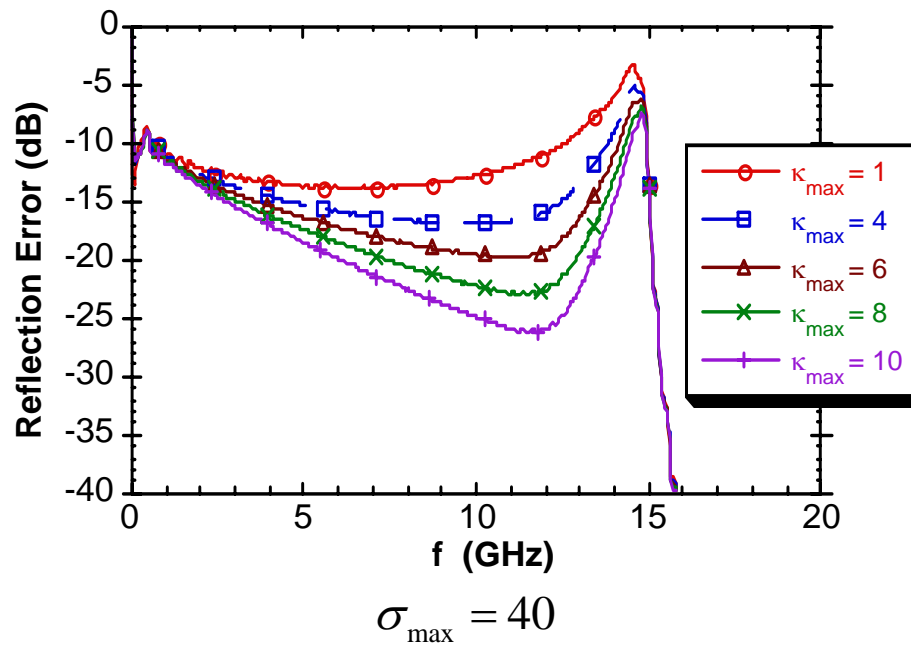
$$\kappa_x(x) = 1 + (\kappa_{\max} - 1) \left(\frac{x}{d} \right)^m$$

Example – Rectangular Waveguide

- Consider a lossless rectangular waveguide with a height of 0.5 cm and a width of 1.0 cm. For these dimensions, the cutoff frequency of the TE_{10} mode is 15 GHz.
- The FDTD lattice has the uniform dimensions $\Delta x = \Delta y = \Delta z = 0.25$ mm.
- The TE_{10} mode is excited in a rectangular waveguide. The time-dependent source was a modulated Gaussian pulse, with center frequency of 20 GHz and half bandwidth of 30 GHz. The field was measured 20 cells from the source (0.5 cm) and three cells from the PML interface. The PML medium was 10 cells thick.
- Reflection error (relative) as σ_{\max} is varied between 5 and 50 and $\kappa_{\max} = 1$.



- Above cutoff, the mode is well absorbed. Below cutoff, only attenuation is due to the waveguide mode.
- Now increase κ



PML for Lossy (Conducting) Media

- Consider the application of PML in a Lossy medium:

$$\begin{bmatrix} \frac{\partial}{\partial y} H_z - \frac{\partial}{\partial z} H_y \\ \frac{\partial}{\partial z} H_x - \frac{\partial}{\partial x} H_z \\ \frac{\partial}{\partial x} H_y - \frac{\partial}{\partial y} H_x \end{bmatrix} = j\omega\epsilon_o \left(\epsilon_r + \frac{\sigma}{j\omega\epsilon_o} \right) \begin{bmatrix} \frac{s_y s_z}{s_x} & 0 & 0 \\ 0 & \frac{s_x s_z}{s_y} & 0 \\ 0 & 0 & \frac{s_x s_y}{s_z} \end{bmatrix} \begin{bmatrix} E_x \\ E_y \\ E_z \end{bmatrix}$$

- Previously, we introduced the constitutive relation for the lossless medium:

$$D_z = \epsilon_o \epsilon_r \frac{s_x}{s_z} E_z. \text{ For a lossy medium, this would be: } D_z = \epsilon_o \epsilon_r \left(1 + \frac{\sigma}{j\omega\epsilon_o} \right) \frac{s_x}{s_z} E_z. \text{ This}$$

would lead to a second-order auxiliary equation.

- Rather, use the constitutive relations:

$$P_z = \frac{s_x}{s_z} E_z, \quad Q_z = s_y P_z$$

- Given $s_i = \kappa_i + \frac{\sigma_i}{j\omega\epsilon_o}$, we can rewrite these as:

$$s_z P_z = s_x E_z \Rightarrow \left(\kappa_z + \frac{\sigma_z}{j\omega\epsilon_o} \right) P_z = \left(\kappa_x + \frac{\sigma_x}{j\omega\epsilon_o} \right) E_z \Rightarrow (j\omega\epsilon_o \kappa_z + \sigma_z) P_z = (j\omega\epsilon_o \kappa_x + \sigma_x) E_z$$

$$Q_z = \left(\kappa_y + \frac{\sigma_y}{j\omega\epsilon_o} \right) P_z \Rightarrow j\omega\epsilon_o Q_z = (j\omega\epsilon_o \kappa_y + \sigma_y) P_z$$

- In the time domain, these are expressed as:

$$\epsilon_o \kappa_z \frac{\partial P_z}{\partial t} + \sigma_z P_z = \epsilon_o \kappa_x \frac{\partial E_z}{\partial t} + \sigma_x E_z$$

$$\epsilon_o \frac{\partial Q_z}{\partial t} = \epsilon_o \kappa_y \frac{\partial P_z}{\partial t} + \sigma_y P_z$$

○ Update procedure (z-projection):

$$Q_{z_{i,j,k+1/2}}^{n+1/2} = \frac{2\varepsilon_o - \Delta t\sigma_y}{2\varepsilon_o + \Delta t\sigma_y} Q_{z_{i,j,k+1/2}}^{n-1/2} + \frac{2\varepsilon_o\Delta t}{2\varepsilon_o + \Delta t\sigma_y} \cdot$$

$$\left\{ \left(H_{y_{i+\frac{1}{2},j,k+\frac{1}{2}}}^n - H_{y_{i-\frac{1}{2},j,k+\frac{1}{2}}}^n \right) / \Delta x - \left(H_{x_{i,j+\frac{1}{2},k+\frac{1}{2}}}^n - H_{x_{i,j-\frac{1}{2},k+\frac{1}{2}}}^n \right) / \Delta y \right\}$$

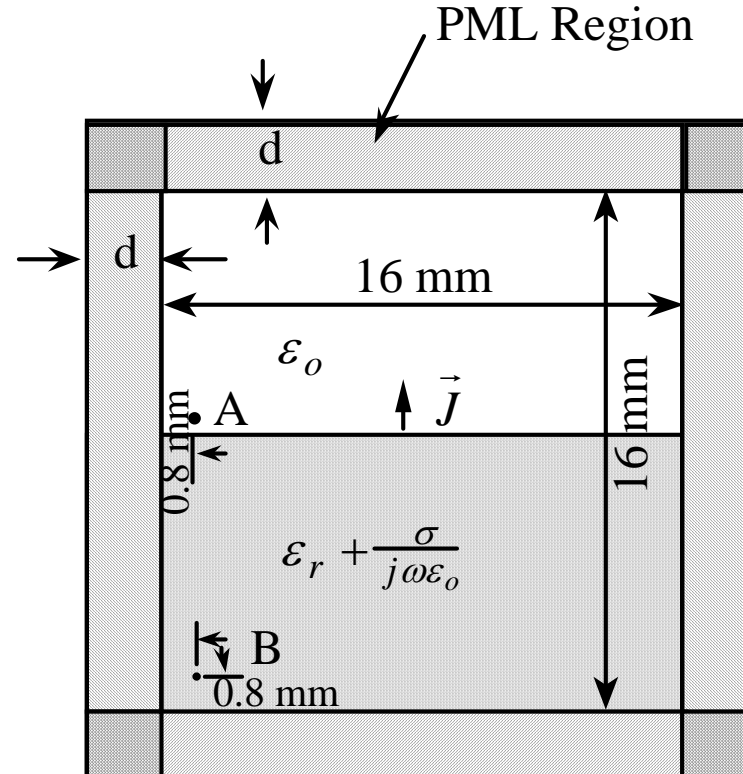
$$\varepsilon_o \kappa_y \frac{P_{z_{i,j,k+1/2}}^{n+1/2} - P_{z_{i,j,k+1/2}}^{n-1/2}}{\Delta t} + \sigma_y \frac{P_{z_{i,j,k+1/2}}^{n+1/2} + P_{z_{i,j,k+1/2}}^{n-1/2}}{2} = \varepsilon_o \frac{Q_{z_{i,j,k+1/2}}^{n+1/2} - Q_{z_{i,j,k+1/2}}^{n-1/2}}{\Delta t}$$

$$\Rightarrow P_{z_{i,j,k+1/2}}^{n+1/2} = \frac{2\varepsilon_o \kappa_y - \Delta t\sigma_y}{2\varepsilon_o \kappa_y + \Delta t\sigma_y} P_{z_{i,j,k+1/2}}^{n-1/2} + \frac{2\varepsilon_o}{2\varepsilon_o \kappa_y + \Delta t\sigma_y} \left(Q_{z_{i,j,k+1/2}}^{n+1/2} - Q_{z_{i,j,k+1/2}}^{n-1/2} \right)$$

$$\varepsilon_o \kappa_z \frac{P_{z_{i,j,k+1/2}}^{n+1/2} - P_{z_{i,j,k+1/2}}^{n-1/2}}{\Delta t} + \sigma_z \frac{P_{z_{i,j,k+1/2}}^{n+1/2} + P_{z_{i,j,k+1/2}}^{n-1/2}}{2} = \varepsilon_o \kappa_x \frac{E_{z_{i,j,k+1/2}}^{n+1/2} - E_{z_{i,j,k+1/2}}^{n-1/2}}{\Delta t} + \sigma_x \frac{E_{z_{i,j,k+1/2}}^{n+1/2} + E_{z_{i,j,k+1/2}}^{n-1/2}}{2}$$

$$\Rightarrow E_{z_{i,j,k+1/2}}^{n+1/2} = \frac{2\varepsilon_o \kappa_x - \sigma_x \Delta t}{2\varepsilon_o \kappa_x + \sigma_x \Delta t} E_{z_{i,j,k+1/2}}^{n-1/2} + \frac{1}{2\varepsilon_o \kappa_x + \sigma_x \Delta t} \left((2\varepsilon_o \kappa_z + \sigma_z \Delta t) P_{z_{i,j,k+1/2}}^{n+1/2} - (2\varepsilon_o \kappa_z - \sigma_z \Delta t) P_{z_{i,j,k+1/2}}^{n-1/2} \right)$$

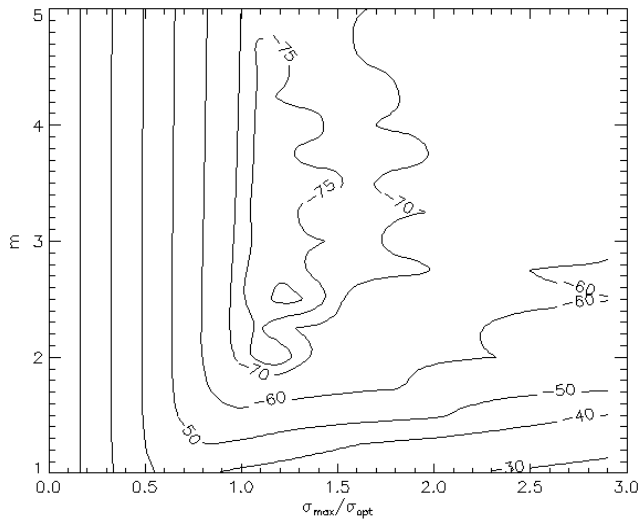
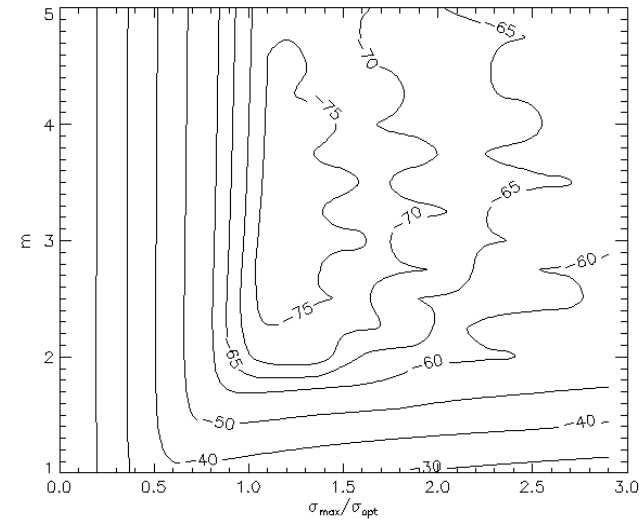
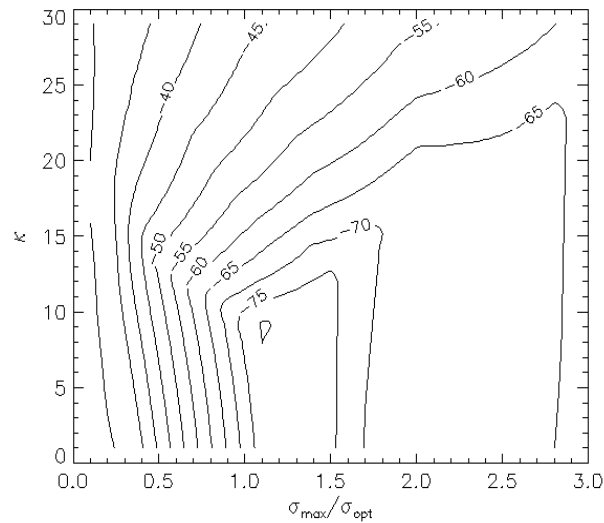
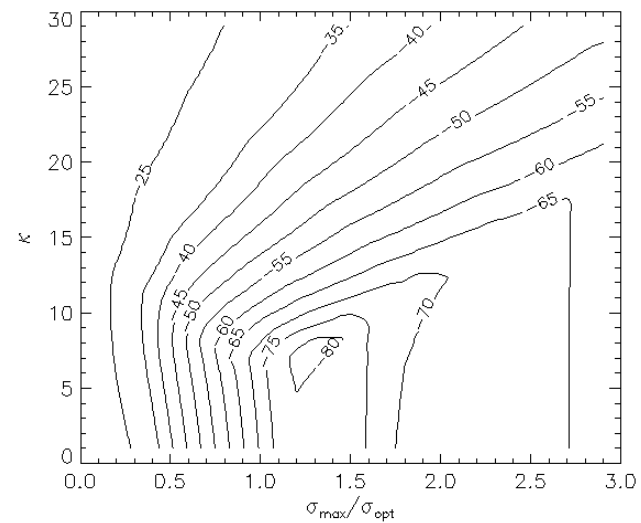
- Repeated for the rest of the E and H-field projections.
- Note that the conductivity requires an additional auxiliary variable.
- Three-step update process for each field projection
- Nevertheless, medium is perfectly matched. The κ terms aide in the absorption of the attenuating and evanescent waves.

EXAMPLE – Dipole over a Lossy Half Space

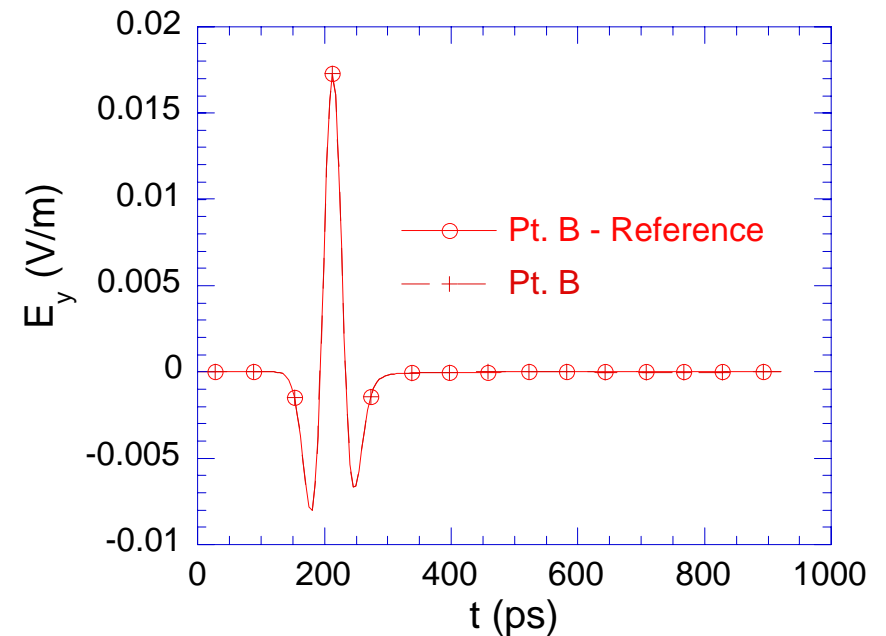
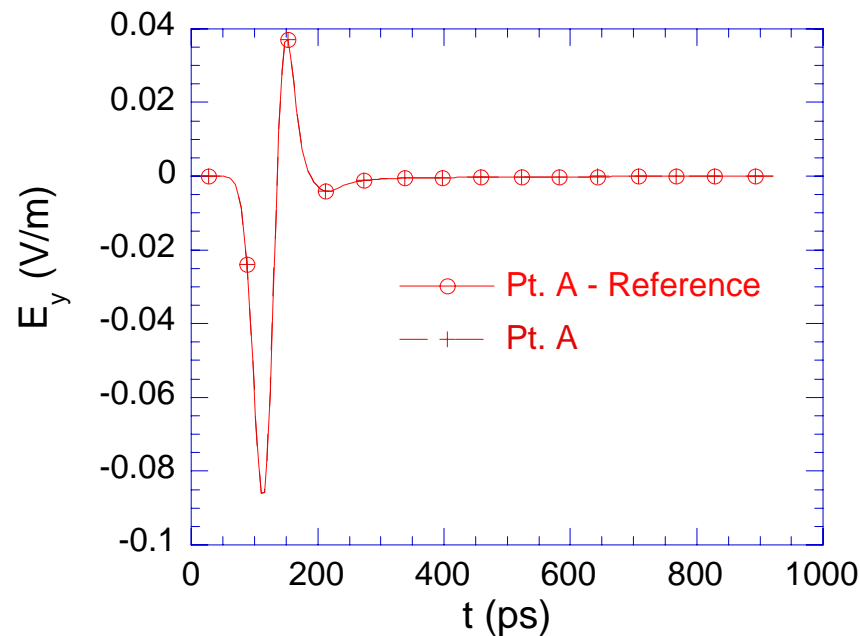
Geometry for the FDTD simulation of a TE_z polarized wave excited by a vertical electric current source above a lossy half space. The working volume was 40 cells by 40 cells ($\Delta x = \Delta y = 0.4$ mm), and the PML layers are 10 cells thick ($d = 4$ mm). ($\epsilon_r = 10$, $\sigma = 0.3$ S/m). (Lossy medium extends thru PML to PEC boundaries)

$$J_y(x_o, y_o, t) = -2 \frac{t - t_o}{t_w} e^{-\left(\frac{t - t_o}{t_w}\right)^2}, \text{ with } t_w = 2.65258 \times 10^{-11} \text{ s \& } t_o = 4 t_w$$

Reflection Error

Point A ($\kappa = 1$)Point B ($\kappa = 1$)Point A ($m = 3$)Point B ($m = 3$)

- Vertical electric field at points *A* and *B* due to the electric current dipole radiating above the lossy half space computed with the PML termination as compared with a reference solution computed on an extremely large grid. 10 cell PML, $\sigma_{\max} = 1.1 \sigma_{\text{opt}}$, $m = 3.5$, $\kappa_{\max} = 7$.



Complex-Frequency Shifted PML Tensor

- The PML still suffers from
 - Large reflections for very slowly varying wave (low frequency, large evanescence, highly-oblique angles of incidence)
 - The majority of the reflection error comes from the front boundary interface c.f., [J. P. Berenger, "Evanescent waves in PML's: Origin of the numerical reflection in wave-structure interaction problems," *IEEE Transactions on Antennas and Propagation*, vol. 47, pp. 1497-1503, 1999.]
 - This is partly related to the pole in the metric tensor at the origin ($\omega = 0$).
 - We can circumvent this by introducing a metric tensor coefficient of the form:

$$s_x = \kappa_x + \frac{\sigma_x}{\alpha_x + j\omega\epsilon_o}$$

- This is referred to as the Complex-Frequency-Shifted (CFS) PML tensor coefficient. First proposed by M. Kuzuoglu and R. Mittra, in "Frequency dependence of the constitutive parameters of causal perfectly matched anisotropic absorbers," *IEEE Microwave and Guided Wave Letters*, vol. 6, pp. 447-449, 1996, for frequency dependent FEM. First proposed for FDTD, with implementation, by Gedney in Chapter 7 of *Advances in Computational Electrodynamics: The Finite-Difference Time-Domain Method*, Allen Taflove, Ed., Artech House, Boston, 1998.
- Consider a wave that is incident on the PML with a complex wave-number:

$$e^{-\gamma_x^i s_x x} = e^{-(\alpha_x^i + j\beta_x^i) s_x x} = e^{-\left(\alpha_x^i + j\beta_x^i\right) \left(\kappa_x + \frac{\sigma_x}{\alpha_x + j\omega\epsilon_o}\right) x} = e^{-\kappa_x \alpha_x^i x} e^{-\frac{\sigma_x}{\alpha_x + j\omega\epsilon_o} \alpha_x^i x} e^{-j\kappa_x \beta_x^i x} e^{-j\omega\sqrt{\mu\epsilon} \cos\theta^i \frac{\sigma_x}{\alpha_x + j\omega\epsilon_o} x}$$

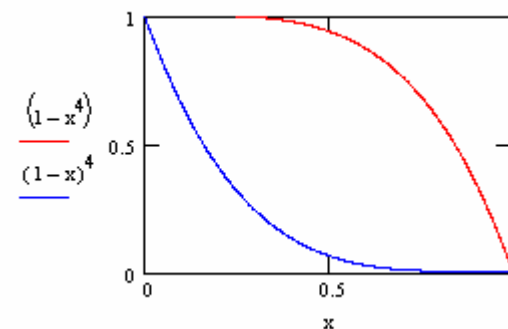
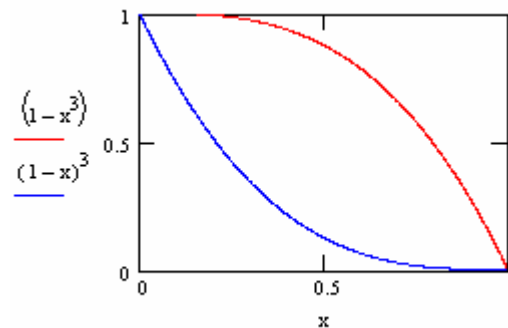
- At very low frequency ($\omega \rightarrow 0$):

$$\approx e^{-\kappa_x \alpha_x^i x} e^{-\frac{\sigma_x}{\alpha_x} \alpha_x^i x}$$

- Which is purely attenuating. In fact, now both κ_x and σ_x attenuate the wave.
- At higher frequencies, where $\omega\epsilon_o \gg \alpha_x$, the CFS PML behaves as the original PML.
- The consequence of this is that we can better attenuate low-frequency interactions with the PML. A rigorous study of this was presented by Berenger in: **“Numerical reflection from FDTD-PMLs: A comparison of the split PML with the unsplit and CFSPML,”** IEEE TRANSACTIONS ON ANTENNAS AND PROPAGATION, vol. 50 (3): pp. 258-265 MAR 2002

- Caveat: For a purely propagating wave, the CFS PML tensor can provide little to no attenuation. Consider a TEM mode with propagation $e^{-j\beta x}$, where $\beta = \omega\sqrt{\mu\epsilon}$.
- In the CFS PML, the wave propagate as: $e^{-j\kappa_x\beta x} e^{-j\beta \frac{\sigma_x}{\alpha_x + j\omega\epsilon_o} x}$.
- In the limit $\omega \rightarrow 0$, this becomes: $e^{-j\kappa_x\beta x} e^{-j\beta \frac{\sigma_x}{\alpha_x} x}$, which has no attenuation at all!
- To circumvent this, we need to scale α_x . It is recommended to scale α_x to be maximum at the interface, and minimum at the back wall.
- Two different polynomial scalings:

$$\alpha_x(x) = \alpha_x^{\max} \left(1 - \left(\frac{x}{d} \right)^m \right), \quad \alpha_x(x) = \alpha_x^{\max} \left(1 - \frac{x}{d} \right)^m$$



Implementing the CFS PML

Method 1: Auxiliary Equation Approach

- Given the CFS tensor coefficients:

$$s_x = \kappa_x + \frac{\sigma_x}{\alpha_x + j\omega\epsilon_o}, \quad s_y = \kappa_y + \frac{\sigma_y}{\alpha_y + j\omega\epsilon_o}, \quad s_z = \kappa_z + \frac{\sigma_z}{\alpha_z + j\omega\epsilon_o}$$

- Lets work with the x -projection of Ampere's Law:

$$j\omega\epsilon\bar{s}E_x = \frac{\partial H_z}{\partial y} - \frac{\partial H_y}{\partial z}, \quad \text{where } \bar{s} = \begin{bmatrix} s_y s_z / s_x & 0 & 0 \\ 0 & s_z s_x / s_y & 0 \\ 0 & 0 & s_x s_y / s_z \end{bmatrix}$$

- Make the substitution:

$$P_x = \frac{1}{s_x} E_x, \quad P_x^z = s_z P_x, \quad P_x^y = s_y P_x^z$$

- Then, from $P_x^y = s_y P_x^z$

$$P_x^y = \left(\kappa_y + \frac{\sigma_y}{\alpha_y + j\omega\epsilon_o} \right) P_x^z \Rightarrow (\alpha_y + j\omega\epsilon_o) P_x^y = [\kappa_y (\alpha_y + j\omega\epsilon_o) + \sigma_y] P_x^z$$

- Transforming this to the time domain:

$$\alpha_y P_x^y + \epsilon_o \frac{\partial}{\partial t} P_x^y = (\kappa_y \alpha_y + \sigma_y) P_x^z + \kappa_t \epsilon_o \frac{\partial}{\partial t} P_x^z$$

- Therefore, to write down the CFS equations, we can use the following procedure:

$$\begin{aligned}
 1. \quad j\omega\epsilon P_x^y &= \frac{\partial H_z}{\partial y} - \frac{\partial H_y}{\partial z} \\
 2. \quad (\kappa_y\alpha_y + \sigma_y)P_x^z + \kappa_y\epsilon_o \frac{\partial}{\partial t}P_x^z &= \alpha_y P_x^y + \epsilon_o \frac{\partial}{\partial t}P_x^y \\
 3. \quad (\kappa_z\alpha_z + \sigma_z)P_x + \kappa_z\epsilon_o \frac{\partial}{\partial t}P_x &= \alpha_z P_x^z + \epsilon_o \frac{\partial}{\partial t}P_x^z \\
 4. \quad \alpha_x E_x + \epsilon_o \frac{\partial}{\partial t}E_x &= (\kappa_x\alpha_x + \sigma_x)P_x + \kappa_x\epsilon_o \frac{\partial}{\partial t}P_x
 \end{aligned}$$

- We can discretize this in a second-order accurate manner as before.
- Problem: We've increased to 4 unknowns per field projection! In 3D, this increases the number of base field vectors from 6 to 24!
- A more efficient procedure was introduced in: [Roden JA, Gedney SD, "Convolution PML (CPML): An efficient FDTD implementation of the CFS-PML for arbitrary media", Microwave and Optical Technology Letters, vol. 27, no. 6, pp. 334-339, Dec. 5, 2000]
- Note that the CPML procedure improves efficiency of the algorithm, but exactly the same reflection properties.

Method 1: Convolutional PML - CPML

- If we combine the split field projections of Berenger, we can express Maxwell's equations in the PML region in a “stretched coordinate form”. Thus,

$$\begin{aligned}
 j\omega\epsilon E_x &= \frac{1}{s_y} \frac{\partial H_z}{\partial y} - \frac{1}{s_z} \frac{\partial H_y}{\partial z}, & -j\omega\mu H_x &= \frac{1}{s_y} \frac{\partial E_z}{\partial y} - \frac{1}{s_z} \frac{\partial E_y}{\partial z} \\
 j\omega\epsilon E_y &= \frac{1}{s_z} \frac{\partial H_x}{\partial z} - \frac{1}{s_x} \frac{\partial H_z}{\partial x}, & -j\omega\mu H_y &= \frac{1}{s_z} \frac{\partial E_x}{\partial z} - \frac{1}{s_x} \frac{\partial E_z}{\partial x} \\
 j\omega\epsilon E_z &= \frac{1}{s_x} \frac{\partial H_y}{\partial x} - \frac{1}{s_y} \frac{\partial H_x}{\partial y}, & -j\omega\mu H_z &= \frac{1}{s_x} \frac{\partial E_y}{\partial x} - \frac{1}{s_y} \frac{\partial E_x}{\partial y}
 \end{aligned}$$

- Note, this is derived by first dividing both sides by s_k , then adding split fields.
- We can then express this in the time domain as:

$$\epsilon \frac{\partial}{\partial t} E_x = \bar{s}_y(t) * \frac{\partial}{\partial y} H_z - \bar{s}_z(t) * \frac{\partial}{\partial z} H_y$$

- Where $\bar{s}_y(t)$ is the inverse Fourier transform of $1/s_y$, and similarly for $\bar{s}_z(t)$

- Given that $s_i = \kappa_i + \frac{\sigma_i}{\alpha_i + j\omega\epsilon_o}$, ($i = x, y, \text{ or } z$), we can show that

$$\bar{s}_i(t) = \frac{\delta(t)}{\kappa_i} - \frac{\sigma_i}{\epsilon_o \kappa_i^2} e^{-\left(\frac{\sigma_i}{\epsilon_o \kappa_i} + \frac{\alpha_i}{\epsilon_o}\right)t} u(t) = \frac{\delta(t)}{\kappa_i} + \zeta_i(t)$$

$$\bar{s}_i(t) = \frac{\delta(t)}{\kappa_i} - \frac{\sigma_i}{\varepsilon_o \kappa_i^2} e^{-\left(\frac{\sigma_i}{\varepsilon_o \kappa_i} + \frac{\alpha_i}{\varepsilon_o}\right)t} u(t) = \frac{\delta(t)}{\kappa_i} + \zeta_i(t)$$

○ Now, we can rewrite the x-projection of Ampere's law as:

$$\varepsilon \frac{\partial}{\partial t} E_x = \frac{1}{\kappa_y} \frac{\partial}{\partial y} H_z - \frac{1}{\kappa_z} \frac{\partial}{\partial z} H_y + \zeta_y(t) * \frac{\partial}{\partial y} H_z - \zeta_z(t) * \frac{\partial}{\partial z} H_y$$

○ At this point, we need to compute the convolutions efficiently.

○ Define the “Discrete Impulse Response” for $\zeta_i(t)$ as:

$$Z_{0_i}(m) = \int_{m\Delta_t}^{(m+1)\Delta_t} \zeta_i(\tau) d\tau = -\frac{\sigma_i}{\varepsilon_o \kappa_i^2} \int_{m\Delta_t}^{(m+1)\Delta_t} e^{-\left(\frac{\sigma_i}{\varepsilon_o \kappa_i} + \frac{\alpha}{\varepsilon_o}\right)\tau} d\tau$$

$$= a_i e^{-\left(\frac{\sigma_i}{\kappa_i} + \alpha\right) \frac{m\Delta_t}{\varepsilon_o}}$$

$$\text{where } a_i = \frac{\sigma_i}{(\sigma_i \kappa_i + \kappa_i^2 \alpha_i)} \left(e^{-\left(\frac{\sigma_i}{\kappa_i} + \alpha_i\right) \frac{\Delta_t}{\varepsilon_o}} - 1.0 \right)$$

○ Then, the discrete convolution of $\zeta_i(t)$ with a discrete function $f(t)$ sampled at $n\Delta t$ is:

$$f(t) * \zeta_i(t) = \sum_{m=0}^{N-1} Z_{0_i}(m) f(n-m)$$

- Inserting this into Ampere's law, and discretizing in time leads to:

○

$$\begin{aligned} \epsilon_r \epsilon_0 \frac{E_{x_{i+\frac{1}{2},j,k}}^{n+1} - E_{x_{i+\frac{1}{2},j,k}}^n}{\Delta_t} = & \frac{H_{z_{i+\frac{1}{2},j+\frac{1}{2},k}}^{n+\frac{1}{2}} - H_{z_{i+\frac{1}{2},j-\frac{1}{2},k}}^{n+\frac{1}{2}}}{\kappa_y \Delta_y} - \frac{H_{y_{i+\frac{1}{2},j,k+\frac{1}{2}}}^{n+\frac{1}{2}} - H_{y_{i+\frac{1}{2},j,k-\frac{1}{2}}}^{n+\frac{1}{2}}}{\kappa_z \Delta_z} \\ & + \sum_{m=0}^{N-1} Z_{o_y}(m) \frac{H_{z_{i+\frac{1}{2},j+\frac{1}{2},k}}^{n-m+\frac{1}{2}} - H_{z_{i+\frac{1}{2},j-\frac{1}{2},k}}^{n-m+\frac{1}{2}}}{\Delta_y} - \sum_{m=0}^{N-1} Z_{o_z}(m) \frac{H_{y_{i+\frac{1}{2},j,k+\frac{1}{2}}}^{n-m+\frac{1}{2}} - H_{y_{i+\frac{1}{2},j,k-\frac{1}{2}}}^{n-m+\frac{1}{2}}}{\Delta_z} \end{aligned}$$

- This is still *too expensive*, since it requires a full summation at every time step!

- Fortunately, given the properties of $Z_{o_i}(m)$, this can be performed in a simplified manner using the “Recursive Convolution Method” [R. J. Luebbers and F. Hunsberger, "FDTD for Nth-Order Dispersive Media," *IEEE Transactions on Antennas and Propagation*, vol. 40, pp. 1297-1301, 1992.]. Thus, the update can be re-written as:

$$\epsilon_r \epsilon_0 \frac{E_{x_{i+\frac{1}{2},j,k}}^{n+1} - E_{x_{i+\frac{1}{2},j,k}}^n}{\Delta_t} = \frac{H_{z_{i+\frac{1}{2},j+\frac{1}{2},k}}^{n+\frac{1}{2}} - H_{z_{i+\frac{1}{2},j-\frac{1}{2},k}}^{n+\frac{1}{2}}}{\kappa_y \Delta_y} - \frac{H_{y_{i+\frac{1}{2},j,k+\frac{1}{2}}}^{n+\frac{1}{2}} - H_{y_{i+\frac{1}{2},j,k-\frac{1}{2}}}^{n+\frac{1}{2}}}{\kappa_z \Delta_z} + \psi_{e_{xy_{i+\frac{1}{2},j,k}}^{n+\frac{1}{2}}} - \psi_{e_{xz_{i+\frac{1}{2},j,k}}^{n+\frac{1}{2}}}$$

where

$$\psi_{e_{xy_{i+\frac{1}{2},j,k}}^{n+\frac{1}{2}}} = b_y \psi_{e_{xy_{i+\frac{1}{2},j,k}}^{n-\frac{1}{2}}} + a_y \left(H_{z_{i+\frac{1}{2},j+\frac{1}{2},k}}^{n+\frac{1}{2}} - H_{z_{i+\frac{1}{2},j-\frac{1}{2},k}}^{n+\frac{1}{2}} \right) / \Delta_y$$

$$\psi_{e_{xz_{i+\frac{1}{2},j,k}}^{n+\frac{1}{2}}} = b_z \psi_{e_{xz_{i+\frac{1}{2},j,k}}^{n-\frac{1}{2}}} + a_z \left(H_{y_{i+\frac{1}{2},j,k+\frac{1}{2}}}^{n+\frac{1}{2}} - H_{y_{i+\frac{1}{2},j,k-\frac{1}{2}}}^{n+\frac{1}{2}} \right) / \Delta_z$$

$$b_i = e^{-\left(\frac{\sigma_i}{\kappa_i} + \alpha_i\right) \frac{\Delta_t}{\epsilon_0}}, \quad (i = x, y, \text{ or } z)$$

- Advantages of the CPML formulation:

1. Reduced the number of auxiliary variables from 3 to 2

2. Lossy medium is similarly treated. Updates do not require additional terms!:

$$\epsilon_r \epsilon_0 \frac{E_{x_{i+\frac{1}{2},j,k}}^{n+1} - E_{x_{i+\frac{1}{2},j,k}}^n}{\Delta_t} + \sigma \frac{E_{x_{i+\frac{1}{2},j,k}}^{n+1} - E_{x_{i+\frac{1}{2},j,k}}^n}{2} = \frac{H_{z_{i+\frac{1}{2},j+\frac{1}{2},k}}^{n+\frac{1}{2}} - H_{z_{i+\frac{1}{2},j-\frac{1}{2},k}}^{n+\frac{1}{2}}}{\kappa_y \Delta_y} - \frac{H_{y_{i+\frac{1}{2},j,k+\frac{1}{2}}}^{n+\frac{1}{2}} - H_{y_{i+\frac{1}{2},j,k-\frac{1}{2}}}^{n+\frac{1}{2}}}{\kappa_z \Delta_z} + \psi_{e_{xy_{i+\frac{1}{2},j,k}}}^{n+\frac{1}{2}} - \psi_{e_{xz_{i+\frac{1}{2},j,k}}}^{n+\frac{1}{2}}$$

3. No more expensive than standard PML terminating a lossy medium

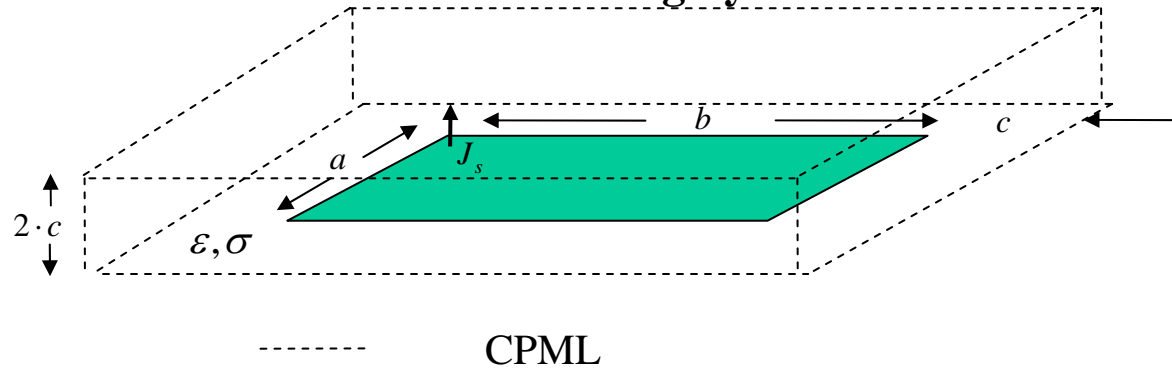
4. The convolutional terms ψ are simply added in as soft source terms – standard FDTD update loops are not corrupted.

5. Very easy to implement in a standard FDTD code with inhomogeneous and lossy medium.

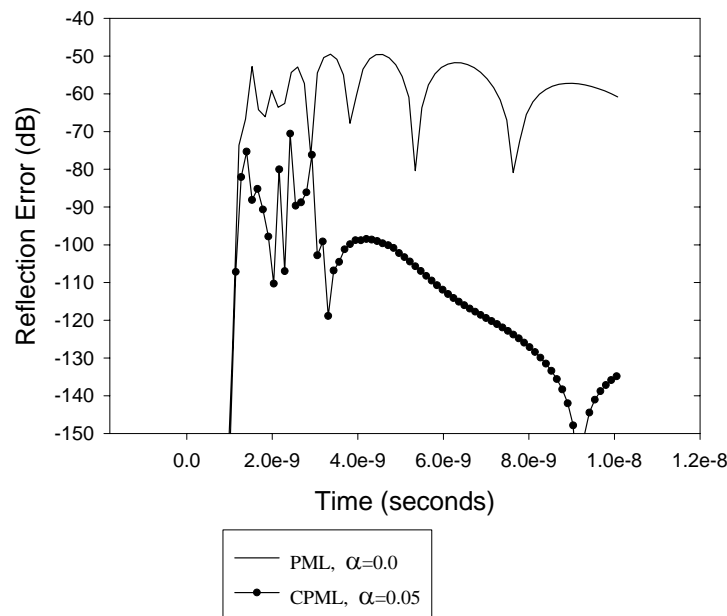
- In practice, $\alpha_i, \kappa_i, \sigma_i$ are scaled along the i -direction. The same rule applies to CPML as PML. You sample $\alpha_i, \kappa_i, \sigma_i$ at the *edge-centers* for E-field updates, and you sample $\alpha_i, \kappa_i, \sigma_i$ at the *face-centers* for H-field updates.

- The update coefficients can then be pre-calculated and stored as *one-dimensional* vectors

EXAMPLE – Scattering by a PEC Plate



$a = 25$ mm, $b = 100$ mm, PML is 10 cells thick, and 3 cells from plate in all dimensions
Maximum relative reflection error over 2,000 time steps for 10 cell thick PML



$\alpha = 0.0$ case:

$$\sigma_{\max} = 0.7 \sigma_{\text{opt}}$$

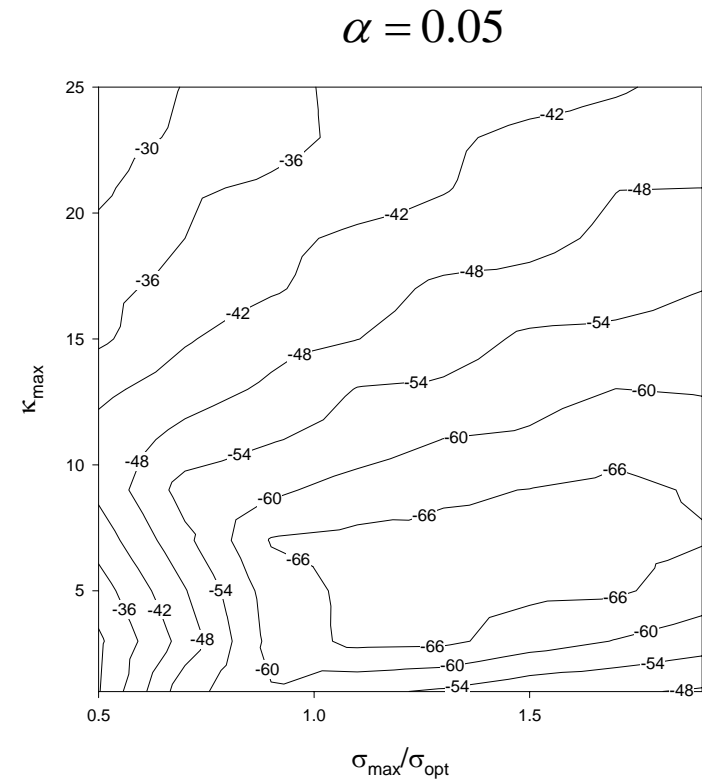
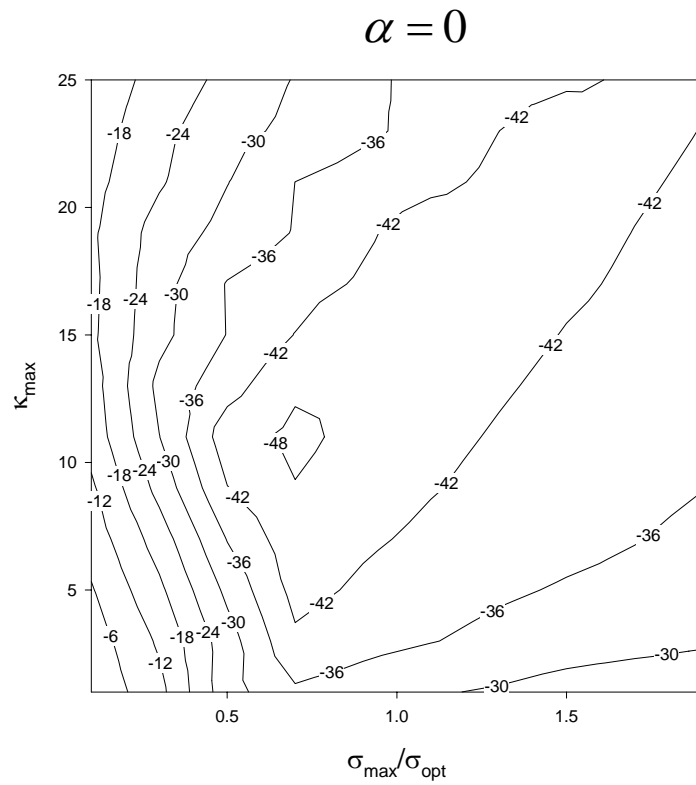
$$\kappa_{\max} = 11$$

$\alpha = 0.05$ case:

$$\sigma_{\max} = 1.1 \sigma_{\text{opt}}$$

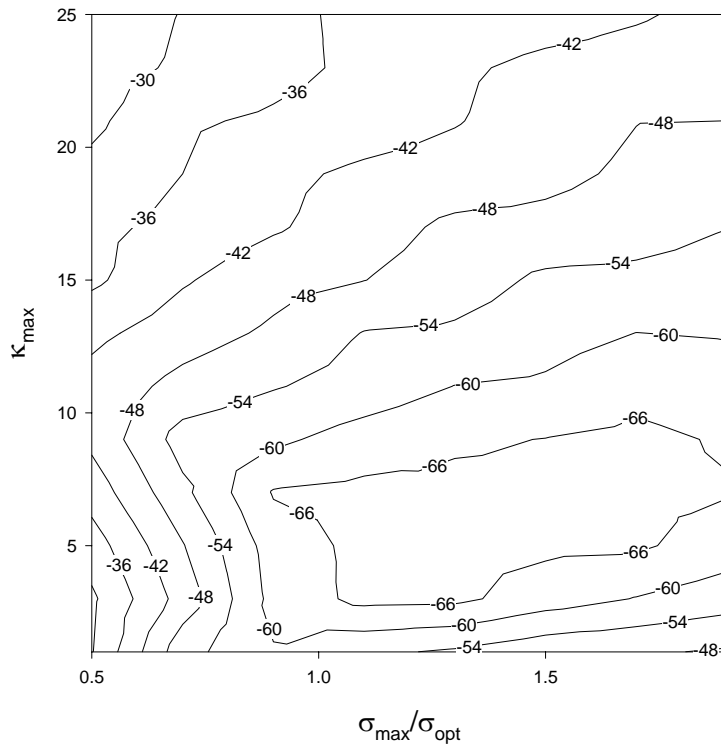
$$\kappa_{\max} = 7$$

- A significant improvement is the late time reflection error.

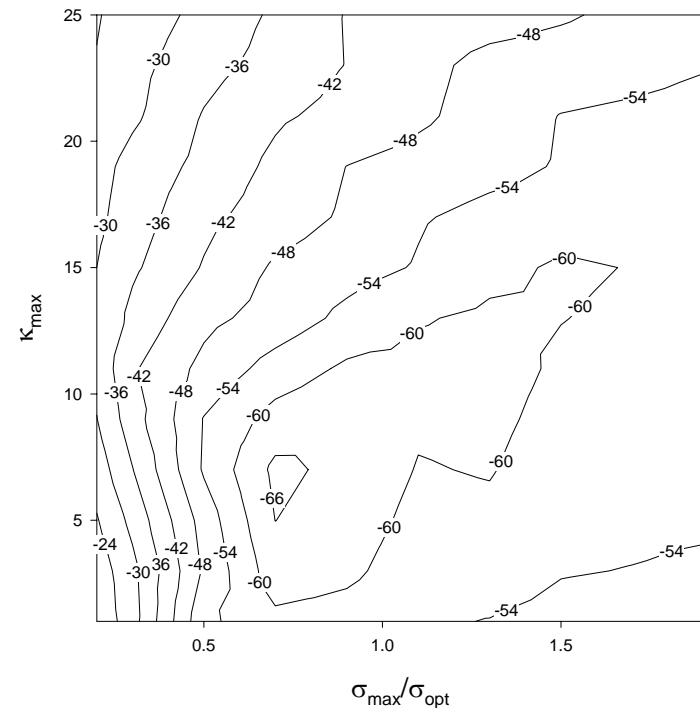


Maximum relative reflection error over 2,000 time steps for 10 cell PML

PML 3 cells from plate & $\alpha = 0.05$



PML 17 cells from plate & $\alpha = 0$



(note PML boundary is equidistant from plate on all sides)

Lattice 1: $126 \times 51 \times 26$ Lattice 2: $154 \times 79 \times 54$

Memory Savings Factor: $2 \times 154 \times 79 \times 54 / 3 \times 126 \times 51 \times 26 = 2.6$

Late Time-Stability of PML

- Consider a PML termination of a single boundary with no overlapping corner regions (a bounded wave guide would be an example).
- For simplicity, assume a lossless, homogeneous region, with a z -normal:

$$\begin{bmatrix} \frac{\partial}{\partial y} H_z - \frac{\partial}{\partial z} H_y \\ \frac{\partial}{\partial z} H_x - \frac{\partial}{\partial x} H_z \\ \frac{\partial}{\partial x} H_y - \frac{\partial}{\partial y} H_x \end{bmatrix} = j\omega\epsilon_o \begin{bmatrix} s_z & 0 & 0 \\ 0 & s_z & 0 \\ 0 & 0 & 1/s_z \end{bmatrix} \begin{bmatrix} E_x \\ E_y \\ E_z \end{bmatrix}, \quad \begin{bmatrix} \frac{\partial}{\partial y} E_z - \frac{\partial}{\partial z} E_y \\ \frac{\partial}{\partial z} E_x - \frac{\partial}{\partial x} E_z \\ \frac{\partial}{\partial x} E_y - \frac{\partial}{\partial y} E_x \end{bmatrix} = -j\omega\mu_o \begin{bmatrix} s_z & 0 & 0 \\ 0 & s_z & 0 \\ 0 & 0 & 1/s_z \end{bmatrix} \begin{bmatrix} H_x \\ H_y \\ H_z \end{bmatrix}$$

- The PML updates for the transverse fields appear in the form of a lossy medium. The normal fields, as a Debye medium. We write these in a two step update process:

$$\frac{\partial}{\partial x} H_y - \frac{\partial}{\partial y} H_x = j\omega\epsilon_o P_z \quad \& \quad E_z = s_z P_z$$

- In the time-domain:

$$\frac{\partial}{\partial x} H_y - \frac{\partial}{\partial y} H_x = \epsilon_o \frac{\partial P_z}{\partial t} \quad \& \quad \frac{\partial E_z}{\partial t} = \frac{\partial P_z}{\partial t} + \frac{\sigma_z}{\epsilon_o} P_z$$

- Comparing these two equations, we recognize that $\frac{\partial P_z}{\partial t}$ is proportional to the transverse derivatives of the transverse magnetic field. We have a dual situation from Faradays law

- In the very late time, as the fields reach steady state, the transverse derivatives of the transverse fields will tend to zero.
- As a consequence $\frac{\partial}{\partial x} H_y - \frac{\partial}{\partial y} H_x = 0 = \epsilon_o \frac{\partial P_z}{\partial t}$
- Therefore, the auxiliary equation reduces: $\frac{\partial E_z}{\partial t} = \frac{\sigma_z}{\epsilon_o} P_z$.
- Where, since $\frac{\partial P_z}{\partial t} = 0$, then P_z is a constant in time. Thus, the solution to the ODE $\frac{\partial E_z}{\partial t} = \frac{\sigma_z}{\epsilon_o} P_z$ is simply: $E_z = \frac{\sigma_z}{\epsilon_o} P_z t + E_{z_0}$, which is a linear function in time! Similarly, for the dual field $H_z = \frac{\sigma_z}{\epsilon_o} Q_z t + H_{z_0}$. Therefore, in the event that the transverse gradient of the fields is zero, the normal fields in the PML can grow linearly in time!

- This has been the topic of some publications:

S. Abarbanel, D. Gottlieb, and J. S. Hesthaven, “Long time behavior of the PML equations in computational electromagnetics,” *Journal of Scientific Computing*, vol. 17, no. 1-4, pp. 405-422, 2002.

E. Becache, P. Petropoulos, & S. D. Gedney, “On the long-time behavior of unsplit perfectly matched layers,” *IEEE Transactions on Antennas and Propagation*, to appear.

S. J. Yakura, D. Dietz, and A. D. Greenwood, “A dynamic stability analysis of the PML method,” Interaction Note Series Note 582, Kirtland Air Force Base, Albuquerque, NM, November 1, 2002

- **Consequences of the late time instability:**

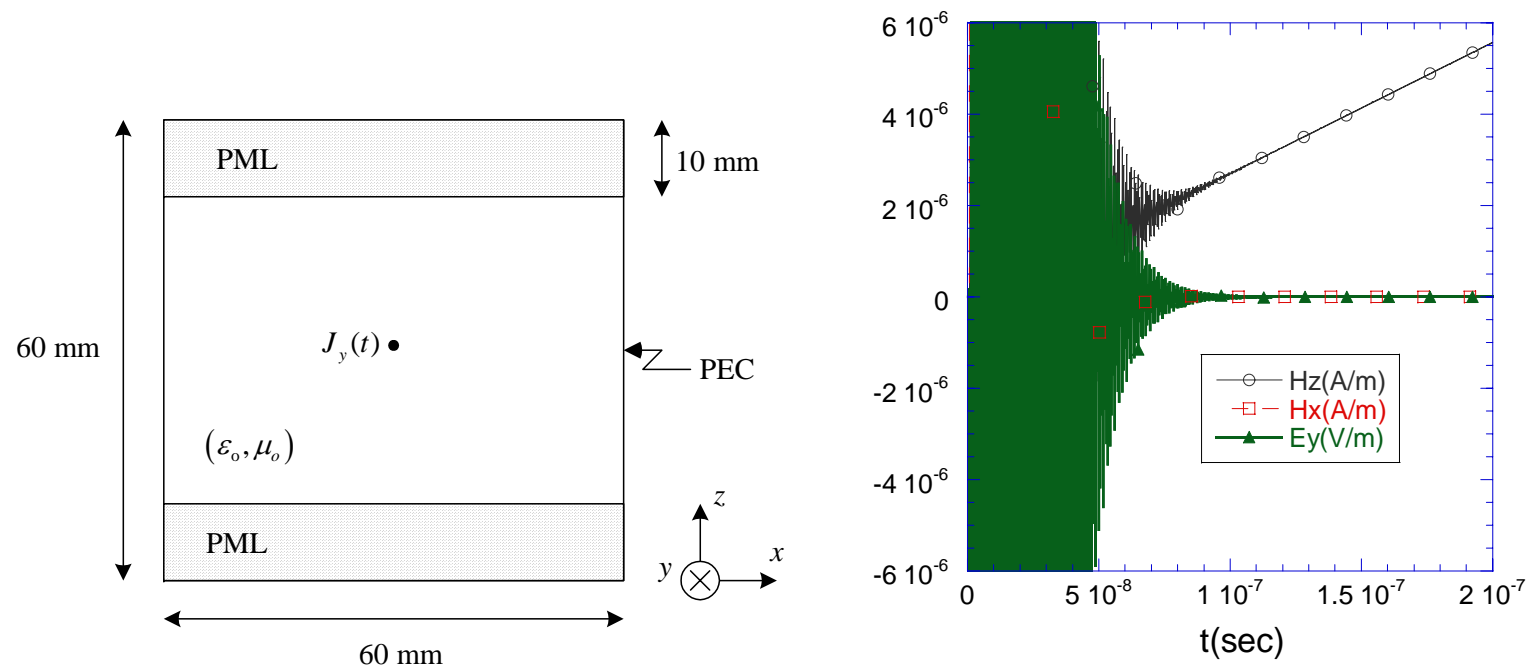
1. The late time instability does not occur until after the fields in the working volume are \sim zero, which is beyond steady state for a radiation/scattering problem
2. The linear growth of the fields only occurs *in* the PML, when using the UPML formulation. \therefore it does not corrupt the fields in the working volume. For the split-field PML, the linear growth can affect the fields in the working volume.
3. If the PML boundaries are overlapping, this problem does not occur. .
4. Late time instability does not occur for CFS PML. Why? The late time-stability is related to the weakly causal nature of the constitutive parameters.

Examples from Bécache, Petropoulos & Gedney

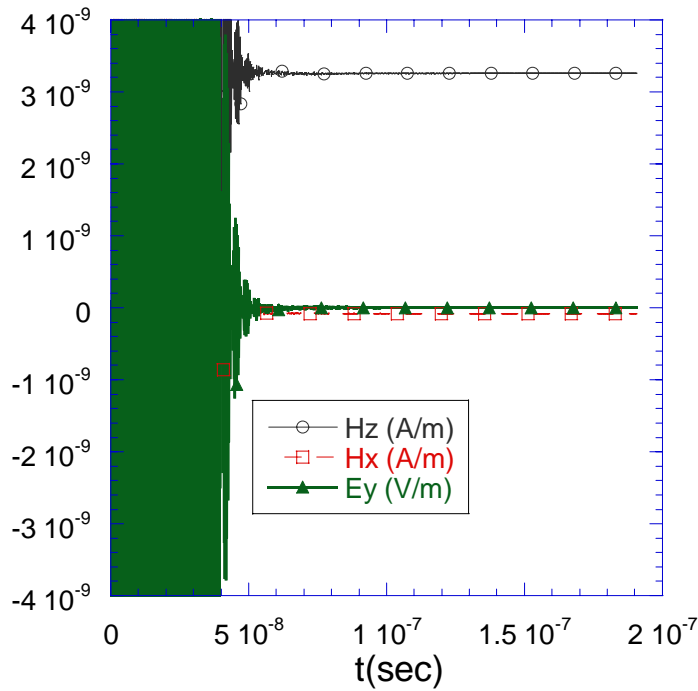
TM_z polarization. $\Delta x = \Delta y = 1\text{ mm}$, $\Delta t = 2.35 \times 10^{-12}\text{ s}$. $J_y(t) = -2 \frac{t}{t_w} e^{\frac{-(t-t_o)^2}{t_w^2}} \sin(2\pi f_c t)$,

with $t_w = 3.183 \times 10^{-10}\text{ s}$, $t_o = 4t_w$, and $f_c = 3 \times 10^9\text{ Hz}$. Standard PML with $m = 4$, $\sigma_{\max} = 10.61\text{ S/m}$, $\kappa_{\max} = 1$.

We are monitoring the fields *inside* the PML in the very late time ($\sim 100,000$ time steps).



Normal field shows linear growth in the late time as predicted!



Repeat the same experiment with CFS PML, with $\alpha = 0.08$. The field remains constant – no linear growth. Here we have:

$$H_z = s_z Q_z = \left(\kappa_z + \frac{\sigma_z}{\alpha_z + j\omega\epsilon_o} \right) Q_z \Rightarrow \alpha_z H_z + \epsilon_o \frac{\partial H_z}{\partial t} = (\kappa_z \alpha_z + \sigma_z) \frac{\partial Q_z}{\partial t} + \sigma_z Q_z$$

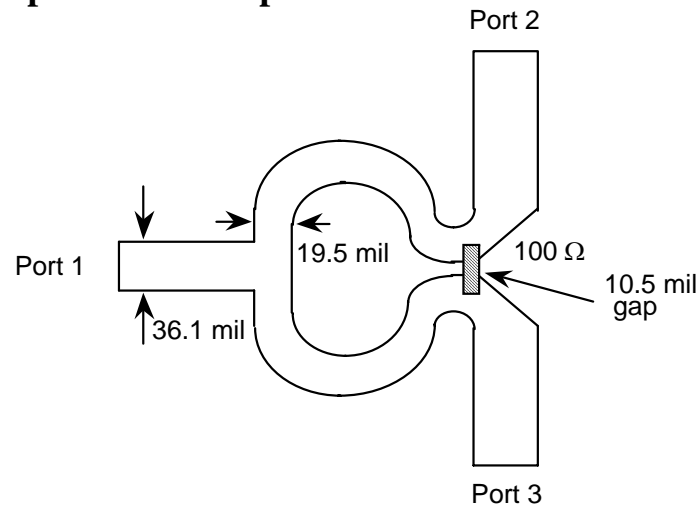
In the late time, if $\frac{\partial Q_z}{\partial t} = 0$, then $\alpha_z H_z + \epsilon_o \frac{\partial H_z}{\partial t} = \sigma_z Q_z$, which has solution: $H_z = \frac{\sigma_z}{\alpha_z} Q_z$.

Therefore, H_z is a non-zero constant in the late time. Nevertheless, it is quite small.

FDTD ANALYSIS OF PRINTED CIRCUITS

- Microwave Circuits:
 - * Communications Systems
 - * Microstrip, Stripline, Co-Planar Wave Guide
 - * Passive and Active Circuit Devices
 - * Printed Antennas

Wilkinson power divider printed on a 15 mil TMM substrate



- Printed Circuit Boards or Packages:
 - * EMC Modeling (Radiation/Coupling)
 - * Signal Integrity on Electrical Interconnect networks with Passive and active Loads

SOURCE MODELING

- Choice of the source will be problem dependent.
- Introduced a number of sources Section 6 of the notes. Most commonly used sources for this type of modeling are:
 - * Voltage Source (Soft Source)
 - * Thévenin Source
 - * Current Sheet
- Analysis of Circuits with linear loads will typically be source independent.
- Typically choose a broad band pulse (Gaussian) providing a broad-band analysis of the device with a single simulation.

PARAMETERIZATION OF CIRCUITS

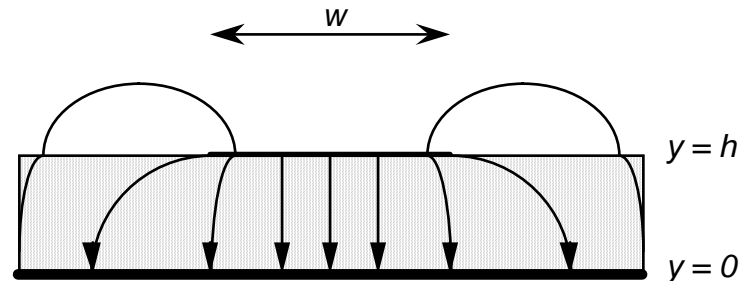
- Fundamental Measured Quantities:
 - * Line Voltage and Current
- Uniform Transmission Line Analysis
 - * Characteristic Line Impedance
 - * Propagation Constant (axial) and effective dielectric
- Network Analysis (General N-port)
 - * Input Impedance
 - * Scattering Parameters
 - * Impedance/Admittance Matrix
 - * Radiated Fields

FUNDAMENTAL MEASURED QUANTITIES

- Line Voltage
 - * Quasi-Static Approximation

$$V_{12} = -\int_2^1 \vec{E} \cdot d\vec{\ell}$$

- * Example: Microstrip Circuit



$$V = -\int_{y=0}^h \vec{E} \cdot d\vec{\ell} = -\sum_{j=1}^{ny1} E_{y_{i,j,k}} \Delta y$$

where, $ny1 = h / \Delta y$

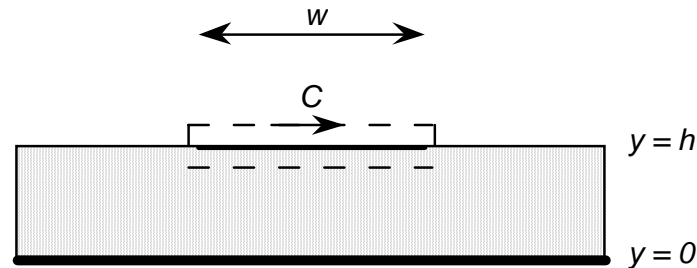
- * Valid if dimensions of the cross-section of the device are electrically small.
- * Most accurate if performed at the physical center of the microstrip

- Line Current

- Quasi-Static Approximation

$$I = \int_S \vec{J} \cdot d\vec{s} \approx \oint_C \vec{H} \cdot d\vec{\ell}$$

- Example: Microstrip Circuit



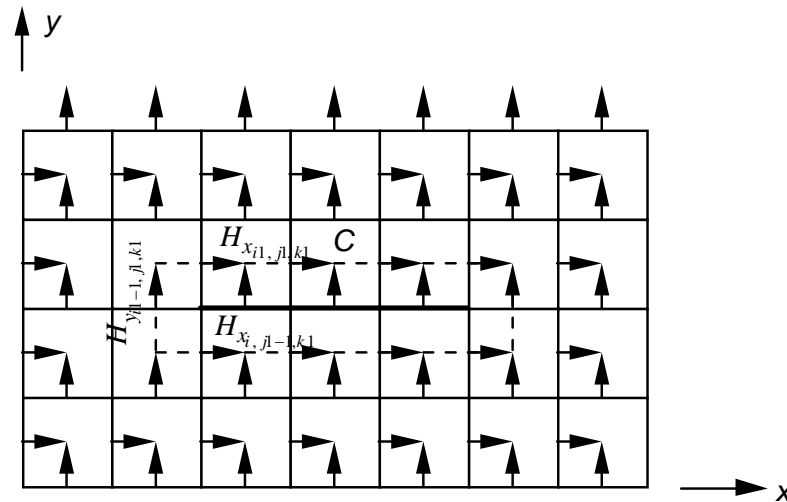
- Approximations:

- Discrete Tangential H-fields are 1/2 cell removed from the conductor surface. Therefore, there is a small amount of displacement current present in the line integral as well.

- Evaluation:

$$\oint_C \vec{H} \cdot d\vec{\ell} \approx \sum_{i=i1}^{i2} \Delta x \left[H_{x_{i,j1,k1}} - H_{x_{i,j1-1,k1}} \right] + \Delta y \left[H_{y_{i1-1,j1,k1}} - H_{y_{i2,j1,k1}} \right]$$

$$\oint_C \vec{H} \cdot d\vec{\ell} \approx \sum_{i=1}^{i2} \Delta x \left[H_{x_{i,j1,k1}} - H_{x_{i,j1-1,k1}} \right] + \Delta y \left[H_{y_{i1-1,j1,k1}} - H_{y_{i2,j1,k1}} \right]$$



LINE IMPEDANCE

- The Generalized Line Impedance can simply be Calculated as

$$Z(\omega) = \frac{V(\omega)}{I(\omega)}$$

where, $V(\omega)$ and $I(\omega)$ are the line voltage and current at a fixed point on the transmission line, and are found by Fourier transforming the time-dependent voltage or currents.

- A difficulty encountered with this formulation is that the transverse magnetic fields and the transverse electric fields are separated by one-half of a cell.
- The voltage and current are further separated by one-half of a time-step.
- This leads to error in the line impedance. Namely, in the discrete space

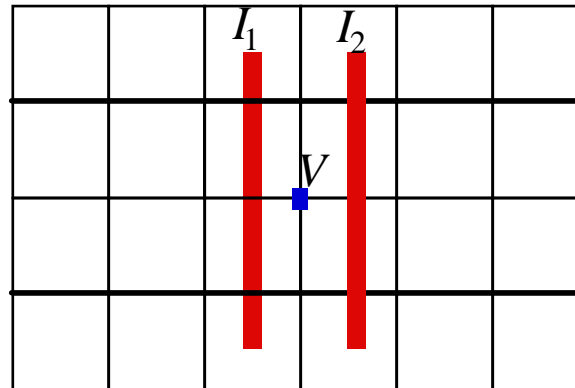
$$\begin{aligned}\tilde{Z}(\omega) &= \frac{V(\omega)e^{-\alpha(z+\Delta z/2)}e^{-j\beta(z+\Delta z/2)}e^{j\omega(t+\Delta t/2)}}{I(\omega)e^{-\alpha z}e^{-j\beta z}e^{j\omega t}} \\ &= \frac{V(\omega)}{I(\omega)}e^{-\alpha\Delta z/2}e^{-j\beta\Delta z/2}e^{j\omega\Delta t/2}\end{aligned}$$

where α and β are the attenuation and propagation constants

- An alternate scheme of computing the line impedance proposed by Fang [IEEE MGWL, vol. 5, pp. 1-6, 1995] helps to overcome this phase shift error.

ACCURATE EVALUATION OF THE LINE IMPEDANCE

Top View



- Compute I_1 and I_2 on either side of the voltage probe
- Compute Characteristic Impedance as:

$$\tilde{Z}(\omega) = \frac{V(\omega)}{\sqrt{I_1(\omega)I_2(\omega)}}$$

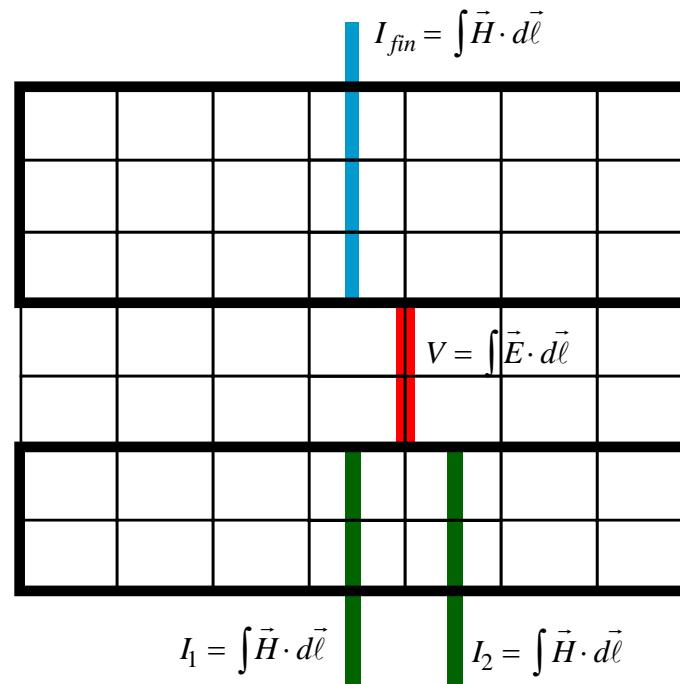
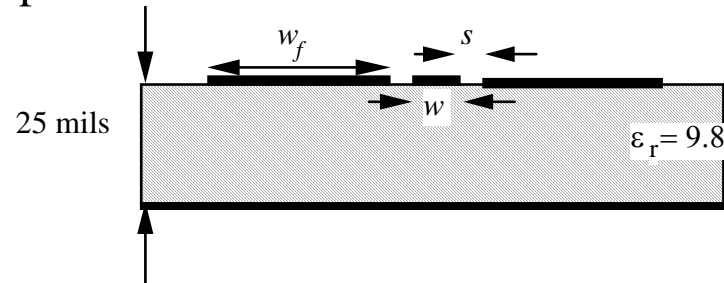
- In an ideal sense:

$$\tilde{Z}(\omega) \approx \frac{V(\omega)e^{-\alpha(z+\Delta z/2)}e^{-j\beta(z+\Delta z/2)}e^{j\omega(t+\Delta t/2)}}{\sqrt{I(\omega)e^{-\alpha z}e^{-j\beta z}e^{j\omega t} \cdot I(\omega)e^{-\alpha(z+\Delta z)}e^{-j\beta(z+\Delta z)}e^{j\omega(t+\Delta t)}}} = \frac{V(\omega)}{I(\omega)}$$

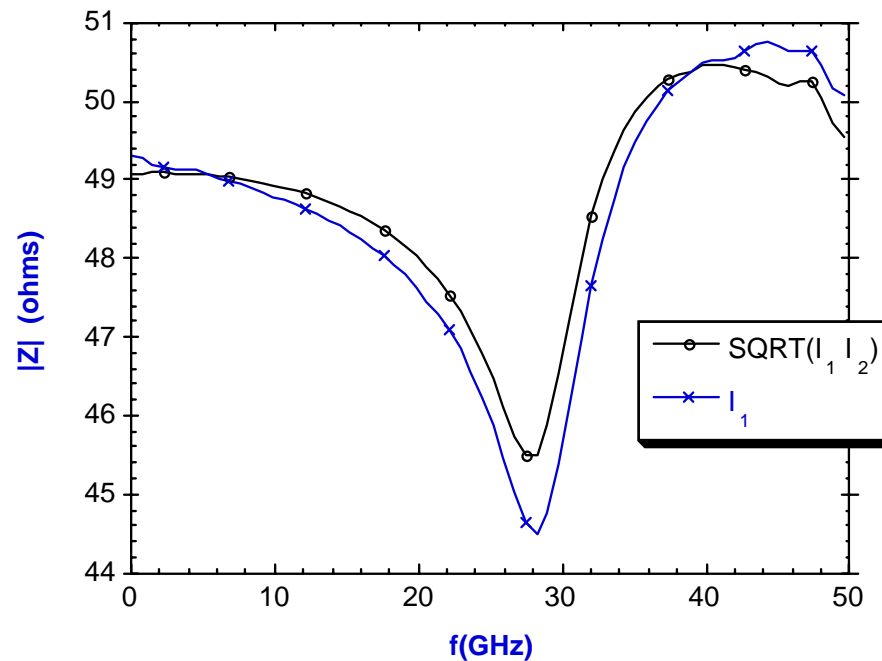
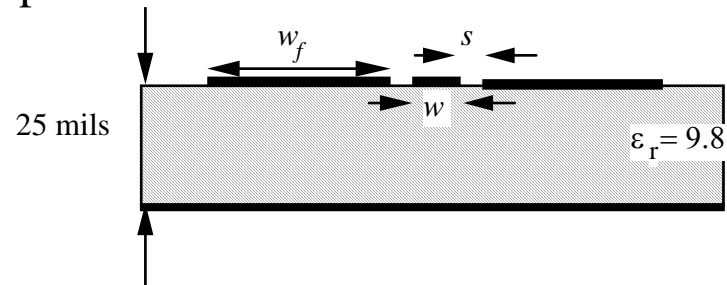
- Thus, the phase Errors Cancel Out, greatly improving the accuracy
- For a uniform line matched at both ends, $\tilde{Z}(\omega)$ represents the characteristic line impedance
- For a uniform line terminated into some load such as a lumped load, antenna, or N-port network, $\tilde{Z}(\omega)$ represents the input impedance of that port.

EXAMPLE OF COMPUTING THE CHARACTERISTIC LINE IMPEDANCE VIA THE FDTD METHOD

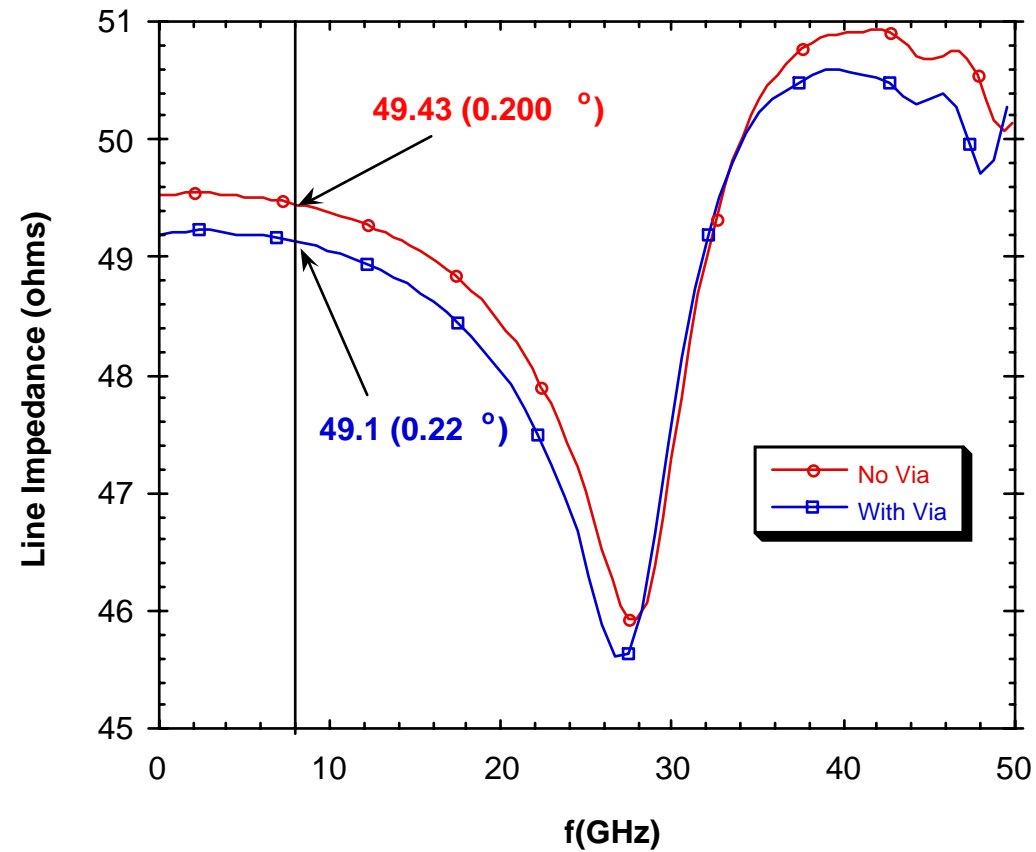
- Grounded Co-Planar WaveGuide (GCPWG)
- Cross section of the uniform GCPWG: $w = 10$ mils, $s = 5$ mils, and $w_f = 40$ mils, and the 50-mil spaced vias were placed at the centers of the outer conductors



- Cross section of the uniform GCPWG: $w = 10$ mils, $s = 5$ mils, and $w_f = 40$ mils, and the 50-mil spaced vias were placed at the centers of the outer conductors



- Comparison of the Line Impedance of the GCPWG loaded with vias, and without vias.



PROPAGATION CONSTANT AND EFFECTIVE DIELECTRIC

- The propagation constant of the fundamental mode can be estimated by simply probing the line voltage or current on a uniform line that is matched at both the source and load ends

- Assuming:

$$\tilde{V}(\omega, z) = V_o e^{-(\alpha_z + j\beta_z)z}$$

- Probe the voltage at two points z_1 and z_2 (where $z_2 > z_1$):

- Then:

$$\frac{\tilde{V}(\omega, z_2)}{\tilde{V}(\omega, z_1)} \cong \frac{V_o e^{-(\alpha_z + j\beta_z)z_2}}{V_o e^{-(\alpha_z + j\beta_z)z_1}} = e^{-(\alpha_z + j\beta_z)(z_2 - z_1)}$$

$$\therefore \alpha_z = -\operatorname{Re} \left\{ \ln \left(\left| \frac{\tilde{V}(\omega, z_2)}{\tilde{V}(\omega, z_1)} \right| \right) \right\} / (z_2 - z_1), \quad \beta_z = -\angle \left(\frac{\tilde{V}(\omega, z_2)}{\tilde{V}(\omega, z_1)} \right) / (z_2 - z_1)$$

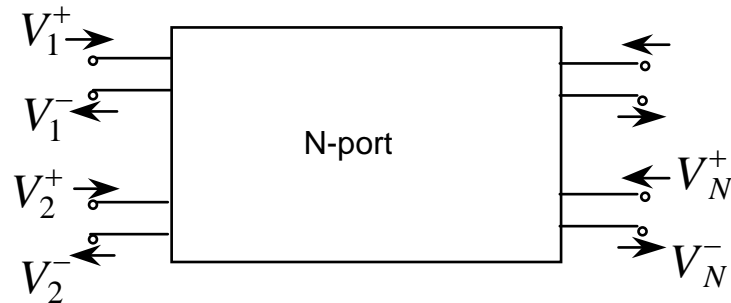
- Then, assuming a quasi-static or TEM approximation,

$$\beta_z \approx \omega \sqrt{\mu_o \epsilon_o \epsilon_{eff}}$$

$$\therefore \epsilon_{eff} \approx \frac{\beta_z^2}{(\omega \sqrt{\mu_o \epsilon_o})^2}$$

SCATTERING PARAMETERS

- A convenient characterization of a microwave circuit device is through its scattering parameters, or the S-parameters
- Scattering Parameters are the elements of the [S]-matrix



- Given an N-port Network, let V_i^+ be the input or incident voltage, and V_i^- be the reflected voltage on the i -th port.

$$\begin{bmatrix} V_1^- \\ V_2^- \\ \vdots \\ V_N^- \end{bmatrix} = \begin{bmatrix} S_{11} & S_{12} & \cdots & S_{1N} \\ S_{21} & S_{22} & & S_{2N} \\ \vdots & & & \vdots \\ S_{N1} & \cdots & & S_{NN} \end{bmatrix} \begin{bmatrix} V_1^+ \\ V_2^+ \\ \vdots \\ V_N^+ \end{bmatrix}$$

- Each term of the S-matrix can be determined as

$$S_{ij} = \left. \frac{V_i^-}{V_j^+} \right|_{V_k^+ = 0 \text{ for } k \neq j}$$

- Note that these are frequency dependent values, and it is assumed that all ports have the same characteristic line impedance

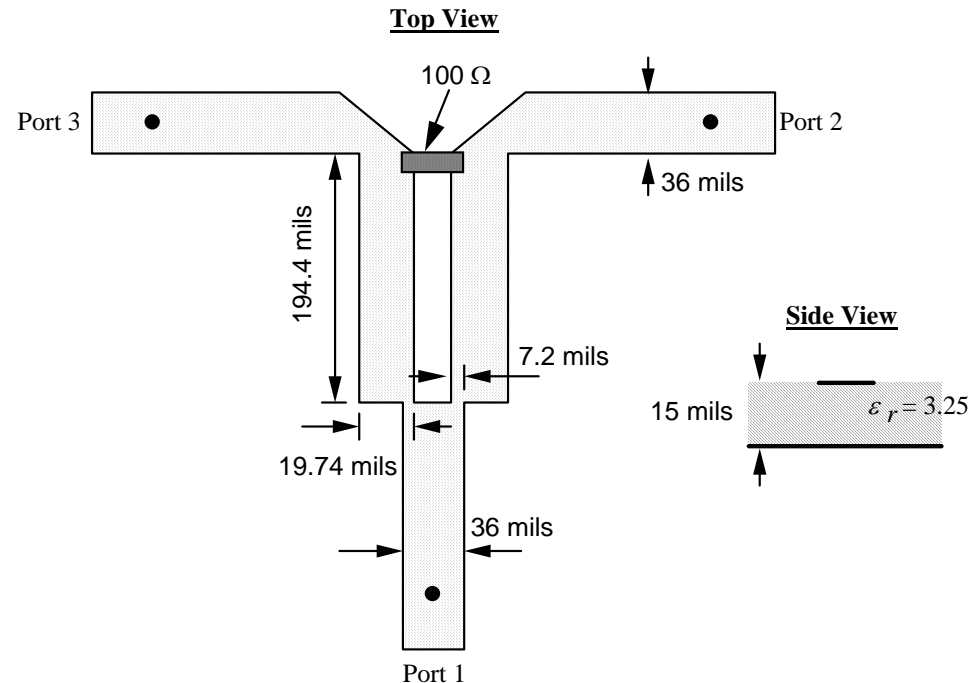
SCATTERING PARAMETERS (CONT'D)

$$S_{ij} = \left. \frac{V_i^-}{V_j^+} \right|_{V_k^+ = 0 \text{ for } k \neq j}$$

- To compute $S_{i,j}$, excite the j -th port, and terminate all ports with a matched load (including the j -th port to avoid multiple reflections).
- Matched condition is most often simulated by terminating the uniform line representing each port into an absorbing boundary wall. This represents a true matched condition, rather than an approximate matched condition which can be achieved using a lumped load.
- Problem: On the j -th port, we can only measure the total line voltage, which is a superposition of the incident and reflected voltage waves. (A soft source is used.)
- To circumvent this, perform an independent simulation of a uniform line for the incident field. To this end, the separation between the source and the port, and the source and the ABC wall must remain unchanged. Otherwise, there will be a phase shift between the incident and total line voltages, leading to errors.
- Then

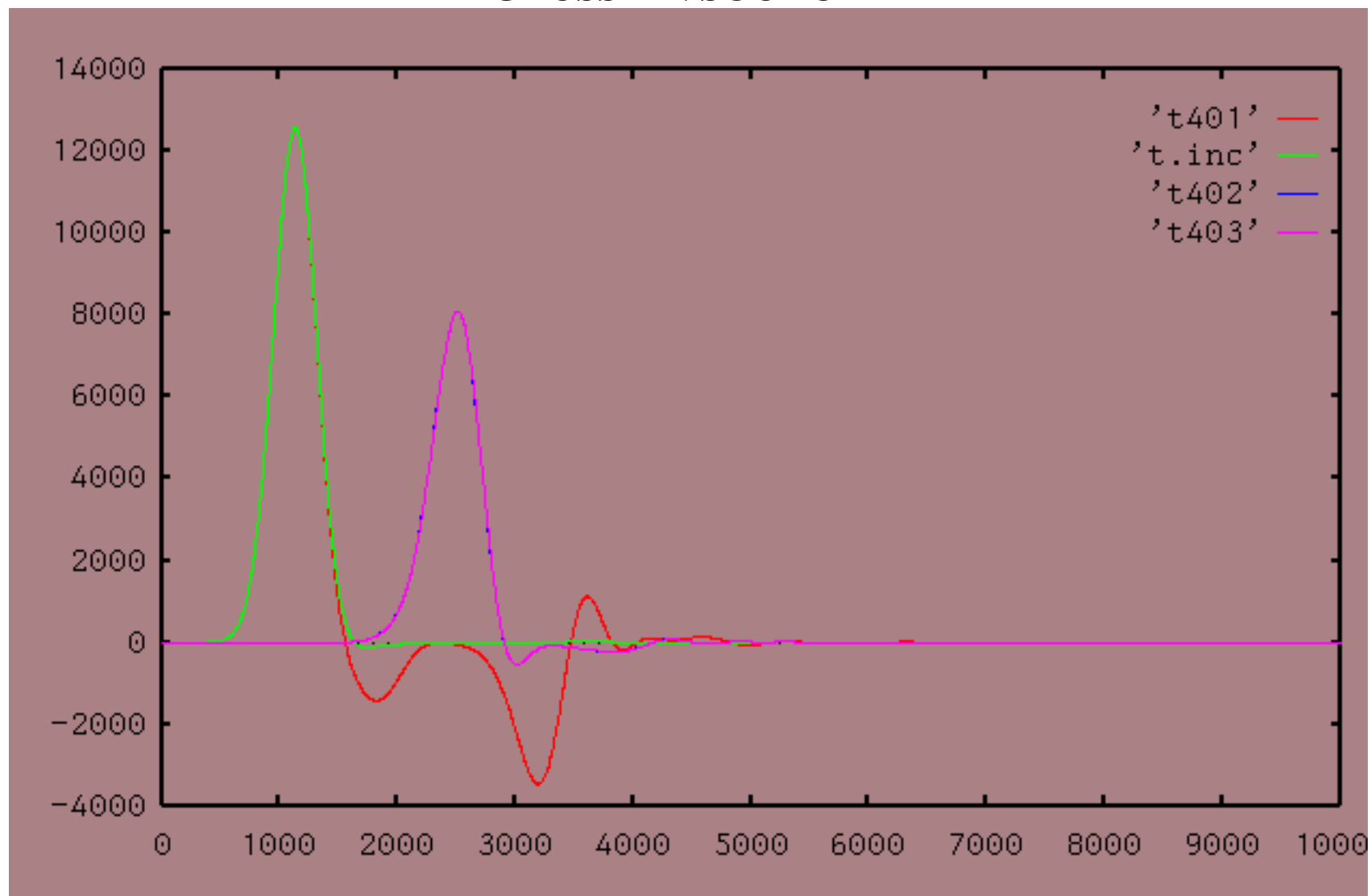
$$S_{ij} = \left. \frac{V_i^-}{V_j^+} \right|_{V_k^+ = 0 \text{ for } k \neq j \text{ and } i \neq j}, \quad S_{jj} = \left. \frac{V_j^t - V_j^+}{V_j^+} \right|_{V_k^+ = 0 \text{ for } k \neq j}$$

EXAMPLE - 3 dB WILKINSON POWER DIVIDER

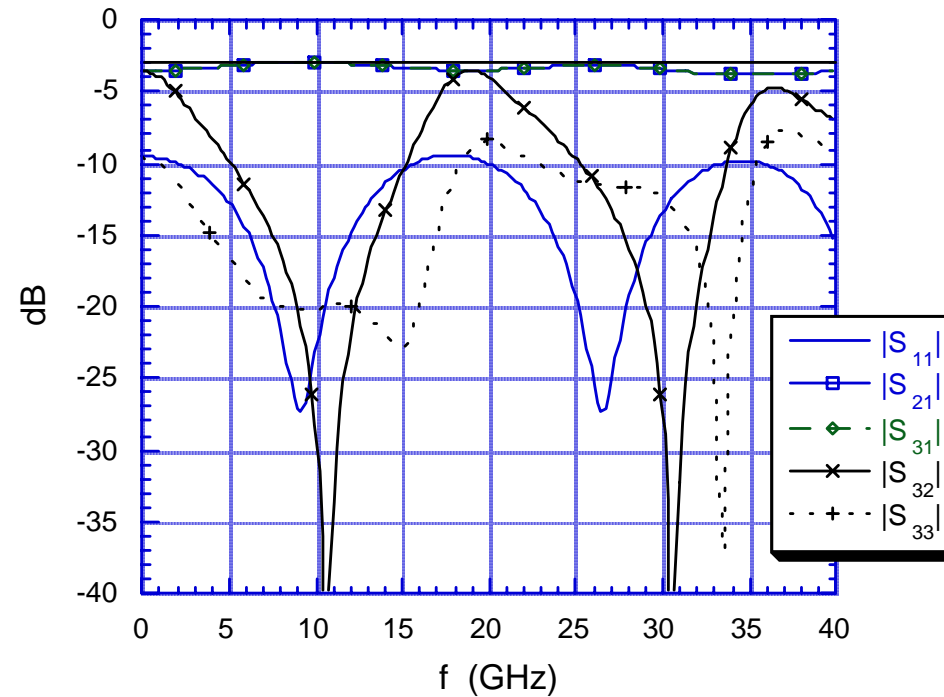


- Simulation Procedure:
 1. Excite Port 1 with an ideal voltage source with a Gaussian pulse profile, match all three ports into ABC walls, and probe the line voltage at all three ports
 2. Excite Port 2 with an ideal voltage source, and probe the line voltages at all three ports which are again matched into ABC walls.
 3. Solve an Auxiliary problem consisting of a uniform microstrip line representing ports 1 & 2. Excite ports with the same pulse, and measure the voltage at port (V_1^+ or V_2^+)
 4. Fourier transform the line voltages, and compute the frequency dependent S-parameters S_{11} , S_{21} , and S_{31} , S_{22} , and S_{32} . By symmetry $S_{12} = S_{21} = S_{13}$, etc.

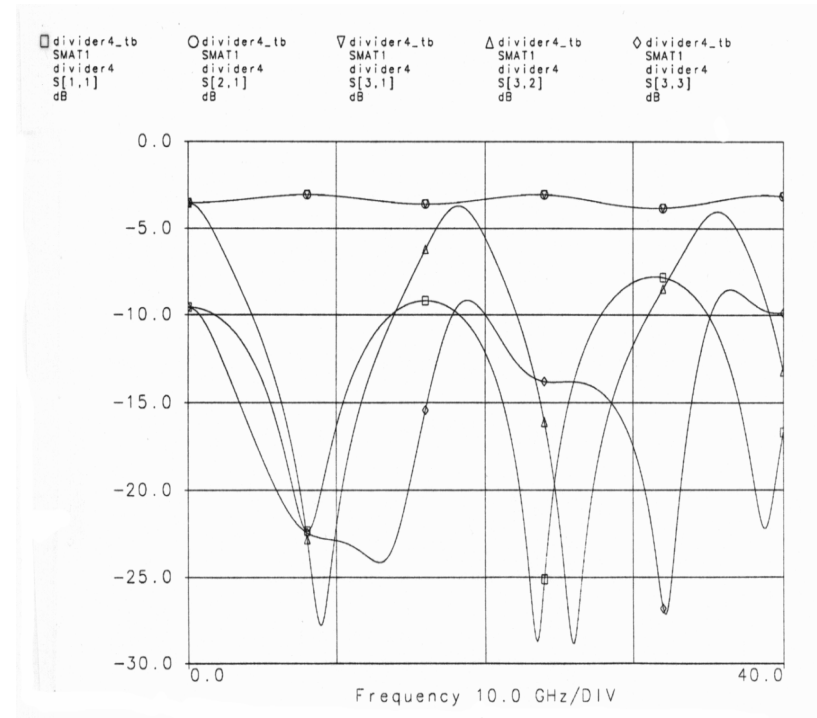
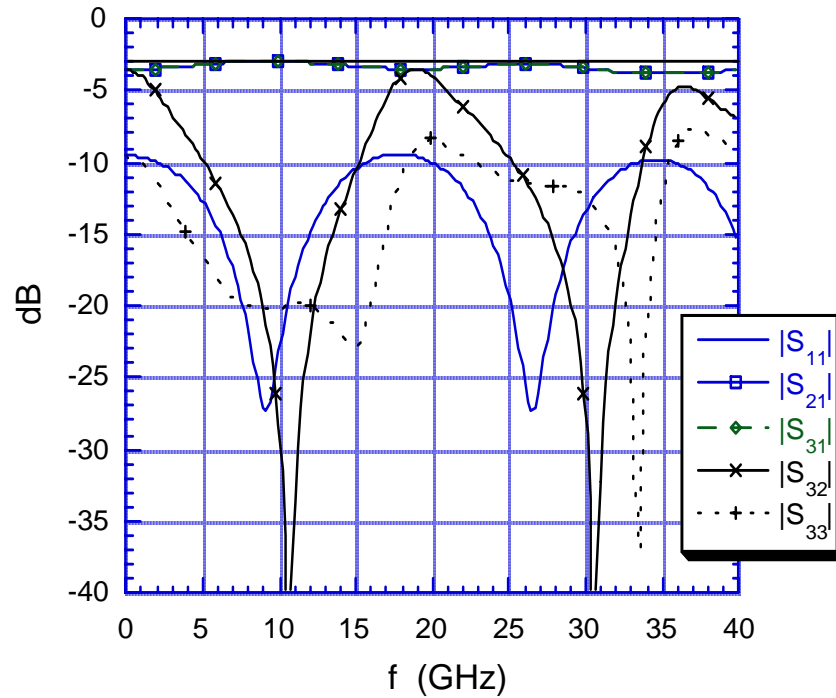
TIME-DEPENDENT PORT VOLTAGES WITH PORT 1 EXCITED BY GAUSSIAN SOURCE



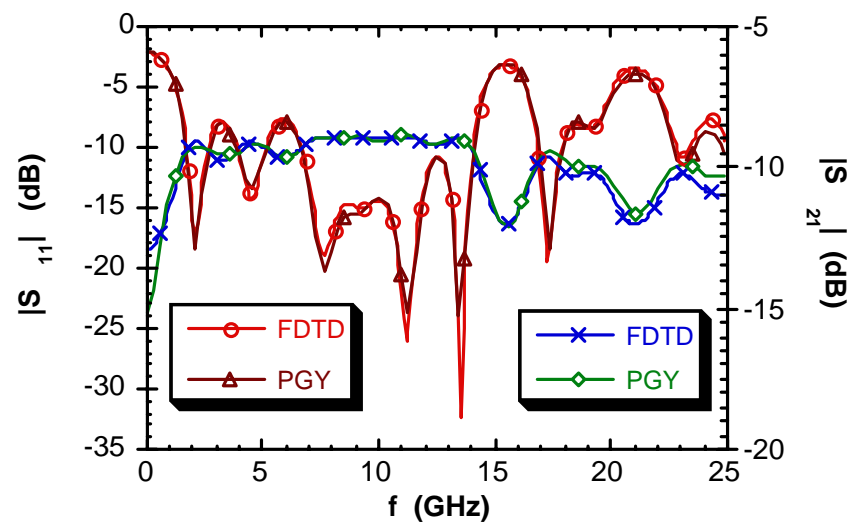
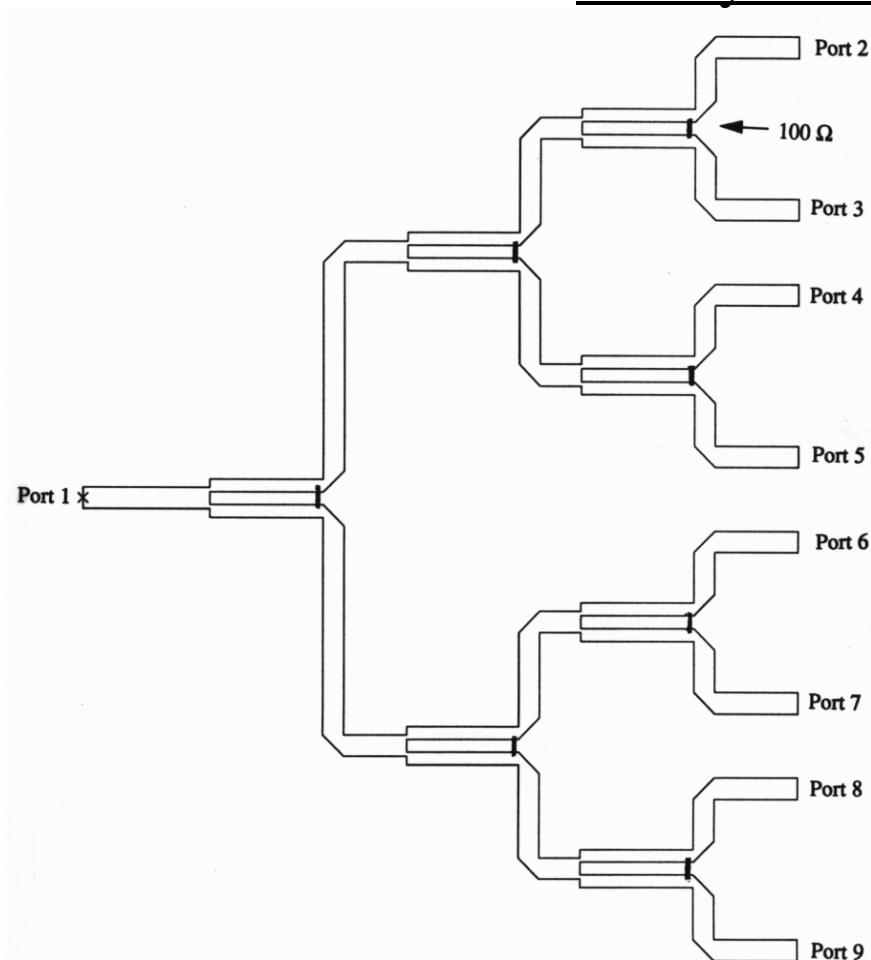
- Magnitude of the S-parameters of the Wilkinson power divider illustrated in Fig. 7 modeled using the FDTD algorithm.



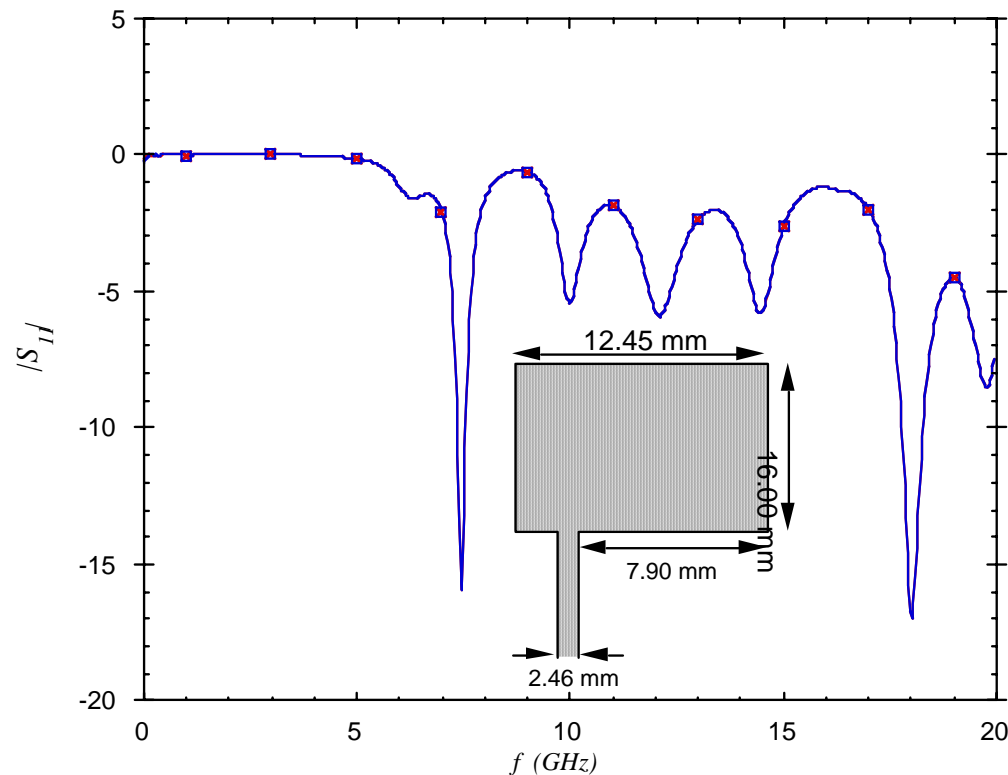
- Compared to HPADs Simulation of the Wilkinson Power Divider:



8-Way Power Divider

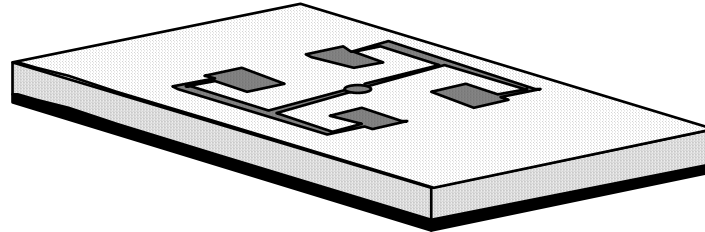


EXAMPLE - 1 PORT PATCH ANTENNA



- $|S_{11}|$ of a microstrip fed patch antenna (superimposed) printed on a 31.25 mil Duroid substrate ($\epsilon_r = 2.2$) computed via the FDTD method. The FDTD lattice is terminated by a 10-cell thick uniaxial PML layer which is placed: — \times — 3 cells from the edge of the patch and 5 cells above the patch, and — \square — 10 cells from the edges of the patch.
- $\Delta x = 0.389$ mm, $\Delta y = 0.4$ mm, $\Delta z = 0.1588$ mm, and $\Delta t = 0.441$ ps.
- How can you compute the input impedance from S_{11} ?

RADIATION FROM PRINTED STRUCTURES



- Previously we detailed the near-field to far-field transformation for radiating structures in a homogeneous space
- Cannot directly apply to structures printed on infinite substrates since a closed surface will require an infinite planar surface, or a surface in an inhomogeneous space.
- From the time-varying fields, equivalent surface currents on the surfaces of conductors, and displacement currents within dielectrics are easily extracted. The far field radiation can then be computed from these currents.
- As previously seen, the far fields can be computed in either the time-domain or the frequency domain. However, for infinite substrates the time delay of the radiated fields is dependent on the observation angle due to multiple reflections in the substrate, it has been elected to first Fourier transform the time-varying currents and compute the far fields in the frequency domain.
- The FDTD method can be used to model printed antennas within multilayered stratified media. If the planar slabs are infinite in extent, then the radiated fields are computed using the surface currents (on the surface of the strips) and the layered Green's function.

RADIATION FROM ANTENNAS ON INFINITE SUBSTRATES

- Given a printed patch antenna on a single substrate that is infinitely planar. The conductors are assumed to be infinitesimally thin and lossless. The equivalent surface current density is computed as

$$\vec{J}(x, y, z, t) = \hat{n} \times (\vec{H}_+(x, y, z^+, t) - \vec{H}_-(x, y, z^-, t)) \Big|_{PEC}$$

- The currents are Fourier Transformed using a DFT or FFT
- The far electric-fields are then computed via the integrals

$$E_\phi = \frac{j\omega\mu_o}{4\pi r} e^{-jk_o r} \int_S \left(F(\theta) \sin \phi J_x - G(\theta) \cos \phi J_y \right) e^{jk_o r' \cos \psi} dA$$

$$E_\theta = -\frac{j\omega\mu_o}{4\pi r} e^{-jk_o r} \int_S \left(G(\theta) \cos \phi J_x + F(\theta) \sin \phi J_y \right) e^{jk_o r' \cos \psi} dA$$

where

$$F(\theta) = \frac{2 \tan(\beta_{z1} h) \cos \theta}{\tan(\beta_{z1} h) \cos \theta - j\Theta(\theta)}, \quad G(\theta) = \frac{2 \tan(\beta_{z1} h) \cos \theta}{\tan(\beta_{z1} h) - j \frac{\epsilon_r}{\Theta(\theta)} \cos \theta},$$

and

$$\beta_{z1} = k_o \Theta(\theta), \quad \text{and,} \quad \Theta(\theta) = \sqrt{\epsilon_r - \sin^2 \theta}.$$

and θ and ϕ are the zenith and azimuthal angles, (origin at center of the antenna)

- These integrals can be derived from a far-field approximation of the exact Green's function using the method of steepest decent [W. Chew, *Waves in Inhomogeneous Media*, Van Nostrand Reinhold, 1989], or using Reciprocity [Jackson and Alexopoulos, *IEEE Trans. on A.P.*, Sept. 85, pp. 976-987]

EFFICIENT COMPUTATION

- If the far fields are needed over a very broad band, the time-varying currents can be Fourier transformed using a fast Fourier-transform (FFT) algorithm. This, however, will require an extremely large data base since the complete time-history for each current element will need to be stored.
- An alternative, is to choose a finite number of discrete frequency points for which the far-field will be evaluated, and perform a discrete Fourier-transform (DFT) throughout the time-updates. Since this involves updating an integral, only one complex number per frequency and per current element need be stored. This is easily stored in core memory.
- Simulation Procedure:
 1. Excite structure with an independent source using standard FDTD lattice terminated with absorbing boundary conditions (open regions), or natural boundary conditions (e.g., ground plane).
 2. Compute the instantaneous current densities on the conductor surfaces from the local tangential H-fields..
 3. Assuming a recursive expression for the DFT, update the DFT at selected discrete frequencies.
 4. After steady state conditions are reached, stop the time-domain simulation, and compute the far fields at the selected angles.

EFFICIENT COMPUTATION OF RADIATED FIELDS (CONT'D)

- For the previous method, assume that there are $M_x \times M_y$ surface currents to store, times M_f frequencies.
- For the radiation pattern, there will be M_ϕ azimuthal angles, and M_θ zenith angles to compute. If a full three-dimensional pattern is desired, typically, one would choose $M_\theta = 180$ (0.5° increments), and $M_\phi = 720$, or a total of ~ 130 k points. Often, only an E and H plane cut are desired, and then $M_\phi = 2$, so only 360 points may be necessary.
- In either case, if $M_x \times M_y \gg M_\theta \times M_\phi$, then a more efficient scheme which would reduce storage would be the following:

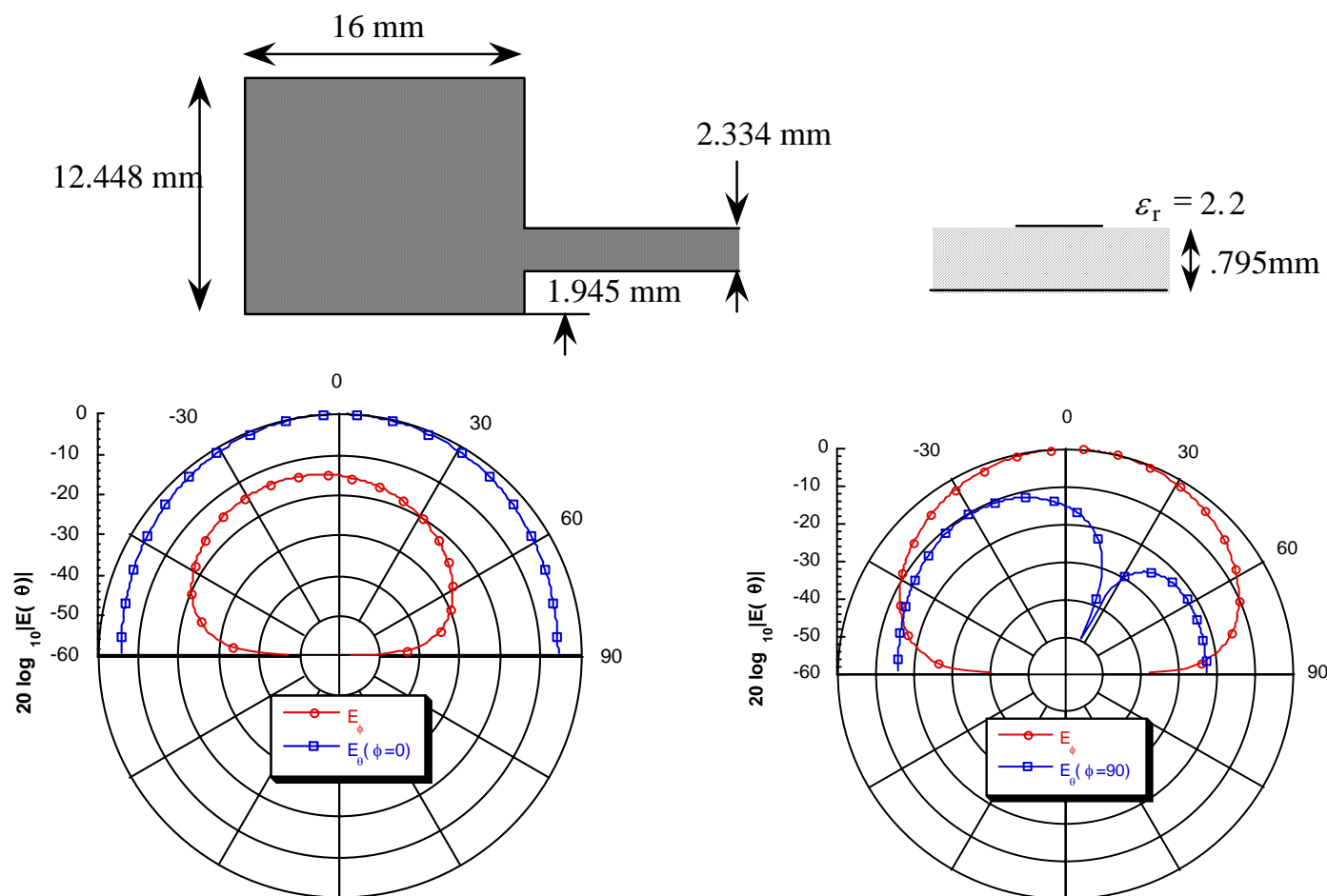
- Excite structure with an independent source.
- Compute the instantaneous current densities on the conductor surfaces from the local tangential H-fields..
- Again assume a recursive expression for the DFT. However, move the summation over the surface inward, and the DFT summation outward.
- Recursively update the fields for each angle θ_j and ϕ_k :

$$E_{\phi_i}(\theta_j, \phi_k) = E_{\phi_i}(\theta_j, \phi_k) + \frac{j\omega_i \mu_o}{4\pi r} e^{-jk_o r} \sum_S \left\{ F(\theta_j) \sin \phi_k J_x \right. \\ \left. - G(\theta_j) \cos \phi_k J_y \right\} e^{jk_o r' \cos \psi_{j,k}} \Delta x \Delta y e^{j\omega_i t} \Delta t$$

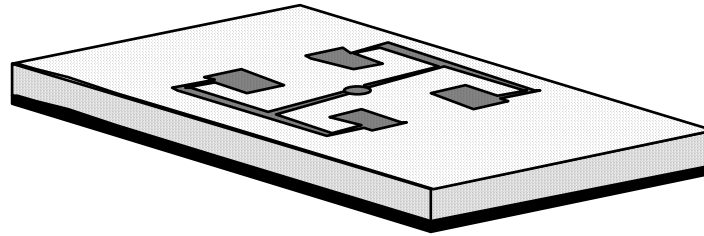
and similarly for E_θ .

- After steady state conditions are reached, stop the time-domain simulation. The fields are already stored in local memory.

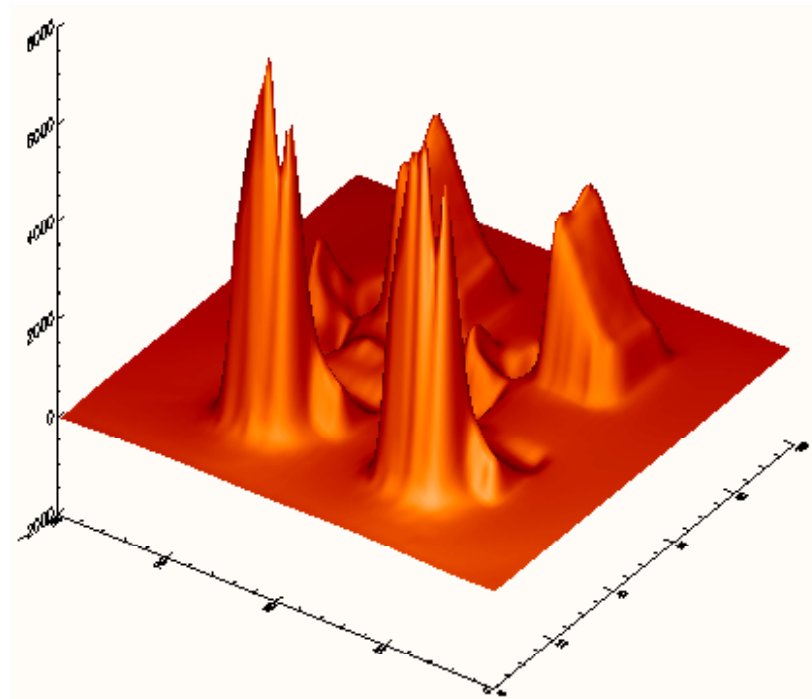
SINGLE PATCH ANTENNA

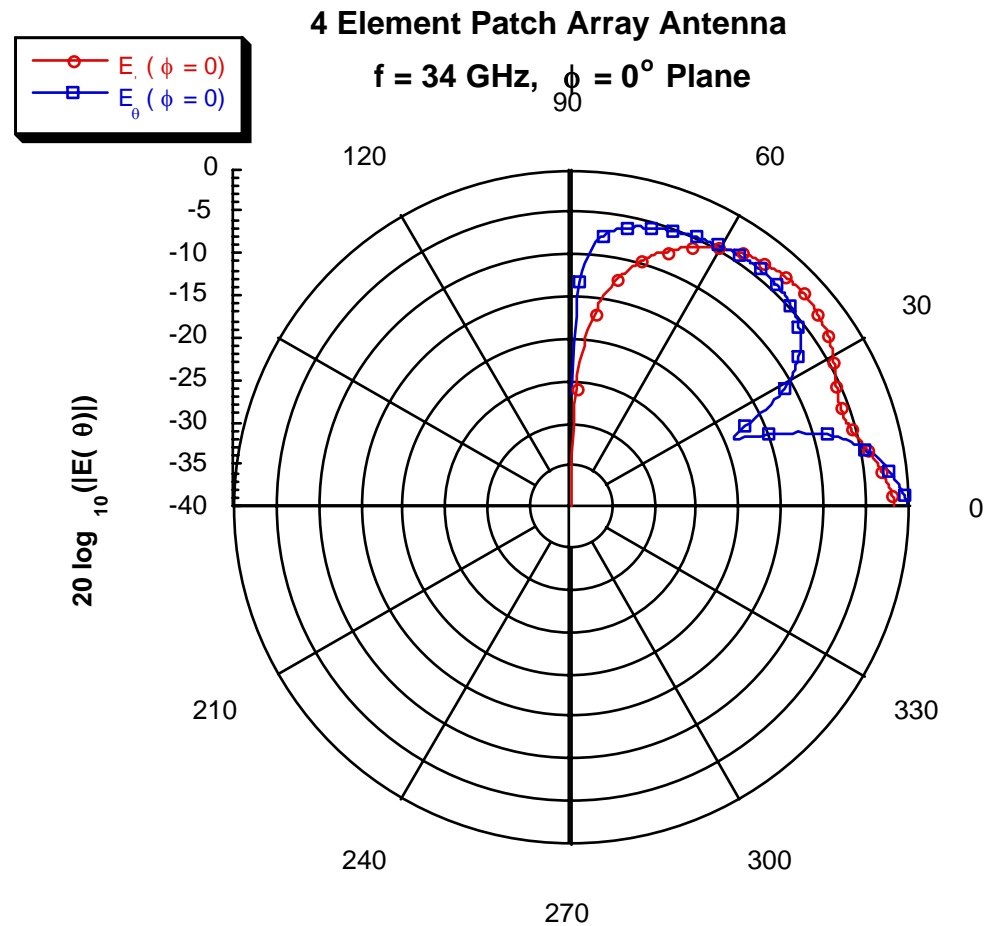


4 Element Patch Array Antenna

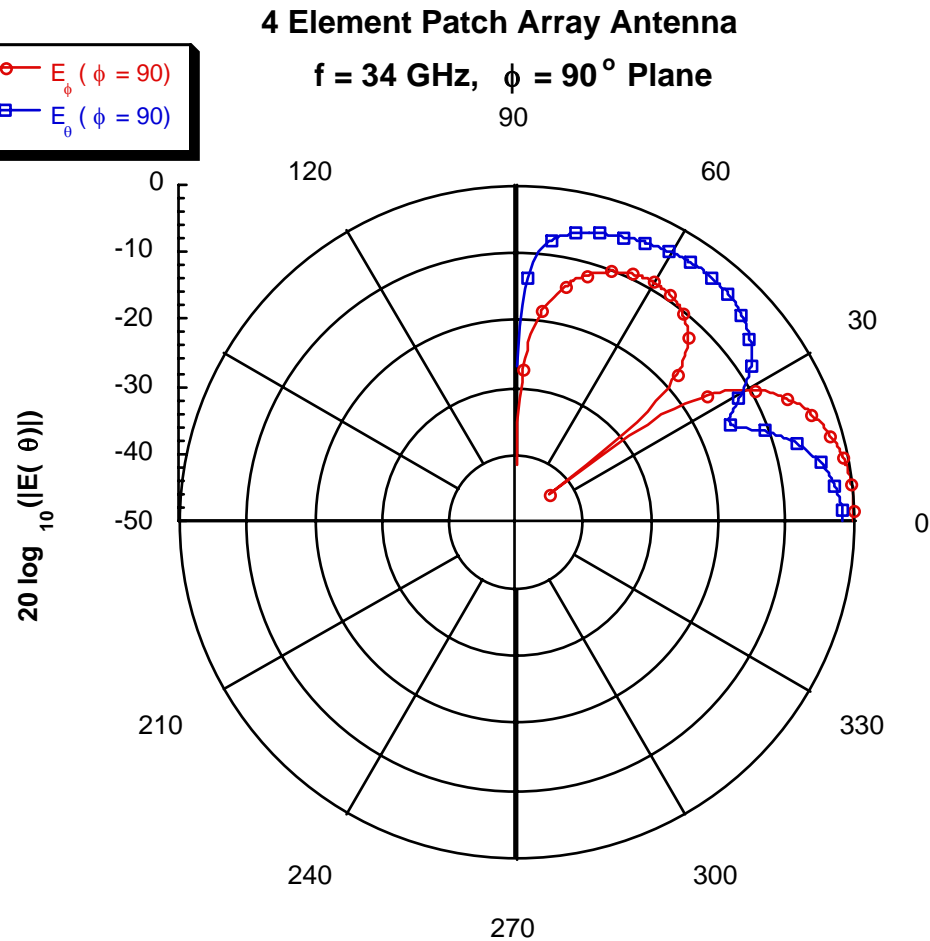


- Center Fed Probe Source ($50\ \Omega$ internal impedance)
- 4 Element Array: E_z just beneath the substrate/conductor surface at time step 1000 (75 ps)





Far field radiation pattern of the four element patch array antenna at 34 GHz – $\phi = 0^\circ$. Note that the electric fields are normalized to the maximum value.



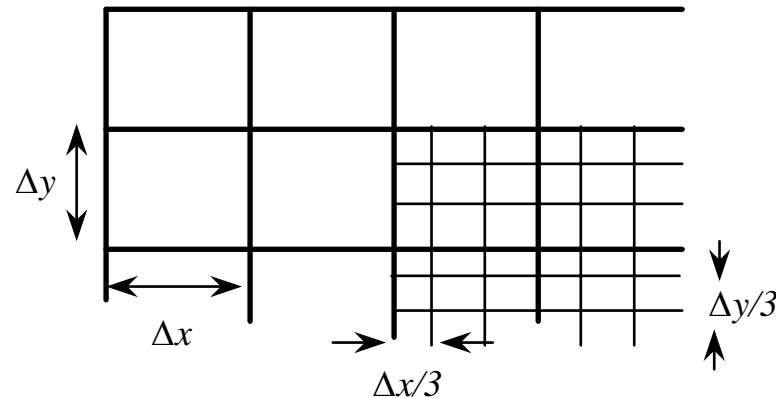
Far field radiation pattern of the four element patch array antenna at 34 GHz – $\phi = 90^\circ$.
 Note that the electric fields are normalized to the maximum value.

NON-UNIFORM FDTD METHODS

- The Previous Lectures have dealt explicitly with FD-TD algorithms based on orthogonal, regular Cartesian lattices.
- Leads to a second-order accurate solution in both space and time. This error, however, is only associated with the differential operators.
- Additional error can be encountered through the boundary conditions imposed on the discrete fields - specifically when boundaries do not align with the uniform grid.
- This has lead to a number of studies of FD-TD based algorithms which rely on *boundary fitted* lattice grids.
 - * Non-Uniform Grid FDTD.
 - * Non-Orthogonal Structured Grid Methods.
 - * Non-Orthogonal Unstructured Grid Methods.
 - * Finite Volume Time-Domain Methods (Unstructured Grids).
- These Techniques offer near second-order accuracy, but offer the advantage of conformal grids.

NON-UNIFORM ORTHOGONAL GRID FDTD METHODS

- Non-Uniform Gridding Can be Achieved Via a Number of Techniques.
 - * Subgridding Methods - Local Refinement of Mesh Based on an Integer Factor:

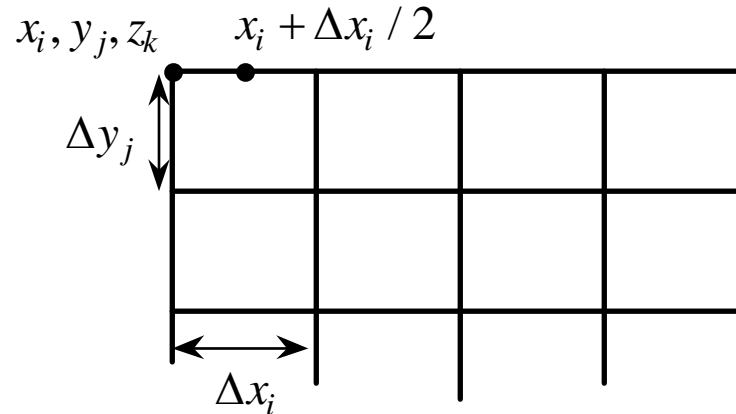


The field can be interpolated in a second-order accurate manner at the interface of the two grids. Time subsampling is used for the refined region. If the grid is subsampled at $\Delta x/m$ and $\Delta y/m$, then $\Delta t_s = \Delta t/m$.^{1,2}

- * Non-Uniform Gridding - Irregular Grid Spacing to conform to problem boundaries:
 - Method is numerically stable.
 - Method is Supraconvergent: Locally First Order, Global Second-Order Accuracy³.

- 1 D. T. Prescott and N. V. Shuley, "A method for incorporating different sized cells into the finite-difference time-domain analysis technique", *IEEE Microwave and Guided Wave Letters*, Vol 2, No. 11, Nov. 1992.
- 2 S. S. Zivanovic, K. S. Yee, and K. K. Mei, "A subgridding method for the time-domain finite-difference method to solve Maxwell's equations," *IEEE Trans Microwave Theory Tech.*, Vol. 39, pp. 471-479, Mar. 1991.
- 3 P. Monk and E. Suli, "A convergence analysis of Yee's scheme on non-uniform grids," *SIAM Journal on Numerical Analysis*, vol. 31, pp. 393-412, April 1994.

IRREGULAR ORTHOGONAL GRID FDTD METHODS



- Vertices of Irregular Grid Defined as 1-Dim. Arrays:

$$\{x_i; i = 1, N_x\}, \quad \{y_j; j = 1, N_y\}, \quad \{z_k; k = 1, N_z\}.$$

- The edge lengths between vertices is also defined as:

$$\{\Delta x_i = x_{i+1} - x_i; i = 1, N_x - 1\}, \{\Delta y_j = y_{j+1} - y_j; j = 1, N_y - 1\}, \{\Delta z_k = z_{k+1} - z_k; k = 1, N_z - 1\}.$$

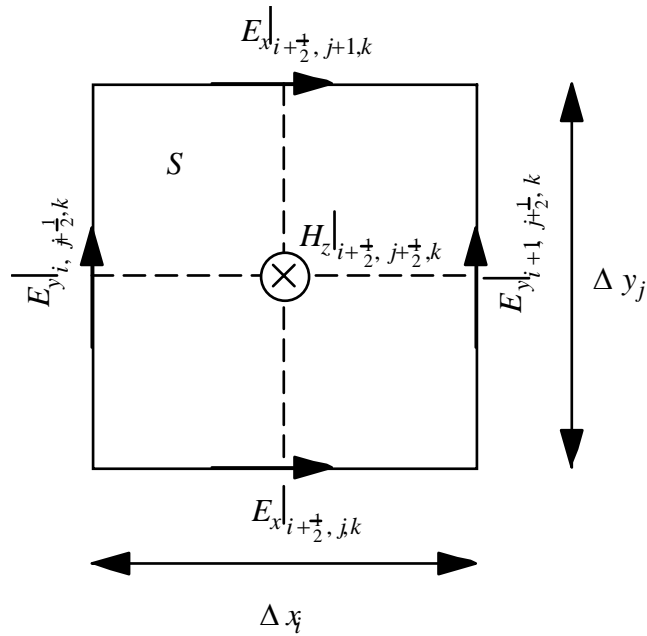
- The cell and edge centers are Defined by the Coordinates:

$$x_{i+\frac{1}{2}} = x_i + \Delta x_i / 2, \quad y_{j+\frac{1}{2}} = y_j + \Delta y_j / 2, \quad z_{k+\frac{1}{2}} = z_k + \Delta z_k / 2$$

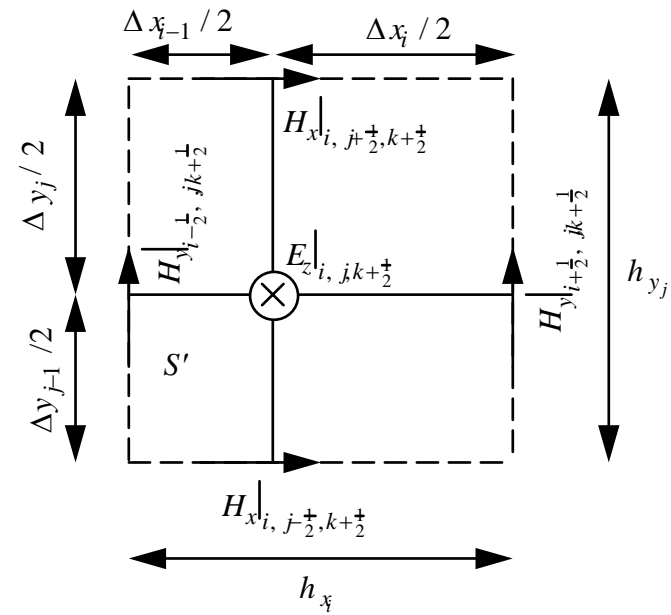
- Introduce a set of dual edge lengths representing the distances between the edge centers:

$$\{h_i^x = (\Delta x_i + \Delta x_{i-1}) / 2; i = 2, N_x\}, \{h_j^y = (\Delta y_j + \Delta y_{j-1}) / 2; j = 2, N_y\},$$

$$\{h_k^z = (\Delta z_k + \Delta z_{k-1}) / 2; k = 2, N_z\}$$



(a)



(b)

Lattice faces bound by lattice edges defining surfaces of integration bound by closed contours. (a) Lattice cell face bound by grid edges and a dual lattice edge passing through its center. (b) Dual lattice face bound by dual edges.

- The electric and magnetic fields, in the discrete non-uniform lattice space, are expressed as:

$$E_x \Big|_{i+\frac{1}{2},j,k}^n \approx E_x(x_{i+\frac{1}{2}}, y_j, z_k, n\Delta t), \quad H_x \Big|_{i,j+\frac{1}{2},k+\frac{1}{2}}^{n+\frac{1}{2}} \approx H_x(x_i, y_{j+\frac{1}{2}}, z_{k+\frac{1}{2}}, (n+\frac{1}{2})\Delta t),$$

$$E_y \Big|_{i,j+\frac{1}{2},k}^n \approx E_y(x_i, y_{j+\frac{1}{2}}, z_k, n\Delta t), \quad H_y \Big|_{i+\frac{1}{2},j,k+\frac{1}{2}}^{n+\frac{1}{2}} \approx H_y(x_{i+\frac{1}{2}}, y_j, z_{k+\frac{1}{2}}, (n+\frac{1}{2})\Delta t),$$

$$E_z \Big|_{i,j,k+\frac{1}{2}}^n \approx E_z(x_i, y_j, z_{k+\frac{1}{2}}, n\Delta t), \quad H_z \Big|_{i+\frac{1}{2},j+\frac{1}{2},k}^{n+\frac{1}{2}} \approx H_z(x_{i+\frac{1}{2}}, y_{j+\frac{1}{2}}, z_k, (n+\frac{1}{2})\Delta t).$$

- The non-uniform FD-TD algorithm is based on a discretization of Maxwell's equations expressed in their integral form, specifically, Faraday's law and Ampère's law:

$$\oint_{C'} \vec{E} \cdot d\vec{\ell} = -\frac{\partial}{\partial t} \iint_{S'} \vec{B} \cdot d\vec{s} - \iint_{S'} \vec{M} \cdot d\vec{s},$$

$$\oint_C \vec{H} \cdot d\vec{\ell} = \frac{\partial}{\partial t} \iint_S \vec{D} \cdot d\vec{s} + \iint_S \sigma \vec{E} \cdot d\vec{s} + \iint_S \vec{J} \cdot d\vec{s}.$$

- The surface integrals are performed over a primary and secondary lattice cell face, respectively, and the contour integral is performed over the edges bounding the faces.

- Evaluating the time derivatives using central difference approximations leads to the Discrete approximation:

$$\begin{aligned}
 & \left[E_x \Big|_{i+\frac{1}{2},j+1,k}^n \Delta x_i - E_x \Big|_{i+\frac{1}{2},j,k}^n \Delta x_i - E_y \Big|_{i+1,j+\frac{1}{2},k}^n \Delta y_j + E_y \Big|_{i,j+\frac{1}{2},k}^n \Delta y_j \right] = \\
 & - \left[\mu_{i+\frac{1}{2},j+\frac{1}{2},k} \frac{H_z \Big|_{i+\frac{1}{2},j+\frac{1}{2},k}^{n+\frac{1}{2}} - H_z \Big|_{i+\frac{1}{2},j+\frac{1}{2},k}^{n-\frac{1}{2}}}{\Delta t} + M_z \Big|_{i+\frac{1}{2},j+\frac{1}{2},k}^{n+\frac{1}{2}} \right] \Delta x_i \Delta y_j \\
 & \left[H_x \Big|_{i,j+\frac{1}{2},k+\frac{1}{2}}^{n+\frac{1}{2}} h_{x_i} - H_x \Big|_{i,j-\frac{1}{2},k+\frac{1}{2}}^{n+\frac{1}{2}} h_{x_i} - H_y \Big|_{i+\frac{1}{2},j,k+\frac{1}{2}}^{n+\frac{1}{2}} h_{y_j} + H_y \Big|_{i-\frac{1}{2},j,k+\frac{1}{2}}^{n+\frac{1}{2}} h_{y_j} \right] = \\
 & \left[\varepsilon_{i,j,k+\frac{1}{2}} \frac{E_z \Big|_{i,j,k+\frac{1}{2}}^{n+1} - E_z \Big|_{i,j,k+\frac{1}{2}}^n}{\Delta t} + \frac{\sigma_{i,j,k+\frac{1}{2}}}{2} \frac{E_z \Big|_{i,j,k+\frac{1}{2}}^{n+1} + E_z \Big|_{i,j,k+\frac{1}{2}}^n}{\Delta t} + J_z \Big|_{i,j,k+\frac{1}{2}}^{n+\frac{1}{2}} \right] h_{x_i} h_{y_j}
 \end{aligned}$$

- $\varepsilon_{i,j,k+\frac{1}{2}}$, $\sigma_{i,j,k+\frac{1}{2}}$, and $\mu_{i+\frac{1}{2},j+\frac{1}{2},k}$ are averaged permittivity, conductivity, and permeability, respectively, about the grid edges as done for the Yee-Algorithm.

- This finally leads to an explicit update scheme:

$$H_z^{n+\frac{1}{2}}\bigg|_{i+\frac{1}{2},j+\frac{1}{2},k} = H_z^{n-\frac{1}{2}}\bigg|_{i+\frac{1}{2},j+\frac{1}{2},k} - \frac{\Delta t}{\mu_{i+\frac{1}{2},j+\frac{1}{2},k}} \left[\left(E_x^n\bigg|_{i+\frac{1}{2},j+1,k} - E_x^n\bigg|_{i+\frac{1}{2},j,k} \right) / \Delta y_j - \left(E_y^n\bigg|_{i+1,j+\frac{1}{2},k} - E_y^n\bigg|_{i,j+\frac{1}{2},k} \right) / \Delta x_i + M_z^{n+\frac{1}{2}}\bigg|_{i+\frac{1}{2},j+\frac{1}{2},k} \right]$$

$$E_z^{n+1}\bigg|_{i,j,k+\frac{1}{2}} = \left(\frac{2\varepsilon_{i,j,k+\frac{1}{2}} - \Delta t \sigma_{i,j,k+\frac{1}{2}}}{2\varepsilon_{i,j,k+\frac{1}{2}} + \Delta t \sigma_{i,j,k+\frac{1}{2}}} \right) E_z^n\bigg|_{i,j,k+\frac{1}{2}} + \left(\frac{2\Delta t}{2\varepsilon_{i,j,k+\frac{1}{2}} + \Delta t \sigma_{i,j,k+\frac{1}{2}}} \right) \cdot$$

$$\left[\left(H_x^{n+\frac{1}{2}}\bigg|_{i,j+\frac{1}{2},k+\frac{1}{2}} - H_x^{n+\frac{1}{2}}\bigg|_{i,j-\frac{1}{2},k+\frac{1}{2}} \right) / h_{y_j} - \left(H_y^{n+\frac{1}{2}}\bigg|_{i+\frac{1}{2},j,k+\frac{1}{2}} - H_y^{n+\frac{1}{2}}\bigg|_{i-\frac{1}{2},j,k+\frac{1}{2}} \right) / h_{x_i} - J_z^{n+\frac{1}{2}}\bigg|_{i,j,k+\frac{1}{2}} \right]$$

- Recall that the time-space stability derived using the Von-Neumann analysis was based on the *Local* discrete field characteristics. This is a result of the explicit nature of the algorithm. Therefore, the stability relationship is governed by the *minimum* grid spacing:

$$\Delta t < 1/c_o \sqrt{1/(\Delta x_{i_{\min}})^2 + 1/(\Delta y_{j_{\min}})^2 + 1/(\Delta z_{k_{\min}})^2}$$

where $\Delta x_{i_{\min}}$, $\Delta y_{j_{\min}}$, and $\Delta z_{k_{\min}}$ are the edge lengths along the x , y , and z directions, respectively, of the *smallest* grid cell in the non-uniform grid.

EFFICIENT IMPLEMENTATION

- Normalize the Fields by their respective edge lengths, i.e.,

$$\tilde{e}_x \Big|_{i+\frac{1}{2},j+1,k}^n = \Delta x_i E_x \Big|_{i+\frac{1}{2},j+1,k}^n, \quad \tilde{h}_x \Big|_{i,j+\frac{1}{2},k+\frac{1}{2}}^{n+\frac{1}{2}} = h_{x_i} H_x \Big|_{i,j+\frac{1}{2},k+\frac{1}{2}}^{n+\frac{1}{2}}$$

- Then:

$$\begin{aligned} \tilde{h}_z \Big|_{i+\frac{1}{2},j+\frac{1}{2},k}^{n+\frac{1}{2}} &= \tilde{h}_z \Big|_{i+\frac{1}{2},j+\frac{1}{2},k}^{n-\frac{1}{2}} - \frac{h_{z_k} \Delta t}{\Delta x_i \Delta y_j \mu_{i+\frac{1}{2},j+\frac{1}{2},k}} \left[\left(\tilde{e}_x \Big|_{i+\frac{1}{2},j+1,k}^n - \tilde{e}_x \Big|_{i+\frac{1}{2},j,k}^n \right) - \right. \\ &\quad \left. \left(\tilde{e}_y \Big|_{i+1,j+\frac{1}{2},k}^n - \tilde{e}_y \Big|_{i,j+\frac{1}{2},k}^n \right) + \tilde{M}_z \Big|_{i+\frac{1}{2},j+\frac{1}{2},k}^{n+\frac{1}{2}} \right] \\ \tilde{e}_z \Big|_{i,j,k+\frac{1}{2}}^{n+1} &= \left(\frac{2\varepsilon_{i,j,k+\frac{1}{2}} - \Delta t \sigma_{i,j,k+\frac{1}{2}}}{2\varepsilon_{i,j,k+\frac{1}{2}} + \Delta t \sigma_{i,j,k+\frac{1}{2}}} \right) \tilde{e}_z \Big|_{i,j,k+\frac{1}{2}}^n + \frac{\Delta z_k}{h_{x_i} h_{y_j}} \left(\frac{2\Delta t}{2\varepsilon_{i,j,k+\frac{1}{2}} + \Delta t \sigma_{i,j,k+\frac{1}{2}}} \right) \cdot \\ &\quad \left[\left(\tilde{h}_x \Big|_{i,j+\frac{1}{2},k+\frac{1}{2}}^{n+\frac{1}{2}} - \tilde{h}_x \Big|_{i,j-\frac{1}{2},k+\frac{1}{2}}^{n+\frac{1}{2}} \right) - \left(\tilde{h}_y \Big|_{i+\frac{1}{2},j,k+\frac{1}{2}}^{n+\frac{1}{2}} - \tilde{h}_y \Big|_{i-\frac{1}{2},j,k+\frac{1}{2}}^{n+\frac{1}{2}} \right) - \tilde{J}_z \Big|_{i,j,k+\frac{1}{2}}^{n+\frac{1}{2}} \right] \end{aligned}$$

• Or:

$$\tilde{h}_z \Big|_{i+\frac{1}{2}, j+\frac{1}{2}, k}^{n+\frac{1}{2}} = \tilde{h}_z \Big|_{i+\frac{1}{2}, j+\frac{1}{2}, k}^{n-\frac{1}{2}} - B_{i+\frac{1}{2}, j+\frac{1}{2}, k} \left[\left(\tilde{e}_x \Big|_{i+\frac{1}{2}, j+1, k}^n - \tilde{e}_x \Big|_{i+\frac{1}{2}, j, k}^n \right) - \right. \\ \left. \left(\tilde{e}_y \Big|_{i+1, j+\frac{1}{2}, k}^n - \tilde{e}_y \Big|_{i, j+\frac{1}{2}, k}^n \right) + \tilde{M}_z \Big|_{i+\frac{1}{2}, j+\frac{1}{2}, k}^{n+\frac{1}{2}} \right]$$

$$\tilde{e}_z \Big|_{i, j, k+\frac{1}{2}}^{n+1} = D_{i, j, k+\frac{1}{2}} \tilde{e}_z \Big|_{i, j, k+\frac{1}{2}}^n + C_{i, j, k+\frac{1}{2}}.$$

$$\left[\left(\tilde{h}_x \Big|_{i, j+\frac{1}{2}, k+\frac{1}{2}}^{n+\frac{1}{2}} - \tilde{h}_x \Big|_{i, j-\frac{1}{2}, k+\frac{1}{2}}^{n+\frac{1}{2}} \right) - \left(\tilde{h}_y \Big|_{i+\frac{1}{2}, j, k+\frac{1}{2}}^{n+\frac{1}{2}} - \tilde{h}_y \Big|_{i-\frac{1}{2}, j, k+\frac{1}{2}}^{n+\frac{1}{2}} \right) - \tilde{J}_z \Big|_{i, j, k+\frac{1}{2}}^{n+\frac{1}{2}} \right]$$

EFFICIENT IMPLEMENTATION (CONT'D)

- High-Level Language Program Structure:
 - * Generate Irregular Grid to Best Fit Boundaries of Problem Geometry.
 - * Identify Source and Probe Locations.
 - * Compute Edge Lengths and Edge Centers and Store in 1D Arrays.
 - * Compute the Averaged Material Parameters.
 - * Compute the Coefficient Arrays.
 - * Initialize Coefficient Arrays for ABC (Note that Higdon ABC or PML is preferable, and uniform grid spacing near the exterior boundary along the normal axis should be maintained).
 - * Perform the Explicit Time-Dependent Solution of the Discrete Fields.
- Note that the recursive update algorithm has the same computational complexity as the regular grid FDTD method with three-dimensional material parameters!
- Furthermore, with the use of an irregular grid, the overall grid size can be greatly reduced, while the time step can be about the same as the regular FDTD method, or even larger!

EXAMPLE 1: PEC CAVITY

- Rectangular cavity with dimensions 0.5 m x 1.0 m x 0.25 m bound by perfect electrical conducting (PEC) walls.
- A random grid spacing for x_i , y_j , and z_k , is assumed, such that:

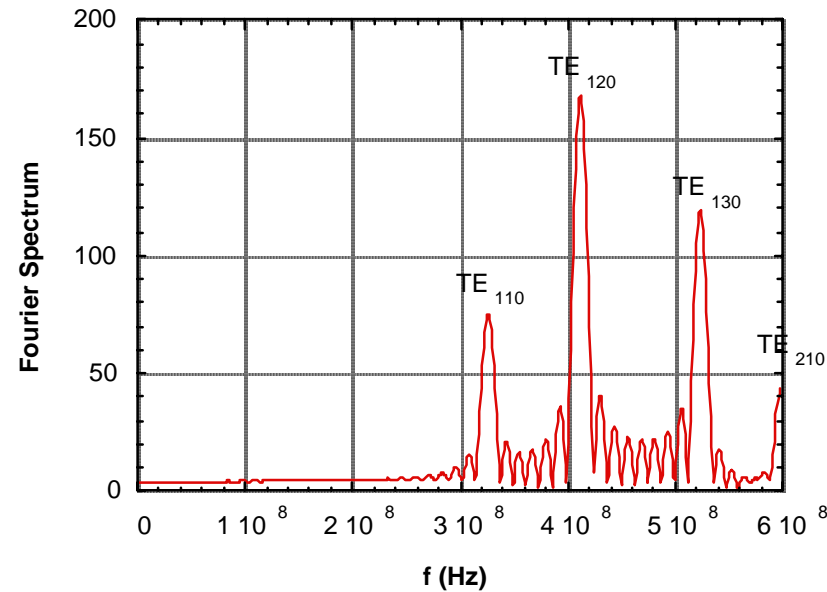
$$\begin{aligned} \{x_i &= (i-1)\Delta x + \frac{1}{2}\Re\Delta x; \quad i = 1, N_x\} \\ \{y_j &= (j-1)\Delta y + \frac{1}{2}\Re\Delta y; \quad j = 1, N_y\} \\ \{z_k &= (k-1)\Delta z + \frac{1}{2}\Re\Delta z; \quad k = 1, N_z\} \end{aligned}$$

where \Re is a random number, and $-\frac{1}{2} \leq \Re \leq \frac{1}{2}$ (note that the boundaries remain fixed).

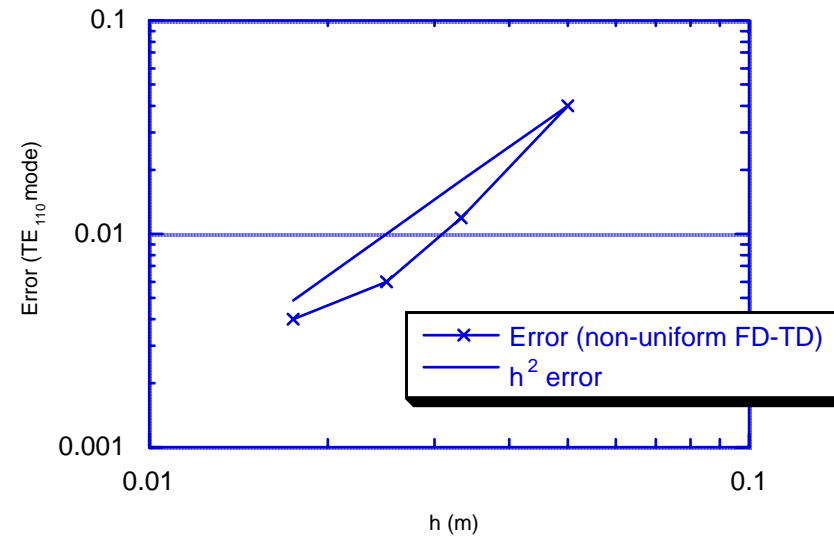
- The cavity is excited with a time varying electric dipole placed off a center axis in the cavity. The electric current is z -directed and has a Gaussian time variation:

$$\vec{J}(t) = \hat{z} e^{-\frac{(t-t_o)^2}{T^2}}$$

where $T = 0.15$ ns, and $t_o = 0.45$ ns.



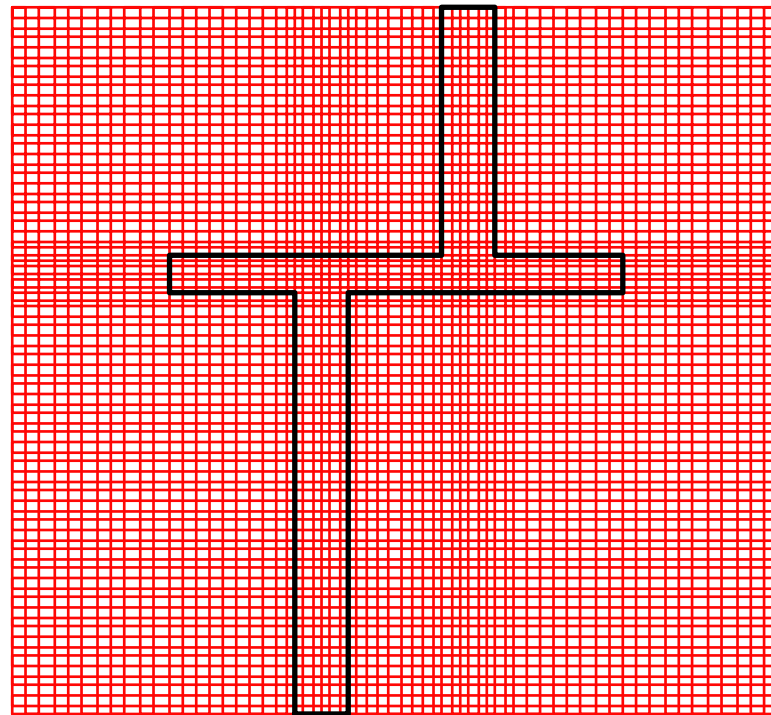
Amplitude of the Fourier transform of the time-varying electric field probed in the resonant cavity for a $21 \times 41 \times 11$ non-uniform lattice with random grid spacing.

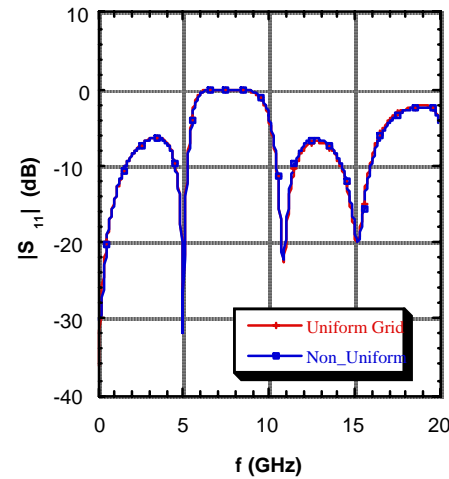


Error convergence of the resonant frequency of the TE₁₁₀ mode computed using the non-uniform FD-TD algorithm.

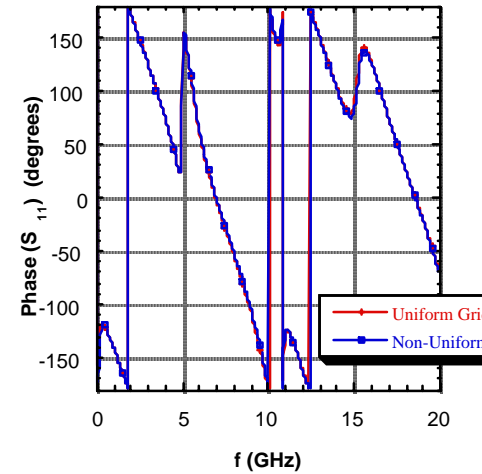
EXAMPLE 2: LOW PASS FILTER

- Microstrip Low Pass Filter printed on 0.794 mm Duroid substrate($\epsilon_r = 2.2$).
- The total lattice had a dimension of $64 \times 76 \times 16$ (compared to $110 \times 80 \times 16$ using traditional FDTD method).
- A global grid size of $\Delta x = 0.64$, $\Delta y = 0.635$, $\Delta z = 0.265$ was used. A time-step of 0.441 ps was used, resulting in 4000 time steps for this simulation. The grid was also locally refined to model the fields more accurately near the microstrip edges.

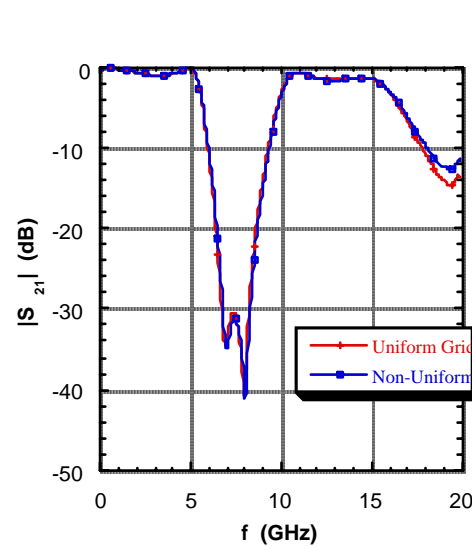




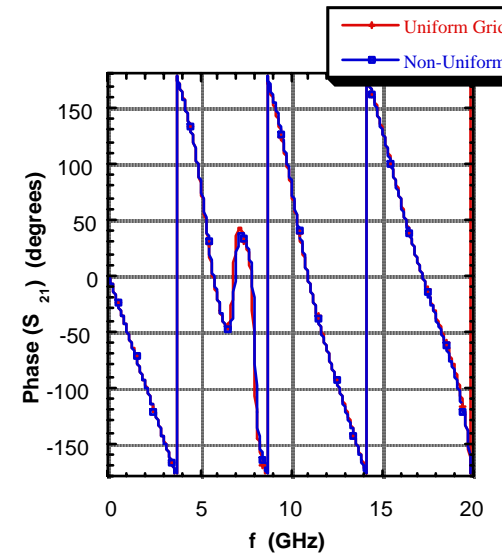
(a)



(b)



(c)



(d)

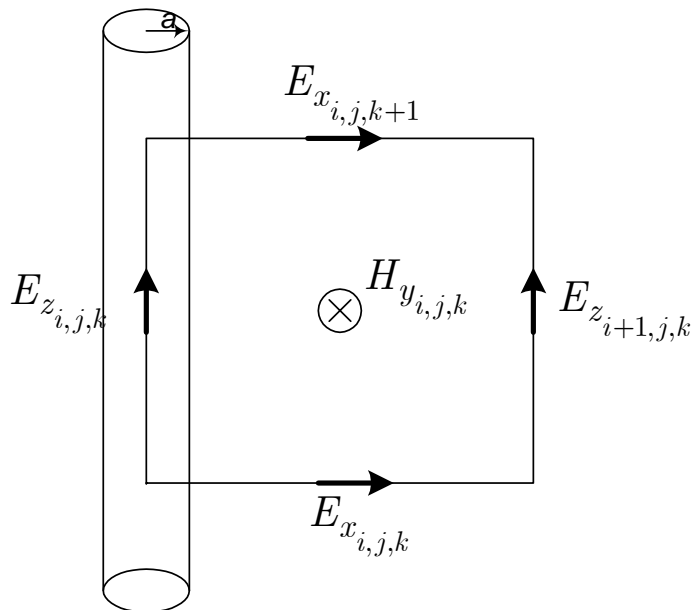
S-parameters for the low-pass filter computed using the traditional FD-TD algorithm and the non-uniform grid FD-TD algorithm. (a) $|S_{11}|$, (b) $\angle S_{11}$, (c) $|S_{21}|$, (d) $\angle S_{21}$.

Subcell Modeling Techniques

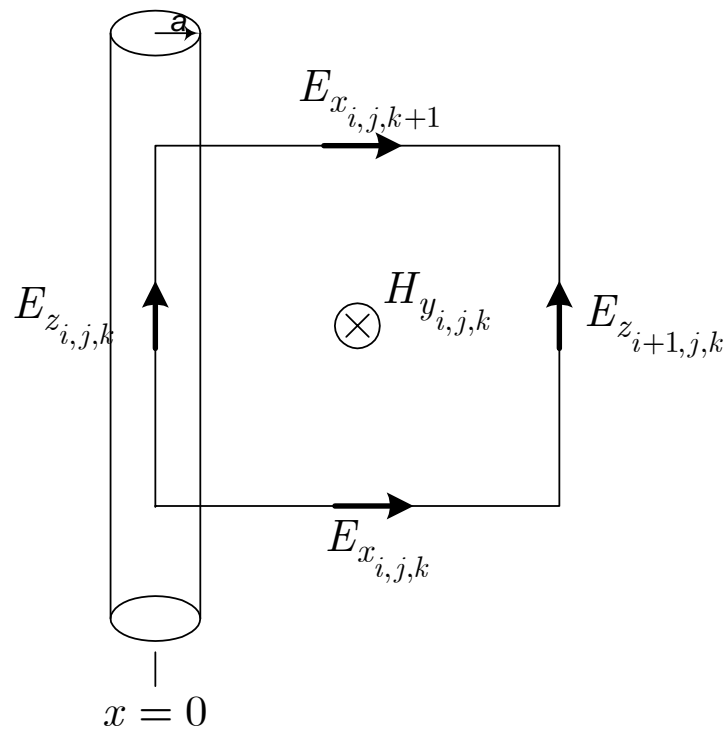
- The Previous Lectures have dealt explicitly with FD-TD algorithms based on orthogonal Cartesian lattices.
- A challenge is presented when modeling structures with fine geometric detail that is very small relative to a wavelength, and to the global problem size.
 - Global cell size and time step can be bound by the smallest geometric detail
 - Need sufficient representation to accurately model boundary and singular field behavior near discontinuities
- Subcell modelling techniques attempt to accurately model the fields near small geometrical discontinuities without the reduction of the global grid. Namely, the model is based on a local approximation of the fields within the cell which the boundary lies. Hence, the methods are referred to as "subcell" models.
- We will discuss subcell models for:
 - Thin wire models
 - Thin slots
 - Thin material sheets
 - Contour Patch model for skew boundaries

Thin Wire Subcell Models

- Many applications require the accurately modeling of field interactions with thin metallic wires
 - Dipole/Monopole Antennas, Wire bonds for PCBs and microwave circuits, Vias or through holes
- If the radius of the wire (a) $\ll \lambda$, the following thin wire model can be employed:



- B.C.: $E_{z_{i,j,k}} = 0$ on the surface of the wire. Realizing this, we will:
 1. We will deform the cell to be $\Delta x - a$ wide
 2. Model the $1/r$ singular behavior of E_x and H_y in the edge normal to the wire axis
 3. Derive an explicit update expression based on Faraday's law expressed in its integral form.



- Let:

$$H_{y_{i,j,k}} = H'_{y_{i,j,k}} \frac{\Delta x}{2} \frac{1}{x}, \quad \& \quad E_{x_{i,j,k}} = E'_{x_{i,j,k}} \frac{\Delta x}{2} \frac{1}{x}$$

- Then, from Faraday's Law:

$$-\mu \iint \frac{\partial \vec{H}}{\partial t} \cdot d\vec{s} = \oint \vec{E} \cdot d\vec{\ell} \Rightarrow$$

$$-\mu \left[H_{y_{i,j,k}}^{n+\frac{1}{2}} - H_{y_{i,j,k}}^{n-\frac{1}{2}} \right] \frac{\Delta z}{\Delta t} \frac{\Delta x}{2} \ln \left(\frac{\Delta x}{a} \right) =$$

$$\left[E_{x_{i,j,k+1}}^n - E_{x_{i,j,k}}^n \right] \frac{\Delta x}{2} \ln \left(\frac{\Delta x}{a} \right) - E_{z_{i+1,j,k}}^n \Delta z$$

- This leads to the explicit update expression:

$$H_{y_{i,j,k}}^{n+\frac{1}{2}} = H_{y_{i,j,k}}^{n-\frac{1}{2}} - \frac{\Delta t \left[E_{x_{i,j,k+1}}^n - E_{x_{i,j,k}}^n \right]}{\mu \Delta z} + \frac{\Delta t E_{z_{i+1,j,k}}^n}{\mu \frac{\Delta x}{2} \ln \left(\frac{\Delta x}{a} \right)}$$

- Note that the update for $E_{x_{i,j,k}}$ is unchanged by the scaling.
- The application of the thin wire model then simply requires a modification of the coefficients of the update of the four magnetic fields surrounding the wire. This is a preprocessing step. Further, the axial electric field is simply zeroed out
- As a result, this is a preprocessing step, and the fundamental FDTD code is unchanged.

Example: Input Impedance of a Thin Wire Dipole[†]

The input impedance of a thin-wire dipole antenna is computed via the FDTD method. The dipole is excited by a voltage gap source. The results below are compared to a Method of Moment calculation when:

$$\Delta x = \Delta y = \Delta z = \ell / 11, \ell / 21, \ell / 41, \ell / 81,$$

[†] Watanabe and Taki, "An improved FDTD Model for the Feeding Gap of a Thin-Wire Antenna," *Microwave and Guided Wave Letters*, Vol 8, pp. 152-154, April 1998.

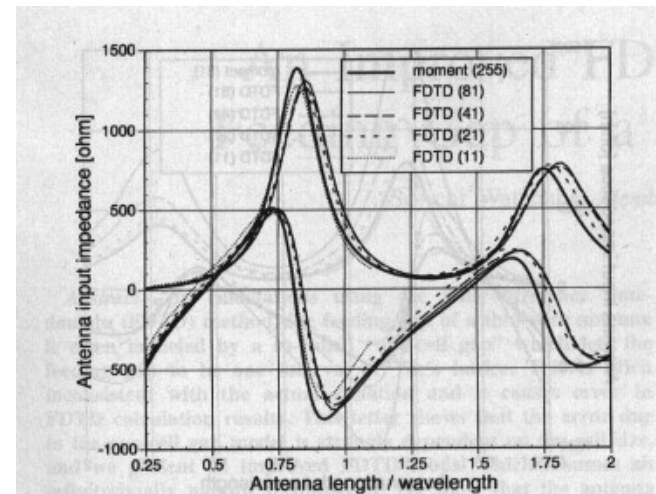


Fig. 5. Input impedance of the thin-wire dipole with the infinitesimal gap. The antenna radius a is $\ell/500$.

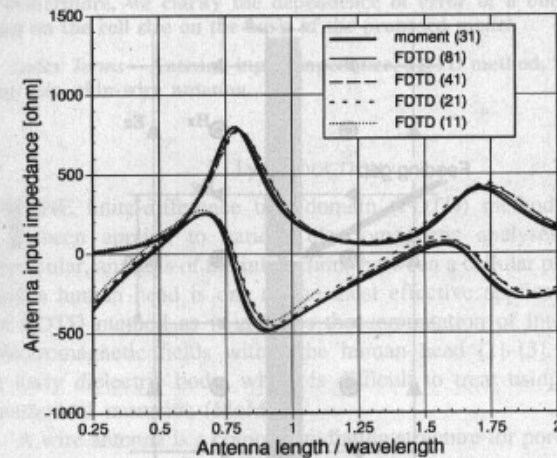


Fig. 6. Input impedance of the thin-wire dipole with the infinitesimal gap. The antenna radius a is $\ell/150$.

This model assumes a delta gap source, where:

$$E_z(gap) = -V\delta(z_o)$$

Thus, in the line integral:

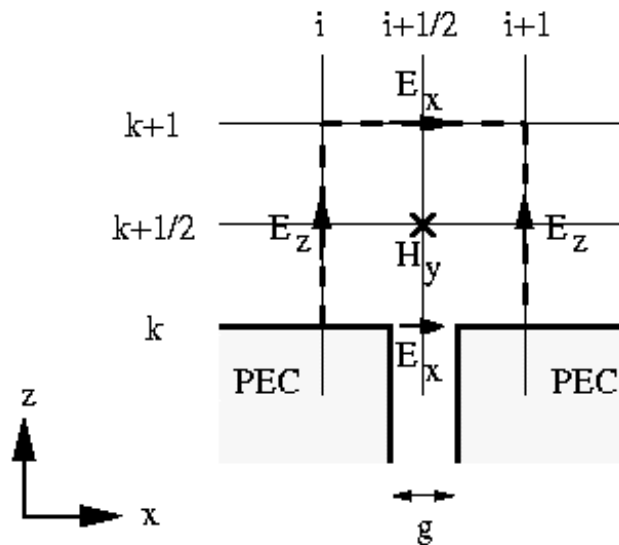
$$\oint \vec{E} \cdot d\vec{\ell} =$$

$$\left[E_{x_{i,j,k+1}}^n - E_{x_{i,j,k}}^n \right] \frac{\Delta x}{2} \ln\left(\frac{\Delta x}{a}\right) - E_{z_{i+1,j,k}}^n \Delta z - V^n$$

$$H_{y_{i,j,k}}^{n+\frac{1}{2}} = H_{y_{i,j,k}}^{n-\frac{1}{2}} - \frac{\Delta t \left[E_{x_{i,j,k+1}}^n - E_{x_{i,j,k}}^n \right]}{\mu \Delta z} + \frac{\Delta t E_{z_{i+1,j,k}}^n + V / \Delta z}{\mu \frac{\Delta x}{2} \ln\left(\frac{\Delta x}{a}\right)}$$

Modeling of Thin Slots

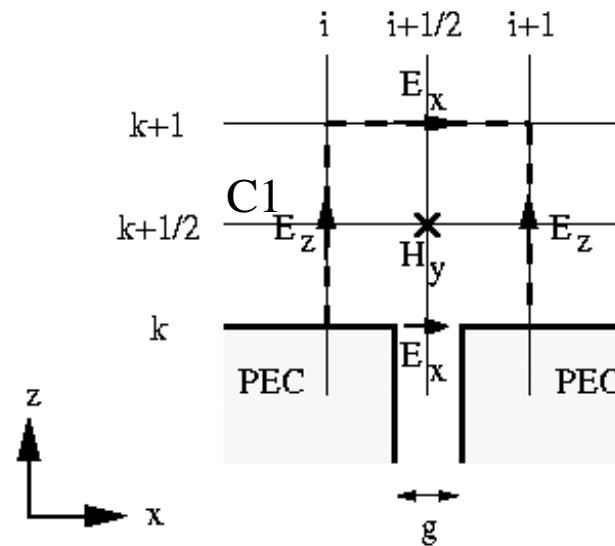
- Next, we consider another class of problems of interest, which involve the electromagnetic interaction with a thin slot. Some examples of these applications include:
 - EMC: EM penetration through thin slots and seams in metallic enclosures
 - Microwave circuits and antennas: EM coupling through slots in a ground plane, or EM radiation from slots in a waveguide wall or ground plane
- We will focus on problems where the slot is narrow and thick relative to the grid size.



- Consider the grids to the right, with C1 and C2

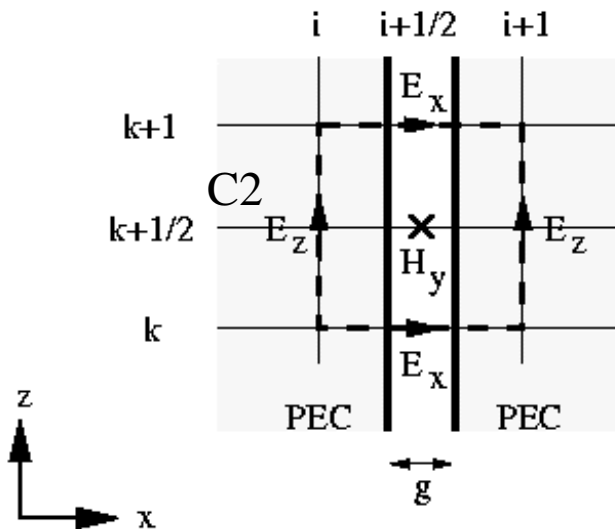
C1:

$$\frac{H_{y_{i,j,k}}^{n+\frac{1}{2}} - H_{y_{i,j,k}}^{n-\frac{1}{2}}}{\Delta t} \Delta x \Delta z = \begin{bmatrix} E_{x_{i,j,k+1}}^n \Delta x - E_{x_{i,j,k}}^n g \\ -E_{z_{i+1,j,k}}^n \Delta z + E_{z_{i,j,k}}^n \Delta z \end{bmatrix}$$



C2:

$$\frac{H_{y_{i,j,k}}^{n+\frac{1}{2}} - H_{y_{i,j,k}}^{n-\frac{1}{2}}}{\Delta t} g \Delta z = \begin{bmatrix} E_{x_{i,j,k+1}}^n g - E_{x_{i,j,k}}^n g \end{bmatrix}$$



- This leads to the explicit updates:

C1:

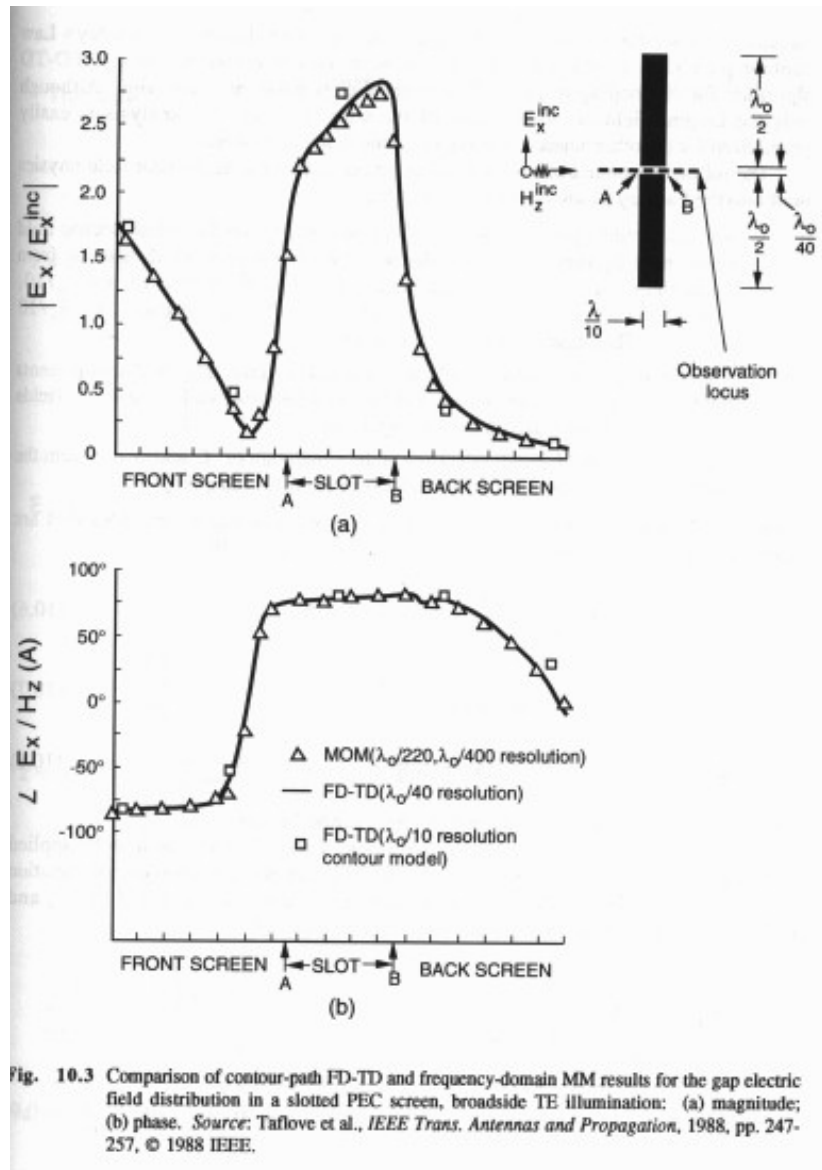
$$H_{y_{i,j,k}}^{n+\frac{1}{2}} = H_{y_{i,j,k}}^{n-\frac{1}{2}} - \frac{\mu_o}{\Delta t} \left[\frac{E_{x_{i,j,k+1}}^n - E_{x_{i,j,k}}^n \frac{g}{\Delta x}}{\Delta z} - \frac{E_{z_{i+1,j,k}}^n - E_{z_{i,j,k}}^n}{\Delta x} \right]$$

C2:

$$H_{y_{i,j,k}}^{n+\frac{1}{2}} = H_{y_{i,j,k}}^{n-\frac{1}{2}} - \frac{\mu_o}{\Delta t} \left[\frac{E_{x_{i,j,k+1}}^n - E_{x_{i,j,k}}^n}{\Delta z} \right]$$

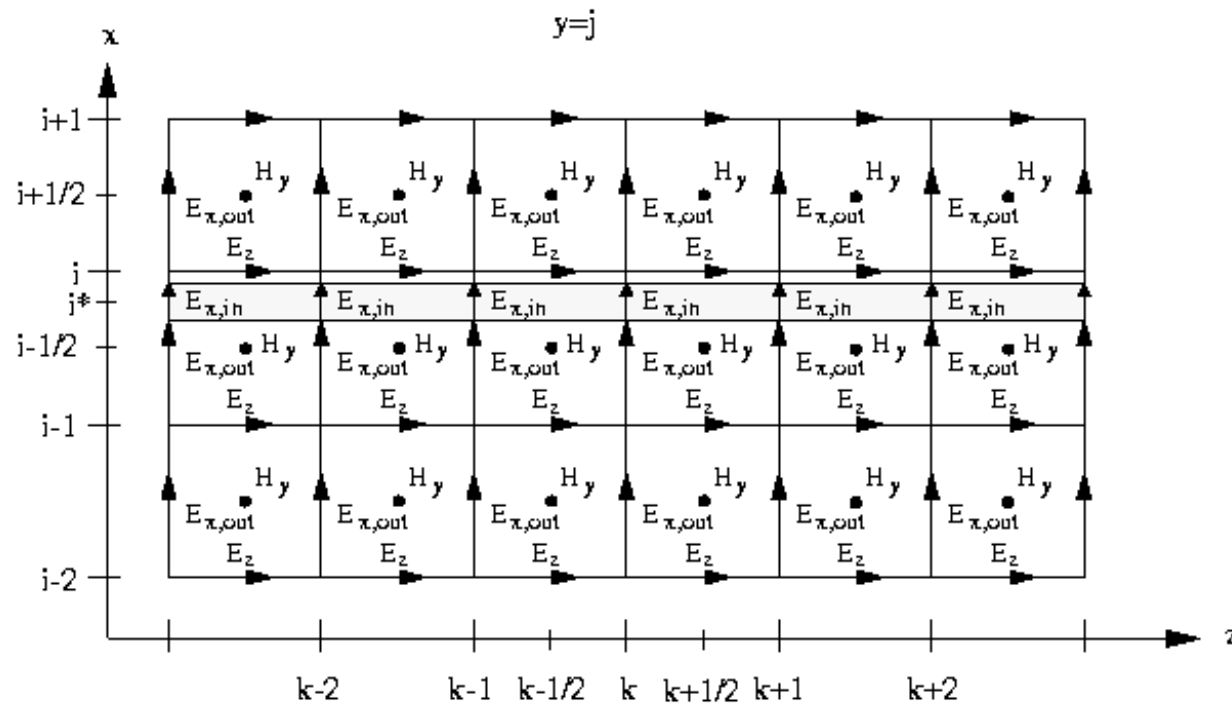
- Note that again, the field updates resemble those of the standard FDTD update scheme. The one difference is that $E_{x_{i,j,k}}^n$ is weighted by $\frac{g}{\Delta x}$. However, $E_{x_{i,j,k}}^n$ is properly weighted (by its edge length), then again, the main FDTD update loops are unchanged.
- It is interesting to observe that the update about C2 is independent of g . The physical width of the slot is actually realized by the slot aperture fields at either end. Only the tangential field is modeled within the slot thereafter.
- For this approximation to be valid, g must be $\ll \lambda$, such that the axial field can be neglected.

Example: Electromagnetic Interaction with a Thin, Narrow Slot



Modeling of Thin Material Sheets

- Assume a thin sheet of lossy dielectric material ($\epsilon_{ts}, \sigma_{ts}, \mu_o$) passing through the FDTD lattice that is normal to the x -axis. The sheet has a thickness $d < \Delta x$, and $d \ll \lambda$.
- The boundary conditions at the surface of the discontinuity is that the tangential electric and magnetic fields are continuous. The normal electric flux density is also continuous - hence, the normal electric field is discontinuous.
- The normal electric field is separated into two contributions, $E_{x,in}$ and $E_{x,out}$ - namely, the normal field "in" and "out" of the dielectric sheet. This allows for the jump discontinuity in E_x .



- Field Updates:

$$E_{x,out_{i,j,k}}^{n+1} = E_{x,out_{i,j,k}}^n + \frac{\Delta t}{\epsilon_o} \left[\frac{H_{z_{i,j,k}}^{n+\frac{1}{2}} - H_{z_{i,j-1,k}}^{n+\frac{1}{2}}}{\Delta y} - \frac{H_{y_{i,j,k}}^{n+\frac{1}{2}} - H_{y_{i,j,k-1}}^{n+\frac{1}{2}}}{\Delta z} \right]$$

$$E_{x,in_{i,j,k}}^{n+1} = \left(\frac{1 - \frac{\sigma_{ts}\Delta t}{2\epsilon_{ts}}}{1 + \frac{\sigma_{ts}\Delta t}{2\epsilon_{ts}}} \right) E_{x,in_{i,j,k}}^n + \left(\frac{\frac{\Delta t}{\epsilon_{ts}}}{1 + \frac{\sigma_{ts}\Delta t}{2\epsilon_{ts}}} \right) \frac{\Delta t}{\epsilon_o} \left[\frac{H_{z_{i,j,k}}^{n+\frac{1}{2}} - H_{z_{i,j-1,k}}^{n+\frac{1}{2}}}{\Delta y} - \frac{H_{y_{i,j,k}}^{n+\frac{1}{2}} - H_{y_{i,j,k-1}}^{n+\frac{1}{2}}}{\Delta z} \right]$$

[Note that the continuity of H_y and H_z is enforced.]

- Tangential Electric Field Updates:

$$E_{y_{i,j,k}}^{n+1} = \left(\frac{1 - \frac{\sigma_{av}\Delta t}{2\epsilon_{av}}}{1 + \frac{\sigma_{av}\Delta t}{2\epsilon_{av}}} \right) E_{y_{i,j,k}}^n + \left(\frac{\frac{\Delta t}{\epsilon_{av}}}{1 + \frac{\sigma_{av}\Delta t}{2\epsilon_{av}}} \right) \left[\frac{H_{x_{i,j,k}}^{n+\frac{1}{2}} - H_{x_{i,j,k-1}}^{n+\frac{1}{2}}}{\Delta z} - \frac{H_{z_{i,j,k}}^{n+\frac{1}{2}} - H_{z_{i-1,j,k}}^{n+\frac{1}{2}}}{\Delta x} \right]$$

$$E_{z_{i,j,k}}^{n+1} = \left(\frac{1 - \frac{\sigma_{av}\Delta t}{2\epsilon_{av}}}{1 + \frac{\sigma_{av}\Delta t}{2\epsilon_{av}}} \right) E_{z_{i,j,k}}^n + \left(\frac{\frac{\Delta t}{\epsilon_{av}}}{1 + \frac{\sigma_{av}\Delta t}{2\epsilon_{av}}} \right) \left[\frac{H_{y_{i,j,k}}^{n+\frac{1}{2}} - H_{y_{i-1,j,k}}^{n+\frac{1}{2}}}{\Delta x} - \frac{H_{x_{i,j,k}}^{n+\frac{1}{2}} - H_{x_{i,j-1,k}}^{n+\frac{1}{2}}}{\Delta y} \right]$$

where,

$$\epsilon_{av} = \left(1 - \frac{d}{\Delta x} \right) \epsilon_o + \frac{d}{\Delta x} \epsilon_{ts}, \quad \sigma_{av} = \frac{d}{\Delta x} \sigma_{ts}$$

Tangential Magnetic Field Updates:

$$H_{y_{i,j,k}}^{n+\frac{1}{2}} = H_{y_{i,j,k}}^{n-\frac{1}{2}} - \left(\frac{\Delta t}{\mu_o \Delta x \Delta z} \right) \left[(\Delta x - d) \left(E_{x,out_{i,j,k+1}}^n - E_{x,out_{i,j,k}}^n \right) + d \left(E_{x,in_{i,j,k+1}}^n - E_{x,in_{i,j,k}}^n \right) \right] \\ - \Delta z \left(E_{z_{i+1,j,k}}^n - E_{z_{i,j,k}}^n \right)$$

$$H_{z_{i,j,k}}^{n+\frac{1}{2}} = H_{z_{i,j,k}}^{n-\frac{1}{2}} - \left(\frac{\Delta t}{\mu_o \Delta x \Delta y} \right) \left[\Delta y \left(E_{y_{i+1,j,k}}^n - E_{y_{i,j,k}}^n \right) - (\Delta x - d) \left(E_{x,out_{i,j+1,k}}^n - E_{x,out_{i,j,k}}^n \right) \right] \\ - d \left(E_{x,in_{i,j+1,k}}^n - E_{x,in_{i,j,k}}^n \right)$$

- Observations:
 - Can still preserve the fundamental FDTD update loops
 - $E_{x,in}^n$ requires a separate update loop and separate storage
 - updates involving $E_{x,in}^n$ can be added in separately after the main update loops of H
 - Tangential E field updates are modified only through the material coefficients.
- Accurately represents the affect of the thin material sheet providing $d \ll \lambda$

Example: Resistive Sheet Loaded Parallel Plate Waveguide[†]

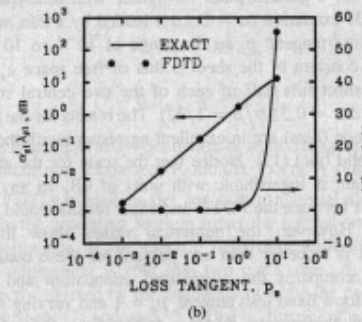
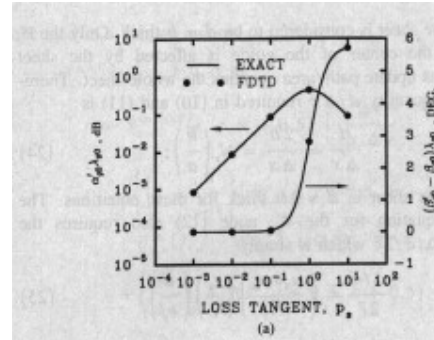
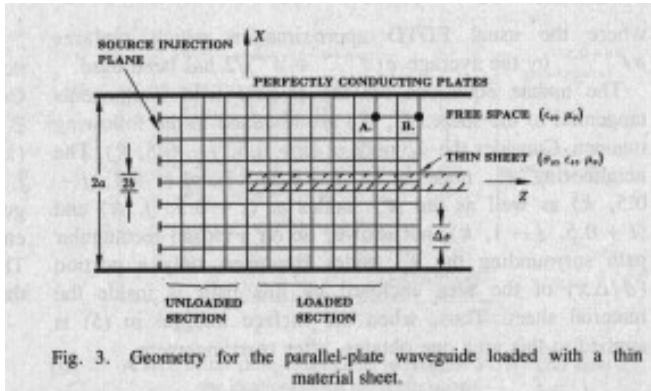


Fig. 4. Comparison of the exact and the subcell FDTD values for $\alpha'_{gi}\lambda_{gi}$ and $(\beta'_{gi} - \beta_{gi})\lambda_{gi}$ for time-harmonic excitation. The loss tangent, p_2 varies from 10^{-4} to 10^2 , sheet thickness $b/\Delta x = 0.5$ ($b/a = 1/32$), $p_x = 1$, $\epsilon_x = \epsilon_0$. (a) TEM mode, $i = 0$. (b) TM₁ mode, $i = 1$.

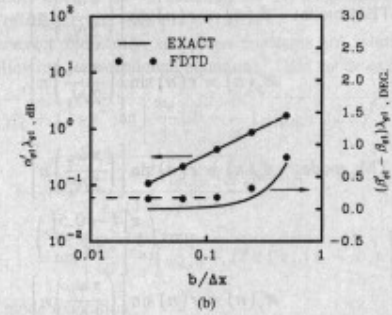
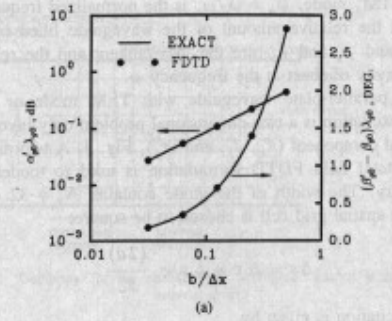


Fig. 5. Comparison of the exact and the subcell FDTD values for $\alpha'_{gi}\lambda_{gi}$ and $(\beta'_{gi} - \beta_{gi})\lambda_{gi}$ for time-harmonic excitation. The sheet thickness $b/\Delta x$ varies from 0.03125 to 0.5 ($b/a = 1/512$ to $1/32$), $p_x = 1$, $\epsilon_x = \epsilon_0$. (a) TEM mode, $i = 0$. (b) TM₁ mode, $i = 1$.

[†]Maloney and Smith, "The Efficient Modeling of Thin Material Sheets in the FDTD Method," *IEEE Transactions on Antennas and Propagation*, Vol. 40, pp. 323-330, March 1992.

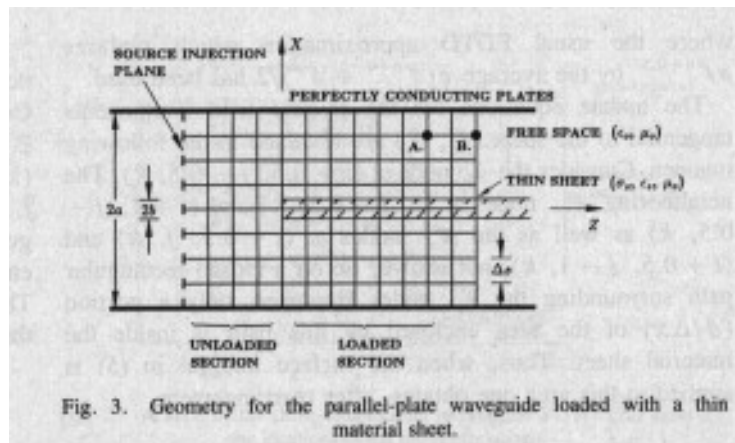
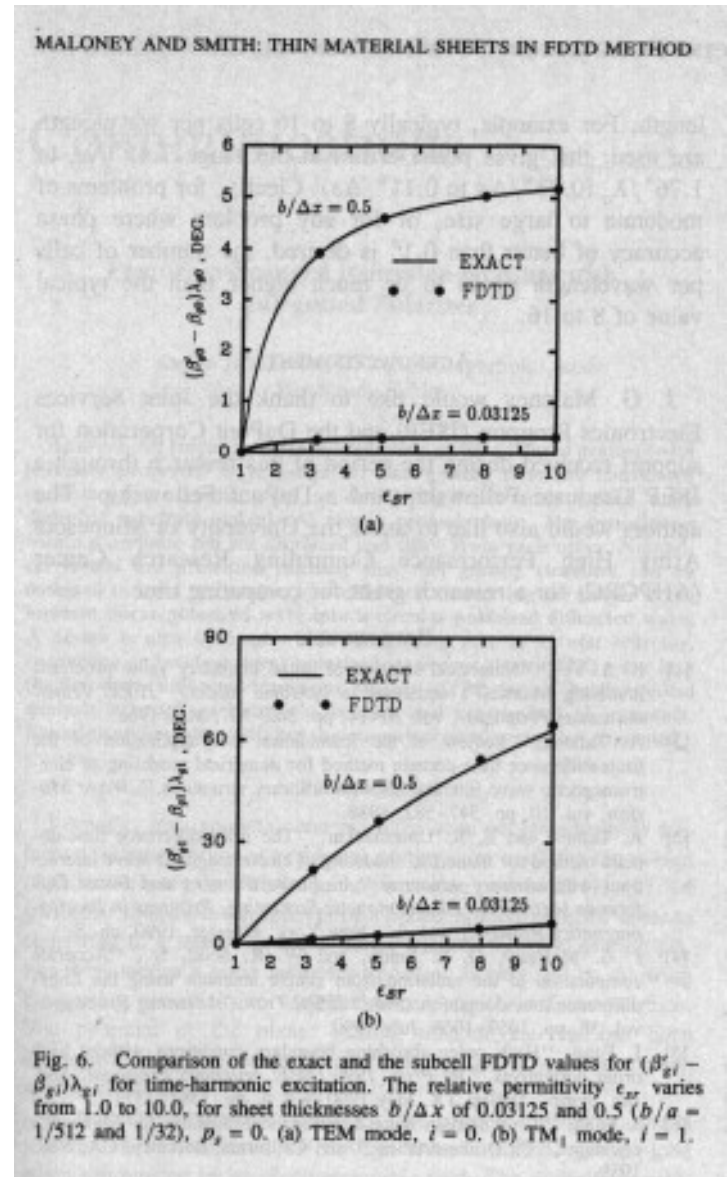
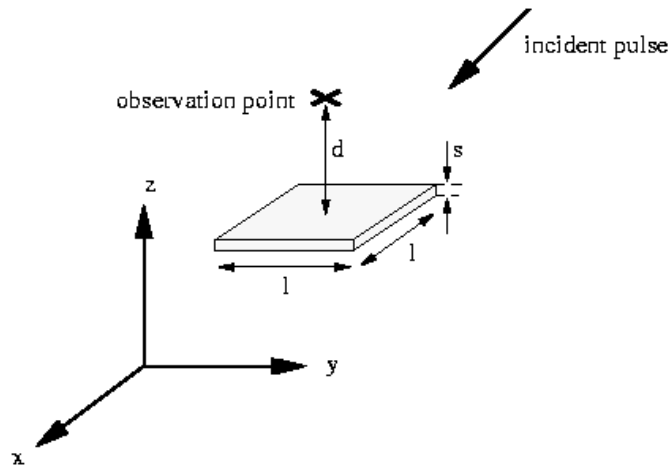
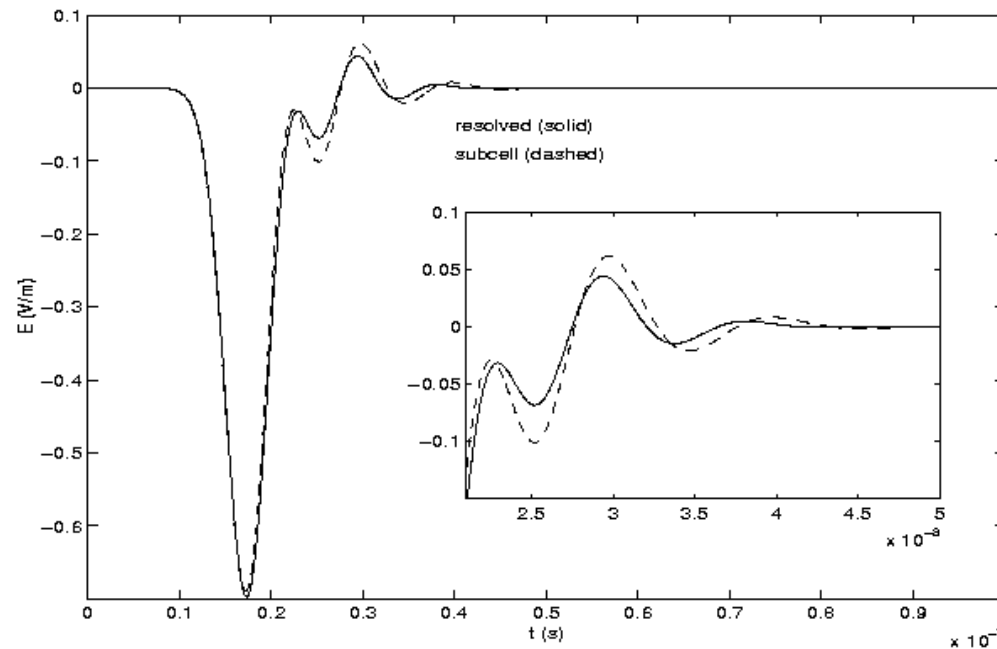


Fig. 3. Geometry for the parallel-plate waveguide loaded with a thin material sheet.

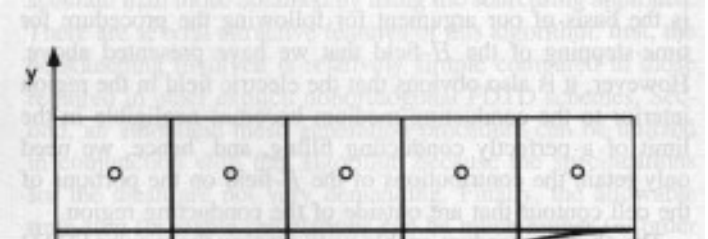


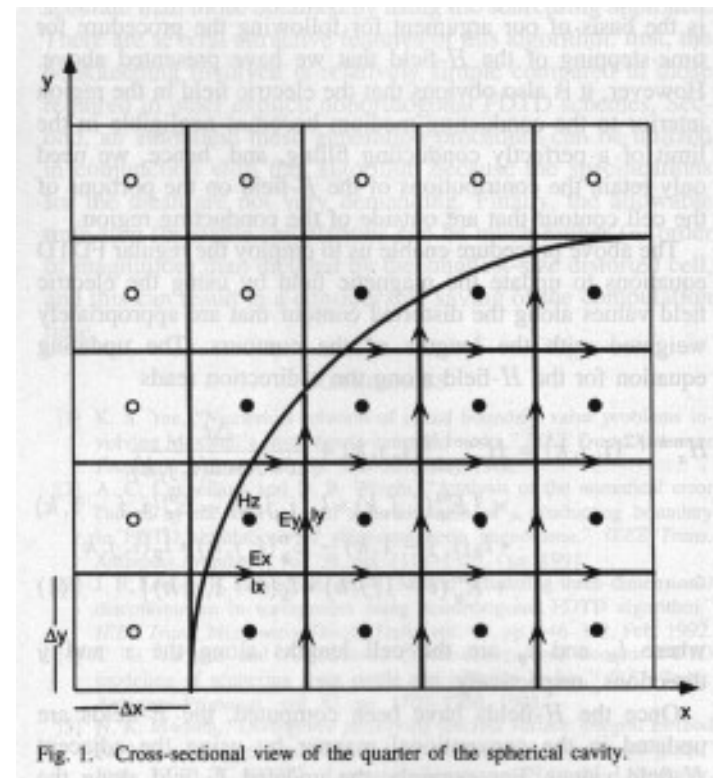
Figure 36: *The thin material sheet.*

Computational parameters:	Case 1	Case 2
Time step, Δt (ns):	0.1	0.04
Number of time steps:	1500	3750
Simulation time (μs):	0.15	0.15
Cell size $\Delta x, \Delta y, \Delta z$ (m):	0.1, 0.1, 0.1	0.025, 0.025, 0.025
Number of cells n_x, n_y, n_z :	24, 24, 61	96, 96, 244
Sheet side, l (m):	0.8	
Thickness, s (m):	0.025	
Material parameters, ϵ, μ, σ :	$\epsilon_0, \mu_0, 200$	
Pulse parameters $a(s^{-1}), b(s)$:	3E8, 1E-8	
Direction of propagation θ, ϕ :	45, 90	
Polarization α, β :	45, -90	



Contour Path Modeling of Irregular Surfaces

- Since God did not make our world rectangular, the FDTD method is forced to approximate irregularly shaped surfaces with staircase approximations.
 - Staircasing leads to boundary error which can supercede dispersive errors
 - To reduce boundary error sufficiently, grid lattice may need to be dramatically refined
 - This leads to additional memory and FLOP's to compute an accurate solution
 - This can be alleviated using several techniques
 1. Non-Orthogonal FDTD Methods
 2. Contour-Patch FDTD Methods
 - Deformed rectangular lattices
- 



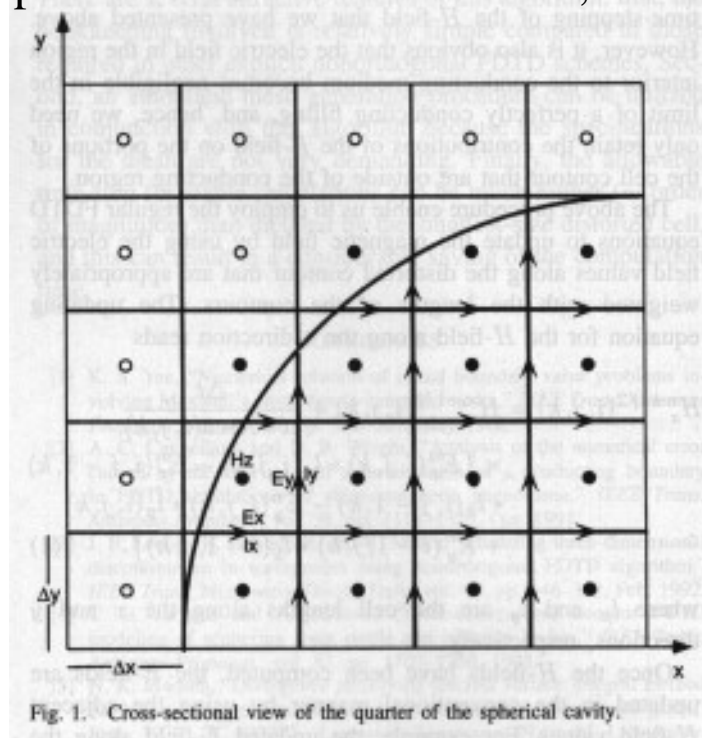
Contour Path FDTD (CPFDTD) Method

- Original CPFDTD method was introduced by Jurgens, et al [1].
 - Method successfully demonstrated to model irregularly shaped objects
 - Suffers from late time instabilities
- Origin of late time instabilities was shown in [2] to be due to the non-reciprocal nature of the CPFDTD method. A stable and accurate scheme was introduced [3,4].
 - Scheme is cumbersome to implement, and intrusive of the base FDTD algorithm
- Stable and simple CPFDTD scheme was recently introduced by Dey and Mittra [5].
 - Scheme is stable, and the most accurate of all the CPFDTD methods introduced [6]
 - This scheme will be the topic of our discussion

- [1] T. Jurgens and A. Taflove, "Three-dimensional contour FDTD modeling of scattering from single and multiple bodies," *IEEE Trans. Antennas and Prop.*, vol. 41, pp. 1803-1708, Dec. 1993
- [2] I. J. Craddock, C. J. Railton, and J. P. BcGeehan, "Derivation and application of a passive equivalent circuit for the FDTD algorithm," *IEEE Microwave and Guided Wave Letters*, vol. 6, pp. 40-42, Jan. 1996.
- [3] C. J. Railton and I. J. Craddock, "Analysis of general 3-D PEC structures using an improved CP-FDTD algorithm," *Electronics Letters*, vol. 31, pp. 1553-1554, Sept. 1995.
- [4] C. J. Railton and I. J. Craddock, "Stabilized CP-FDTD algorithm for the analysis of arbitrary 3D PEC structures," *Proc. Inst. Elect. Eng.*, vol. 143, pt. H, pp. 367-372, Oct. 1996.
- [5] S. Dey and R. Mittra, "A locally conformal FDTD algorithm for modeling 3D PEC objects," *IEEE Microwave and Guided Wave Letters*, vol. 7, pp. 273-275, Sept. 1997.
- [6] C. J. Railton and J. Schneider, "An analytical and numerical analysis of several locally conformal FDTD schemes," *IEEE Trans. On Microwave Theory and Techniques*, vol. 47, pp. 56-66, Jan. 1999.

Contour Path FDTD (CPFDTD) Method (cont'd)

- Consider the cross-section of a quadrant of a spherical surface positioned within an FDTD lattice
- Near the surface of the boundary, the cells are distorted.
 - The electric fields are located on the edges of the cells (as indicated by the arrows)
 - The magnetic fields are assumed to be positioned at the cell centers - even if the cell center happens to lie outside of the PEC boundary (as indicated by the filled circles)
- Faraday's law is performed in its integral form over the deformed cell faces
- Ampere's law is represented in differential form, assuming undeformed cells



Field Updates

- From Faraday's Law:

$$H_{z_{i,j,k}}^{n+\frac{1}{2}} = H_{z_{i,j,k}}^{n-\frac{1}{2}} - \frac{\Delta t}{\mu A_{i,j,k}} \left[E_{y_{i+1,j,k}}^n l_{y_{i+1,j,k}} - E_{y_{i,j,k}}^n l_{y_{i,j,k}} - E_{x_{i,j+1,k}}^n l_{x_{i,j+1,k}} + E_{x_{i,j,k}}^n l_{x_{i,j,k}} \right]$$

where $A_{i,j,k}$ is the face area

- From Ampere's Law:

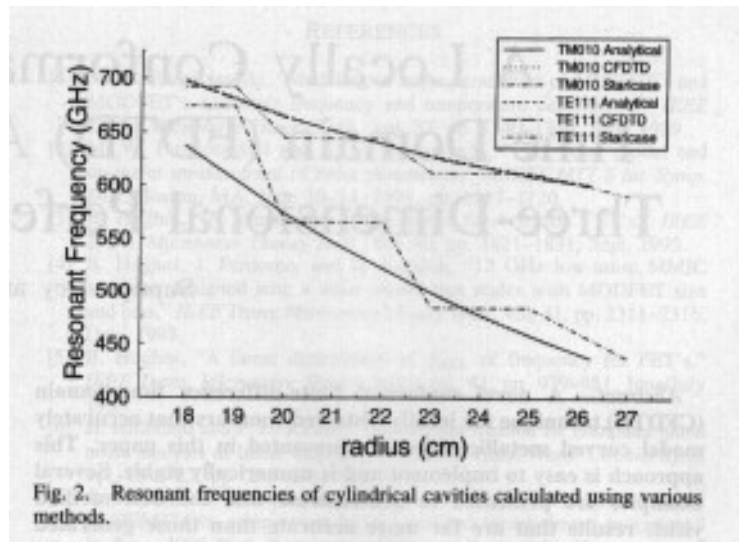
$$E_{x_{i,j,k}}^{n+1} = E_{x_{i,j,k}}^n + \frac{\Delta t}{\varepsilon} \left[\frac{H_{z_{i,j,k}}^n - H_{z_{i,j-1,k}}^n}{\Delta y} - \frac{H_{y_{i,j,k}}^n - H_{y_{i,j,k-1}}^n}{\Delta z} \right]$$

- Observations:

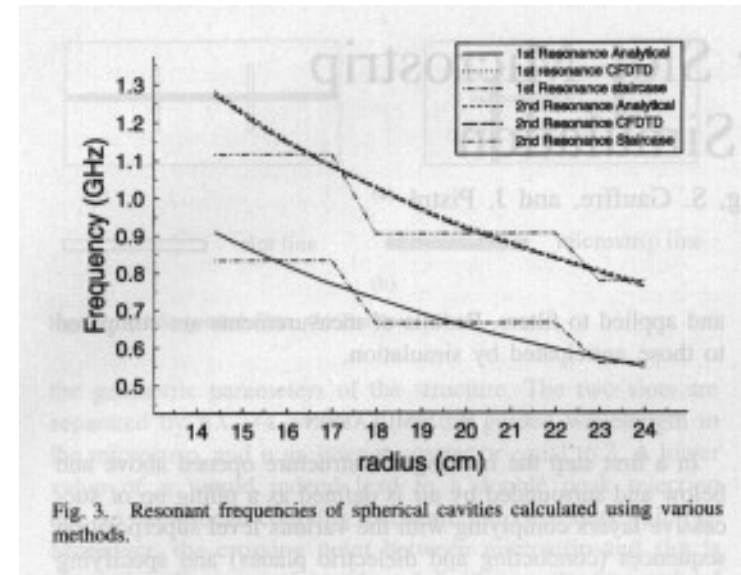
- Scheme can be incorporated directly into the FDTD algorithm. Only the update coefficients need to be modified - a preprocessing step
- Scheme is stable, since method is reciprocal
- Dey and Mittra report:
 1. If the area of the smallest distorted cell is $> 1.5 \%$ of the undistorted cell area, the time step should be reduced by 50 % of the Courant Limit
 2. If the area of the smallest distorted cell is $> 2.5 \%$ of the undistorted cell area, the time step should be reduced by 30 % of the Courant Limit
 3. If the ratio between the maximum length of the side of a cell and its area is < 15 , the time step should be reduced by 50 % of the Courant Limit
 4. If the ratio between the maximum length of the side of a cell and its area is < 10 , the time step should be reduced by 30 % of the Courant Limit

Examples of the CPFDTD Method

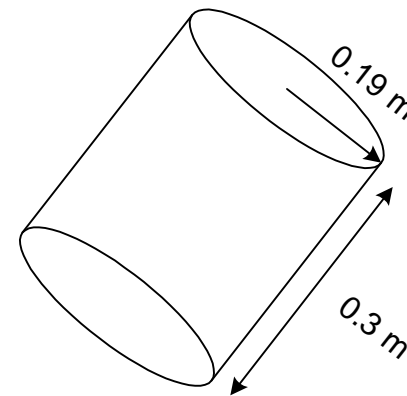
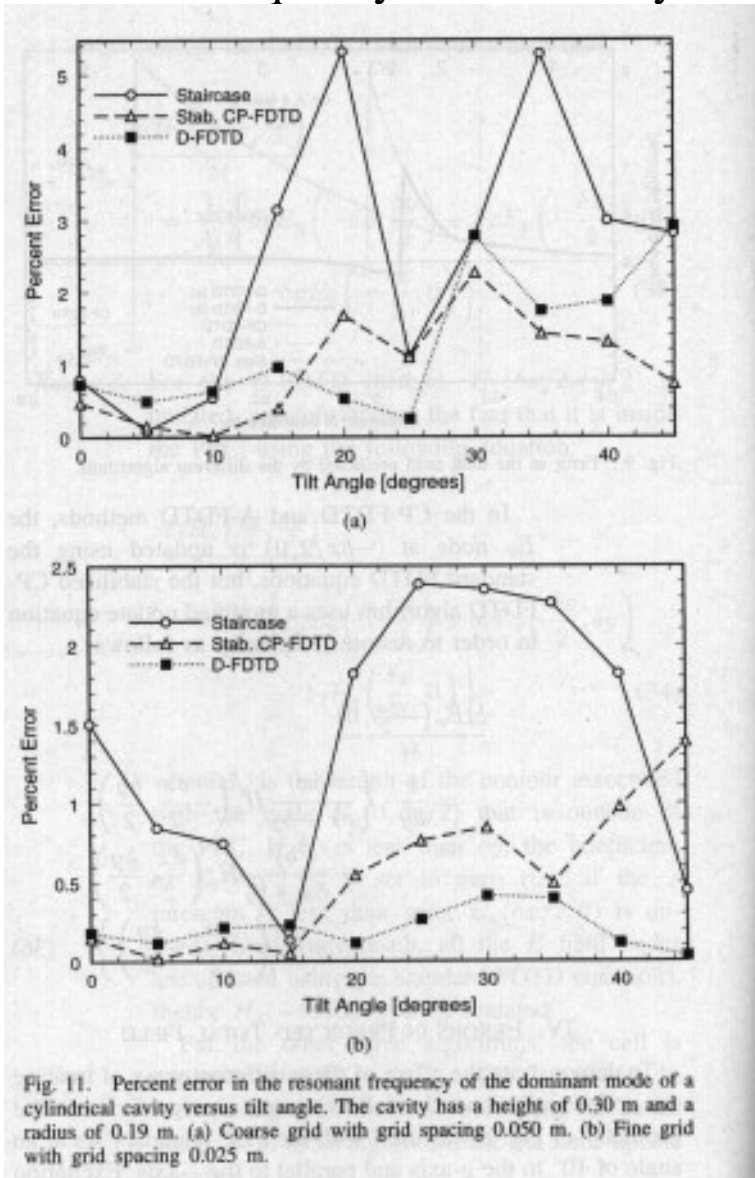
Resonant Frequency of a Cylindrical Cavity [5]:



Resonant Frequency of a Spherical Cavity [5]:



Resonant Frequency of a Tilted Cylindrical Cavity [6]:



- How would you modify the CPFDTD method to open PEC boundaries rather than closed?

Conformal FDTD Model of Dielectric Surfaces

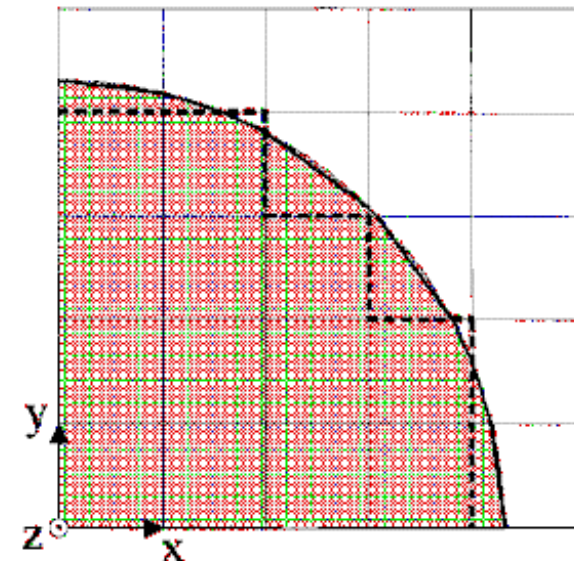
- Previous discussion was limited to non-penetrable conductor surfaces
- Not applicable to penetrable materials such as dielectrics
- Applications:
 - Dielectric Resonators - microwave circuit applications, Photonic Bandgap (PBG) structures, antenna radomes or sheaths
- Conformal FDTD method will be based on both deforming the cell and introducing an effective tensor representation [1,2]
 - Effective permittivity tensor is necessary due to the different properties of the normal and tangential electric field

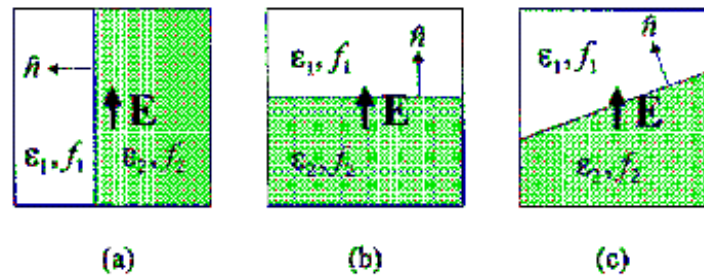
[0] Nadobny J, Sullivan D, Wlodarczyk W, et al. , "A 3-D tensor FDTD-formulation for treatment of sloped interfaces in electrically inhomogeneous media," *IEEE T. Antennas and Propagation*, vol. 51 (8), pp. 1760-1770, August 2003

[1] J.-Y. Lee and N.-H. Myung, "Locally tensor conformal FDTD method for arbitrary dielectric surfaces," *Microwave and Optical Technology Letters*, vol. 23, No. 4, pp. 245-249, Nov. 20, 1999.

[2] R. D. Meade, et al., "Accurate theoretical analysis of photonic band-gap materials," *Phys. Rev. B*, vol. 48, pp. 8434-8437, 1993.

[3] D. E. Aspnes, "Local-field effects and effective-medium theory: a microscopic perspective," *American Journal of Physics*, vol. 50, pg. 704-709, 1982.





- The behavior of the electric field at the surface of a dielectric interface will depend on the field polarization
- We've seen that we can average the permittivity in a cell

- (a) Tangential

$$\varepsilon_{\text{tan}} = \frac{A_1}{A} \varepsilon_1 + \frac{A_2}{A} \varepsilon_2$$

- (b) Normal

$$\frac{1}{\varepsilon_n} = \frac{A_1}{A} \frac{1}{\varepsilon_1} + \frac{A_2}{A} \frac{1}{\varepsilon_2}$$

- Skew (c)

- The skew boundary is a combination of the tangential and normal contributions
- Based on effective media theory [1-3]:

$$\varepsilon_{\text{eff}} = \begin{bmatrix} \varepsilon_n n_x^2 + \varepsilon_{\text{tan}} n_y^2 & (\varepsilon_n - \varepsilon_{\text{tan}}) n_x n_y & 0 \\ (\varepsilon_n - \varepsilon_{\text{tan}}) n_x n_y & \varepsilon_n n_y^2 + \varepsilon_{\text{tan}} n_x^2 & 0 \\ 0 & 0 & \varepsilon_{\text{tan}} \end{bmatrix}$$

where, the unit vector normal to the surface is: $\hat{n} = n_x \hat{x} + n_y \hat{y}$ and ε_{tan} and ε_n are defined above

- This can be generalized to a three-dimensional surface

Consider the limiting case when $n_x = 1$, $n_y = 0$

$$\epsilon_{eff} = \begin{bmatrix} \epsilon_n & 0 & 0 \\ 0 & \epsilon_{tan} & 0 \\ 0 & 0 & \epsilon_{tan} \end{bmatrix}$$

- Similarly along other axes
- The field update is performed in the following order:
 1. Update the electric flux densities $\vec{D}_{i,j,k}^{n+1}$ using the direct FDTD updates based on Ampere's law
 2. Compute the electric fields from $\vec{D}_{i,j,k}^{n+1}$ using the constitutive relationship
 3. Update the magnetic fields based on Faraday's law

- Constitutive Relationship

$$\vec{E}_{i,j,k}^{n+1} = \varepsilon^{-1} \vec{D}_{i,j,k}^{n+1}$$

where

$$\varepsilon_{eff}^{-1} = \begin{bmatrix} \frac{\varepsilon_n n_y^2 + \varepsilon_{\tan} n_x^2}{\Delta} & -\frac{(\varepsilon_n - \varepsilon_{\tan}) n_x n_y}{\Delta} & 0 \\ -\frac{(\varepsilon_n - \varepsilon_{\tan}) n_x n_y}{\Delta} & \frac{\varepsilon_n n_x^2 + \varepsilon_{\tan} n_y^2}{\Delta} & 0 \\ 0 & 0 & \frac{1}{\varepsilon_{\tan}} \end{bmatrix}$$

and, where

$$\Delta = \varepsilon_{\tan} \varepsilon_n (n_x^4 + n_y^4 + 2n_y^2 n_x^2) = \varepsilon_{\tan} \varepsilon_n (n_x^2 + n_y^2)^2 = \varepsilon_{\tan} \varepsilon_n$$

Constitutive Relationships:

$$E_{x_{i,j,k}}^{n+1} = \left(\frac{n_x^2}{\varepsilon_n} + \frac{n_y^2}{\varepsilon_{\tan}} \right) D_{x_{i,j,k}}^{n+1} + \left(\frac{1}{\varepsilon_n} - \frac{1}{\varepsilon_{\tan}} \right) n_x n_y \bar{D}_{y_{i,j,k}}^{n+1}$$

$$E_{y_{i,j,k}}^{n+1} = \left(\frac{1}{\varepsilon_n} - \frac{1}{\varepsilon_{\tan}} \right) n_x n_y \bar{D}_{x_{i,j,k}}^{n+1} + \left(\frac{n_x^2}{\varepsilon_{\tan}} + \frac{n_y^2}{\varepsilon_n} \right) D_{y_{i,j,k}}^{n+1}$$

$$E_{z_{i,j,k}}^{n+1} = \frac{1}{\varepsilon_{\tan}} D_{z_{i,j,k}}^{n+1}$$

where, $\bar{D}_{x_{i,j,k}}^{n+1}$ and $\bar{D}_{y_{i,j,k}}^{n+1}$ are averaged as:

$$\bar{D}_{x_{i,j,k}}^{n+1} = \frac{1}{4} \left[D_{x_{i,j,k}}^{n+1} + D_{x_{i,j+1,k}}^{n+1} + D_{x_{i-1,j,k}}^{n+1} + D_{x_{i-1,j+1,k}}^{n+1} \right]$$

$$\bar{D}_{y_{i,j,k}}^{n+1} = \frac{1}{4} \left[D_{y_{i,j,k}}^{n+1} + D_{y_{i+1,j,k}}^{n+1} + D_{y_{i,j-1,k}}^{n+1} + D_{y_{i+1,j-1,k}}^{n+1} \right]$$

Example 1: Rotated Planar Interface [1]

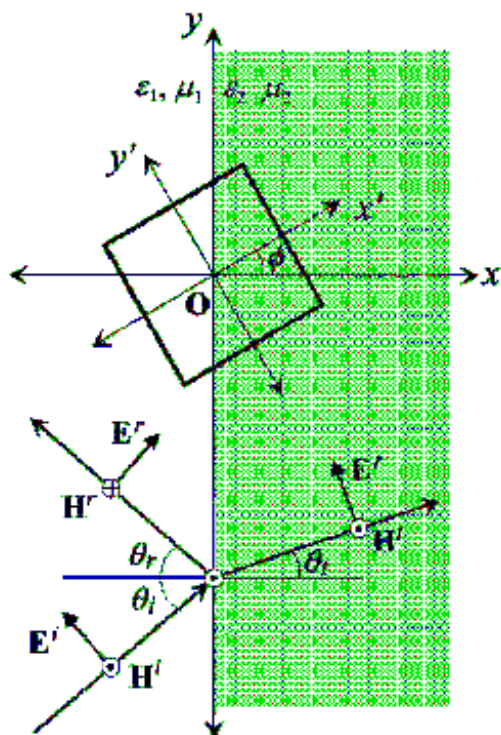


Figure 2 Uniform plane wave incident on a planar interface and a rotated square test cell

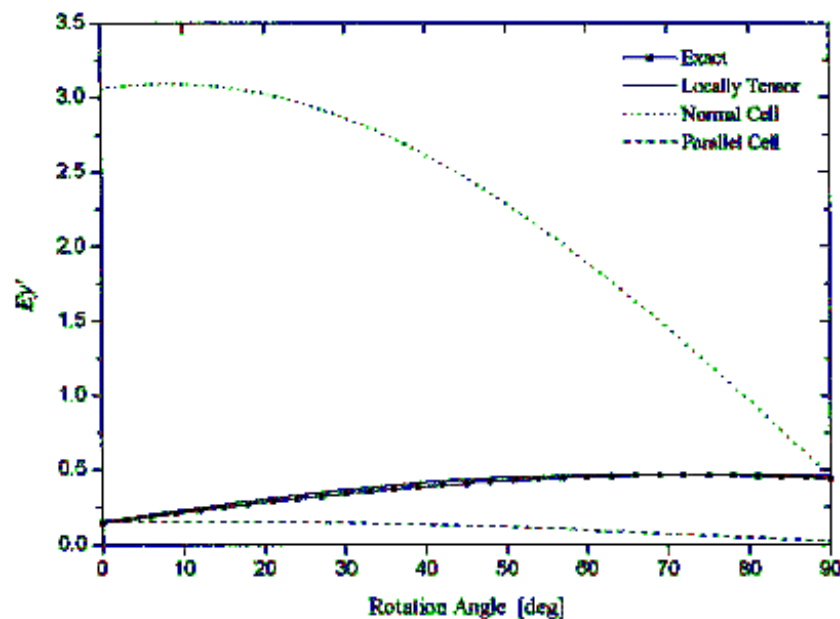


Figure 3 2-D planar interface test

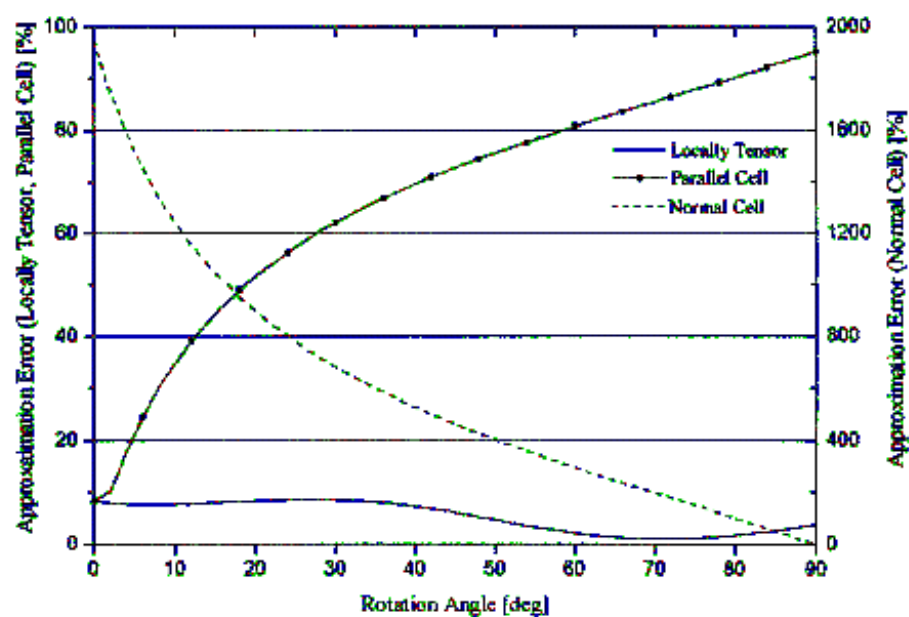


Figure 4 Approximation error

$$\text{approximation error} = \frac{|E_{y', \text{exact}} - E_{y', \text{approx}}|_{\max}}{|E_{y', \text{exact}}|_{\max}}$$

Example 2: Dielectric Cylinder [1]

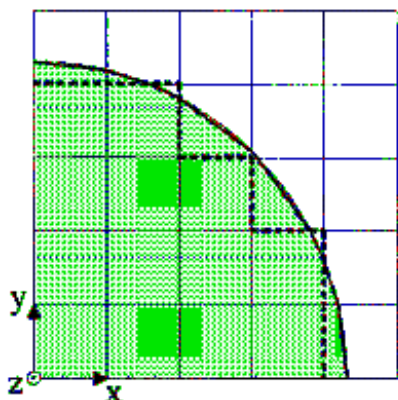


Figure 6 2-D quarter dielectric circular cylinder and FDTD grid structure

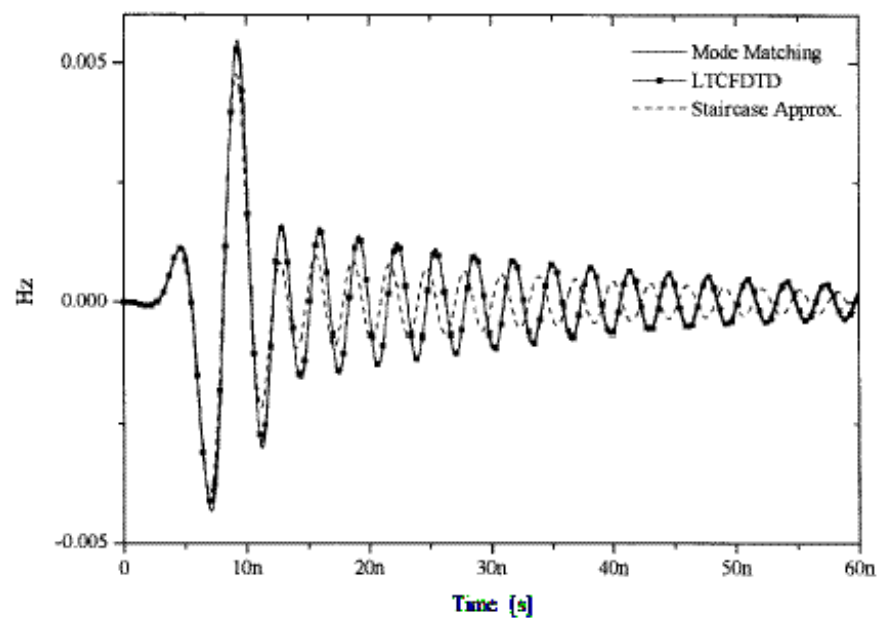


Figure 7 Magnetic field at the center point of a dielectric circular cylinder

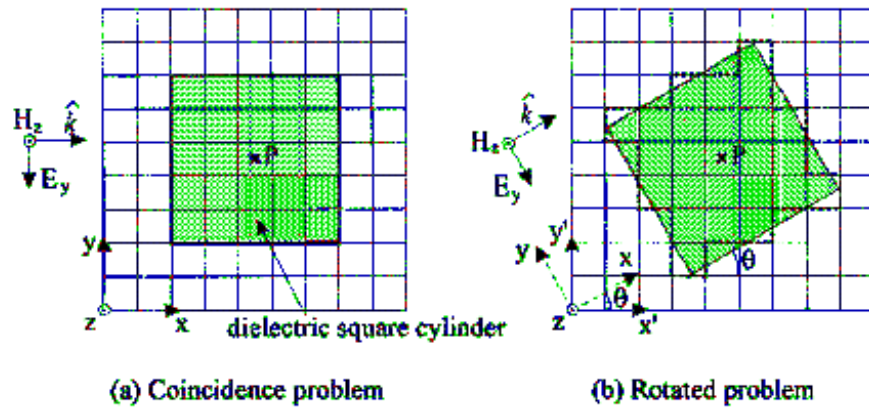


Figure 8 2-D dielectric square cylinder and FDTD grid structure

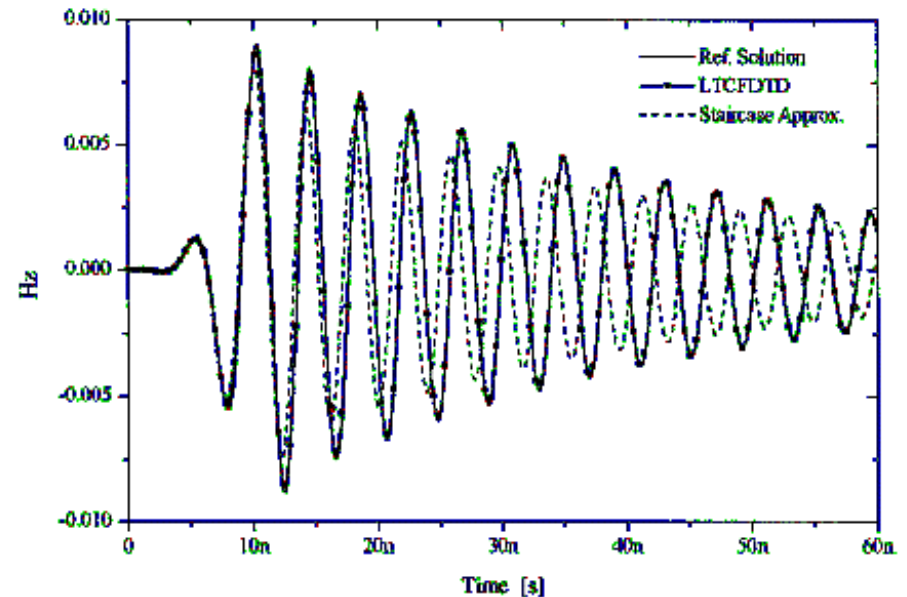


Figure 9 Magnetic field at the center point of a dielectric square cylinder

- Observations
 - Method appears to offer excellent accuracy as compared to a staircase approximation with a coarse grid
 - Late time stability? It is uncertain given the averaging terms. Needs to be validated.
 - Method could be extended to 3-D

Assume a three-dimensional surface with unit normal:

$$\hat{n} = \cos \phi \sin \theta \hat{x} + \sin \phi \sin \theta \hat{y} + \cos \theta \hat{z}$$

Define the rotational tensor:

$$\bar{\bar{T}} = \begin{bmatrix} \sin \theta & 0 & \cos \theta \\ 0 & 1 & 0 \\ -\cos \theta & 0 & \sin \theta \end{bmatrix} \begin{bmatrix} \cos \phi & \sin \phi & 0 \\ -\sin \phi & \cos \phi & 0 \\ 0 & 0 & 1 \end{bmatrix}$$

and the permittivity tensor:

$$\bar{\varepsilon}_{eff} = \begin{bmatrix} \varepsilon_n & 0 & 0 \\ 0 & \varepsilon_{tan} & 0 \\ 0 & 0 & \varepsilon_{tan} \end{bmatrix}$$

Then applying rotation of coordinates, the constitutive relation can be defined as:

$$\bar{\varepsilon}_{eff} \bar{\bar{T}} \vec{E} = \bar{\bar{T}} \vec{D}$$

Finally, define:

$$\bar{\bar{\varepsilon}}_{eff} = \bar{\bar{T}}^{-1} \bar{\varepsilon}_{eff} \bar{\bar{T}} =$$

$$\begin{bmatrix} \cos^2 \phi \sin^2 \theta \varepsilon_n + (\sin^2 \phi \sin^2 \theta + \cos^2 \theta) \varepsilon_{tan} & \cos \phi \sin \phi \sin^2 \theta (\varepsilon_n - \varepsilon_{tan}) & \cos \phi \sin \theta \cos \theta (\varepsilon_n - \varepsilon_{tan}) \\ \cos \phi \sin \phi \sin^2 \theta (\varepsilon_n - \varepsilon_{tan}) & \sin^2 \phi \sin^2 \theta \varepsilon_n + (\cos^2 \phi \sin^2 \theta + \cos^2 \theta) \varepsilon_{tan} & \sin \phi \sin \theta \cos \theta (\varepsilon_n - \varepsilon_{tan}) \\ \cos \phi \sin \theta \cos \theta (\varepsilon_n - \varepsilon_{tan}) & \sin \phi \sin \theta \cos \theta (\varepsilon_n - \varepsilon_{tan}) & \cos^2 \theta \varepsilon_n + \sin^2 \theta \varepsilon_{tan} \end{bmatrix}$$

This can be more conveniently expressed in terms of the unit normal vector:

$$\epsilon_{eff} = \begin{bmatrix} n_x^2 \epsilon_n + (n_y^2 + n_z^2) \epsilon_{tan} & n_x n_y (\epsilon_n - \epsilon_{tan}) & n_x n_z (\epsilon_n - \epsilon_{tan}) \\ n_x n_y (\epsilon_n - \epsilon_{tan}) & n_y^2 \epsilon_n + (n_x^2 + n_z^2) \epsilon_{tan} & n_y n_z (\epsilon_n - \epsilon_{tan}) \\ n_x n_z (\epsilon_n - \epsilon_{tan}) & n_y n_z (\epsilon_n - \epsilon_{tan}) & n_z^2 \epsilon_n + (n_x^2 + n_y^2) \epsilon_{tan} \end{bmatrix}$$

This leads to a full, three-dimensional tensor relationship.

$$\bar{\bar{\epsilon}}_{eff} \vec{E} = \vec{D}$$